

ASSOCIATIONS OF POLYCYCLIC AROMATIC HYDROCARBONS (PAHs)
WITH PARTICULATES IN
THE ENVIRONMENT

by

JEJAL REDDY BATHI

A DISSERTATION

Submitted in partial fulfillment of the requirements for the degree of
Doctor of Philosophy in the Department of Civil,
Construction, and Environmental Engineering
in the Graduate School of
The University of Alabama

TUSCALOOSA, ALABAMA

2008

Copyright Jejal Reddy Bathi 2008
ALL RIGHTS RESERVED

Submitted by Jejal Reddy Bathi in partial fulfillment of the requirements for the degree of Doctor of Philosophy specializing in Civil Engineering.

Accepted on behalf of the faculty of the Graduate School by the dissertation committee:

Karen Boykin, Ph.D.

Robert H. Findlay, Ph.D.

Rocky S. Durrans, Ph.D.

Sergey B. Mirov, Ph.D.

Shirley E. Clark, Ph.D.

Robert E. Pitt, Ph.D.
Chairperson

Kenneth J. Fridley, Ph.D.
Department Chairperson

Date

David A. Francko, Ph.D.
Dean of the Graduate School

Date

LIST OF ABBREVIATIONS AND SYMBOLS

ANOVA	Analysis of variance
CO ₂	Carbon dioxide
COD	Chemical oxygen demand
C.I.	Confidence interval
DB-5	5% Divinylbenzene
DL	Detetction limit
GC	Gas chromatography
gm	Gram
Filtered	Runoff samples with particulate matter separated
ft	Feet
H	Henry's law constant
HMW	High molecular weight
K _{OC}	Soil-organic partition coefficient
K _{OW}	Octanol-water partition coefficient
kg	Kilogram
L	Liter
LOM	Large organic material
LOM	Low molecular weight
mL	mili liter
MSD	Mass spectroscopy detector

NIST	National Institute of Standards and Technology
OC	Organic content
PAHs	Polycyclic aromatic hydrocarbons
PCBs	Polychlorinated biphenyls
POPs	Persistent organic pollutants
p-value	Probability value
QA	Quality assurance
QC	Quality control
SS	Suspended solids
TD	Thermal desorption
Un-filtered	Runoff samples collected as it is
US EPA	United States Environmental Protection Agency
USGS	United States Geological Service
w/o LOM	With out large organic material
µg	Microgram
µL	Microliter
µm	Micrometer
%	Percent
<	Less than
>	Greater than

ACKNOWLEDGMENTS

First I would like to express my sincere gratitude to my advisor, Dr. Robert Pitt, for his patience, guidance and insightfulness. I hope that one day I can have the vision and creativity he has. A special thank you to Dr. Robert Findlay for his guidance and support throughout this research work. Without your expertise, the development of thermal desorption analytical technique would not have been possible. I would also like to thank you all other committee members: Dr. Karen, Dr. Durrans, Dr. Mirov and Dr. Shirley Clark for your contributions and suggestions. I would also take this opportunity to thank NSF EPSCoR Center for Optical Sensors and Spectroscopies for funding this work in part (Grant No. EPS-0447675).

I gratefully acknowledge my fellow graduate students, Hunter, Kimberly, Vijay for their contributions to collect and process the sediment samples. And also, Celina, Humberto, Laith and class of spring 2007 Experimental Design and Field Sampling, CE 484/584 for their contributions to this research work. Sincere thank you to Jennifer Mosher and Janna Brown of Biological Sciences for teaching me analytical protocol and assisting with sample analyses.

My acknowledgment never ends without thanking my parents, Anji Reddy and Padma for their love and encouragement. Also, my special thank you to my brothers: B.A.Reddy and B.V.N Reddy, to sister-in-laws: Chandrakala and Sunitha for their constant support. Additionally, I would also like to thank you my in-laws: N.S.Reddy and

Aruna Kumari and my brother in-law Sunil Reddy for their confidence in me. Last but not least a very special thank you to my lovely wife Sumana for everything.

CONTENTS

LIST OF ABBREVIATIONS AND SYMBOLS	ii
ACKNOWLEDGEMENTS	iv
LIST OF TABLES	x
LIST OF FIGURES	xvi
ABSTRACT	xxxi
CHAPTERS:	
I INTRODUCTION	1
II LITERATURE REVIEW	4
2.1 Sources of PAHs in the Environment	4
2.2 Fates of PAHs in the environment	8
2.2.1 PAHs associations with particulate matter	10
2.3 Suspended solids in stormwater	15
2.4 Analytical methods for measuring PAHs in environmental samples	22
2.5 Need for research	25
2.6 Dissertation research	26
III EXPERIMENTAL DESIGN	27
3.1 Hypotheses	27
3.2 Quantification of Selected PAHs on Size Fractionated Particulate Matter ...	30
3.3 Quantification of the Material Composition of Sediment Samples	31

3.4 Developing a Thermal Desorption Analytical Technique for Analyses of PAHs	32
3.5 Fugacity-based Partition Calculations for an Environmental System under Equilibrium Conditions.....	32
3.6 Quality Control and Quality Assurance	34
3.7 Sediment Sample Collection and Processing	35
IV FATE MODELING	43
4.1 Fugacity Modeling	43
4.2 Multi Chamber Treatment Train (MCTT) Study	47
4.2.1 Comparing Model Predictions with MCTT PAH Data	48
4.3 Studying the Effects of Environmental Factors on PAHs Associations with Particulate Material using Fugacity Calculations	51
4.4 Conclusions.....	56
V ANALYTICAL METHOD DEVELOPMENT	58
5.1 Development of New Analytical Techniques	58
5.2 Analysis Procedure	59
5.2.1 Tube Conditioning	59
5.2.2 Tube Packing	60
5.2.3 Analysis.....	61
5.3 Thermal Desorption Method Optimization.....	62
5.3.1 Optimal conditions of thermal desorption system	64
5.4 Testing Method for Linearity.....	65

5.5 Analysis of a Standard Sample using the Developed Method	65
5.5.1 Presence of sulfur	66
5.5.2 Moisture in the sample	66
5.6 Comparison of Recoveries from Two Different Solid Matrices	67
5.7 Method Detection Limit (MDL)	68
5.8 Recovery Calculations using the Standard NIST Solid Matrix Sample	71
5.9 Specifications of GC Column and Operating Conditions	74
5.10 Conclusions	75
VI URBAN STREAM SEDIMENT CHARACTERISTICS	76
6.1 Sediment Particle Sizes	76
6.2 Thermal Chromatography	80
6.3 Chemical Oxygen Demand	87
6.4 Conclusions	92
VII PAHs CONCENTRATIONS ON SEDIMENT PARTICLES	94
7.1 Testing the Concentrations for Variability	95
7.1.1 Comparing the Concentrations at the Three Creeks	95
7.1.2 Comparing PAH Concentrations for Different Particle Size Ranges ..	101
7.2 Relationships between COD and PAH Concentrations	106
7.3 Summary	107
VIII CONCLUSIONS	109
8.1 Hypothesis 1 Findings	111

8.2 Hypothesis 2 Findings	113
REFERENCES	116
APPENDICES:	
A PROPERTIES AND FATE MODELING OF PAHs	120
B THERMAL DESORPTION ANALYTICAL METHOD DEVELOPMENT	128
C STATISTICAL ANALYSES OF THE DATA.....	147

LIST OF TABLES

2.1 Organic Compounds Detected at Different Urban Source Areas (Source: Pitt et al.1999)	5
2.2 Concentrations and partitioning of selected PAHs in urban stormwater samples (Pitt et al. 1999)	13
4.1 Assumed System Parameters	45
4.2 MacKay Level 1 Calculated Fugacity Capacities and Percentage Partitioning of Selected PAHs with Different Environmental Phases	46
4.3 Percentage of samples detected	48
4.4 Variables used in fugacity partition predictions	49
4.5 Model Predicted Percentage of Partitions.....	49
4.6 MCTT Observed Percentage of Partitions (non-detects in filtered samples are replaced with half of DL).....	50
4.7 24 Factorial Design Showing Experimental Conditions for 16 Runs (Box et al. 1978)	52
4.8 Values Used in Factorial Analysis of Modeled PAH Associations.....	52
4.9 Model Predicted Portioning of Anthracene with 24 Factorial Design Variables	54
4.10 Calculated Effects of Factors and their Interactions on the Associations of Anthracene with Different Media	54
5.1 Regression Coefficient Values for Linearity test.....	65

5.2 Comparison of Peak Areas for Two Solid Matrices	67
5.3 Method detection and Quantification Limits	70
5.4 Calculated Method Recovery Using NIST Sediment Standard	73
5.5 One-Way ANOVA P values for PAHs Concentrations of Coarser and Grinded Samples	74
6.1 Percentage Associations and Standard Deviations of Particles of Individual Size Ranges for Cribbs Mill Creek Sediment Samples	77
6.2 Percentage Associations and Standard Deviation of Particles of Individual Size Ranges for Hunter Creek Sediment Samples	78
6.3 Percentage Associations and Standard Deviation of Particles of Individual Size Ranges for Carroll's Creek Sediment Samples	78
6.4 Ray (1997) Thermal Chromatography Method Parameters	81
6.5 Percentage of Weight Losses over Temperature Ranges for Cribbs Mill Creek Sediment Samples	82
6.6 Percentage of Weight Losses over Temperature Ranges for Hunter Creek Sediment Samples	83
6.7 Percentage of Weight Losses over Temperature Ranges for Carroll's Creek Sediment Samples	84
6.8 Observed COD Values of Sediment Samples from Cribbs Mill Creek	88
6.9 Observed COD Values of Sediment Samples from Hunter Creek	88
6.10 Observed COD Values of Sediment Samples from Carroll's Creek	89
6.11 ANOVA P Values of Regression of COD and Sediment Material Weight Loss on Heating	92
7.1 Two-Way ANOVA P Values for Analyte Concentrations	95

7.2. One Way Location ANOVA Results Comparing Analyte Concentrations by Particle Sizes	98
7.3. One Way ANOVA P Values for PAHs Concentration by Particle Size.....	103
7.4 Summery of Cluster groups for Cribbs Mill Creek Sediments (at similarity levels greater than 75%).....	104
7.5 Summery of Cluster groups for Hunter Creek Sediments (at similarity levels greater than 75%).....	104
7.6 Summery of Cluster groups for Carroll’s Creek Sediments (at similarity levels greater than 75%).....	105
7.7 Two-Way ANOVA Analysis Results for PAH to COD Concentration Ratios	106
A.1 Model Predicted Portioning of Benzo(a)anthracene with 24 Factorial Design Variables	120
A.2 Calculated Effects of Factors and their Interactions on the Associations of Benzo(a)anthracene with Different Media.....	121
A.3. Model Predicted Portioning of Chrysene with 24 Factorial Design Variables.....	123
A.4 Calculated Effects of Factors and their Interactions on the Associations of Chrysene with Different Media.....	123
A.5 Physical Chemical Properties of PAHs (Source: ATSDR, 1995)	127
B.1. NIST Certified Weights and Method Calculated Weights of PAH Analytes in the Standard Sediment	132
B.2 Calculated Concentrations of Analytes in Coarser 710 - 1400 μ m Sediment Composite Sample and in Corresponding Grinded Sample	141
B.3 Calculated Concentrations of Analytes in Coarser 1400 - 2800 μ m Sediment Composite Sample and in Corresponding Grinded Sample	142
C.1 Observed Concentrations of Naphthalene at Cribbs Mill Creek.....	147
C.2 Observed Concentrations of Fluorene at Cribbs Mill Creek.....	147

C.3 Observed Concentrations of Phenanthrene at Cribbs Mill Creek	148
C.4 Observed Concentrations of Anthracene at Cribbs Mill Creek.....	148
C.5 Observed Concentrations of Fluoranthene at Cribbs Mill Creek.....	149
C.6 Observed Concentrations of Pyrene at Cribbs Mill Creek.....	149
C.7 Observed Concentrations of Benzo(a)anthracene at Cribbs Mill Creek	150
C.8 Observed Concentrations of Chrysene at Cribbs Mill Creek.....	150
C.9 Observed Concentrations of Benzo(b)flourantrene at Cribbs Mill Creek.....	151
C.10 Observed Concentrations of Benzo(a)pyrene at Cribbs Mill Creek	151
C.11 Observed Concentrations of Indeno(1,2,3-cd)pyrene at Cribbs Mill Creek	152
C.12 Observed Concentrations of Dibenz(a,h)anthracene at Cribbs Mill Creek.....	152
C.13 Observed Concentrations of Benzo(ghi)perylene at Cribbs Mill Creek	153
C.14 Observed Concentration of Naphthalene at Hunter Creek.....	153
C.15 Observed Concentration of Fluorene at Hunter Creek.....	154
C.16 Observed Concentration of Phenanthrene at Hunter Creek	154
C.17 Observed Concentration of Anthracene at Hunter Creek.....	155
C.18 Observed Concentration of Fluranthene at Hunter Creek	155
C.19 Observed Concentrations of Pyrene at Hunter Creek	156
C.20 Observed Concentrations of Benzo(a)anthracene at Hunter Creek	156
C.21 Observed Concentrations of Chrysene at Hunter Creek	157
C.22 Observed Concentrations of Benzo(b)flourantrene at Hunter Creek.....	157
C.23 Observed Concentrations of Benzo(a)pyrene at Hunter Creek	158

C.24 Observed Concentrations of Indeno(1,2,3-cd)pyrene at Hunter Creek.....	158
C.25 Observed Concentrations of Dibenz(a,h)anthracene at Hunter Creek	159
C.26 Observed Concentrations of Benzo(ghi)perylene at Hunter Creek.....	159
C.27 Observed Concentrations of Naphthalene at Carroll's Creek.....	160
C.28 Observed Concentration of Fluorene at Carroll's Creek.....	160
C.29 Observed Concentration of Phenanthrene at Carroll's Creek	161
C.30 Observed Concentrations of Anthracene at Carroll's Creek	161
C.31 Observed Concentrations of Fluranthene at Carroll's Creek	162
C.32 Observed Concentrations of Pyrene at Carroll's Creek	162
C.33 Observed Concentrations of Benzo(a)anthracene at Carroll's Creek	163
C.34 Observed Concentrations of Chrysene at Carroll's Creek	163
C.35 Observed Concentrations of Benzo(b)fluoranthene at Carroll's Creek	164
C.36 Observed Concentrations of Benzo(a)pyrene at Carroll's Creek.....	164
C.37 Observed Concentrations of Indeno(1,2,3-cd)pyrene at Carroll's Creek.....	165
C.38 Observed Concentrations of Dibenz(a,h)anthracene at Carroll's Creek	165
C.39 Observed Concentrations of Benzo(ghi)perylene at Carroll's Creek.....	166
C.40 Ratios of Concentrations over CODs ($\mu\text{g/gm}$) for Cribbs Mill Creek.....	236
C.41 Ratios of Concentrations over CODs ($\mu\text{g/gm}$) for Hunter Creek	240
C.42 Ratios of Concentrations over CODs ($\mu\text{g/gm}$) for Carroll's Creek	244
C.43 Analyte Concentration and COD Regression Analyses Results for Cribbs Mill Creek Sediments	248

C.44 Analyte Concentration and COD Regression Analysis Results for Hunter Creek
Sediment..... 253

C.45 Analyte Concentration and COD Regression Analysis Results for Carroll's Creek
Sediments..... 258

LIST OF FIGURES

2.1 Type 1 (discrete) settling of spheres in water at 10oC (Reynolds 1982)	16
2.2 Inlet particle size distributions observed at the Monroe Street wet detention pond.....	17
2.3. Tenth percentile particle sizes for stormwater inlet flows (Pitt et al. 1997) .	19
2.4. Fiftieth percentile particle sizes for stormwater inlet flows (Pitt et al. 1997)	19
2.5 Ninetieth percentile particle sizes for stormwater inlet flows (Pitt et al. 1997) .	20
2.6 Particle size distribution by source area, (Source: Morquecho et al. 2005) ...	22
3.1 Aerial photograph of Cribbs Mill Creek, sampling point (Source: Googlemap, www.google.com)	36
3.2 Concrete channel along Cribbs Mill Creek.....	37
3.3 Aerial photograph of Hunter Creek sampling location (Source: Googlemap, www.google.com)	38
3.4 Sampling location at Hunter Creek.....	38
3.5. Layer of grease material at the outfall of an automobile maintenance shop which is entering Hunter Creek adjacent to the sampling location	39
3.6. Carroll’s Creek sampling location aerial view (Source: Googlemap, www.google.com)	40
3.7 Closer view of sampling location along Carroll’s Creek.....	41
3.8 Residential area along Carroll’s Creek with known SSO history.....	41
4.1 Percentage of PAH partitioning with solids versus PAH Log (KOW), Log (KOC)	47
4.2 Comparisons of observed and calculated PAH associations with particulate	

material	51
4.3 Probability plot of effects of partitioning of Anthracene with air	55
4.4 Probability plot of effects of partitioning of Anthracene with water.....	55
4.5 Probability plot of effects of partitioning of Anthracene with air	56
5.1 Tubes conditioning oven (Source: SIS product manual)	60
5.2 Schematic of packed desorption tube (Source: SIS product manual)	61
5.3 Graphics of AutoDesorb™ (Source: SIS application notes)	62
5.4 Desorption time versus peak areas for Pyrene.....	63
5.5 Desorption time versus peak areas for Benz(ghi)perylene.....	64
5.6 Relationship between naphthalene weights in NIST standards and method calculated weights.....	69
6.1 Observed creek sediment particle size distributions.....	77
6.2 Box and whisker plots of particle sizes for Cribbs Mill Creek sediment samples.....	79
6.3 Box and whisker plots of particle sizes for Hunter Creek sediment samples..	79
6.4 Box and whisker plots of particle sizes for Carroll’s Creek sediment samples..	80
6.5 Comparison of weight loss over temperature range of 104 – 550°C (total volatile content)	85
6.6 Comparison of weight loss over temperature range of 240 – 365°C (leaves and grass)	85
6.7 Comparison of weight loss over temperature range of 365 – 470°C (Rubber)	86

6.8 Comparison of weight loss over temperature range of 470 – 550°C (Asphalt)	86
6.9 Observed cumulative COD of creek sediments by particle size	89
6.10 Comparison of COD results from three creeks by sediment particle size category	90
6.11 Weight loss over temperature range of 104 - 550°C versus observed COD for Cribbs Mill Creek	90
6.12 Weight loss over temperature range of 104 - 550°C versus observed COD for Hunter Creek	91
6.13 Weight loss over temperature range of 104 - 550°C versus observed COD for Carroll's Creek	91
7.1 Probability plots of pyrene concentrations (for < 45µm all creeks were different, for 45 - 90µm Hunter Creek was higher than others)	96
7.2 Sample Effort Needed for Paired Testing (Power of 80% and Confidence of 95%) (Burton and Pitt 2002)	101
A.1 Probability plot of effects of partitioning of benzo(a)anthracene with air	121
A.2 Probability plot of effects of partitioning of benzo(a)anthracene with water	122
A.3 Probability plot of effects of partitioning of benzo(a)anthracene with suspended solids	122
A.4 Probability plot of effects of partitioning of chrysene with air	124
A.5 Probability plot of effects of partitioning of chrysene with water	124
A.6 Probability plot of effects of partitioning of chrysene with suspended solids	125
A.7 Structures of selected PAHs	126

B.1 Chromatogram of NIST standard with dominant peaks of sulfur compounds	129
B.2 Chromatogram of NIST standard with ice plugging problem.....	130
B.3 Chromatogram of freeze dried NIST standard with copper.....	131
B.4 Relation between fluorene weights in NIST standards and method calculated weights	133
B.5 Relation between phenanthrene weights in NIST standards and method calculated weights.....	133
B.6 Relation between anthracene weights in NIST standards and method calculated weights.....	134
B.7 Relation between fluranthene weights in NIST standards and method calculated weights.....	134
B.8 Relation between pyrene weights in NIST standards and method calculated weights	135
B.9 Relation between benzo(a)anthracene weights in NIST standards and method calculated weights.....	135
B.10 Relation between chrysene weights in NIST standards and method calculated weights.....	136
B.11 Relation between benzo(b)flouranthene weights in NIST standards and method calculated weights.....	136
B.12 Relation between benzo(a)pyrene weights in NIST standards and method calculated weights.....	137
B.13 Relation between indeno(1,2,3-cd)pyrene weights in NIST standards and method calculated weights.....	137
B.14 Relation between dibenz(a,h)anthracene weights in standards and method calculated weights.....	138

B.15 Relation between benzo(ghi)perylene weights in NIST standards and method calculated weights.....	138
B.16 Residual Plots of method response for naphthalene, fluorene, phenanthrene, anthracene, fluranthene, pyrene in NIST sediment standard	139
B.17 Residual Plots of method response for benzo(a)anthracene, chrysene, benzo(a)pyrene, beno(b)flouranthene, indeno(1,2,3-cd)pyrene, dibenz(a,h)anthracene, benzo(ghi)perylene in NIST sediment standard ...	140
B.18 Normal probability plots for concentrations of naphthalene, fluorene, phenanthrene, anthracene, fluoranthene, pyrene in 710 - 14000 μ m size composite sample.....	143
B.19 Normal probability plots for for benzo(a)anthracene, chrysene, benzo(a)pyrene, beno(b)flouranthene, indeno(1,2,3-cd)pyrene, dibenz(a,h)anthracene, benzo(ghi)perylene in 710 - 1400 μ m size composite sample	144
B.20 Normal probability plots for concentrations of naphthalene, fluorene, phenanthrene, anthracene, fluoranthene, pyrene in 1400 - 2800 μ m size composite sample.....	145
B.21 Normal probability plots for for benzo(a)anthracene, chrysene, benzo(a)pyrene, Beno(b)flouranthene, Indeno(1,2,3-cd)pyrene, dibenz(a,h)anthracene, benzo(ghi)perylene in 1400 - 2800 μ m size composite sample	146
C.1 Probability plots for naphthalene concentrations	167
C.2 Probability plots for fluorene concentrations	168
C.3 Probability plots for phenanthrene concentrations.....	169
C.4 Probability plots for anthracene concentrations	170
C.5 Probability plots for fluranthene concentrations	171
C.6 Probability plots for pyrene concentrations	172
C.7 Probability plots for benzo(a)anthracene concentrations	173

C.8 Probability plots for chrysene concentrations	174
C.9 Probability plots for benzo(b)fluoranthrene concentrations.....	175
C.10 Probability plots for benzo(a)pyrene concentrations	176
C.11 Probability plots for indeno(1,2,3-cd)pyrene oncentrations.....	177
C.12 Probability plots for dibenz(a,h)anthracene concentrations.....	178
C.13 Probability plots for benzo(ghi)perylene concentrations	179
C.14 Box Whisker plots for concentrations of naphthalene by particle size	180
C.15 Box Whisker plots for concentrations of fluorene by particle size	181
C.16 Box Whisker plots for concentrations of phenanthrene by particle size....	182
C.17 Box Whisker plots for concentrations of anthracene by particle size	183
C.18 Box Whisker plots for concentrations of fluoranthene by particle size	184
C.19 Box Whisker plots for concentrations of pyrene by particle size	185
C.20 Box Whisker plots for concentrations of benzo(a)anthracene by particle size	186
C.21 Box Whisker plots for concentrations of chrysene by particle size	187
C.22 Box Whisker plots for concentrations of benzo(b)flouranthene particle size	188
C.23 Box Whisker plots for concentrations of benzo(a)pyrene particle size	189
C.24 Box Whisker plots for concentrations of indeno(1,2,3-cd)pyrene by particle size	190
C.25 Box Whisker plots for concentrations of dibenz(a,h)anthracene by particle size	191

C.26 Box Whisker plots for concentrations of benzo(ghi)perylene by particle size	192
C.27 Box Box Whisker lot for naphthalene concentration with particle size range < 45µm	193
C.28 Box Whisker lot for naphthalene concentration with particle size range 45 – 90µm	193
C.29 Box Box Whisker lot for naphthalene concentration with particle size range 90 – 180µm	193
C.30 Box Whisker lot for naphthalene concentration with particle size range 180 – 355µm	194
C.31 Box Whisker lot for naphthalene concentration with particle size range 355 – 710µm	194
C.32 Box Box Whisker lot for naphthalene concentration with particle size range 710 – 1400µm	194
C.33 Box Whisker lot for naphthalene concentration with particle size range 1400 – 2800µm	195
C.34 Box Whisker lot for naphthalene concentration with particle size range > 2800µm	195
C.35 Box Whisker lot for naphthalene concentration with LOM.....	195
C.36 Box Box Whisker Plot for fluorene concentration on particle size range < 45µm	196
C.37 Box Whisker Plot for fluorene concentration on particle size range 45 – 90µm	196
C.38 Box Whisker Plot for fluorene concentration on particle size range 90 – 180µm	196
C.39 Box Box Whisker Plot for fluorene concentration on particle size range 180 - 355µm	197

C.40 Box Whisker Plot for fluorene concentration on particle size range 355 – 710 μm	197
C.41 Box Box Whisker Plot for fluorene concentration on particle size range 710 - 1400 μm	197
C.42 Box Whisker Plot for fluorene concentration on particle size range 1400 – 2800 μm	198
C.43 Box Whisker Plot for fluorene concentration on particle size range > 2800 μm	198
C.44 Box Whisker Plot for fluorene concentration on LOM.....	198
C.45 Box Whisker Plot for Phenanthrene Concentration on Particle Size Range < 45 μm	199
C.46 Box Whisker plot for phenanthrene concentration on particle size range 45 – 90 μm	199
C.47 Box Whisker plot for phenanthrene concentration on particle size range 90 – 180 μm	199
C.48 Box Whisker plot for phenanthrene concentration on particle size range 180 - 355 μm	200
C.49 Box Box Whisker plot for phenanthrene concentration on particle size range 355 - 710 μm	200
C.50 Box Whisker plot for phenanthrene concentration on particle size range 710 - 1400 μm	200
C.51 Box Whisker plot for phenanthrene concentration on particle size range 1400 - 2800 μm	201
C.52 Box Box Whisker plot for phenanthrene concentration on particle size range > 2800 μm (w/o LOM)	201
C.53 Box Whisker plot for phenanthrene concentration on LOM.....	201

C.54 Box Whisker plot for anthracene concentration on particle size range < 45 μm	202
C.55 Box Whisker plot for anthracene concentration on particle size range 45 – 90 μm	202
C.56 Box Whisker plot for anthracene concentration on particle size range 90 – 180 μm	202
C.57 Whisker plot for anthracene concentration on particle size range 180 – 355 μm	203
C.58 Whisker plot for anthracene concentration on particle size range 355 – 710 μm	203
C.59 Whisker plot for anthracene concentration on particle size range 710 – 1400 μm	203
C.60 Whisker plot for anthracene concentration on particle size range 1400 – 2800 μm	204
C.61 Whisker plot for anthracene concentration on particle size range > 2800 μm (w/o LOM)	204
C.62 Box Whisker plot for anthracene concentration with LOM.....	204
C.63 Box Whisker plot for fluoranthene Concentration on particle size range < 45 μm	205
C.64 Box Whisker plot for fluoranthene Concentration on particle size range 45 – 90 μm	205
C.65 Whisker plot for fluoranthene Concentration on particle size range 90 – 180 μm	205
C.66 Whisker plot for fluoranthene Concentration on particle size range 180 – 355 μm	206
C.67 Whisker plot for fluoranthene Concentration on particle size range 355 – 710 μm	206

C.68 Box Whisker plot for fluoranthene Concentration on particle size range 710 - 1400 μm	206
C.69 Whisker plot for fluoranthene Concentration on particle size range 1400 – 2800 μm	207
C.70 Box Whisker plot for fluoranthene Concentration on particle size range > 2800 μm (w/o LOM)	207
C.71 Box Whisker plot for fluoranthene concentration with LOM.....	207
C.72 Box Whisker plot for pyrene concentration with particle size range < 45 μm	208
C.73 Whisker plot for pyrene concentration with particle size range 45 - 90 μm	208
C.74 Whisker plot for pyrene concentration with particle size range 90 - 180 μm	208
C.75 Box Whisker plot for pyrene concentration with particle size range 180 – 355 μm	209
C.76 Box Box Whisker plot for pyrene concentration with particle size range 355 - 710 μm	209
C.77 Box Whisker plot for pyrene concentration with particle size range 710 – 1400 μm	209
C.78 Box Whisker plot for pyrene concentration with particle size range 1400 – 2800 μm	210
C.79 Box Whisker plot for pyrene concentration with particle size range > 2800 μm	210
C.80 Box Whisker plot for pyrene concentration with LOM	211
C.81 Box Whisker plot for benzo(a)anthracene concentration with particle size range < 45 μm	211

C.82 Box Whisker plot for benzo(a)anthracene concentration with particle size range 45 - 90 μm	211
C.83 Box Whisker plot for benzo(a)anthracene concentration with particle size range 90 - 180 μm	212
C.84 Box Whisker plot for benzo(a)anthracene concentration with particle size range 180 - 355 μm	212
C.85 Box Whisker plot for benzo(a)anthracene concentration with particle size range 355 - 710 μm	212
C.86 Box Box Whisker plot for benzo(a)anthracene concentration with particle size range e 710 - 1400 μm	213
C.87 Box Box Whisker plot for benzo(a)anthracene concentration with particle size range 1400 - 2800 μm	213
C.88 Box Whisker plot for benzo(a)anthracene concentration with particle size range > 2800 μm (w/o LOM)	213
C.89 Box Whisker plot for benzo(a)anthracene concentration with LOM.....	214
C.90 Box Whisker plot for chrysene concentration with particle size range < 45 μm	214
C.91 Box Whisker plot for chrysene concentration with particle size range 45 – 90 μm	214
C.92 Box Whisker plot for chrysene concentration with particle size range 90 – 180 μm	215
C.93 Box Whisker plot for chrysene concentration with particle size range 180 – 355 μm	215
C.94 Box Whisker plot for chrysene concentration with particle size range 355 – 710 μm	215
C.95 Box Whisker plot for chrysene concentration with particle size range 710 – 1400 μm	216

C.96 Box Whisker plot for chrysene concentration with particle size range 1400 – 2800µm	216
C.97 Box Whisker plot for chrysene concentration with particle size range > 2800µm (w/o LOM)	216
C.98 Box Whisker plot for Chrysene concentration with LOM.....	217
C.99 Box Whisker plot for Benzo(b)fluoranthrene concentration with particle size range < 45µm	217
C.100 Box Whisker plot for Benzo(b)fluoranthrene concentration with particle size range 45 - 90µm.....	217
C.101 Box Whisker plot for Benzo(b)fluoranthrene concentration with particle size range 90 - 180µm.....	218
C.102 Box Whisker plot for Benzo(b)fluoranthrene concentration with particle size range 180 - 355µm.....	218
C.103 Box Whisker plot for Benzo(b)fluoranthrene concentration with particle size range 355 - 710µm.....	218
C.104 Box Whisker plot for Benzo(b)fluoranthrene concentration with particle size range 710 - 1400µm.....	219
C.105 Box Whisker plot for Benzo(b)fluoranthrene concentration with particle size range 1400 - 2800µm.....	219
C.106 Box Whisker plot for Benzo(b)fluoranthrene concentration with particle size range < 2800µm (w/o LOM)	219
C.107 Box Whisker plot for benzo(b)fluoranthrene concentration with LOM ..	220
C.108 Box Whisker plot for benzo(a)pyrene concentration on particle size range < 45µm	220
C.109 Whisker plot for benzo(a)pyrene concentration with particle size range 45 – 90µm	220

C.110 Whisker plot for benzo(a)pyrene concentration with particle size range 90 – 180µm	221
C.111 Whisker plot for benzo(a)pyrene concentration with particle size range 180 - 355µm.....	221
C.112 Whisker plot for benzo(a)pyrene concentration with particle size range 355 - 710µm.....	221
C.113 Whisker plot for benzo(a)pyrene concentration with particle size range 710 - 1400µm.....	222
C.114 Whisker plot for benzo(a)pyrene concentration with particle size range 1400 - 2800µm.....	222
C.115 Whisker plot for benzo(a)pyrene concentration with particle size range > 2800µm (w/o LOM)	222
C.116 Box Whisker plot for benzo(a)pyrene concentration with LOM	223
C.117 Box Whisker plot for indeno(1,2,3-cd)pyrene concentration with particle size range < 45µm.....	223
C.118 Box Whisker plot for indeno(1,2,3-cd)pyrene concentration with particle size range 45 - 90µm.....	223
C.119 Box Whisker plot for indeno(1,2,3-cd)pyrene concentration with particle size range 90 - 180µm.....	224
C.120 Box Whisker plot for indeno(1,2,3-cd)pyrene concentration with particle size range 180 - 355µm.....	224
C.121 Box Whisker plot for indeno(1,2,3-cd)pyrene concentration with particle size range 355 - 710µm.....	224
C.122 Box Whisker plot for indeno(1,2,3-cd)pyrene concentration with particle size range 710 - 1400µm.....	225
C.123 Box Whisker plot for indeno(1,2,3-cd)pyrene concentration with particle size range 1400 - 2800µm.....	225

C.124 Box Whisker plot for indeno(1,2,3-cd)pyrene concentration with particle size range > 2800 μ m (w/o LOM)	225
C.125 Box Whisker plot for indeno(1,2,3-cd)pyrene concentration with LOM	226
C.126 Box Whisker plot for dibenz(a,h)anthracene concentration with particle size range < 45 μ m	226
C.127 Box Whisker plot for dibenz(a,h)anthracene concentration with particle size range 45 - 90 μ m	226
C.128 Box Whisker plot for dibenz(a,h)anthracene concentration with particle size range 90 - 180 μ m	227
C.128 Box Whisker plot for dibenz(a,h)anthracene concentration with particle size range 180 - 355 μ m	227
C.130 Box Whisker plot for dibenz(a,h)anthracene concentration with particle size range 355 - 710 μ m	227
C.131 Box Whisker plot for dibenz(a,h)anthracene concentration with particle size range 710 - 1400 μ m	228
C.132 Box Whisker plot for dibenz(a,h)anthracene concentration with particle size range 1400 - 2800 μ m	228
C.133 Box Whisker plot for dibenz(a,h)anthracene concentration with particle size range > 2800 μ m (w/o LOM)	228
C.134 Box Whisker plot for dibenz(a,h)anthracene concentration with LOM...	229
C.135 Box Whisker plot for Benzo(ghi)perylene concentration with particle size range < 45 μ m	229
C.136 Box Whisker plot for Benzo(ghi)perylene concentration with particle size range 45 - 90 μ m	229
C.137 Box Whisker plot for benzo(ghi)perylene concentration with particle size range 90 - 180 μ m	230

C.138 Box Whisker plot for benzo(ghi)perylene concentration with particle size range 180 - 355um	230
C.139 Box Whisker plot for benzo(ghi)perylene concentration with particle size range 355 - 710um	230
C.140 Box Whisker plot for benzo(ghi)perylene concentration with particle size range 710 - 1400um	231
C.141 Box Whisker plot for benzo(ghi)perylene concentration with particle size range 1400 - 2800um	231
C.142 Box Whisker plot for benzo(ghi)perylene concentration with particle size range > 2800um (w/o LOM)	231
C.143 Box Whisker plot for Benzo(ghi)perylene concentration with LOM	232
C.144 Cluster analyses of PAHs concentration by particle size for Cribbs Mill Creek	233
C.145 Cluster Analyses of PAHs concentration by particle size for Hunter Creek	234
C.146 Cluster analyses of PAHs concentration by particle size for Carroll's Creek	235

ABSTRACT

Polycyclic aromatic hydrocarbons (PAHs) in urban runoff can occur both in soluble and particulate-associated forms. Because of their low volatility (low Henry's Law constant), high octanol-water partition coefficients (K_{OW}) and high soil organic coefficients (K_{OC}), many of the PAHs are preferentially adsorbed to particulate matter. As a part of this research, fugacity based partition calculations were performed to identify the percentage of associations of selected PAHs with different phases in the aquatic environment under equilibrium conditions. The partition prediction calculations showed high associations of PAHs with sediments than in the liquid portion or in the air, especially for high molecular weight PAHs.

PAH analyses in environmental samples are challenging because of the relatively low concentrations and the complexity of the mixtures in the samples. Most of the available standard procedures are time consuming, manual work oriented, and requiring large amounts of organic solvents. As one of the objectives of this research, developed a faster and less labor intensive analysis procedure by using thermal desorption techniques for analyses of selected PAHs in environmental sediment samples.

Understanding the association of contaminants with different particle sizes is important for determining the most effective treatment of runoff. The composition of the sediment (organic matter and other litter, vs. inert soil) may effect the association of PAHs with the sediment. The sediment material composition is likely effected by the

source areas contributing for sediments. One of the goals of this research work was to quantify the material compositions, associated chemical oxygen demand and associated PAH concentrations in size fractionated sediment samples collected from three different creeks. The sediments at these creeks were affected by runoff from different major land use source areas. Overall the PAH concentrations were found to be affected by sediment particle sizes and sampling location. The large organic material component of the sediments were found to have higher concentrations of PAHs compared to other sediment sizes. Contamination by hydrocarbons at one of the sampling sites also affected the observed PAH concentrations, especially for the small particle sizes.

CHAPTER I

INTRODUCTION

Polycyclic aromatic hydrocarbons (PAHs) are an example of persistent organic pollutants of concern (Cheung et al. 2006). As an example, some of the PAHs have been determined to be carcinogenic by several regulatory agencies (US Environmental Protection Agency (EPA), US Department of Health and Human Services (DHHS) and the International Agency for Research on Cancer (IARC)). After the Clean Water Act (1972) was implemented, point source discharges of PAHs from industrial activities were substantially reduced. The remaining non-point sources, such as from stormwater runoff, became a dominant factor in contribution of these hydrocarbons to the environment (US EPA 200b, Van Metre et al. 2000). Because of their low volatility (low Henry's Law constant), high octanol-water partition coefficients (K_{OW}) and high soil organic coefficients (K_{OC}), many are preferentially adsorbed to particulate matter.

PAH analyses in environmental samples are challenging because of the relatively low concentrations and the complexity of the mixtures in the samples. Typically, environmental sample analyses for PAHs involves three major steps: 1) Sample preparation 2) sample cleanup, extraction and concentration, and 3) final detection and quantification. Most of the available standard procedures are time consuming, manual

work oriented, and also are ineffective for detecting PAH compounds associated with suspended solids in water samples. As one of the objectives of this research, I developed a faster and less labor intensive analysis procedure by using thermal desorption techniques for environmental sediment samples.

Understanding the association of contaminants with different particle sizes is important for determining the most effective treatment of runoff. PAHs in urban runoff can occur in soluble and particulate-associated forms; however, studies have identified particulate associated PAHs as the most abundant (Pitt et al. 1999; Barbara et al. 2003; Hwang and Foster 2005). As a part of this research, fugacity based partition calculations were performed to identify the percentage of associations of selected PAHs with different phases in the aquatic environment under equilibrium conditions. The partition prediction calculations showed similar trends of high associations of PAHs with sediments than in the liquid portion or in the air, especially for high molecular weight PAHs.

Variations in organic content of the particulate matter has been reported to affect the particulate PAH associations (Zhou et al. 1998). Recent investigations have also found high PAH concentrations associated with large organic material trapped in stormwater floatable controls (Rushton 2006). The composition of the sediment (organic matter and other litter, vs. inert soil) should effect the association of PAHs with the sediment. The sediment material composition is likely effected by the source areas contributing for sediments. One of the goals of this research work was to quantify the material compositions, associated chemical oxygen demand and associated PAH concentrations in size fractionated sediment samples collected from three different creeks. The sediments at these creeks were affected by runoff from different major land

use source areas. Overall the PAH concentrations were found to be affected by sediment particle sizes and sampling location. The large organic material component of the sediments were found to have higher concentrations of PAHs compared to other sediment sizes. Contamination by hydrocarbons at one of the sampling sites also affected the observed PAH concentrations, especially for the small particle sizes.

CHAPTER II

LITERATURE REVIEW

2.1 Sources of PAHs in the Environment

PAHs are ubiquitous environmental contaminants. Sources of PAHs can be broadly classified as pyrogenic (combustion origin) and petrogenic (petroleum origin). A greater abundance of high molecular weight (HMW) PAHs indicates likely pyrogenic sources, while a greater abundance of low molecular weight (LMW) PAHs implies likely petrogenic origins of the PAHs (Boehm and Farrington 1984). Naphthalene, Fluorene, Anthracene, Phenanthrene are examples of low molecular weight PAHs, while benzo(*k*)fluoranthene, benzo(*a*)pyrene, indeno(*cd*)pyrene and benzo(*ghi*)perylene are examples of high molecular weight PAHs. Tracking the sources of PAHs based on the molecular weight of PAHs alone may not be accurate. Table 2.1 lists frequently detected PAHs in the environment, and their likely primary sources (Pitt et al. 1995). In contrast to what one would expect, high molecular weight PAHs, which are assumed to be pyrogenic in origin, were noted to be from original petroleum sources. Of course, some of these primary petroleum materials have undergone combustion in transportation and industrial operations. Tracking the sources of PAHs based on the presence of LWM or HMW PAHs also becomes questionable as the PAHs are released into the environment and undergo chemical, physical and biological changes (Countway et al. 2003). Physical changes (such as evaporation, or physical transport of by air or water from one location to

other), chemical changes (such as photo transformation of PAHs to daughter products), and biological changes (such as biotransformation of the PAHs), changes their profile in the environment. Differentiating the sources of PAHs based on observed PAH molecular weights may be a useful tool if the samples analyzed for PAHs are assumed not to be affected by any of these modifications.

Table 2.1 Organic Compounds Detected at Different Urban Source Areas (Source: Pitt et al.1999)

Toxicant	Maximum Concentration (µg/L)	Detection Frequency at Urban Source Areas (%)	Likely Primary Source
Benzo(a)anthracene	60	12	Gasoline, Wood Preservative
Benzo(b)fluoranthene	226	17	Gasoline, Motor Oils
Benzo(k)fluoranthene	221	17	Gasoline, Bitumen, Oils
Benzo(a)pyrene	300	17	Asphalt, Gasoline, Oils
Fluoranthene	128	23	Oils, Gasoline, Wood Preservative
Naphthalene	296	13	Coal Tar, Gasoline, Insecticides
Phenanthrene	69	10	Oils, Gasoline, Coal Tar
Pyrene	102	19	Oils, Gasoline, Bitumen, Coal Tar, Wood Preservative

Over time, many changes have occurred affecting industrialization with the affect of increased discharges of pollutants. Prior to the 1800s, the bulk of PAH discharges to the environment were of natural origin, or received limited contributions from anthropogenic sources (Van Metre et al. 2000). Van Metre et al. (2000) reported modest to dramatic increases over time in total PAH concentrations in sediment cores of ten lakes and reservoirs in six U.S. metropolitan areas. This study indicated there was a shift in the sources of PAH contamination from uncombusted to combusted fossil fuels. The increase in PAH sediment concentrations was in coincidence with the increase in automobile use

and power production, both major consumers of fossil fuels. Similarly, Kuklick et al. (1997) examined sediment samples from three South Carolina estuaries, Winyah Bay, Charleston Harbor and the North Edisto River estuary. The concentrations of total PAHs were extremely variable, ranging from $33 \mu\text{g kg}^{-1}$ dry weight in the Edisto River estuary to $9600 \mu\text{g kg}^{-1}$ dry weight in some areas of urbanized Charleston Harbor. These data show the large effect that urbanization has on sediment PAH contamination.

PAHs are considered to be some of the most important organic toxicant pollutants in stormwater runoff. The magnitude of PAH pollution in runoff depends on the type of the contributing source area. Pitt et al. (1999) examined stormwater PAHs from more than 100 samples collected from different sources area sheetflows, and some receiving waters, in and around Birmingham, AL. The source areas represented by the samples included roofs, parking areas, storage areas, streets, loading docks, and vehicle service areas, plus nearby urban creeks, in residential, commercial, industrial and mixed land use areas. The concentrations of the different PAHs detected varied considerably among the different source areas. Vehicle servicing areas and parking areas were found to have the highest concentrations of PAHs in the runoff, and higher concentrations were associated with longer interevent periods between rains. McCready et al. (2000) also examined PAH contamination of stormwater runoff and resultant contamination of aquatic systems. They examined surface sediment samples from 124 sites in Sydney Harbor, Australia, for 16 of the EPA identified priority PAHs. They also found that the PAH concentrations varied widely, from < 100 to $380,000 \mu\text{g kg}^{-1}$ total PAHs, depending on the sampling location. The spatial distribution of PAHs indicated increased concentrations of PAHs nearer to

areas where stormwater enters the harbor, indicating that urban runoff is a major source of PAHs into Sydney Harbor.

Dry deposition of prior industrial and automobile emissions of PAHs is likely a major source of PAHs to urban waters. However, it is important to factor the yield of these materials to the actual runoff and receiving waters when conducting mass balances. As an example, Pitt (1987) found that only about half of the smallest particulates (<50 μm) on impervious surfaces actually are removed during most rains. If these surfaces are directly connected to the drainage system, these particulates would be effectively transported to the receiving waters. Impervious surfaces that drain to landscaped areas have less of their washed-off particulates actually enter receiving waters, and dry deposition to pervious areas would have very little of their contributions enter receiving waters. Dry deposition falling directly onto water surfaces would obviously have 100% yields to the receiving waters. Therefore, dry deposition of PAHs to receiving waters is more obvious in urban areas than in non-urban areas due to the greater land surface coverage of impervious surfaces in urban areas.

When PAHs are discharged to the atmosphere they will partition between particulate and gaseous phases. The PAH contributions to wet and dry deposition are a function of their vapor exchange across the air-water interface. Wet and dry deposition have been reported as the major transport processes for atmospheric PAHs to the aquatic environment (Terzi et al. 2005). The density and magnitude of PAH emission sources in an area affects the amount of dry deposition. For example, emissions from vehicular exhaust and from industries in urban areas will increase the deposition rate of PAHs. Webber (1983) investigated dry deposition of PAHs in urban and non-urban locations of

southeastern Virginia over a 16 month period from November 1980 to February 1982. They found that the mean PAH deposition rate was $27 \mu\text{g m}^{-2}\text{yr}^{-1}$, and was higher in urban locations compared to non-urban locations.

Seasons may also have an effect on the deposition rates of PAHs. Seasonal differences in environmental conditions such as rain characteristics, temperature, and wind speed, plus possible changes in source area contributions, likely affect the deposition characteristics of PAHs in any area. Ollivon et al. (2001) found from their study in Paris, France that the bulk deposition rate (wet plus dry deposition) for six selected PAHs during the summer was $69 \mu\text{gm}^{-2}\text{yr}^{-1}$, the winter deposition rate was higher, at $165 \mu\text{gm}^{-2}\text{yr}^{-1}$. The observed higher deposition rates in the winter could have been caused by increases in source PAH emissions to the atmosphere in the form of domestic heating.

PAHs in urban runoff can occur in both particulate and soluble forms, although studies have identified the particulate forms as being the most predominate (Pitt et al. 1999). According to the Hwang and Foster (2005) study on urban stormwater runoff in Washington DC, particulate-associated PAHs account for 68-97% of total PAHs in the runoff. The particulate-bound PAHs tend to settle and accumulate in receiving water sediments.

2.2 Fates of PAHs in the environment

PAHs present in surface waters can volatilize photolyze, oxidize, biotransform, bind to suspended particles or sediment, or accumulate in aquatic organisms. In sediments, PAHs can biodegrade or accumulate in aquatic organisms (ATSDR).

Photodegradation of PAHs involves the transformation of PAHs to different intermediate products which are finally transformed to end products of carbon dioxide and water. Environmental conditions such as humic acid, concentrations of oxygen, etc., play an important role in the rate of photo transformations of PAHs in the environment. Analyses of the direct photolysis of pyrene by Parmer et al. (1993) (using GS/MS) showed that pyrene yields six compounds or groups of isomers. He also found that direct photolysis products of benzo(a)pyrene included five groups of compounds or isomers. The study identified these photolysis products tentatively as oxygen-addition products, hydroxyl-addition products, phthalate esters, and three or four carbon degradation products. The study also identified that among the four parameters considered (potential sensitizers, humic material, pH, and suspended sediment), the amount of humic material was the most important parameter affecting the rate of photodegradation of pyrene. Similarly, Clark et al. (2006) found that photodegradation of pyrene in aqueous solutions increases as the ionic strength of the solution increases, and decreases with increases in concentrations of humic acid, or decreases in oxygen concentrations.

Similar to photo transformation, biotransformation of PAHs also involves the formation of intermediate bio-transformed products which will then further undergo biotransformation to form final carbon dioxide and water products. According to Atlas et al. (2005), bacterial metabolism of naphthalene represents the typical biotransformation mechanism of this PAH in the environment. The aerobic bacterial metabolism of naphthalene involves the oxidative action of the naphthalene dioxygenase enzyme, which forms intermediate naphthalene dihydrodiols. The dihydrodiols are then dehydrogenated

with the help of dehydrogenase enzymes to form salicylic acid, which is finally metabolized via catechols resulting in final carbon dioxide and water.

The overall biotransformation rate of hydrocarbons in solids is strictly limited by a variety of parameters (Rockne et al. 2002). The biotransformation, and hence the persistence of environmental contaminants, is mostly influenced by the physical/chemical properties of the contaminant, the presence of a viable microbial population to transform the contaminants, the environmental conditions such as temperature, and pH suitable for microbial biotransformation activities (Alexander 1999). The aqueous solubility of PAHs decreases as the number of rings in the molecules increase, which influences the biodegradability of the compound. Sherrill and Saylor (1980) found that PAH degradation was directly related to temperature. PAH degrading bacteria have been documented to be temperature sensitive; a *Mycobacterium* sp. that was shown to mineralize a series of PAHs, including pyrene, grew well at temperatures between 24 and 30°C (Heitkamp et al. 1988). The rate of mineralization and hence the biotransformation of anthracene and naphthalene will be controlled by oxygen content (Bauer and Capone 1985). Similarly, pH and redox potential may effect the biotransformation of PAHs, with the highest degradation rates of benzo(a)pyrene found to occur at pH 8.0, and at all pH values, benzo(a)pyrene and naphthalene biotransformation increased with increasing redox potential (Hambrick et al. 1980).

2.2.1 PAHs associations with particulate matter

When PAHs are released into the environment, they will partition into different phases (air, water, solids) which affect their treatability and how they should be analyzed.

Sorption plays an important role in the fate of these organic contaminants. Due to their extremely low solubility and their hydrophobic nature, most PAHs are predominantly associated with particulate matter. Partitioning of PAHs between different phases in the environment also depends on the physical and chemical properties of the phases.

The solid-water sorption coefficient (K_d) of a contaminant indicates its quantity distribution between the aqueous and solid phases of the system at equilibrium. According to Boethling et al. (2000), the organic carbon normalized sorption coefficient (K_{oc}) approach is the most appropriate procedure for estimating the sorption coefficients, where:

$$K_{oc} = \frac{K_d}{oc} \quad (\text{eq. 2.1})$$

The K_d is the solid-water sorption coefficient and OC is the organic fraction of the solid. There are many regression models available to estimate the $\text{Log } K_{oc}$ of PAHs from $\text{Log } K_{ow}$, where K_{ow} is the octonal water partition coefficient, for example:

$$\text{Log } K_{oc} = 0.904 \log K_{ow} - 0.006 \quad (\text{Chiou et al. 1983}) \quad (\text{eq. 2.2})$$

$$\text{Log } K_{oc} = 1.000 \log K_{ow} - 0.210 \quad (\text{Karichhoff et al. 1979}) \quad (\text{eq. 2.3})$$

Regression equations relating the $\text{Log } K_{oc}$ and $\text{Log } S$ are also available in the literature, where S is the solubility of PAH in water, for example:

$$\text{Log } K_{oc} = \log S + 0.44 \quad (\text{Karichhoff et al. 1979}) \quad (\text{eq. 2.4})$$

In general, the relationship between the dissolved and sorbed chemical concentrations of PAHs is non-linear in nature which can be represented by the Freundlich isotherm:

$$C_{\text{sord}} = K_f \cdot (C_w)^n ; \quad (\text{eq. 2.5})$$

The C_{sorb} is the concentration of the sorbed chemical, K_f is the Freundlich constant, C_w is the concentration of the dissolved chemical, and n reflects the nonlinearity, with n equal to one representing a linear partition relationship.

Under equilibrium conditions, the partition coefficients discussed above may be effective in predicting the PAH partition concentrations in the liquid and solid phases, but these predictions may not be accurate for real time systems which are not usually at equilibrium. Differences between predicted sorption coefficients and actual measured observations were seen by Hwang et al. (2006) in their study of PAHs in stormwater samples along the lower Anacostia River in Washington, D.C. Though the report did not provide the details about how different the predicted and observed values were, they reported that the concentrations of particulate-bound PAHs were higher than the predicted concentrations, as one could expect based on analyses of the solid-water partition coefficient (K_d).

High K_{oc} (or high K_{ow}) values of a pollutant indicate its higher affinity to adsorb to solids in the environment. PAHs are hydrophobic in nature, with their relatively high K_{oc} and K_{ow} constants (values are shown in Table A.5). Due to their hydrophobic nature, in the aquatic environment, PAHs tend to accumulate more on particulate matter than in the liquid partition, and this is most obvious for high molecular weight PAHs. Many researchers have examined the partitioning behavior of PAHs in the aquatic environment. As shown on Table 2.2, Pitt et al. (1998 and 1999) has examined stormwater samples in different locations in the United States and found that PAHs are more predominant in the particulate form than in the dissolved form.

Table 2.2 Concentrations and partitioning of selected PAHs in urban stormwater samples (Pitt et al. 1999)

Contaminant	Amount of Contaminant (μg)			% Association	
	Non-filtered water	Filtered water (In water Phase)*	Associated with particulate solids (by difference)	Water	Particulate Solids
Fluoranthene	28	7	21	25	75
Pyrene	31	2	29	8	92
Benzo(a)anthracene	32	<0.5	>31.5	<1.5	>98.5
Benzo(b)fluoranthene	61	<0.5	>60.5	<0.8	>99.2
Benzo(k)fluoranthene	47	<0.5	>46.5	<1.1	>98.9
Benzo(a)pyrene	70	<0.5	>69.5	<0.7	>99.3
Benzo(g,h,i) perylene	20	<0.5	>19.5	<2.5	>97.5

* The detection limits for the PAHs was about 0.5 $\mu\text{g}/\text{L}$

Factors that affect the PAH associations with the particulate matter in the aquatic environment include the physical and chemical properties of the specific PAH contaminant, the physical and chemical properties of the aquatic medium, and the physical and chemical properties of the particulate matter. For the purpose of understanding such affects Zhou et al. (1998) studied the relationships between the concentrations of fluoranthene and pyrene on suspended solids with salinity, suspended solids concentration and particulate organic carbon, in the Humber estuary, UK. The concentrations of selected PAHs on suspended solids showed no correlation with the salinity of the samples, while concentrations of suspended solids and particulate organic carbon showed a clear relationship with concentrations of PAHs on the suspended solids. Concentrations of suspended solids in the samples showed negative correlations with the concentrations of selected PAHs on suspended solids, whereas particulate organic content showed positive correlations with the concentrations of particulate-associated PAHs. This

study also showed that higher concentrations of PAHs are likely associated with the finer particles (generally classified as clay material which have large surface areas per unit weight), compared to the coarser particles (generally classified as sand particles which have comparatively less organic matter which are needed for greater sorption of PAHs) .

A similar pattern was observed by Aryal et al. (2005) who monitored suspended solids and PAHs associated with fractionated suspended solids in highway runoff for four rain events (samples were only collected during the initial 3 mm of runoff) at an inlet point of treatment facilities for a highway drainage system in Winterthur, Switzerland. The measured concentrations of PAHs in fine fractions ($<45\mu\text{m}$) were higher than their concentrations in coarse fractions ($>45\mu\text{m}$).

Barbara et al. (2003), of the U.S. Geological Survey, examined PAHs in simulated rainfall water runoff and particulates collected from four parking lot test plots. Results indicated that the coal-tar-sealed parking lots had higher concentrations of PAHs than those from any other examined type of surface. The reported average total PAH concentrations in particulates in the runoff from the parking lots were 3,500,000 $\mu\text{g}/\text{kg}$ from coal-tar-sealed, 620,000 $\mu\text{g}/\text{kg}$ from asphalt-sealed, and 54,000 $\mu\text{g}/\text{kg}$ from unsealed parking lots.

Rushton et al. (2006) studied the association of selected PAHs on gross solids while analyzing the performance of a Continuous Deflection Separation (CDS) retrofit unit installed to control stormwater discharging to the Hillsborough River, south Florida. The gross solids, consisting of litter, leaves, trash and sediment, collected by the CDS unit was found to have a wide range of concentrations for the selected PAHs. They found high concentrations of PAHs on the gross solids that had high organic content.

2.3 Suspended solids in stormwater

Particles in stormwater samples can be fractionated by using sieving/filtration, or centrifugal action. Particle sizes are more commonly measured based on their settling velocities, and using automated instruments such as a Coulter Counter Multi Sizer III which measure particle volume for many size increments. Automated instruments are usually used for measuring the particle sizes due to higher resolution and rapid analytical response times. Most of the particles in stormwater at outfall locations, by mass, are in the range of 1 to 100 μm , corresponding to laminar settling conditions (Burton and Pitt 2002). For discrete particles, the settling velocities and hence the particle sizes, can be predicted by Stokes's and Newton's settling equations. Figure 2.1 shows the relationship between settling velocities, particle sizes, laminar and turbulent flow conditions, and specific gravity.

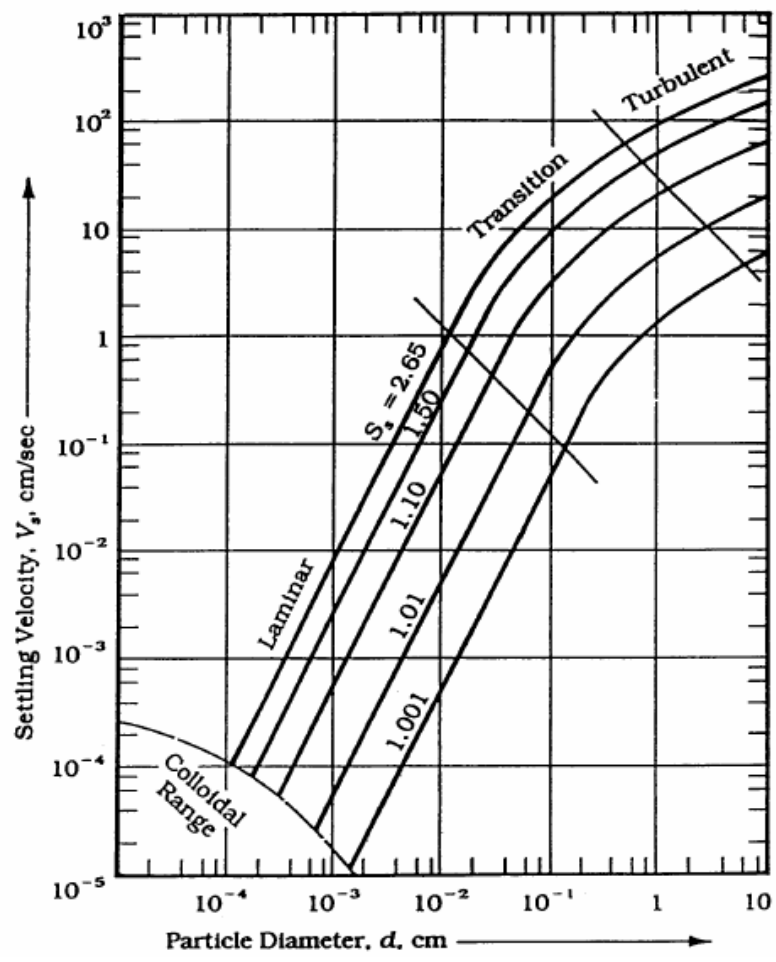


Figure 2.1 Type 1 (discrete) settling of spheres in water at 10° C (Reynolds 1982).

Pitt et al. (1997) obtained stormwater particle size data for many different source area sheetflows in the Birmingham, Alabama, area during their PAH study. The data did not indicate any significant differences in particle size distributions for different source areas and land uses, except that roof runoff had substantially smaller particle sizes compared to the other source areas. Deposition (dry and wet) of particles from the atmosphere is the main source contributing to the roof runoff particles and hence these particles are generally smaller in sizes than the particles observed from other surface stormwater runoff sources.

Sample line velocities in automatic samplers may not be high enough to collect the largest material, plus the line diameter may be smaller than some of the bed load material, and hence most monitored stormwater particle distributions may not include bed load components (Burton and Pitt 2002). House et al. (1993) studied the Monroe St. (Madison, WI) detention pond. The USGS and WI DNR installed special bed load samplers that trapped the bed load material for analysis. Particle size distributions for 16 seasonal samples were analyzed. The bed load material was comprised of the largest material, of sizes 300 or 400 μm , and larger, and comprised about 10 percent of the annual total solids loading, by weight, as shown on Figure 2.2 Although the bed load solids fraction was not a large portion of the total transported solids and pollutants, they represent the largest particle sizes flowing in the stormwater and can be easily trapped in most detention ponds and catchbasins.

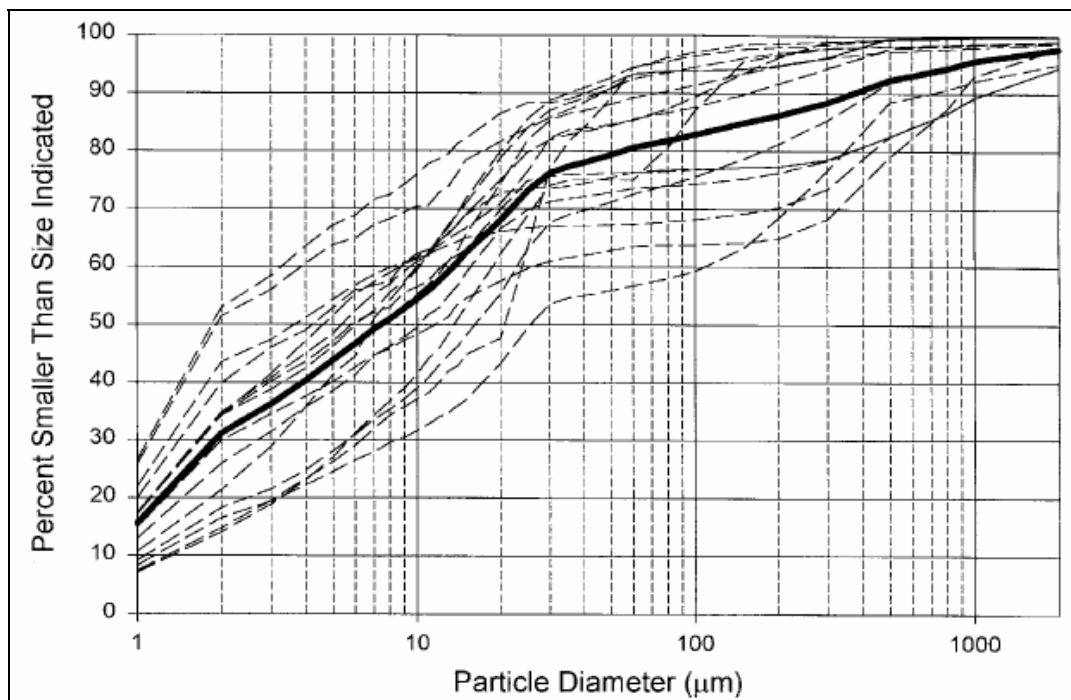


Figure 2.2 Inlet particle size distributions observed at the Monroe Street wet detention pond.

According to Pitt et al. (1997), the particle size distributions of stormwater at different locations in an urban area greatly affect the ability of different source area and storm drain inlet controls in capturing particulate-bound pollutants in stormwater. Pitt et al (1995) conducted particle size analyses on 121 stormwater samples collected from three states, (southern New Jersey, Birmingham, Alabama, and at several cities in Wisconsin) in areas that were not affected by stormwater controls. They measured the particle sizes using a Coulter Counter Multi-Sizer II and verified the results with microscopic, sieve, and settling column tests. Among all the samples they analyzed, the samples from New Jersey had the smallest particle sizes, followed by the samples from Wisconsin, and then Birmingham, Alabama, which had the largest particles. The New Jersey samples were collected from gutter flows in a residential neighborhood that was xeroscaped, and were collected using manual “dipper” samplers of cascading water at drainage system inlets. Wisconsin samples were obtained from several source areas, including parking areas and gutter flows mostly from residential, but from some commercial areas. Birmingham samples were collected from a long-term parking area using automatic samplers. Figures 2.3 through 2.5 show grouped box and whisker plots showing the particle sizes (in μm) corresponding to the 10th, 50th (median) and 90th percentile of the cumulative distributions for the three areas. The median particle sizes ranged from 0.6 to 38 μm , and averaged 14 μm . The 90th percentile sizes (90% of all particles, by mass, were larger) ranged from 0.5 to 11 μm , and averaged 3 μm .

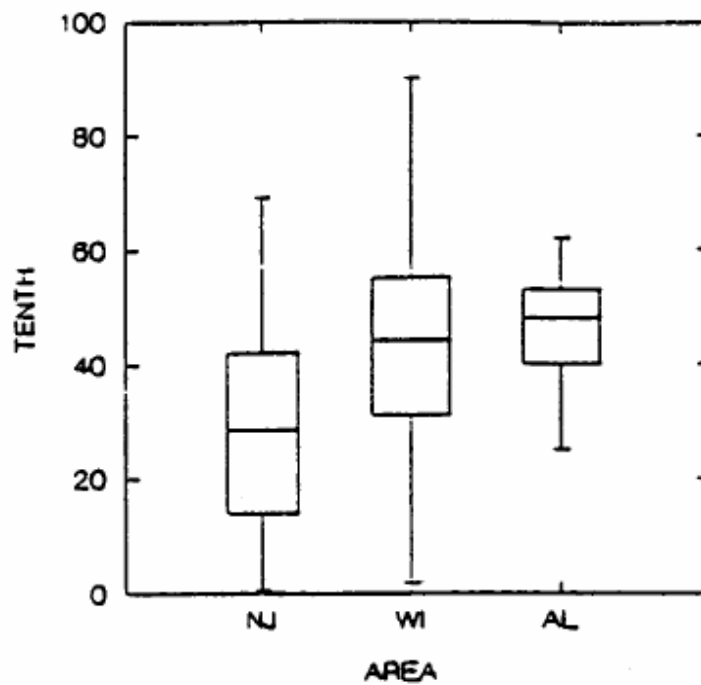


Figure 2.3. Tenth percentile particle sizes for stormwater inlet flows (Pitt et al. 1997)

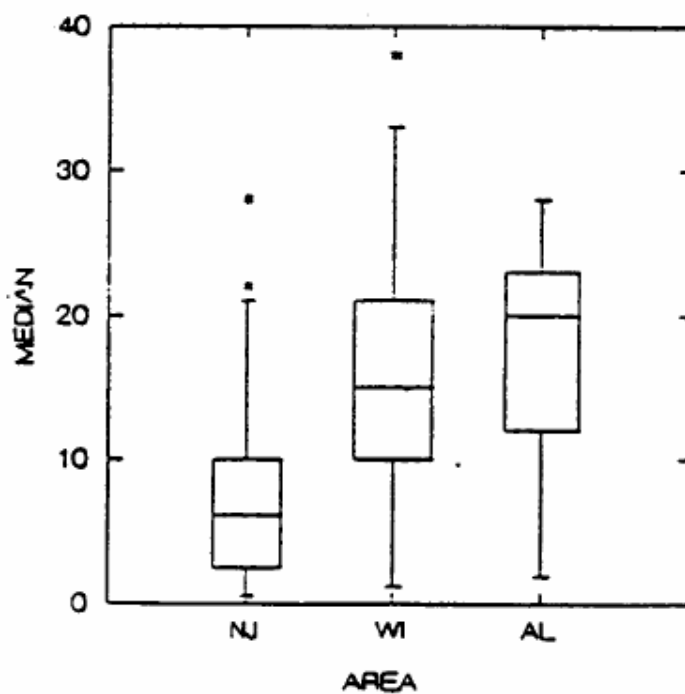


Figure 2.4. Fiftieth percentile particle sizes for stormwater inlet flows (Pitt et al. 1997)

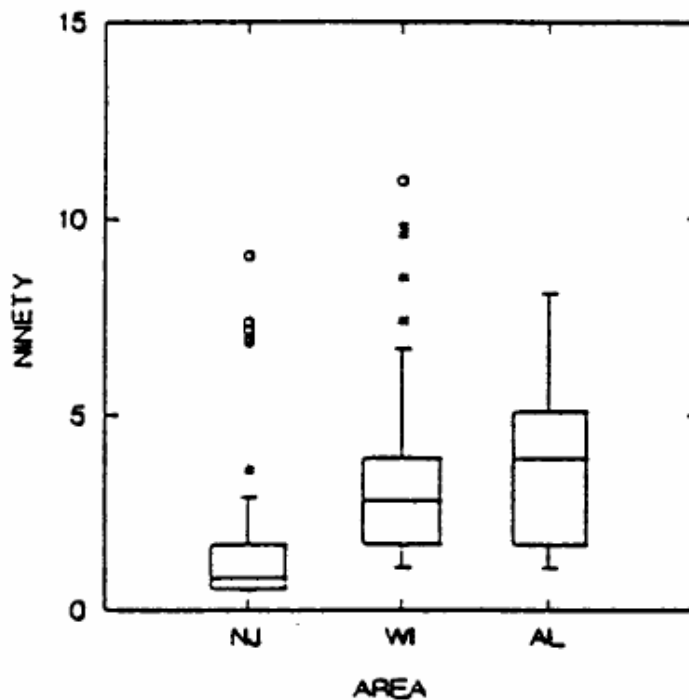


Figure 2.5 Ninetieth percentile particle sizes for stormwater inlet flows (Pitt et al. 1997)

Aryal et al. (2005) monitored suspended solids in highway runoff for four rain events at an inlet point at a treatment facility for a highway drainage system in Winterthur, Switzerland. During the initial 3 mm of flow, they found that coarser SS fractions (106 – 250 μm and $>250 \mu\text{m}$) showed power growth relationships with TSS, whereas for the SS fractions $<20 \mu\text{m}$ and 20 – 40 and 45 – 106 μm , the values are clustered at a lower range of TSS values. There were no further increases in SS concentration found at the higher TSS concentration region indicating that TSS concentrations in runoff with high TSS will only be influenced by coarser particles in the runoff at this location.

An increase in runoff discharges proportionally increases the erosion power, thus increasing the suspended solids it carries into water bodies, which will end up in the bottom sediment of water bodies. Hwang et al. (2006) has observed similar relations

between the discharge rate (ton per min) and total suspended solids (mg/L) in the runoff in the lower Anacostia River area in Washington, D.C. They reported that the TSS in some storm flow samples that had flow rates above about 150 t/min (metric ton per minute) exceeded the benchmark level of 100 mg/L.

Morquecho (2005) analyzed different source area runoff samples for heavy metal concentrations for different particle sizes in and around Tuscaloosa and Birmingham, AL. The particle distributions observed may better indicate the expected particle size that may be observed in the sediment samples analyzed as part of this research. Figure 2.6 shows the observed particle size distribution in the runoff samples collected from storm drain inlets, roofs and mixed source areas of roofs and parking lots. For most of the samples, the TSS particle median sizes were between 20 and 90 μm , and very few samples were found with large fractions of larger sizes. The source area samples did show large amounts of the larger particles (generally, 10 to 20% of the sample particulate masses were associated with particulates larger than 1,500 μm , particles that would not be effectively transported in the stormwater drainage system).

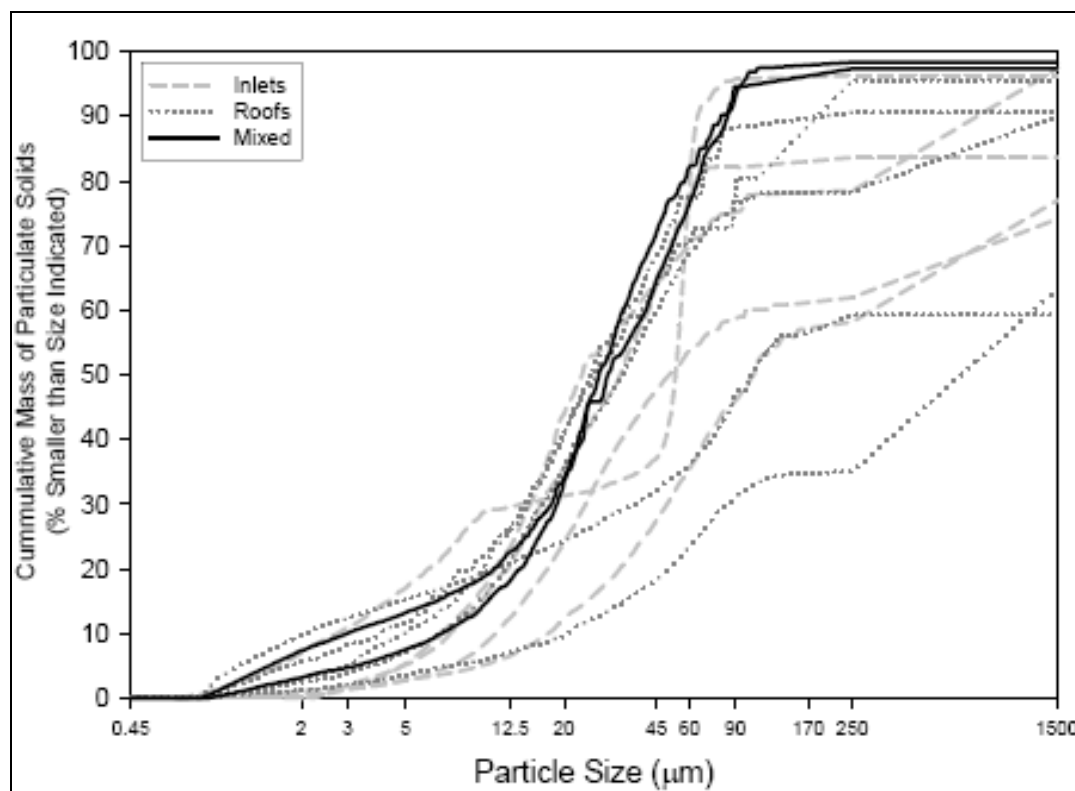


Figure 2.6 Particle size distribution by source area, (Source: Morquecho et al. 2005)

2.4 Analytical methods for measuring PAHs in environmental samples

The general analytical procedure for polycyclic aromatic hydrocarbons (PAHs) and other organic contaminants (such as pesticides) involves sample collection, sample preparation and extraction, and final determination. In most cases, problematic PAH concentrations in water are typically low, emphasizing the extraction and concentration steps in the analytical process. Final detection of these contaminants is usually carried out with gas chromatography with a mass spectrophotometer detector.

Water or solid samples to be analyzed for PAH contamination usually undergo solvent extraction prior to analysis. Liquid-liquid extraction by separatory funnel, continuous extraction, or solid-phase extraction, are the most common extraction

methods for liquid samples. Soxhlet, automated Soxhlet, and ultrasonic extraction methods are the common solvent extraction methods for PAHs from solid samples.

Solid-phase extraction (SPE) is the most common method used for the extraction and concentration of trace organic contaminants in water samples (Synder et al. 2003). EPA method 3535, under SW-846, explains the applicability, operation and limitations of the method. Organics from a known volume of liquid sample are extracted using a solid phase extraction device (a solid-phase sorption substrate on a filter stand) and then the targeted analytes are eluted from the solid-phase media using an appropriate solvent. However, suspended solids present in the sample can cause analytical and technical problems in sample concentration and final detection, including plugging of the SPE cartridges and disks, which will cause the extraction to last for several hours, or even render it impossible, and difficulty in extracting the organics from the particulates, as SPE was developed to extract organics from filtered water samples.

Continuous extraction of liquid samples for PAHs, as described in EPA method 3520, is more efficient (based on recovery) for samples containing particulate concentrations of up to 1% (10,000 mg/L) that can cause emulsions. However, this method requires expensive glassware, uses fairly large volumes of solvents, and requires extraction times of 6 to 24 hours. EPA method 3510C describes the separatory funnel liquid-liquid extraction procedure for organics in aqueous samples. This extraction process concentrates the analytes into a small volume of organic solvent. This procedure includes the serial extraction of aqueous samples with methylene chloride in a separatory funnel. This method may also require cleanup steps after the separation funnel extraction to remove interferences. This procedure is moderately labor intensive and requires careful

attention to ensure acceptable recoveries, and uses moderate quantities of organic solvents.

EPA method 3540 describes the Soxhlet procedure for extraction of PAHs from solid matrices. A known amount of solid sample is mixed with anhydrous sodium sulfate and placed into an extraction thimble, or between two plugs of glass wool, and continuously extracted using an appropriate solvent. The extraction method may provide efficient extraction, but it requires about 16 to 24 hours for single samples and uses large volumes of solvent.

EPA method 3550, described under SW-848, outlines the detailed procedure of using ultrasonic energy for the extraction of semivolatile organic compounds from solid matrices. This method is comparatively efficient, requiring shorter times for extraction, but has less extraction efficiency. Ultrasonic extraction methods also use relatively large volumes of solvent, requires an expensive piece of equipment, and requires large amounts of sample if low concentrations of the analyte is of interest.

Generally, PAHs are most effectively extracted from liquid samples at a neutral pH with methylene chloride. The commonly used solvents for extraction of PAHs from solid matrices are dichloromethane, cyclohexane, benzene, and methanol. Evaporation is usually employed to concentrate the solvents containing the extracted organics. The separation and detection methods are further described in EPA methods 8100 and 8310. These traditional approaches for extraction and evaporation are labor-intensive and time consuming. These methods are also prone to contamination introduced by impurities in the solvents, and also use large quantities of organic solvents in the process that could cause environmental contamination and hazards to the operators.

2.5 Need for research

The literature mentioned above have identified adsorption on particulate matter as the main transport and fate mechanism of PAHs in the environment. Studies have illustrated that increases in urbanization are associated with increases of PAH contamination in the environment. The increase in PAH contamination poses a great threat to the environment due to toxic and carcinogenic effects (USEPA 1997; CA EPA 1990a and 1990b; ATSDR 1995), thus necessitating more effective treatment methods. Understanding the distribution of contaminants is important for effective and economical treatment of PAHs in runoff. While much work has been done in identifying the main fate of PAHs in surface waters, there is little information available concerning PAH contamination for different particle sizes; this information is needed for developing effective treatment technologies and more effective modeling of PAH sources and fate.

Filtration and sedimentation are the unit processes usually used for advanced treatment of stormwater to remove particulate solids and associated contaminants, such as PAHs. Along with the concentration of suspended solids, the size of the suspended solids greatly affects the performance of the control devices used (such as sedimentation ponds). By understanding the association of PAHs with particulate solids size fractions, better designs of control methods will be possible. Efficient quantification methods for PAH contamination of sediment will also help in identifying locations to be targeted for priority cleanup of contaminated sites after natural disasters.

2.6 Dissertation research

The dissertation research specifically addresses the following steps:

- Perform PAHs partition calculations in the environment using equilibrium based fugacity model to understand the fate of PAHs in environment
- Develop and test analytical procedures for PAH analyses by incorporating thermal desorption techniques
- Quantify the concentrations of selected PAHs on size fractionated particulate matter in creek sediments
- Identify the basic organic material composition of size fractionated particulate matter in creek sediments
- Verify the fugacity modeling calculations based on site specific measured conditions

CHAPTER III

EXPERIMENTAL DESIGN

3.1 Hypotheses

The objective of this dissertation research work is to determine the associations of polycyclic aromatic hydrocarbons (PAHs) with size fractionated solids in urban stream sediments. The literature review and preliminary analyses indicated that the association of PAHs with particulate matter in the aquatic environment is their most important form and greatly affects their fate. Therefore, the removal of particulate matter in discharges would also dramatically reduce discharges of the associated PAHs. The design and performance of stormwater treatment devices is highly dependent on the size of the particles to be controlled. Therefore, knowing the specific PAH concentrations associated with different particle size groups will help in the design of more effective stormwater controls and will enable more accurate predictions of the fates of discharged PAHs to urban receiving waters. Knowing the associations of PAHs with different particle sizes will also enable more efficient restoration of waters contaminated by natural disasters, or accidental releases of hydrocarbons. The following hypotheses statements for this dissertation research are based on the literature review and preliminary analyses.

Hypothesis 1: PAHs are strongly associated with particulate matter and variations in key characteristics of the sediment affect these associations.

Prediction 1: PAHs are hydrophobic in nature and have low vapor pressures which make them strongly associated with particulate matter in the aquatic environment. Generally, urban sediments are composed of sand, clay, silt, and organic material. PAHs strongly sorb to the organic matter and hence the concentrations of PAHs in sediments depend on the sediment material composition. Smaller sized particles have larger surface areas compared to large particles and hence, greater amounts of PAHs, per unit particle weight, are associated with the small particles. The small particles may also have larger fractions of organic matter, also causing greater concentrations of PAHs.

Research Activities 1: a) Perform fugacity prediction model analyses to calculate the partitioned concentrations of PAHs in urban aquatic environments under equilibrium conditions. These results were compared with historical values of particulate and filterable PAHs obtained during prior field studies.

b). Quantify PAH concentrations on different particle size classes of creek sediments using TD/GC/MS.

c) Analyze the sediment for chemical oxygen demand (COD) using HACH method 8000 and for different possible combustible materials (paper, leaves/grasses, rubber, and asphalt) using “Thermal Chromatography” where the sediment is subjected to increasing temperatures and measurements are made of the accumulative loss in weight.

Critical Tests 1: a) The fugacity model estimates for the partitioned PAH values for air, water, suspended sediment, sediment and biota were evaluated. The percentage of the partitioned amounts of individual PAHs into air, water and sediment phases were graphically represented and statistically evaluated, reflecting the variability of the observations for different conditions.

b) The analyzed PAH concentrations in the particulate matter were analyzed with the help of cluster and NAOVA analyses. All the analyzed data are clustered into groups based on the concentrations of the PAHs and sample characteristics.

Hypothesis 2: Sediment affected by historical events, such as contamination by sewage overflows or runoff from automobile service areas, will have higher concentrations of PAHs compared to non-affected sediment.

Prediction 2: PAHs are strongly associated with organic matter in sediments. Sewage contamination of the sediment may increase the organic content of the sediment, causing higher concentrations of sediment-bound PAHs.

Research Activities 2: Collected and analyzed sediment samples for PAH contamination from two similar urban creeks, one with no historical sewage contamination, and the other with no past history of sewage contamination. Contamination from commercial stormwater from automobile service areas were examined through sampling at another site with known contamination for comparison to the uncontaminated urban site.

Critical Test 2: Assessed the PAH concentrations in the collected sediment samples from the three creeks. Cluster and ANOVA analyses were used to identify natural groupings of site characteristics that explain the variabilities in measured PAH values. The most important groupings of data, represented by short stalks in the dendograms and with significant factors in the ANOVA analyses, contained the sediment and site characteristics of greatest interest.

3.2 Quantification of Selected PAHs on Size Fractionated Particulate Matter

The research activities reported in this dissertation was conducted in two stages. The first stage of the research was the development and testing of an analytical procedure for PAHs associated with particulates using newly developed thermal desorption techniques. The second stage of the research included the collection and analysis of samples and their evaluations in relation to the research hypotheses. The sediment samples were collected from three different creeks in and around the cities of Tuscaloosa and Northport, Alabama. The sediment samples collected from these three creeks represent sediments affected by stormwater runoff from residential areas only (in a creek that was previously studied and confirmed to have to historical sewage contamination); sediments affected by known sewer overflows (as reported to ADEM), and sediments affected by runoff from commercial areas only. All the sediment samples collected were fractionated based on particle sizes and the analyses were conducted on each size group.

The numbers of samples needed to be collected to provide statistically relevant conclusions are calculated using following equation (Burton and Pitt 2002):

$$n = [\text{COV} (Z_{1-\alpha} + Z_{1-\beta})/\text{error}]^2 \quad (\text{eq. 3.1})$$

Where, n = number of samples required, α = False positive rate ($1 - \alpha$ is degree of confidence), β = False negative rate ($1 - \beta$ is the power), $Z_{1-\alpha}$ = Z score corresponding to $1 - \alpha$, $Z_{1-\beta}$ = Z score corresponding to $1 - \beta$, Error = Allowable error, COV = Coefficient of variation.

The above formula can be used to calculate the number of samples required for PAH analyses to obtain statistically valid results, with a 95% degree of confidence (the corresponding Z score is 1.645), a power of 80% (the corresponding Z score is 0.85),

allowable error of 25%, and with an expected COV of 0.3. With these data quality objectives, a minimum of 9 samples for each particle size would be needed. If the COV is larger (likely), the confidence and power will decrease for this sample size. The overall variability in the PAH concentrations will be reduced by stratified random sampling using the sampling locations as different sample categories. A total of 15 samples will be collected for this research, 5 sediment composites from each of the 3 creeks. Each of these 15 samples will be separated into 9 particle sizes (including separation of the largest size into organic and inert fractions) for individual PAH analyses.

PAH contamination of each particle size range is quantified and represented by exploratory data analyses methods, such as box and whisker plots and probability plots. These plots are supplemented with statistical analyses (such as ANOVA) to identify the presence of significant differences in PAHs contamination based on particles sizes.

3.3 Quantification of the Material Composition of Sediment Samples

The composition of the material present in the sediments was analyzed by using ‘Thermal Chromatography’ (an expansion of the volatile solids analyses) techniques (Ray 1997). Under this research objective, the main focus was to quantify the amount of paper debris, grass and leave material, rubber, and asphalt in the size fractionated sediments. The quantified individual materials present in the sediments and the COD results were tested for possible relation with the help of regression analyses.

3.4 Developing a Thermal Desorption Analytical Technique for Analyses of PAHs

The thermal desorption procedure which was employed as a sample preparation step for the GC/MSD analyses of PAHs in particulates was developed as part of this research. Initially, experiments were conducted by spiking pre-conditioned glass wool with known standard PAH mixtures. To test the repeatability of the analytical procedure, three samples of glass wool were spiked with 200ng of liquid PAHs standard and analyzed using TD/GC/MS. The coefficients of variation in the resulting peaks areas of the analytes were calculated and evaluated. The recovery of the selected PAHs from sediment particles was examined by measuring the recovery of analytes from the NIST standard sediment. These recovery calculations were performed for different sizes of fractionated solid particles being examined to measure any variability of recovery as a function of particle size. Two composite sediment samples in the size ranges of 710 - 1400 μ m and 1400 - 2800 μ m were prepared from all the samples collected at the three creeks. Portions of the composite sediment samples were ground to a size < 180 μ m. The composite sediment samples and the ground composite sediment samples were analyzed separately for PAHs concentration. The resultant PAH concentrations in the samples were compared for consistency.

3.5 Fugacity-based Partition Calculations for an Environmental System under Equilibrium Conditions

Mackay fugacity level 1 (Mackay et al. 1992) calculations to predict the partitioning of PAHs among the environmental phases is only applicable for equilibrium conditions. Prediction fate model calculations for selected PAHs were performed based

on typical environmental conditions and with the assumption of system equilibrium.

Based on this model, the partition percentages of selected PAHs into different phases were calculated. The equations involved in the model calculations are:

$$C = Z * f \quad (\text{or}) \quad f = \frac{M}{\sum(V_i * Z_i)} \quad (\text{eq. 3.2})$$

Where, C = Concentration of contaminant, mol/m³; Z = fugacity capacity constant, mol/m³; f = fugacity, Pa; V_i = Volume of the corresponding phases; and Z_i = fugacity capacities of phases for air, water, sediment, suspended sediment, and fish for i = 1, 2, 3, 4, 5 respectively and are defined as follows.

$$Z_1 = \frac{1}{RT} \quad (\text{eq. 3.3})$$

$$Z_2 = \frac{1}{H} \quad (\text{eq. 3.4})$$

$$Z_3 = Z_2 * P_3 * \phi_3 * \frac{K_{OC}}{1000} \quad (\text{eq. 3.5})$$

$$Z_4 = Z_2 * P_4 * \phi_4 * \frac{K_{OC}}{1000} \quad (\text{eq. 3.6})$$

$$Z_5 = Z_2 * P_5 * L * \frac{K_{OW}}{1000} \quad (\text{eq. 3.7})$$

Where R = gas constant (8.314 J/mol K), T = absolute temperature (K), H= Henry's law constant (Pa.m³/mol), K_{OC} = Organic-water partition coefficient, K_{OW} = Octonal-water partition coefficient, P₃ = density of sediment (kg/m³), P₄ = density of suspended sediment (kg/m³), Ø₃= organic fraction of sediment, Ø₄= organic fraction of suspended sediment, P₅ = density of fish in the aquatic system (kg/m³), L= Lipid content of fish.

Predicted partition values calculated using this model were employed in studying the affect of selected environmental parameters on the associations of PAHs with different media compartments. Factorial analyses techniques are used for studying the affect of the parameters, namely, organic content of sediment particles, temperature of the system, concentration of selected PAH, and concentration of sediment particles in the system.

3.6 Quality Control and Quality Assurance

Quality control and quality assurance techniques were used during all parts of the research, from sample collection to laboratory analyses, including data statistical analyses. All the glassware employed in the analyses work were soap washed and rinsed with ultrapure 18 mega ohm water and were subjected to drying at elevated temperature of about 450°C for 6 hours. Thermal desorption tubes and needles used in the TD/GC/MS process were subjected to thermal conditioning prior to analyses. The thermal desorption tube conditioning procedure is described in Chapter 5 of this report. The GC/MS instrument performance was tested with the help of liquid standards added to glass wool. Only certified reagent grade solvents were used in the analyses process. All the certified analytical standards used for developing standard reference curves were obtained from SUPELCO[®], which were then further diluted to different concentrations in hexane solvent. Recovery of the thermal desorption PAH extraction technique was calculated by analyzing three samples of the NIST sediment. Analytical method detection limits were calculated by measuring the variability of the method response of the NIST standard sediment analyses. NIST sediment samples were freeze dried to remove as much

moisture as possible, as the remaining moisture after the standard drying of the sediment caused cryo fusing which blocked the capillary tubes preventing any analyses. All the creek sediment samples were collected in glass bottles and were dried at 104°C in an oven. To avoid trace contamination, all the samples were placed in aluminum trays for drying. The dried sediment samples were fractionated based on particle sizes using a mechanical shaker. Only stainless steel sieves were used. The processed sediment particles were covered in aluminum foil and stored at 4°C until they were analyzed for PAHs. There was no need for freeze drying of sediment samples, unlike NIST sediment, as their analysis gave clear separation of analytical peaks in resulting chromatograms with good abundance. Every day before the start of sample analysis, the mass spectrometer was auto tuned using the standard tuning file, and after every few sediment sample runs solvent analyses were performed to clear up any potential contaminated depositions in the inlet and as well as in capillary column.

3.7 Sediment Sample Collection and Processing

Sediment samples were collected from three different creeks in and around Tuscaloosa and Northport, AL. The three creeks are Cribbs Mill Creek, Carroll's Creek, and Hunter Creek. One sampling area along each of the three creeks was chosen in such a way that the sediment analysis scheme for PAHs represents the sediments affected by known source area contributions.

Cribbs Mill Creek is an urban creek in Tuscaloosa, Alabama which originates at a small stormwater runoff ditch at the Veterans Affairs Hospital on Veterans Memorial Parkway. Cribbs Mill Creek then joins Cypress Creek at Friday Lake before emptying

into the Black Warrior River. A sampling point along the creek was chosen on a concrete lined channel in a residential neighborhood. Medium density single-family dwellings are located on both sides of this concrete lined creek channel. The chosen sampling point is towards the downstream end of the concrete channel reach which is a few hundred feet long. The sediment (bed load) on the concrete channel is therefore mainly affected by the runoff from the surrounding residential areas, with minimal bank erosion material. This creek was extensively studied by Pitt et al. (2005) as part of an EPA study on inappropriate discharges. No sanitary sewage discharges were ever identified along this creek during this prior three year study.

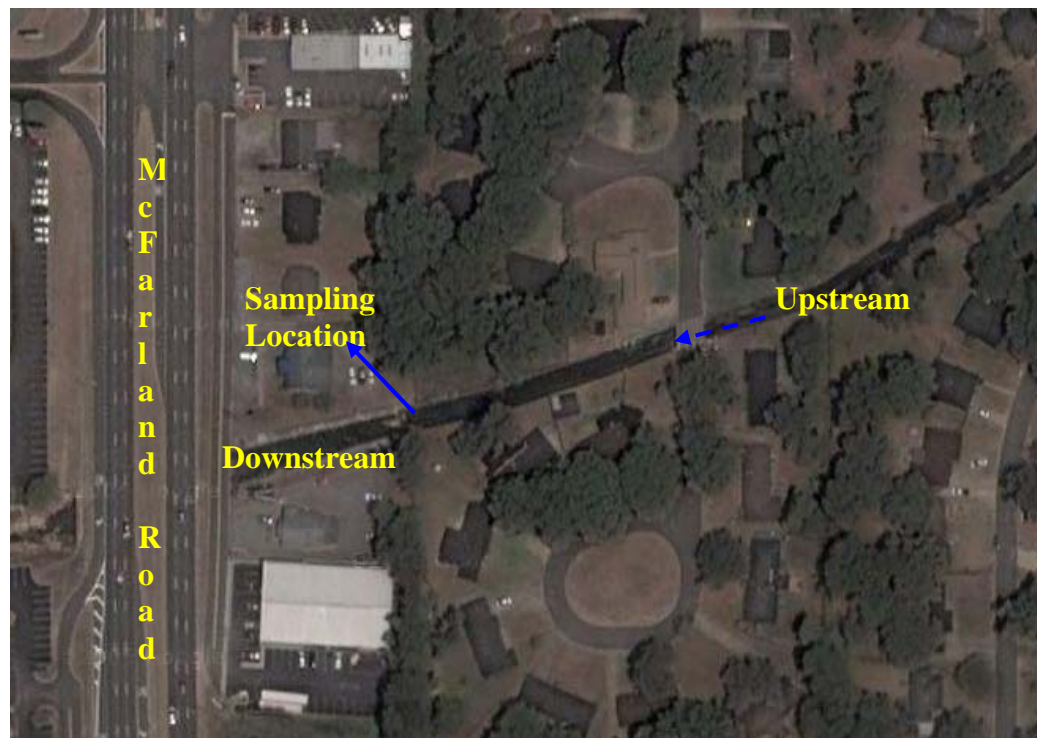


Figure 3.1 Aerial photograph of Cribbs Mill Creek, sampling point (Source: Googlemap, www.google.com)



Figure 3.2 Concrete channel along Cribbs Mill Creek

Hunter Creek is an urban creek whose watershed area is within the cities of Tuscaloosa and Northport. Hunter Creek originates in Tuscaloosa County and passes through the Northport city limits before joining the Black Warrior River. The sediment at the sampling location (where creek crosses Hunter Creek road) is mostly affected by the runoff from heavy traffic along McFarland Blvd., commercial areas, and runoff from temporary trailer residential areas. Physical observations at the site indicate that an outfall from an automobile maintenance shop on the side of the creek was directly affecting the sediment at the sampling location. The PAH analyses results from this sampling location will represent PAH contamination in creek sediments by commercial sources.



Figure 3.3 Aerial photograph of Hunter Creek sampling location (Source: Googlemap, www.google.com)



Figure 3.4 Sampling location at Hunter Creek



Figure 3.5. Layer of grease material at the outfall of an automobile maintenance shop which is entering Hunter Creek adjacent to the sampling location

Carroll's Creek is located in Northport and Tuscaloosa, although most of the watershed is located in Northport. The Carroll's Creek watershed area is also located in two counties, Fayette County and Tuscaloosa County. The creek starts in Fayette County and joins Lake Tuscaloosa in Tuscaloosa County. The sediment at the sampling location chosen along the creek is directly affected by runoff from a high density residential area on one side of the creek and forested lands on the other side of the creek. The residential area near the sampling location has a recent history of sanitary sewer overflows (SSOs). As indicated in Consent Order NO. 07-139-CWP from the Alabama Department of Environmental Management (ADEM) to the City of Northport issued in July 2007, there were three SSO incidents during 2006 at the residential area near the sampling location. In February 2006 sewage overflowed into the creek during an intense lightning storm which caused high intensity rains. A reported 42,000 gallons of sewage overflowed at this location and entered the creek. The second incident was in March 2006, when a

wastewater line ruptured and leaked 2,000 gallons of sewage into the creek. The third recently reported incident was in July 2006 when 30,000 gallons of SSO discharged into the creek due to a sewer pump failure in the neighborhood.



Figure 3.6. Carroll's Creek sampling location aerial view (Source: Googlemap, www.google.com)



Figure 3.7 Closer view of sampling location along Carroll's Creek



Figure 3.8 Residential area along Carroll's Creek with known SSO history

The sampling locations will therefore provide a variety of local conditions for comparison:

- Cribbs Mill Creek: residential areas with no history of sanitary sewage contamination

- Carroll's Creek: residential areas with a documented history of sanitary sewage contamination
- Hunter Creek: heavy commercial contamination associated with automobile maintenance facilities

All the samples were collected in pre-cleaned and autoclaved glass sample bottles using a manual dipper sampler made from polypropylene. The collected sediment samples were dried in aluminum trays at 104°C to remove moisture and were then sieved using a mechanical shaker and a set of sieves. All of the chemical analyses were conducted on the material retained by the sieves having openings of 45, 90, 180, 355, 710, 1,400 and 2,800 µm. In addition, the largest size fraction was separated into inert and organic fractions, with the large organic material (mostly leaves) manually separated for separate analyses. The fractionated sediment samples were stored at 4°C until they were analyzed. All the size fractionated sediment particles were analyzed for PAH concentrations using TD/GC/MS.

CHAPTER IV

FATE MODELING

4.1 Fugacity Modeling

The fugacity models described by Mackay et al. (1992) are methods that are useful to determine the partitioning of a chemical contaminant into different phases once they are released into the environment. Fugacity reflects the tendency of an organic compound to prefer one phase (liquid, solid, or gas) over another phase. It is often defined as the escaping tendency of a chemical substance from a phase. At a given temperature and pressure, an organic chemical will have a different fugacity for each phase. The phase with the lowest fugacity will be the most favorable, and will have the lowest Gibbs free energy.

Mackay's level I method (which does not consider bioaccumulation rates or kinetics) was used as a preliminary assessment of potential associations of the PAHs into the different main phases at equilibrium. This model is based on the physical-chemical properties of the chemical contaminant and the media. These properties include temperature, flows and accumulations of air, water and solid matter. The composition of the media is also an important property of the media. The physical-chemical properties of the contaminant chemical include the partition coefficients, Henry's law constant, and solubility of the contaminant. Equations involved in the model calculations are shown below.

$$C = Z * f \quad (\text{or}) \quad f = \frac{M}{\sum (V_i * Z_i)} \quad (\text{eq. 4.1})$$

Where C = Concentration of contaminant, mol/m³, Z = fugacity capacity constant, mol/m³, f = fugacity, Pa, M = Moles of contaminate, V_i = Volume of the corresponding phases and Z_i = fugacity capacities of air, water, sediment, suspended sediment, and fish for i = 1, 2, 3, 4, and 5 respectively and are defined as follows.

$$Z_1 = \frac{1}{RT} \quad (\text{eq. 4.2})$$

$$Z_2 = \frac{1}{H} \quad (\text{eq. 4.3})$$

$$Z_3 = Z_2 * P_3 * \phi_3 * \frac{K_{OC}}{1000} \quad (\text{eq. 4.4})$$

$$Z_4 = Z_2 * P_4 * \phi_4 * \frac{K_{OC}}{1000} \quad (\text{eq. 4.5})$$

$$Z_5 = Z_2 * P_5 * L * \frac{K_{OW}}{1000} \quad (\text{eq. 4.6})$$

Where R = gas constant (8.314 J/mol K), T = absolute temperature (K), H= Henry's law constant (Pa.m³/mol), K_{OC} = Organic-water partition coefficient, K_{OW} = Octonal-water partition coefficient, P₃ = density of sediment (kg/m³), P₄ = density of suspended sediment (kg/m³), ϕ_3 = organic fraction of sediment, ϕ_4 = organic fraction of suspended sediment, P₅ = density of fish in the aquatic system (kg/m³), L= Lipid content of fish.

The percentage of the total quantity of each PAH that is partitioned into individual phases were calculated using the system volumes, densities, and organic fractions as shown on Table

4.1. Selected PAHs and their physical and chemical properties used in model prediction are shown in the Table A.5.

Table 4.1 Assumed System Parameters

Parameter	Air	Water	Soil	Sediment	SS	Fish
Volume (m ³)	1.0E+14	2.0E+11	9.0E+09	1.0E+08	1.0E+06	2.0E+05
Density (kg/m ³)	1.2E+00	1.0E+03	2.4E+03	2.4E+03	1.5E+03	1.0E+03
Organic Fraction	-	-	0.02	0.04	0.2	0.05 (Lipid Content Weight/Weight)

The model predicted fugacity capacities and the percentage partition by weight for selected PAHs into air, water, suspended sediment, sediment and fish (biota) are shown on Table 4.2. The values indicate, as expected, that for many of the PAHs, the compounds are mostly partitioned with the sediment phase than with the other phases. The low molecular weight PAHs naphthalene, fluorene, phenanthrene, and anthracene (which have fewer carbon rings) are mostly partitioned into the air or water phases compared to those having higher molecular weights. Figure 4.1 shows the relationship between percentage partitioning of PAHs onto sediment phase and their Log (K_{ow}), Log (K_{oc}). PAHs with Log (K_{ow}) or Log (K_{oc}) values greater than about 4.5 are mostly partitioned with the sediment phase compared to other phases. Of the PAHs examined, only naphthalene, fluorene, and phenanthrene are expected to be predominantly associated with the air phase.

Table 4.2 MacKay Level 1 Calculated Fugacity Capacities and Percentage Partitioning of Selected PAHs with Different Environmental Phases

PAH	Z ₁	Z ₂	Z ₃	Z ₄	Z ₅	F	% Partition by Weight				
							Air	Water	Sediment	SS	Fish
Naphthalene	4.0E-04	2.1E-02	3.3E+00	1.0E+01	9.3E-01	1.7E-05	89.7	9.5	0.7	0.0	0.0
Fluorene	4.0E-04	4.7E-02	3.3E+01	1.0E+02	2.0E+00	1.1E-05	76.0	17.7	6.2	0.2	0.0
Phenanthrene	4.0E-04	3.9E-02	5.2E+01	1.6E+02	1.7E+00	7.0E-06	73.5	14.4	13.0	0.3	0.0
Anthracene	4.0E-04	5.6E-01	7.6E+02	2.4E+03	4.1E+03	2.8E-06	17.5	49.3	29.8	1.0	0.4
Fluoranthene	4.0E-04	1.5E+00	5.5E+03	1.7E+04	6.6E+01	5.4E-07	4.4	33.2	60.5	1.9	0.0
Pyrene	4.0E-04	5.3E-01	1.9E+03	6.0E+03	2.3E+01	1.1E-06	11.7	30.6	55.9	1.8	0.0
Benzo(a)anthracene	4.0E-04	1.5E+01	2.9E+05	9.0E+05	1.1E+05	2.0E-08	0.1	9.2	87.9	2.8	0.1
Chrysene	4.0E-04	1.2E+14	2.4E+18	7.5E+18	5.4E+15	2.4E-21	0.0	9.2	88.1	2.8	0.0
Benzo(b)fluoranthrene	4.0E-04	8.2E-01	4.3E+04	1.4E+05	6.1E+03	1.4E-07	0.9	3.5	92.7	2.9	0.0
Benzo(a)Pyrene	4.0E-04	2.0E+01	1.1E+07	3.3E+07	1.5E+05	5.9E-10	0.0	0.4	96.6	3.0	0.0
Indeno(1,2,3-cd)pyrene	4.0E-04	3.3E+14	5.1E+19	1.6E+20	1.5E+16	6.9E-23	0.0	1.3	95.8	3.0	0.0
Dibenz(a,h)anthracene	4.0E-04	1.3E+03	4.3E+08	1.3E+09	5.9E+04	1.5E-11	0.0	0.6	96.4	3.0	0.0
Benzo(g,h,i)perylene	4.0E-04	7.0E+01	1.1E+07	3.4E+07	5.2E+05	5.8E-10	0.0	1.3	95.7	3.0	0.0

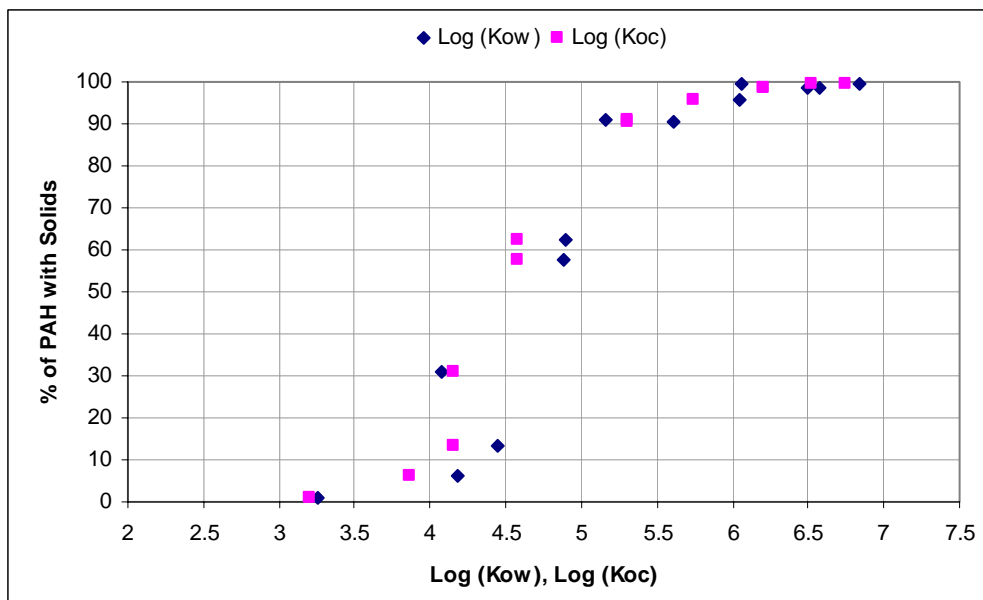


Figure 4.1 Percentage of PAH partitioning with solids versus PAH Log (K_{ow}), Log (K_{oc})

4.2 Multi Chamber Treatment Train (MCTT) Study

As a part of the MCTT study, Pitt et al. (1995 and 1999) collected stormwater sheet flow samples from source areas in three different land uses (residential, commercial, and industrial) that were analyzed for PAHs, and other constituents to identify critical source areas of toxicants. Sheet flow samples were obtained from roofs, parking areas, storage areas, streets, vehicle service areas, landscaped areas, urban creeks, and detention ponds.

All the samples collected were divided and analyzed twice: one split was analyzed un-filtered and the second split was filtered first through a 0.45 μm membrane filter to remove the particulate solids and analyzed to represent only the water-associated fraction of the PAHs. The particulate-associated fraction was determined by difference. PAH concentrations associated with the particulate solids were therefore calculated using the particulate solids concentrations for each sample. Twenty-two of the 58 samples analyzed

contained detectable PAH concentrations, but very few had detectable concentrations in the filtered sample fraction.

Table 4.3 shows the percentage of detection of individual PAHs in un-filtered samples, and in both un-filtered and filtered samples. The decreased percentage of detection for the filtered samples compared to the un-filtered samples indicates the analytes are mostly associated with the particulate solids in the samples. The decrease in percentage of detection in the filtered samples is more common for the high molecular weight PAHs than for the low molecular weight PAHs, indicating that the high molecular weight PAHs have a greater portion associated with the particulates.

Table 4.3 Percentage of samples detected

PAH	% of Samples Having Detected PAH Concentrations	
	In Un-filtered Samples	In both Un-filtered and Filtered Samples
Naphthalene	16	12
Anthracene	9	2
Fluoranthene	26	12
Phenanthrene	12	0
Benzo(a)anthracene	12	0
Benzo(b)fluoranthene	22	0
Benzo(k)fluoranthene	22	0
Chrysene	9	0
Pyrene	19	7
Benzo(a)pyrene	22	0

4.2.1 Comparing Model Predictions with MCTT PAH Data

For comparison purpose, fugacity model calculations were performed by assuming the absence of air, sediment and biota in the in the environment system, only examining associations with the water and the suspended particulate matter. Table 4.4 shows the values of the variables used in the fugacity model calculations. Table 4.5

shows the calculated partitioning percentages of the PAHs associated with the water and the suspended particulate matter.

Table 4.4 Variables used in fugacity partition predictions

Variable	Value
Sample (system) volume	1 L
Organic fraction of suspended solids	0.2
Concentration of Contaminant	150 µg/L
Suspended Solids Concentration	50 mg/L
Temperature	25°C

Table 4.5 Model Predicted Percentage of Partitions

PAH	Z ₁	Z ₂	F	Amount Associated (kg)		% Association	
				Water	SS	Water	SS
Naphthalene	2.1E-02	1.0E+01	5.4E-02	1.5E-04	2.3E-06	98	2
Fluorene	4.7E-02	1.0E+02	1.8E-02	1.4E-04	1.0E-05	93	7
Phenanthrene	3.9E-02	1.6E+02	1.9E-02	1.3E-04	1.9E-05	88	12
Anthracene	5.6E-01	2.4E+03	1.3E-03	1.3E-04	1.9E-05	88	12
Fluoranthene	5.8E-04	6.7E+00	9.2E-01	1.1E-04	4.1E-05	73	27
Pyrene	9.0E-01	1.0E+04	6.0E-04	1.1E-04	4.1E-05	73	27
Benzo(a)anthracene	1.5E+01	9.0E+05	1.5E-05	5.0E-05	1.0E-04	33	67
Chrysene	1.2E+14	7.5E+18	1.8E-18	5.0E-05	1.0E-04	33	67
Benzo(b)fluoranthene	8.2E-01	1.4E+05	1.1E-04	2.3E-05	1.3E-04	15	85
Benzo(k)fluoranthene	9.5E-03	3.3E+03	5.0E-03	1.2E-05	1.4E-04	8	92
Benzo(ghi)perylene	7.0E+01	3.4E+07	4.6E-07	8.9E-06	1.4E-04	6	94
Benzo(a)pyrene	2.1E+01	3.5E+07	5.1E-07	2.7E-06	1.5E-04	2	98

The MCTT observed PAH partitioning between water and particulate matter is shown on Table 4.6. These percentages were calculated by replacing the non-detected values in the filtered samples with half of the detection limit (0.25 µg/L) to represent likely average concentrations. Figure 4.2 contains plots of the predicted vs. the observed associations. This plot shows that the fugacity equilibrium model under-predicted the

percentage of the PAHs associated with the particulate matter compared to the observed conditions. This trend was found to be more obvious for the low molecular weight PAHs. As stated earlier in this chapter, the fugacity level I procedure assumes equilibrium conditions. It is possible that the real time observed samples collected during the MCTT project may not have at equilibrium. Physical and chemical properties (such as the organic content) of the particulate matter also effect the partitioning of the analytes. Variations in concentrations of the PAHs associated with the particulate matter can depend on the source areas and local activities. As an example, Mahler et al. (2005) found that particulate bond PAHs in runoff from coal-tar sealed asphalt parking lots was 65 times higher than found from un-sealed parking lots. It is important to note that the actual importance of particulate matter in transporting PAHs in the urban environment is likely greater than predicted using chemical modeling tools.

Table 4.6 MCTT Observed Percentage of Partitions (non-detects in filtered samples are replaced with half of DL)

PAH	% Association	
	Water	Particulate Matter
Naphthalene	22	78
Fluorene	3	97
Phenanthrene	2	99
Anthracene	8	92
Fluoranthene	29	71
Pyrene	19	81
Benzo(a)anthracene	3	99
Chrysene	1	99
Benzo(b)fluoranthene	1	99
Benzo(k)fluoranthene	2	98
Benzo(ghi)perylene	1	99
Benzo(a) pyrene	1	99

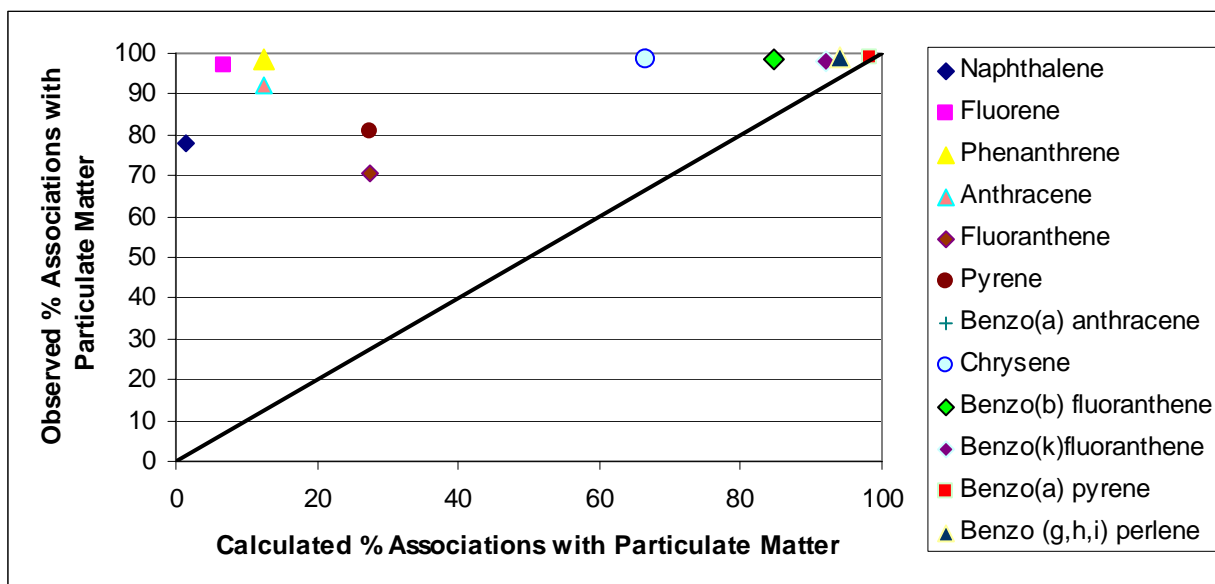


Figure 4.2 Comparisons of observed and calculated PAH associations with particulate material

4.3 Studying the Effects of Environmental Factors on PAHs Associations with Particulate Material using Fugacity Calculations

The effects of assumed important environmental factors on the partitioning of the PAHs with different media were studied using a full 2^4 factorial experimental design (Box et al. 1978). The factorial experimental design identifies the effects of individual variables, and also the effects of interactions of the variables, on the PAH concentrations. These effects were calculated using a table of contrasts. This table shows the averages of the differences between the sums of the analyte concentrations when the factor is at its maximum value and at its minimum value. Probability plots of the calculated effects for the factors indicates those factors and interactions that are not likely associated with random processes. The design matrix used in this factorial study is shown in Table 4.7. The '+' and '-' sign in the matrix indicates the factor at its high and low respectively.

The low and high values of the factors were chosen based on typical observations for stormwater and urban receiving waters, and are shown in the Table 4.8. Combination of factors, example 'AB' shows the interaction of 'A' factor and factor 'B,' similarly, for example 'ABCD' indicates the 4-way interaction of 'A', 'B', 'C', and 'D.'

Table 4.7 2⁴ Factorial Design Showing Experimental Conditions for 16 Runs (Box et al. 1978)

Run	A	B	C	D	AB	AC	AD	BC	BD	CD	ABC	ABD	ACD	BCD	ABCD
1	+	+	+	+	+	+	+	+	+	+	+	+	+	+	+
2	+	+	+	-	+	+	-	+	-	-	+	-	-	-	-
3	+	+	-	+	+	-	+	-	+	-	-	+	-	-	-
4	+	+	-	-	+	-	-	-	-	+	-	-	+	+	+
5	+	-	+	+	-	+	+	-	-	+	-	-	+	-	-
6	+	-	+	-	-	+	-	-	+	-	-	+	-	+	+
7	+	-	-	+	-	-	+	+	-	-	+	-	-	+	+
8	+	-	-	-	-	-	-	+	+	+	+	+	+	-	-
9	-	+	+	+	-	-	-	+	+	+	-	-	-	+	-
10	-	+	+	-	-	-	+	+	-	-	-	+	+	-	+
11	-	+	-	+	-	+	-	-	+	-	+	-	+	-	+
12	-	+	-	-	-	+	+	-	-	+	+	+	-	+	-
13	-	-	+	+	+	-	-	-	-	+	+	+	-	-	+
14	-	-	+	-	+	-	+	-	+	-	+	-	+	+	-
15	-	-	-	+	+	+	-	+	-	-	-	+	+	+	-
16	-	-	-	-	+	+	+	+	+	+	-	-	-	-	+

(+indicates factor at its high value, - indicates factor at its low value)

Table 4.8 Values Used in Factorial Analysis of Modeled PAH Associations

Variable	Low value	High value
Temperature (A), °C	5	25
Concentration of PAH compound (B), µg/L	10	300
Concentration of Suspended Solids(C), mg/L	10	500
Organic Fraction of Suspended Solids (D)	0.05	0.2

A hypothetical system with air, water, and suspended particulate matter phases was assumed to study the effects of selected factors on the partitioning with different phases. As an example anthracene analyses calculations are shown here. The analyses

calculation results for benzo(a)anthracene and chrysene are shown in the Appendix A. Table 4.9 shows the predicted portioned moles of anthracene into air, water and suspended particulate matter under different combinations of the factors of the 2^4 factorial design. Table 4.10 shows the calculated effects of different combinations of the factors in portioning of anthracene with air, water and suspended particulate matter.

Figures 4.3, 4.4 and 4.5 are probability plots of the effects of the factors and their interactions on partitioning anthracene into the three main phases. The probability plot for the air phase (Figure 4.3) indicates that the concentration of anthracene (or total amount of anthracene) (B) in the system has positive effects in partitioning of anthracene into the air phase. However, the concentration of suspended particulate matter (C), and combinations of suspended particulate matter concentration and anthracene concentration (BC) have negative effects on anthracene partitioning into the air. In the case of partitioning into the water phase (Figure 4.4), the concentration of anthracene (B) was found to have the greatest positive effect, and the concentration of the suspended particulate matter (C) had a significant negative effect (the higher the particulate matter concentration, more of the anthracene is associated with the sediment). Figure 4.5 shows the probability plot of effects of anthracene partitioning with suspended particulate matter. The significant factors were the concentration of the anthracene (B) and the concentration of the particulate matter (C). The organic content (D) of the particulate matter also affects the partitioning of the anthracene with suspended particulate matter, but to a lesser extent. Similar kind of results were also shown for factorial analyses of benzo(a)anthracene partitioning.

Table 4.9 Model Predicted Portioning of Anthracene with 2⁴ Factorial Design Variables

Factor Value				Moles of Anthracene Partitioned with		
A	B	C	D	Air	Water	Particulate Matter
+	+	+	+	2.3E-13	2.8E-08	3.9E-08
+	+	+	-	4.2E-13	5.0E-08	1.8E-08
+	+	-	+	5.5E-13	6.5E-08	1.8E-09
+	+	-	-	5.6E-13	6.7E-08	4.7E-10
+	-	+	+	7.8E-15	9.3E-10	1.3E-09
+	-	+	-	1.4E-14	1.7E-09	5.9E-10
+	-	-	+	1.8E-14	2.2E-09	6.2E-11
+	-	-	-	1.9E-14	2.2E-09	1.6E-11
-	+	+	+	8.0E-14	1.6E-08	5.1E-08
-	+	+	-	7.8E-14	1.6E-08	5.2E-08
-	+	-	+	3.1E-13	6.3E-08	4.0E-09
-	+	-	-	3.3E-13	6.6E-08	1.0E-09
-	-	+	+	2.7E-15	5.4E-10	1.7E-09
-	-	+	-	6.2E-15	1.3E-09	9.9E-10
-	-	-	+	1.0E-14	2.1E-09	1.3E-10
-	-	-	-	1.1E-14	2.2E-09	3.5E-11

Table 4.10 Calculated Effects of Factors and their Interactions on the Associations of Anthracene with Different Media

Factors/ Interactions	Calculated Effect		
	Air	Water	Suspended Solids
A	1.0E-13	6.2E-09	-6.2E-09
B	3.9E-13	4.5E-08	2.0E-08
C	-2.5E-13	-2.0E-08	2.0E-08
D	-2.7E-14	-3.4E-09	1.2E-08
AB	8.0E-14	6.0E-09	-6.0E-09
AC	3.0E-15	5.5E-09	-5.5E-09
AD	-2.3E-14	-2.6E-09	2.6E-09
BC	-1.9E-13	-1.9E-08	1.9E-08
BD	-2.5E-14	-3.0E-09	3.0E-09
CD	-2.0E-14	-2.3E-09	2.3E-09
ABC	3.7E-15	5.3E-09	-2.3E-09
ABD	-2.2E-14	-2.6E-09	2.6E-09
ACD	-2.4E-14	-3.0E-09	3.0E-09
BCD	-1.8E-14	-2.0E-09	1.1E-09
ABCD	-2.3E-14	-3.0E-09	3.0E-09

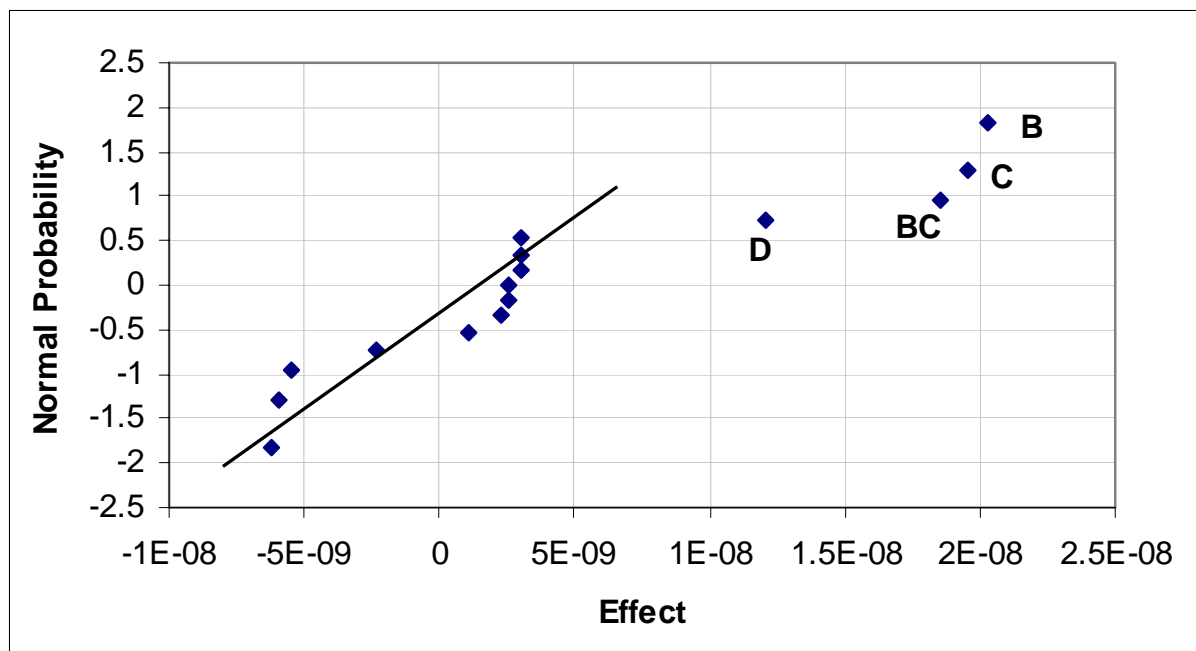


Figure 4.5 Probability plot of effects of partitioning of Anthracene with air

4.4 Conclusions

MacKay's level I fugacity model was used to predict partitioning fractions of selected PAHs associated with different phases (water, sediment, air, biota). This modeling approach indicated that except for the low molecular weight PAHs (naphthalene, fluorene, phenanthrene, and anthracene) all the other studied PAHs are predominantly partitioned with the sediment phase. The level I fugacity model, which assumes system equilibrium, was found to under predict the PAH partitioning with the particulate matter when compared with observed particulate and filtered PAH observations from prior research that examined stormwater treatment of PAHs. A 2^3 full factorial design study was conducted for an air, water and suspended solids hypothetical system for anthracene and benzo(a)anthracene and chrysene. This example PAHs were

found to partition into all three phases, and its behavior was mainly affected by their initial concentration in the system components.

CHAPTER V

ANALYTICAL METHOD DEVELOPMENT

5.1 Development of New Analytical Techniques

Model prediction calculations and available literature (Pitt et al. 1999 and Hwang et al. 2006) have shown that particulate associations are the main fate of many of the PAHs in the aquatic environment. It is therefore essential that the analytical methods used for PAH analyses be sensitive to particulate forms of the contaminants, and that separate analyses of the particulate and filtered portions also be conducted, if possible. Traditional Solid Phase Extraction (SPE) methods for PAHs may not be suitable for preparing samples having high concentrations of suspended solids due to extremely low recoveries during the extraction process (Pitt et al. 1999). Separating the solids from the liquid and analyzing the individual sample portions (filtered and particulate fractions) separately is one method for complete PAH analyses. Soxhlet (EPA method SW-848), automated soxhlet (EPA method 3540), and ultrasonic extraction (EPA method 3550) methods are the common solvent extraction methods for PAHs from solid samples. However, these methods have some inherent disadvantages, such as requiring large amounts of samples and large volumes of organic solvents, they are time consuming and complex, and involve multi-step processes that are subject to errors (Zhang et al. 1994).

Another aspect of this research modified and tested an alternative PAH extraction procedure that used a newly available SIS AutoDesorbTM thermal desorption method. Thermal extraction, or thermal desorption, techniques use elevated temperatures as a means to transfer the analytes from solid sample matrices to the gaseous analytical system. The analytes desorbed from the solid sample matrices are concentrated in a cryotrap at the head of a GC column. The concentrated analytes are then separated and detected using a standard GC column and MS detector which is similar to the analysis of liquid samples when concentrated into a solvent. The equipment used during this method development included the AutoDesorbTM unit, glass wool, Tenax®, PAH liquid standards obtained from SUPELCO® (47930-U QTM PAH Mix), NIST1941b sediment standard, desorption tubes and tube conditioning oven, GC (HP6890N), and MS (HP5975).

5.2 Analysis Procedure

5.2.1 Tube Conditioning

Prior to the use of the thermal desorption tubes for the analysis of samples, the thermal desorption tubes need to be conditioned at elevated temperatures. The conditioning of the tubes helps in removing all foreign materials which may cause sample cross contamination, or memory peaks in the sample analysis. The tube conditioning was performed with the help of high purity nitrogen gas. Initially, the tubes were flow conditioned at room temperature for several minutes to get rid of oxygen from the interiors of the tubes. After initial purging of the tubes at room temperature, the tubes were heated up to 350°C at a rate of 4°/min while purging with nitrogen gas. The tubes were maintained at elevated temperatures of 350°C for four hours. Throughout the

conditioning process, the nitrogen flow is maintained at about 60 mL/min. At the end of the four hours at the elevated temperature, the tubes were removed from the conditioning oven and placed in the cooling rack at the rear of the oven and allowed to cool for 10 minutes. When the tubes are cooled, the tubes were immediately capped on both ends with the pre-conditioned steel caps. The same procedure was used for conditioning the needles.



Figure 5.1 Tubes conditioning oven (Source: SIS product manual)

5.2.2 Tube Packing

The thermal desorption tubes are made of stainless steel and are 4 mm in internal diameter and 100 mm long and threaded at both ends. Conditioned tubes are packed with the sample to be analyzed. Both ends of the tubes are plugged with glass wool to hold the sample in place and to reduce the loss of fine particulates into the analytical stream that would plug the needle and accelerate contamination of the MS.

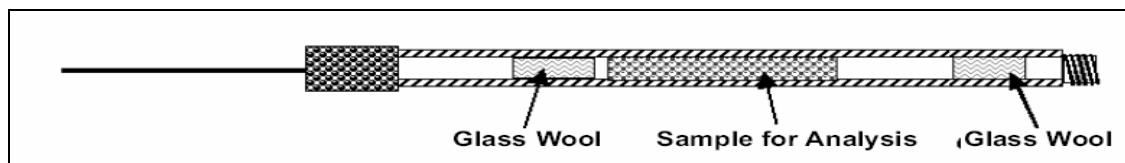


Figure 5.2 Schematic of packed desorption tube (Source: SIS product manual)

5.2.3 Analysis

The packed tubes, which are ready for analysis, are then loaded onto the system carousel. Once the analysis process is initiated with the help of the AutoDesorb™ software from the remote control system, the desorption tube is purged to remove oxygen, excess water, and volatile materials that are resident in the tube. The needle is then lowered into the GC inlet and the injection period starts, followed by purging. The injection time period is set based on the instrument response to allow the injection port pressures to equilibrate and the proper split flow to be reached before the injection time expires. At the end of the injection time, the heater blocks close around the desorption tube and the tube is heated at a rate specified in the method. Carrier gas transports the desorbed analytes into the inlet of the GC. The cryotrap then traps the analytes entering the GC inlet by condensing the organic gases and focus the analytes for their concentration. The cryotrap is then heated up ballistically to release the focused analytes instantaneously into the GC column, where the analytes are separated based on their volatility and then detected by the MS, based on their charge to mass ratios.

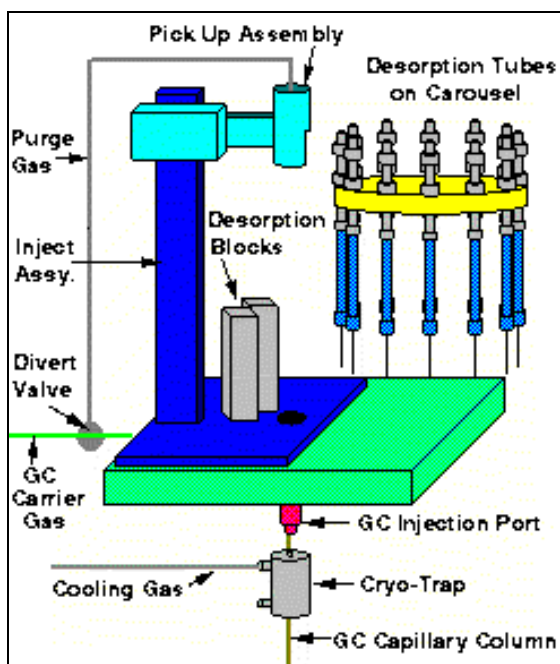


Figure 5.3 Graphics of AutoDesorb™ (Source: SIS application notes)

5.3 Thermal Desorption Method Optimization

The selected conditions for the thermal desorption extraction were determined based on a series of experiments conducted to obtain optimal recovery of analytes from the solid samples and to have good separation of the analytical peaks. For this purpose, standard solid samples were prepared by spiking 10 μ L of the 20 mg/L PAH mixed standard onto pre-treated glass wool. The thermal desorption unit was subjected to different desorption times and desorption temperatures. The final desorption temperatures that were tested ranged from 250°C to 375°C. Final desorption temperature of 350°C produced higher peaks of individual PAHs. Similarly, different desorption times were tested to obtain maximum peak areas. A series of runs was made with different holding times at the final desorption temperature. The final temperature holding times tested ranged from 1 min to 20 min. It was found that the peak areas obtained for individual PAHs increased as the holding time increased from 1 min to 15 min, but then decreased

as the holding time further increased to 20 min. Therefore, the optimum desorption time for the highest recovery of PAHs was found to be 15 min. For three replicate runs, the coefficients of variation (COV) showed that low molecular weight and high molecular weight PAHs have high variations in the peak areas (naphthalene 49%, fluorene 24%, dibenzo(a,h)anthracene 15%, benzo(ghi)perylene 16%), while the intermediate PAHs had much lower variations (COVs ranging from 0.5% - 4.0%).

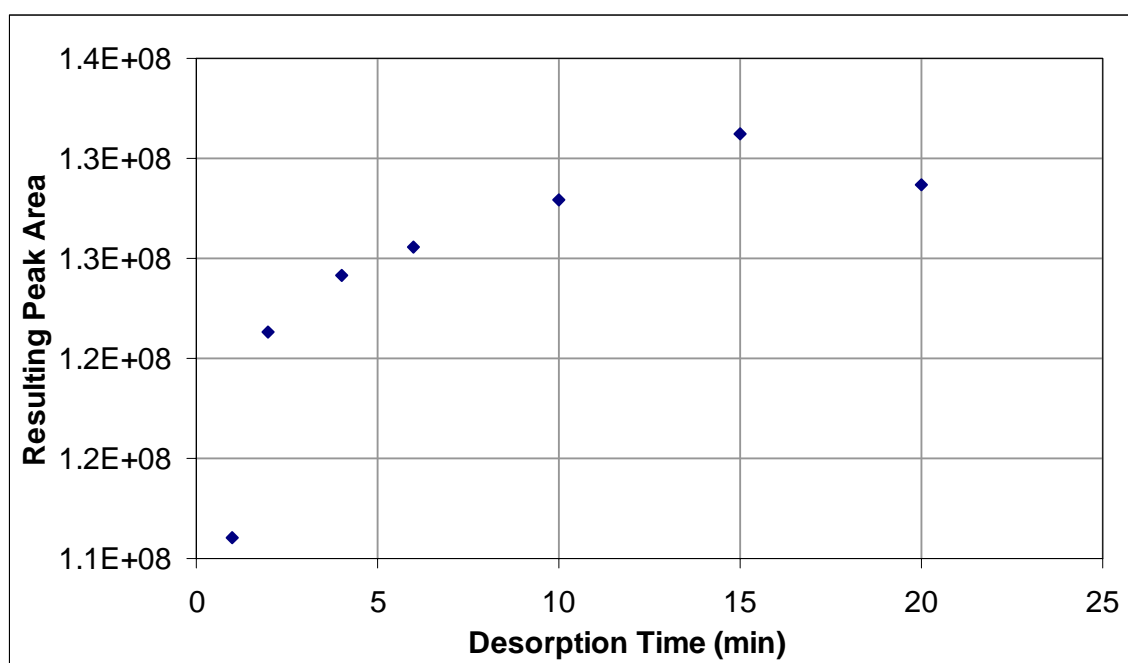


Figure 5.4 Desorption time versus peak areas for Pyrene

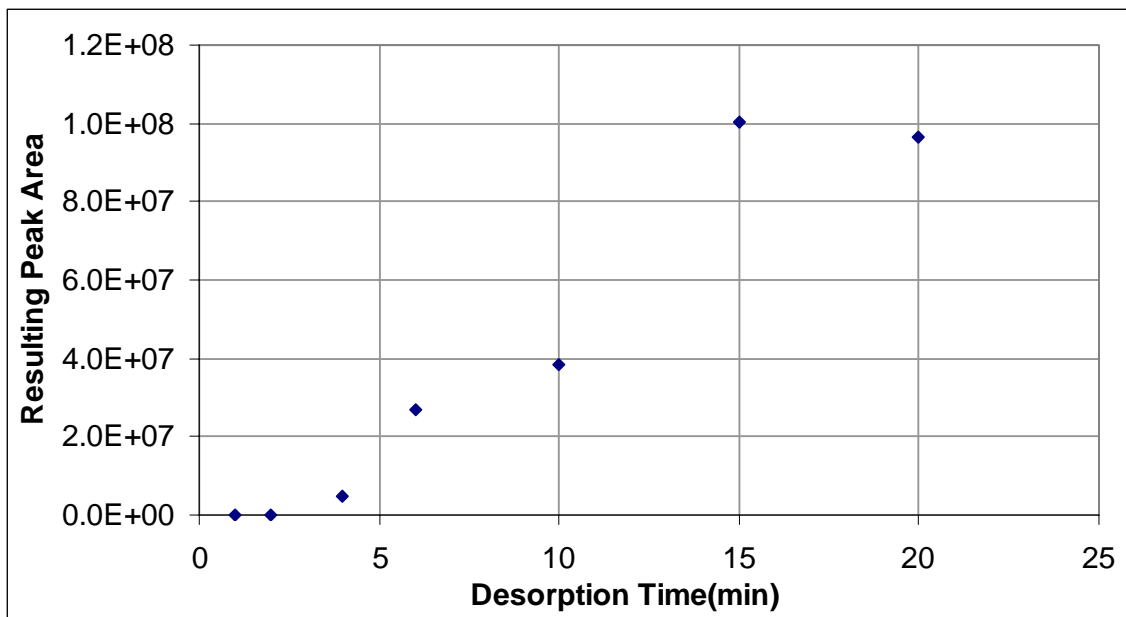


Figure 5.5 Desorption time versus peak areas for Benz(ghi)perylene

5.3.1 Optimal conditions of thermal desorption system

Purge duration:	1.00 min
Injection duration:	1.00 min
Initial temperature:	50°C
Temperature ramp rate:	100°C
Final temperature:	350°C
Final temperature holding time:	15 min
Cryo-trap:	enabled
Cryo cool temperature:	-40°C
Cryo heat temperature:	300°C
Cryo heat duration:	10.00 min
GC start time:	26.50 min

5.4 Testing Method for Linearity

The developed method was tested for linear responses for selected PAHs. For these tests, challenge solid matrices were prepared by spiking Tenax® with 10, 50, 100, 200 and 400 ng of the PAH liquid standard mixture. The obtained regression index of determination (R^2) values for selected PAHs are reasonable for this method, and are shown in Table 5.1.

Table 5.1 Regression Coefficient Values for Linearity test

PAH	R^2
Naphthalene	0.9958
Fluorene	0.9848
Phenanthrene	0.9969
Anthracene	0.9944
Fluoranthene	0.9978
Pyrene	0.9975
Benz(a)anthracene	0.9934
Chrysene	0.9961
Benz(b)fluoranthrene	0.9925
Benz(a)pyrene	0.9881
Indeno(1,2,3-cd)pyrene	0.9619
Dibenzo(a,h)anthracene	0.9593
Benz(ghi)perylene	0.9357

5.5 Analysis of a Standard Sample using the Developed Method

A marine sediment standard, NIST1941b obtained from the National Institute of Standards and Technology (NIST), was tested using the developed method. This standard sample was collected from Chesapeake Bay at the mouth of Baltimore (MD) Harbor near the Francis Scott Key Bridge using a Kynar-coated grab sampler. The standard is certified for 119 different constituents of PAHs, PCBs and chlorinated pesticides. The sample was ground and sieved so the sediment particles were finer than 150 μm .

A 10 mg portion of NIST1941 was subjected to the analysis with the operational conditions determined during the method development. Most of the analytes present in the standard sample were detected and clear individual peaks were shown. There were two major problems identified during the analysis of the standard material using thermal desorption GS/MS analysis, as discussed below.

5.5.1 Presence of sulfur

Due to the presence of sulfur in the sediment sample, there were many unwanted sulfur-containing analyte peaks in the gas chromatogram. Sulfur products of PAHs bond to particulate solids and makes them difficult to extract. As copper forms copper sulfide when reacted with sulfur, the addition of small amounts of copper into the thermal desorption tube, along with the sediment sample, helped in avoiding the sulfur products of PAHs. Figure B.1 shows the chromatogram with unwanted peaks of sulfur products of PAHs.

5.5.2 Moisture in the sample

High moisture content of the standard sample caused ice plugging in the GC column during the cryofocusing step and obstructed the flow of analytes through the column. This caused tremendous reductions in the peak areas obtained for the individual analytes, and in some cases, there were no peaks observed. To reduce the water content in the sample, samples were freeze dried before analysis. Figure B.2 shows the chromatogram for samples containing high moisture content. Figure B.3 shows the

chromatogram obtained for freeze dried NIST sediment sample along with added small amounts of pre-cleaned copper.

5.6 Comparison of Recoveries from Two Different Solid Matrices

The research initially examined the PAH recoveries from glass wool compared to Tenax spiked with PAH mixtures. This was performed by spiking the wool and 10 mg of Tenax with 20 ng/ μ L of the PAH standard mixture. The recovery of low molecular weight PAHs (having fewer numbers of rings) was more in the case of Tenax than for the glass wool, whereas for the high molecular weight PAHs (having more rings), the recovery of PAHs from glass wool was greater than from the Tenax matrix. The comparative recovery calculations clearly showed that the recoveries of analytes vary depending on solid matrices. Tenax (an adsorbent resin) represents environmental solid samples more closely than does glass wool and hence the recoveries from the Tenax matrix indicate a more reasonable recovery factor of analytes from real environmental samples.

Table 5.2 Comparison of Peak Areas for Two Solid Matrices

PAH	Mean Area		Ratio of Area
	Glass Wool	10mg Tenax	Glass Wool/Tenax
Naphthalene	22788021	61202757	0.37
Fluorene	63267375	71902289	0.88
Phenanthrene	93644340	98973951	0.95
Anthracene	97919751	99626677	0.98
Fluoranthene	114127323	116877318	0.98
Pyrene	112801392	113481063	0.99
Benz(a)anthracene	125345520	122965363	1.02
Chrysene	127764095	127548616	1.00
Benz(b)fluoranthrene	137369218	137484565	1.00
Benz(a)pyrene	129740976	115008192	1.13
Indeno(1,2,3-cd)pyrene	128386541	90639701	1.42
Dibenz(a,h)anthracene	77365639	47015167	1.65
Benz(ghi)perylene	83206184	50522238	1.65

5.7 Method Detection Limit (MDL)

The method detection limit can be defined as the minimum amount of substance that can be detected with a given confidence. NIST sediment samples of different weights, ranging from 3 mg to 60 mg were analyzed using the developed method. For each analyte, a plot was made comparing the known analyte quantity in the NIST standard to the measured amount (Figure 5.6). Significant departures from a linear response indicate the upper and lower limits of the useful quantitative range of the method. A regression analysis was performed on the data for each analyte providing further information about the method. Ideally, the slope generated from these regression analyses should be 1. A slope significantly different from 1 indicates a bias in the method. The standard error of the regression may be used to estimate the detection limit (DL) of the method (McCormick and Roach 1987).

$$DL = Y_0 + S_y Z_\alpha \quad (\text{eq. 5.1})$$

Where,

DL = detection limit of the method

Y_0 = The intercept of the regression equation

S_y = Standard error of the regression

Z_α = The area under the normal curve associated with a one-tail probability for a given confidence level.

In this report standard error and detection limits are presented for a 95% confidence level.

Concentrations less than the detection limit only indicates the presence of the analyte.

The limit of quantification (LOQ) can be calculated by using equation (McCormick and Roach 1987).

$$LOQ = Y_0 + 2S_y Z_\alpha \quad (\text{eq. 5.2})$$

The corresponding weights of analytes in the NSIT sediment samples and method calculated weights of analytes are shown in the Tables B.1. Figures B.4 through B.15 in shows the linear relation of standard sediment analyte weights and method calculated analyte weights. For analytes indeno(1,2,3-cd)pyrene and dibenz(a,h)anthracene the linear line was forced to pass through the origin as the intercepts were found to be insignificant (P value for indeno(1,2,3-cd)pyrene was 0.327 and for dibenz(a,h)anthracene was 0.263). The Table 5.3 shows the calculated DL and QL of the method. The residual probability graphs are shown in the Figures B.16 AND B.17, and were found to be normal with 95% C.I.

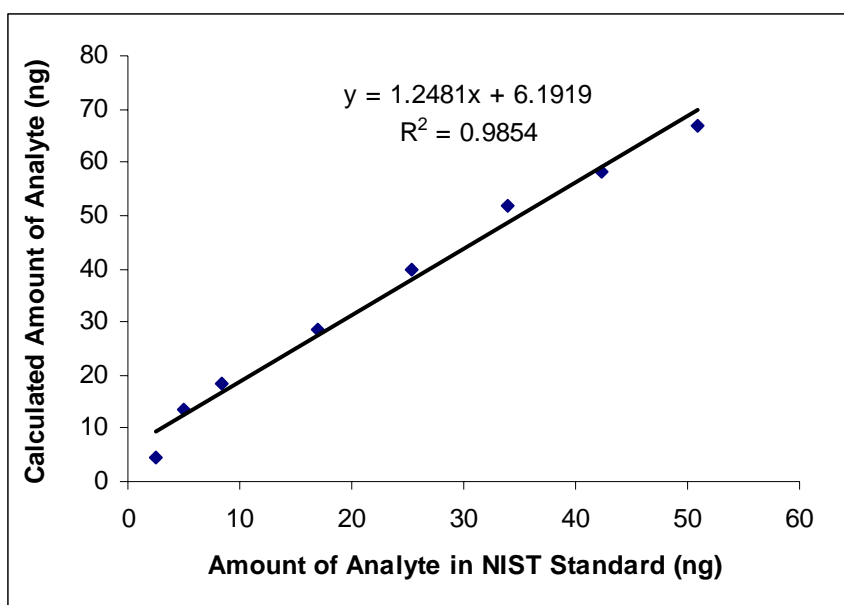


Figure 5.6 Relationship between naphthalene weights in NIST standards and method calculated weights

Table 5.3 Method detection and Quantification Limits

PAH	Y-intercept (P Value)	Slope (P Value)	Standard Error	% R²	Detection Limit (ng)	Lower Quantification Limit (ng)
Naphthalene	6.09 (0.013)	1.24 (0.000)	2.15	98.5	9.63	13.17
Fluorene	0.58 (0.012)	1.53 (0.000)	1.24	96.4	2.62	4.66
Phenanthrene	4.47 (0.002)	0.85 (0.000)	1.16	97.1	6.37	8.27
Anthracene	3.2 (0.001)	0.42 (0.001)	0.38	94.1	3.83	4.47
Fluranthene	1.78 (0.002)	0.33 (0.000)	0.54	98.8	2.67	3.55
Pyrene	7.34 (0.000)	0.43 (0.000)	1.5	93.2	9.81	12.28
Benzo(a) anthracene	1.77 (0.000)	0.22 (0.000)	0.29	96.8	2.25	2.73
Chrysene	0.31 (0.002)	0.25 (0.000)	1.41	96.5	2.63	4.95
Benzo(b) flouranthrene	3.55 (0.000)	0.23 (0.000)	0.36	97.6	4.15	4.74
Benzo(a)pyrene	3.37 (0.002)	0.42 (0.000)	0.5	97.5	4.2	5.03
Indeno(1,2,3-cd) pyrene	0	0.32 (0.001)	0.62	93.1	1.34	2.36
Dibenz(a,h) anthracene	0	0.43 (0.051)	0.64	52.2	1.05	2.09
Benzo(ghi) perylene	0.13 (0.0482)	0.14 (0.000)	0.51	97.1	0.97	1.82

5.8 Recovery Calculations using the Standard NIST Solid Matrix Sample

The percentage recovery of the analytes from the sample matrices using the developed method was further tested by comparing analyte concentrations by TD/GC/MS with the certified NIST sample concentrations. Three samples of 27 mg each were subjected to TD/GC/MS and the concentrations of the analytes were calculated based on resulting chromatogram peak areas. Table 5.4 shows these measured analyte concentrations using the TD/GC/MS process, along with the certified NIST concentrations, and the calculated recovery factors. The acceptable range of extraction recoveries for PAHs from liquid samples using SPE methods are also shown in Table 5.4. Even though the calculated recoveries for some of the analytes have low percentage values, almost all are still in the acceptable ranges of listed recoveries. The calculated recoveries ranged from 33 to 142 percent. Other than the recovery of naphthalene and fluorene which were found to be slightly outside of the upper limit of the acceptable range of recoveries, all other samples were found to be with the acceptable range of recoveries established for the aqueous samples. In general, one would expect higher percentages of recovery of analytes from aqueous samples compared to solid samples.

Differences between the concentrations of analytes in coarse sediment samples and in the same samples that were ground were examined to quantify the effect of particle sizes on the recovery of selected PAHs. Two composite sediment samples in the size ranges of 710 – 1400 μm and 1400 – 2800 μm were prepared from all the samples collected at the three creeks. Portions of the composite sediment samples was ground in the ball mill to a size $< 180\mu\text{m}$. The coarser composite sediment samples and their ground samples were analyzed separately for the PAHs. Three replicates of each sample

portion were analyzed. The resulted PAH concentrations in composite sediment sample and in corresponding grinded sediment sample are shown in the Table B.2 and B.3. The probability plots of resulted concentrations are shown in the Figure B.18 through B.21, and were found to normal. The ANOVA analyses of the measured concentrations of PAHs in the coarser ungrounded and ground samples resulted in high P values (> 0.05) for all comparisons, except for one (Benzo(a)pyrene for the 710-1400 sample) indicating that there were no significant differences detected between the ground and unground samples (Table 5.5). This indicated that the recovery of the PAHs were not likely affected by sediment particle sizes.

PAHs are preferentially associated with organic matter. The thermal chromatography results (Chapter VI) showed that these sediment samples are mostly composed of inert material and only small portions were organic (leaves and grass material, for example) The PAHs are likely associated with the surfaces of the particulates where smaller pieces of the organic matter may be attached. It is likely that there are only small portions of PAHs throughout the sediment particles (the exception being the asphaltic material that was detected in only very small fractions). The extraction process is obviously much more efficient in stripping off PAHs that are attached to the outer surfaces of the particulates than from the inner portions of the sediment particles. The results of these tests, comparing ground and unground sample PAH concentrations, indicated that additional amounts of PAHs were not found within the sediment material itself.

Table 5.4 Calculated Method Recovery Using NIST Sediment Standard

PAH	NIST Concentration, µg/kg, (95% C.I)			TD/GC/MS Measured Concentration µg/kg, (Standard Deviation)	% Recovery	¹ Acceptable Range of % Recovery From EPA Methods (Aqueous Samples)	² Acceptable Range of % Recovery From <i>Standard Methods</i> (Aqueous Samples)
	Minimum	Maximum	Average				
Naphthalene	753	943	848	1064 (329)	125	*D – 122	21 – 133
Fluorene	70	100	85	121 (17)	142	D – 142	59 – 121
Phenanthrene	362	450	406	446 (112)	110	D – 155	54 -120
Anthracene	166	202	184	192 (37)	104	NG	NG
Fluranthene	601	701	651	406 (64)	62	14 – 123	26 – 137
Pyrene	542	620	581	189 (33)	33	D – 140	52 – 115
Benzo(a)anthracene	310	360	335	365 (65)	109	33 – 143	33 – 143
Chrysene	260	322	291	407 (116)	140	17 – 168	17 – 168
Benzo(b)flouranthrene	432	474	453	157 (107)	35	24 – 159	24 – 159
Benzo(a)pyrene	341	375	358	148 (74)	41	17 – 163	17 – 163
Indeno(1,2,3- cd)pyrene	284	398	341	116 (86)	34	NG	NG
Dibenz(a,h)anthracene	43	63	53	24 (15)	46	NG	NG
Benzo(g,h,i)perylene	262	352	307	133 (88)	43	NG	NG

*D: detected, result must be greater than zero

¹ acceptable range of recoveries for EPA method 610 for analysis of organic chemicals from municipal and industrial wastewater, as provided under 40 CFR part 136.1.

² acceptable range of recoveries for extraction of liquid sample as provided in the standard methods for the examination of water and wastewater (2005).

NG: Not given

Table 5.5 One-Way ANOVA P values for PAHs Concentrations of Coarser and Grinded Samples

PAH	ANOVA P Value (95% C.I)	
	710 - 1400 μ m	1400 - 2800 μ m
Naphthalene	0.122	0.128
Fluorene	0.064	0.118
Phenanthrene	0.618	0.052
Anthracene	0.776	0.204
Fluranthene	0.786	0.135
Pyrene	0.516	0.076
Benzo(a)anthracene	0.052	0.368
Chrysene	0.36	0.249
Benzo(b)flouranthrene	0.342	0.409
Benzo(a)pyrene	0.048	0.45
Indeno(1,2,3-cd)pyrene	0.175	0.67
Dibenz(a,h)anthracene	0.376	0.294
Benzo(ghi)perylene	0.100	0.660

5.9 Specifications of GC Column and Operating Conditions

The GC column employed in these analyses was a J&W Scientific DB-5MS + DG column from Agilent Technologies. The column has a 30 meter length, and a 0.25mm internal diameter and a film thickness of 0.25 μ m. The operating temperature range of the column is - 60 $^{\circ}$ C to 350 $^{\circ}$ C. GC operating conditions were:

Initial temperature:	50 $^{\circ}$ C, hold for 1.00 minute
Final temperature:	300 $^{\circ}$ C hold for 20.00min
Ramp 1:	20 $^{\circ}$ C/min from 50 $^{\circ}$ C to 140 $^{\circ}$ C
Ramp 2:	6 $^{\circ}$ C/min from 140 $^{\circ}$ C to 300 $^{\circ}$ C
Injector temperature:	300 $^{\circ}$ C
Injection volume:	1 μ L
Carrier gas:	Helium at 35 cm/sec
Mode:	Constant flow

5.10 Conclusions

Determining the fraction of the pollutant associated with particulate matter is very important as it can be a significant portion of the total pollutant mass. The most commonly used method (solids phase extraction, SPE) for analyzing the total PAH content of water samples may not be effective if the sample has a large fraction of particulate-bound PAHs, as the recovery of PAHs from sediment samples is poor when using SPE. The traditional methods for PAH analyses in sediments (such as Soxhlet extraction) are labor intensive, time consuming and also require large amounts of solvents which may cause environmental and operator safety problems.

The recently developed thermal desorption technique for PAH extraction from solid samples is effective and relatively rapid. During this research, the thermal desorption method showed good linearity over a wide range of concentrations of PAHs and sediment sample quantities. The calculated recoveries of the method were also in an acceptable range. The TD method requires less operator time and also produces the final analysis results faster compared to most other methods, especially if additional sample drying is not needed. The new technique doesn't involve any solvents and therefore avoids potential environmental and safety problems. However, this technique doesn't completely prevent fines from entering the capillary tube and the detector; therefore it requires more frequent maintenance of the GC/MS. The use of internal standards will help determine when maintenance is needed, based on monitoring the sensitivity of the detector. In addition, the TD method also requires very dry samples to prevent ice blockages in the inlet. Extra time and care is therefore needed in drying the samples before the thermal extraction process.

CHAPTER VI

URBAN STREAM SEDIMENT CHARACTERISTICS

Concentrations of PAHs associated with urban creek sediment particles may vary depending on the characteristics of the sediments. Some of the different characteristics of the sediments that may affect PAH associations that were investigated during this research included particle sizes, material composition and contamination history. This chapter describes these creek sediment characteristics.

6.1 Sediment Particle Sizes

Five samples from each of three creeks (Cribbs Mill Creek, Hunter Creek, and Carroll's Creek) were collected and processed for particle size distributions (psd). The samples were collected in pre-cleaned and autoclaved glass sample bottles using a manual dipper sampler made from polypropylene. The collected sediment samples were dried then sieved using a mechanical shaker. A set of sieves having openings of 45, 90, 180, 355, 710, 1400 and 2,800 μm were used to fractionate the sediment particles. In addition, large organic material (leaves and other debris) were manually separated from the largest particle fraction for separate analyses.

Figure 6.1 shows the particle size distributions, and Tables 6.1, 6.2, and 6.3 shows the percentage associations and standard deviations of associations of particles with

individual size ranges for these sediment samples. In all cases, the particles in the size range of 180 to 355 μm were most dominant in the sediments, as shown in the box and whisker plots on Figures 6.2, 6.3, 6.4. Overall, most of the particles are distributed in the size range of 90 to 710 μm .

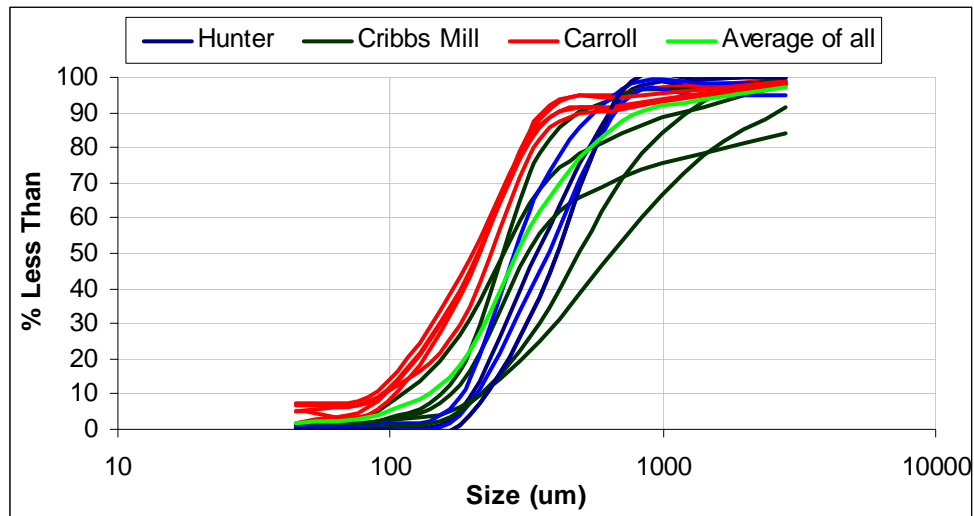


Figure 6.1 Observed creek sediment particle size distributions

Table 6.1 Percentage Associations and Standard Deviations of Particles of Individual Size Ranges for Cribbs Mill Creek Sediment Samples

Size Range (μm)	Percentage Associations						
	Sample 1	Sample 2	Sample 3	Sample 4	Sample 5	Average	Standard Deviation
<45	1.0	0.4	0.4	0.8	0.1	0.5	0.3
45 – 90	4.1	1.9	1.6	1.7	0.4	1.9	1.2
90 – 180	21.4	14.4	10.3	3.9	4.3	10.9	6.6
180 - 355	41.6	61.5	43.1	18.8	25.0	38.0	15.0
355 - 710	16.0	16.6	16.4	28.4	41.0	23.7	9.8
710 - 1400	7.7	1.6	6.5	24.0	22.0	12.4	8.9
1400 – 2800	6.0	1.7	5.9	13.9	7.1	6.9	3.9
>2800 (w/o LOM)	2.2	1.9	15.7	8.5	0.0	5.7	5.8
> 2800 LOM	0.9	1.2	1.0	2.2	1.5	1.4	0.5

LOM: large organic matter (mostly leaves, with some other organic debris)

w/o LOM: with the large organic matter removed

Table 6.2 Percentage Associations and Standard Deviation of Particles of Individual Size Ranges for Hunter Creek Sediment Samples

Size Range (μm)	Percentage Associations						
	Sample 1	Sample 2	Sample 3	Sample 4	Sample 5	Average	Standard Deviation
<45	0.2	0.1	0.3	0.1	0.1	0.2	0.1
45 – 90	0.7	0.4	1.0	0.2	0.2	0.5	0.3
90 – 180	4.4	3.7	7.5	1.1	1.0	3.5	2.4
180 - 355	46.2	40.4	59.4	36.3	36.2	43.7	8.6
355 - 710	42.8	48.1	28.6	58.3	58.3	47.2	11.1
710 - 1400	3.5	2.0	1.2	3.7	3.7	2.8	1.0
1400 – 2800	0.8	0.4	0.4	0.4	0.4	0.5	0.2
> 2800 (w/o LOM)	1.3	4.8	1.5	0.1	0.1	1.6	1.7
> 2800 LOM	1.0	0.2	0.2	0.1	0.2	0.4	0.3

LOM: large organic matter (mostly leaves, with some other organic debris)

w/o LOM: with the large organic matter removed

Table 6.3 Percentage Associations and Standard Deviation of Particles of Individual Size Ranges for Carroll's Creek Sediment Samples

Size Range (μm)	Percentage Associations						
	Sample 1	Sample 2	Sample 3	Sample 4	Sample 5	Average	Standard Deviation
<45	2.0	3.5	1.0	2.3	4.0	2.6	1.1
45 – 90	6.2	7.4	5.0	6.8	4.9	6.1	1.0
90 – 180	31.2	32.2	31.7	29.8	20.5	29.1	4.4
180 - 355	48.6	43.0	51.4	46.6	53.1	48.5	3.6
355 - 710	7.3	5.3	5.3	6.6	8.2	6.5	1.1
710 - 1400	2.4	3.2	2.4	3.3	4.4	3.1	0.7
1400 – 2800	1.6	3.4	1.8	2.3	3.3	2.5	0.7
>2800 (w/o LOM)	0.7	1.9	1.4	2.2	1.7	1.6	0.5
> 2800 LOM	0.0	0.3	0.1	0.2	0.1	0.1	0.1

LOM: large organic matter (mostly leaves, with some other organic debris)

w/o LOM: with the large organic matter removed

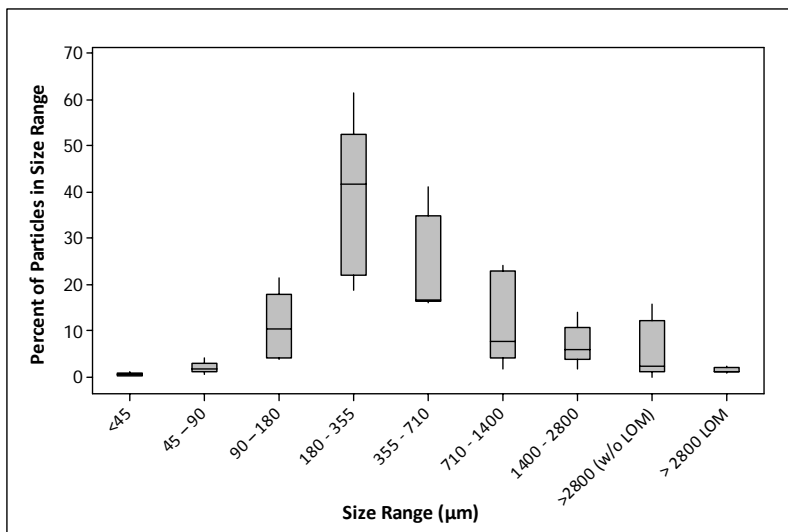


Figure 6.2 Box and whisker plots of particle sizes for Cribbs Mill Creek sediment samples.

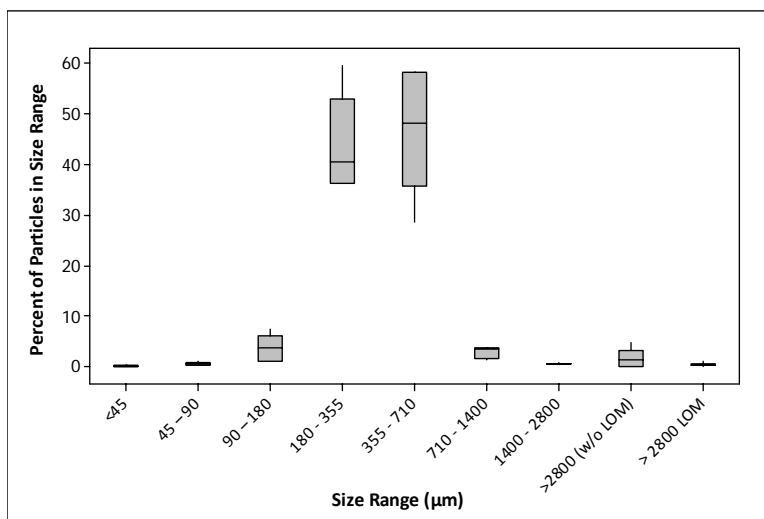


Figure 6.3 Box and whisker plots of particle sizes for Hunter Creek sediment samples

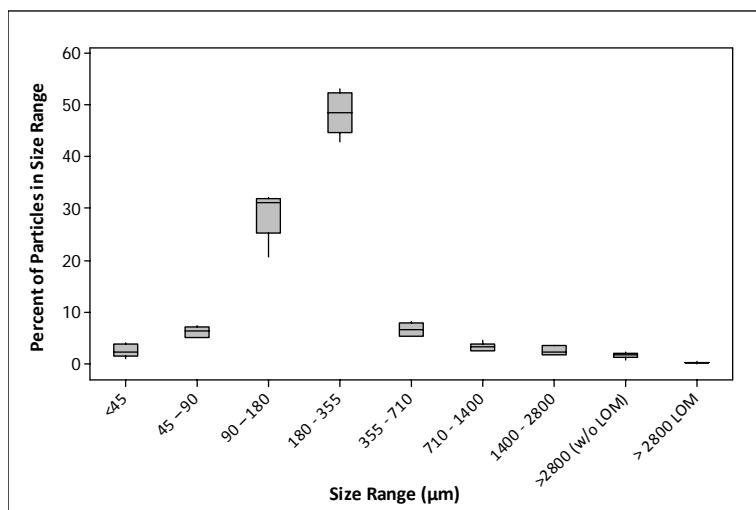


Figure 6.4 Box and whisker plots of particle sizes for Carroll's Creek sediment samples

6.2 Thermal Chromatography

A thermal chromatography method was developed by Ray (1997) to identify the components of urban dirt samples collected from Madison, WI, streets. This method was used to identify the major components of the sediment samples. Identifying the amount of leaves and grass material associated with the sample indicates the amount of organic material in the sample. A known amount of sediment sample was placed in a crucible that was heated progressively to higher temperatures, at set intervals, from 105 to 550°C. The heating process started with a temperature of 105°C to dry the samples. After 105°C, 240°C was the next temperature, then 365°C, then 470°C, and finally 550°C to complete the process. A heating time of 1 hour at each temperature was maintained to ensure stable weights. After each heating interval, the crucible (with sample) was cooled and weighed in order to determine the percent mass burned off for each material since the last temperature. Table 6.4 shows the corresponding temperatures where different material will be combusted, based on Ray's (1997) earlier work. Material lost between

240 and 365°C indicates the amount of leaves and grass associated with each particle size that may preferentially sorb PAHs, while material lost between 365 and 550°C indicates rubber and asphalt that likely has substantial PAH compounds as part of the component material.

Table 6.4 Ray (1997) Thermal Chromatography Method Parameters

Temperature (°C)	Material Lost at These Temperatures
up to 104	Moisture
104 - 240	Paper debris
240 - 365	Leaves and grass
365 - 470	Rubber
470 - 550	Asphalt
Above 550	Remaining material is inert (mostly soil)

A composite sediment sample from the five sediment samples collected at each sampling location was prepared and subjected to the thermal chromatography analysis. Tables 6.5, 6.6 and 6.7 show the thermal chromatography results for the sediment composite samples from Cribbs Mill Creek, Hunter Creek, and Carroll's Creek, respectively. These results show that almost all of the material was inert, except for the large leaf fraction. Figure 6.5 compares the percentage of the total weight loss over the temperature of 104 - 550°C for the different particle sizes and sampling locations. The sediment samples from Cribbs Mill Creek are found to have highest weight loss indicating that those sediment samples had higher proportions of combustible components compared to the sediment samples from other two creeks. Figure 6.6 compares the weight losses associated with the temperature range 240 – 365°C for the different creeks and sediments. Material lost in this temperature range was associated with organic material such as leaves and grass.

As described in the hypothesis under Experimental Design chapter, one could expect a greater organic content for the Carroll's Creek sediment as this creek had a past history of sewer overflow contamination. However, the thermal chromatography results showed that the sediment samples from Cribbs Mill Creek, which did not have any indications of sewage contamination, were associated with the highest weight loss over the temperature range of 240 – 365°C and hence are associated with higher proportions of organic material compared to other two creeks. It is expected that the Cribbs Mill Creek sediment samples did not have much mass contributions from bank erosion soil material, as the sampling stretch was concrete-lined. There was an obvious greater amount of algae present on the channel lining in Cribbs Mill Creek than in the other creeks. Lower proportions of organic material from Carroll's Creek may be because, the sediments at the sampling point were diluted with inert eroded material from the stream banks, the organic material from sewer overflows may have been scoured and transported from the area of historical contamination, or the organic material from the SSOs could have been degraded in the time since the overflows.

Table 6.5 Percentage of Weight Losses over Temperature Ranges for Cribbs Mill Creek Sediment Samples

Size Range (µm)	Percentage of Weight Loss (gm) Between Temperatures (°C)					Percentage of Inert Material
	105 – 240 (paper debris)	240 – 365 (leaves and grass)	365 – 470 (rubber)	470 – 550 (asphalt)	105 – 550 (total volatile content)	
<45	3.7	1.9	0.0	1.9	7.4	85.2
45 - 90	1.0	2.9	1.0	0.0	4.8	90.4
90 - 180	0.2	0.8	0.6	0.0	1.7	96.6
180 – 355	0.2	0.8	0.5	0.0	1.6	96.9
355 – 710	0.5	1.7	1.2	0.0	3.4	93.2

710 - 1400	2.6	5.1	3.3	0.0	11.0	77.9
1400 - 2800	3.8	8.6	0.0	6.0	18.4	63.2
>2800 (w/o LOM)	0.8	15.7	0.0	2.8	19.4	61.2
>2800 LOM	Na	Na	na	na	na	na

na: sample not available

LOM: large organic matter (mostly leaves, with some other organic debris)

w/o LOM: with the large organic matter removed

Table 6.6 Percentage of Weight Losses over Temperature Ranges for Hunter Creek Sediment Samples

Size Range (µm)	Percentage of Weight Loss (gm) Between Temperatures (°C)					Percentage of Inert Material
	105 – 240 (paper debris)	240 - 365 (leaves and grass)	365 – 470 (rubber)	470 – 550 (asphalt)	105 – 550 (total volatile content)	
<45	2.2	0.5	0.0	0.3	3.1	96.9
45 - 90	1.2	0.6	0.0	0.4	2.3	97.7
90 - 180	0.4	0.3	0.0	0.2	0.8	99.2
180 - 355	0.4	0.0	0.2	1.6	2.2	97.8
355 - 710	0.2	0.1	0.0	0.3	0.6	99.4
710 - 1400	1.8	2.0	0.7	1.0	5.5	94.5
1400 - 2800	2.7	6.0	2.3	0.7	11.6	88.4
>2800 (w/o LOM)	1.5	2.8	0.6	1.1	6.0	94.0
>2800 LOM	8.6	42.5	28.3	1.3	80.8	19.2

LOM: large organic matter (mostly leaves, with some other organic debris)

w/o LOM: with the large organic matter removed

Table 6.7 Percentage of Weight Losses over Temperature Ranges for Carroll's Creek Sediment Samples

Size Range (μm)	Percentage of Weight Loss (gm) Between Temperatures ($^{\circ}\text{C}$)					Percentage of Inert Material
	105 - 240 (paper debris)	240 - 365 (leaves and grass)	365 - 470 (rubber)	470 - 550 (asphalt)	105 - 550 (total volatile content)	
<45	1.1	1.0	0.9	0.8	3.9	96.1
45 - 90	0.5	0.8	0.5	0.7	2.5	97.5
90 - 180	0.4	0.3	0.4	0.3	1.4	98.6
180 - 355	0.4	0.5	0.3	0.4	1.5	98.5
355 - 710	0.5	0.6	0.5	0.2	1.9	98.1
710 - 1400	1.4	3.5	2.7	1.1	8.7	91.3
1400 - 2800	1.0	4.6	2.5	1.2	9.3	90.7
>2800 (w/o LOM)	0.8	1.0	7.0	0.7	9.5	90.5
>2800 LOM	20.4	33.5	3.9	0.9	58.6	41.4

LOM: large organic matter (mostly leaves, with some other organic debris)

w/o LOM: with the large organic matter removed

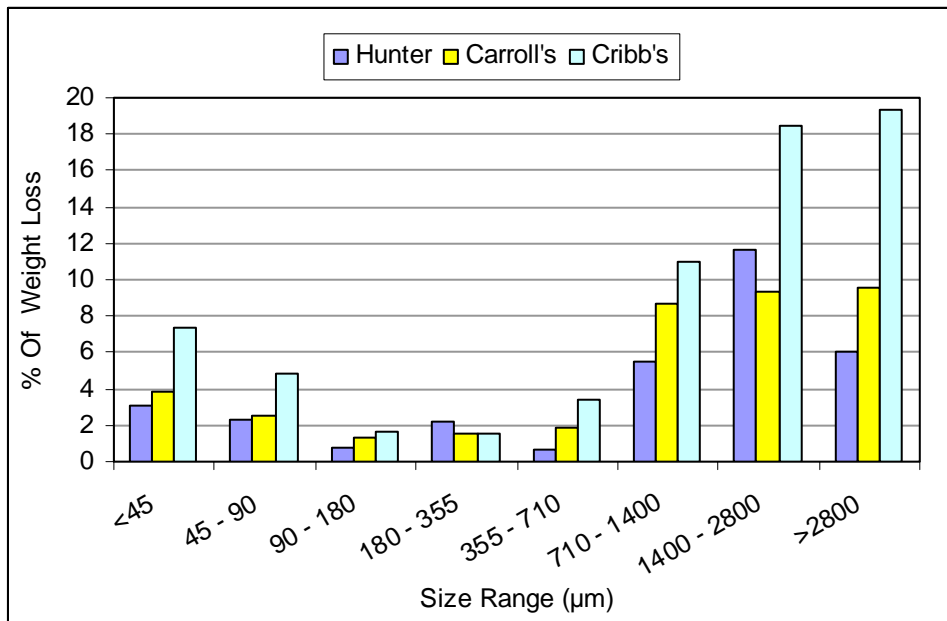


Figure 6.5 Comparison of weight loss over temperature range of 104 – 550°C (total volatile content)

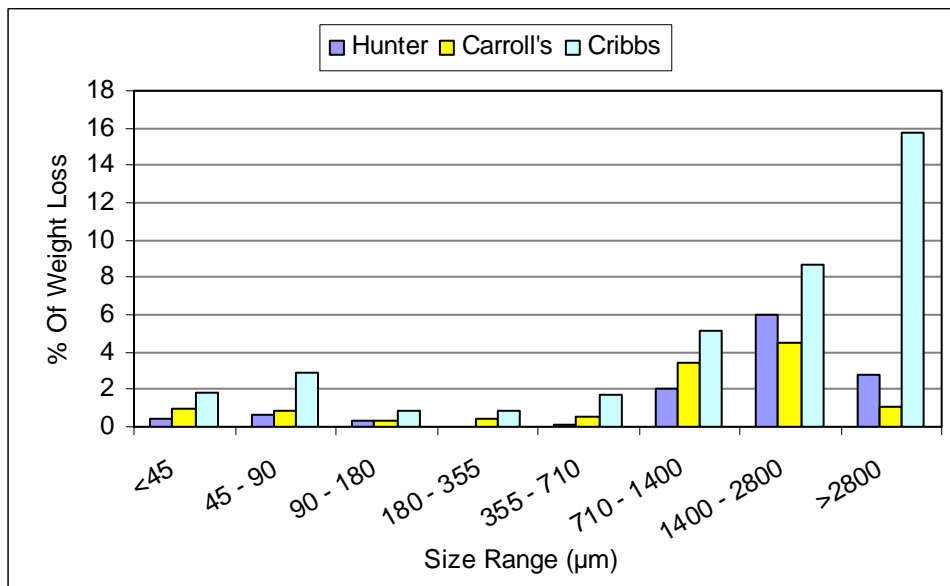


Figure 6.6 Comparison of weight loss over temperature range of 240 – 365°C (leaves and grass)

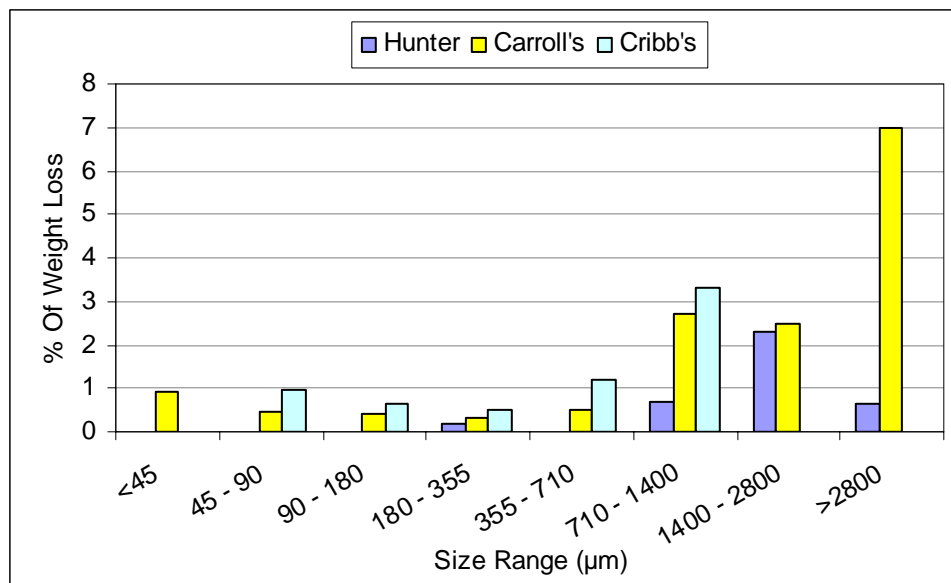


Figure 6.7 Comparison of weight loss over temperature range of 365 – 470°C (Rubber)

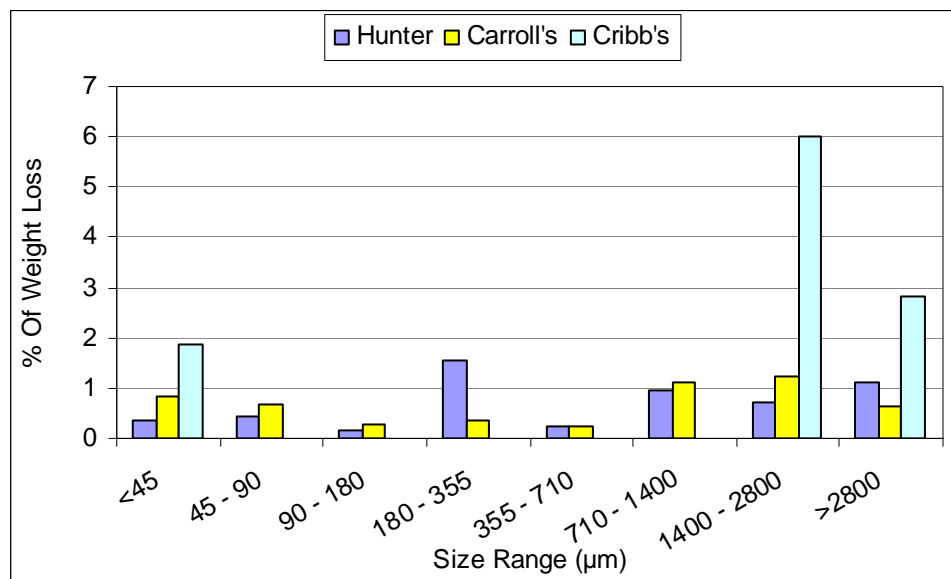


Figure 6.8 Comparison of weight loss over temperature range of 470 – 550°C (Asphalt)

6.3 Chemical Oxygen Demand

The size-fractionated sediment samples from the three creeks were analyzed for Chemical Oxygen Demand (COD) using HACH method 8000, as shown on Tables 6.8, 6.9 and 6.10. These results showed similar trends from the three creeks. Smaller ($< 90\mu\text{m}$) and larger ($> 355\mu\text{m}$) particles were found to have higher concentrations of COD (mg COD/kg dry sediment) compared to intermediate sized particles. This trend is similar to total volatile content observations made previously. The accumulative COD mass, with respect to the observed psd of the sediment particles, showed that particles of $355\mu\text{m}$ in size were associated with the median mass of the creek sediment COD (Figure 6.9). Half of the mass is associated with smaller particles and half is associated with larger particles. Figure 6.10 shows that expect for the size range $710 - 1400 \mu\text{m}$, the observed COD values for Cribbs Mill Creek were found to be higher than the observed COD values of other two creeks. Regression graphs, Figures 6.11, 6.12, and 6.13 show direct correlations between total weight loss between 104 and 550°C and on the sediment COD concentrations. The ANOVA P values of regression shown in the table were also well below 0.05 indicating strong relations between weight loss of sediments on heating and associated COD concentrations. The constant terms (y-intercepts) in the regression equations for Hunter Creek and Carroll's Creek were found to be insignificant ($P>0.05$) and the regression equations therefore do not include this term (the regression line was forced to pass through the origin). It is likely that the thermal tests are good indicators of sediment organic content, and can also help identify major volatile components of the material.

Table 6.8 Observed COD Values of Sediment Samples from Cribbs Mill Creek

Size Range (μm)	COD (mg COD/kg dry sediment)						
	Sample 1	Sample 2	Sample 3	Sample 4	Sample 5	Average	Standard Deviation
<45	5.2E+07	1.4E+08	8.7E+07	1.3E+08	2.0E+08	1.2E+08	5.6E+07
45 – 90	3.3E+07	1.3E+08	4.6E+07	1.3E+08	1.5E+08	9.5E+07	5.2E+07
90 – 180	1.3E+07	5.1E+07	3.5E+07	5.5E+07	7.1E+07	4.5E+07	2.2E+07
180 – 355	7.1E+06	5.6E+07	2.8E+07	4.1E+07	7.6E+07	4.2E+07	2.6E+07
355 – 710	4.5E+07	2.9E+07	6.6E+07	2.9E+07	1.3E+08	6.0E+07	4.2E+07
710 – 1400	9.5E+07	1.5E+08	1.3E+08	4.2E+07	1.6E+08	1.2E+08	4.7E+07
1400 – 2800	1.4E+08	1.1E+08	1.5E+08	1.2E+08	1.3E+08	1.3E+08	1.7E+07
>2800 (w/o LOM)	1.6E+08	2.0E+08	1.6E+08	1.1E+08	1.3E+08	1.5E+08	3.3E+07
>2800 LOM	1.2E+09	1.1E+09	2.0E+09	1.9E+09	2.0E+09	1.6E+09	4.5E+08

LOM: large organic matter (mostly leaves, with some other organic debris)

w/o LOM: with the large organic matter removed

Table 6.9 Observed COD Values of Sediment Samples from Hunter Creek

Size Range (μm)	COD (mg COD/kg dry sediment)						
	Sample 1	Sample 2	Sample 3	Sample 4	Sample 5	Average	Standard Deviation
<45	7.5E+07	3.9E+07	4.4E+07	6.5E+07	5.2E+07	5.5E+07	1.5E+07
45 – 90	4.4E+07	2.8E+07	3.1E+07	8.4E+07	2.2E+07	4.2E+07	2.5E+07
90 – 180	1.3E+07	7.8E+06	1.0E+07	1.4E+07	7.9E+06	1.1E+07	3.0E+06
180 – 355	8.6E+05	3.4E+06	4.0E+06	4.1E+06	4.9E+06	3.4E+06	1.5E+06
355 – 710	4.6E+06	5.0E+06	6.6E+06	6.2E+06	1.2E+07	6.9E+06	3.1E+06
710 - 1400	2.9E+07	6.6E+07	3.1E+07	1.9E+07	1.4E+08	5.7E+07	5.0E+07
1400 – 2800	1.1E+08	7.0E+07	9.1E+07	5.2E+06	1.8E+08	9.1E+07	6.2E+07
>2800 (w/o LOM)	3.9E+07	4.9E+07	3.3E+06	4.7E+07	5.4E+07	3.8E+07	2.0E+07
>2800 LOM	1.2E+09	1.3E+09	1.4E+09	1.6E+09	1.7E+09	1.5E+09	2.1E+08

LOM: large organic matter (mostly leaves, with some other organic debris)

w/o LOM: with the large organic matter removed

Table 6.10 Observed COD Values of Sediment Samples from Carroll's Creek

Size Range (µm)	COD (mg COD/kg dry sediment)						
	Sample 1	Sample 2	Sample 3	Sample 4	Sample 5	Average	Standard Deviation
<45	2.2E+07	6.5E+07	4.3E+07	5.0E+07	5.9E+07	4.8E+07	1.7E+07
45 - 90	1.4E+07	2.1E+07	2.4E+07	3.2E+07	3.1E+07	2.4E+07	7.6E+06
90 - 180	1.2E+07	1.1E+07	1.1E+07	1.3E+07	1.7E+07	1.3E+07	2.6E+06
180 - 355	9.4E+06	1.3E+07	1.1E+07	1.7E+06	1.6E+07	1.0E+07	5.4E+06
355 - 710	3.4E+07	4.3E+07	3.8E+07	5.7E+07	5.7E+07	4.6E+07	1.1E+07
710 - 1400	1.3E+08	9.2E+07	1.1E+08	1.7E+08	1.2E+08	1.2E+08	2.9E+07
1400 - 2800	6.0E+07	1.1E+08	1.7E+08	8.7E+07	1.1E+08	1.1E+08	3.9E+07
>2800 (w/o LOM)	1.1E+08	7.7E+07	9.9E+07	9.3E+07	1.1E+08	9.7E+07	1.3E+07
>2800 LOM	1.3E+09	1.2E+09	1.0E+09	1.5E+09	1.3E+09	1.3E+09	1.9E+08

LOM: large organic matter (mostly leaves, with some other organic debris)

w/o LOM: with the large organic matter removed

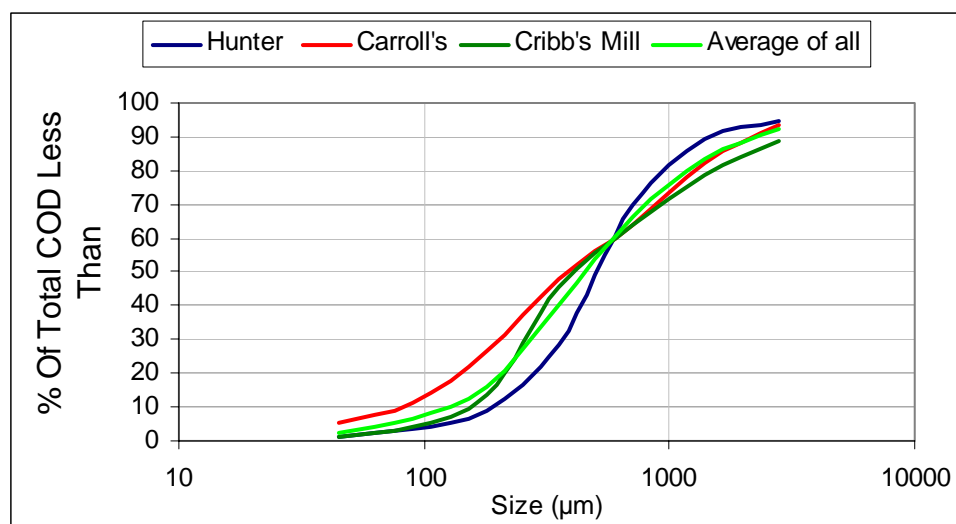


Figure 6.9 Observed cumulative COD of creek sediments by particle size

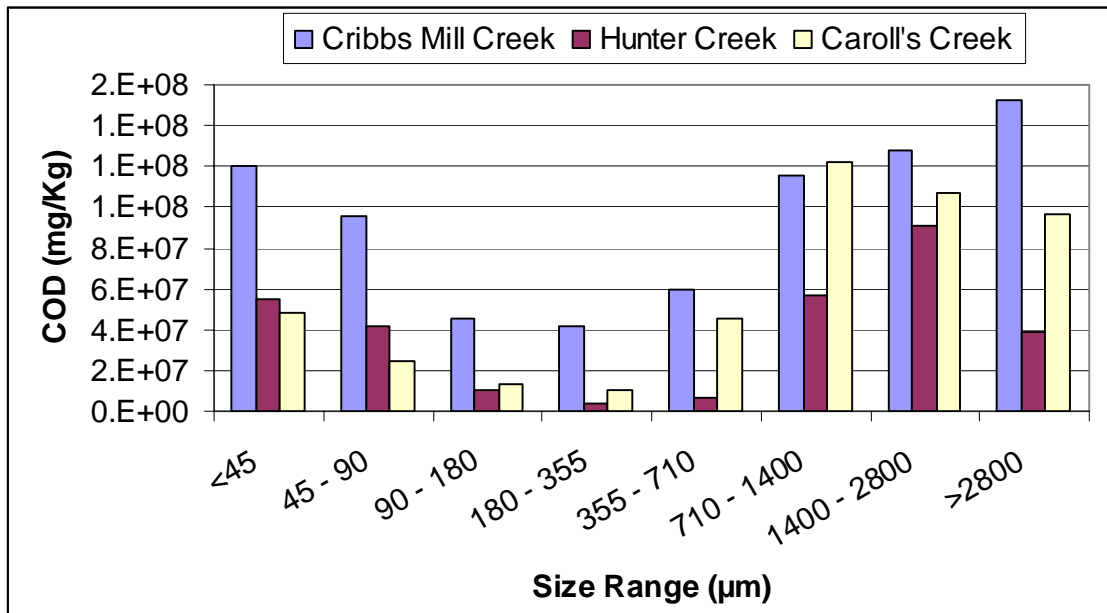


Figure 6.10 Comparison of COD results from three creeks by sediment particle size category

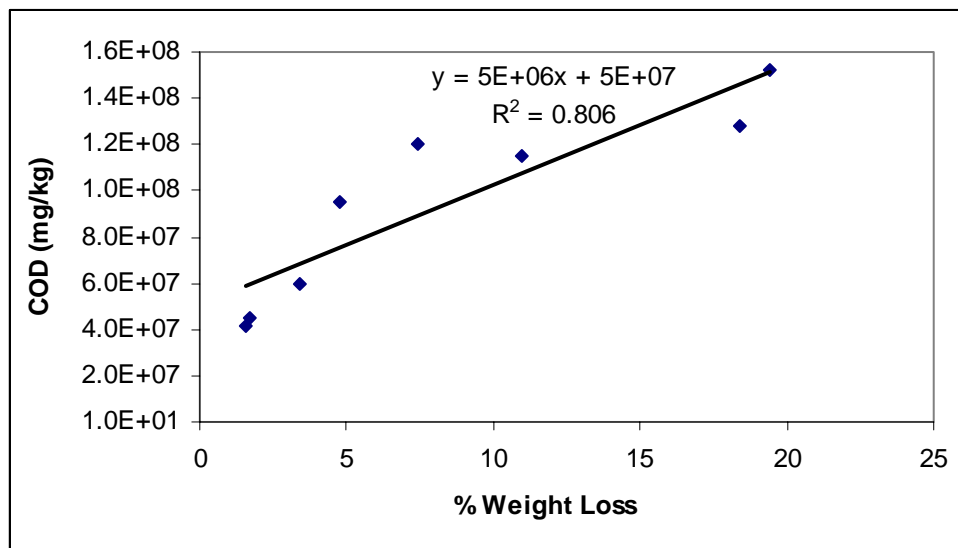


Figure 6.11 Weight loss over temperature range of 104 - 550°C versus observed COD for Cribbs Mill Creek

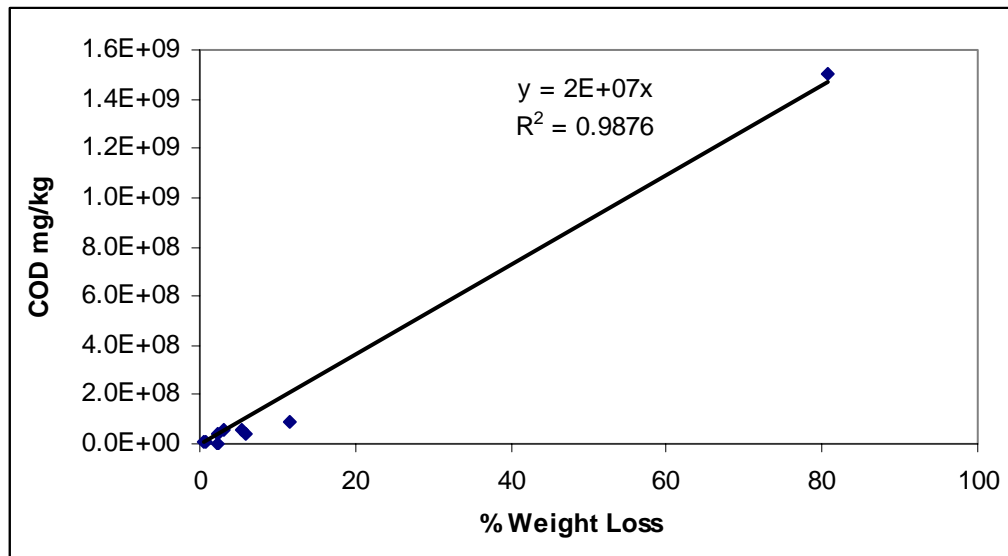


Figure 6.12 Weight loss over temperature range of 104 - 550°C versus observed COD for Hunter Creek

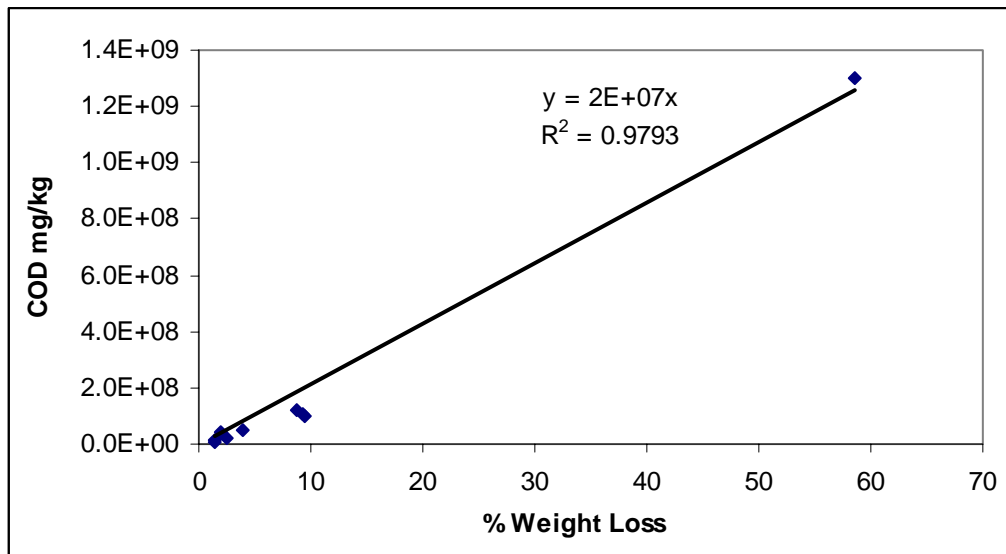


Figure 6.13: Weight loss over temperature range of 104 - 550°C versus observed COD for Carroll's Creek

Table 6.11 ANOVA P Values of Regression of COD and Sediment Material Weight Loss on Heating

Creek	P Value	
	Slope	Constant
Cribbs Mill Creek	0.002	0.004
Hunter Creek	0.000	-
Carroll's Creek	0.001	-

6.4 Conclusions

Analysis of sediment samples indicated that most of the particles were distributed in the 90 to 710 μm size range. Thermal chromatography results showed that the samples from Cribbs Mill creek have higher percentage of weight losses of material on heating (except for size fraction 180 – 355 μm) (Figure 6.5), indicating these contain larger fractions of combustible material compared to the other two creeks. The higher weight losses in the 240 – 365 °C temperature range (associated with organic material) for Cribbs Mill creek samples compared to other two creeks may be because these sediment samples were collected on a concrete lined channel section and were not effected by channel erosion products. The concrete channel also had obvious large quantities of attached algae that may also have affected the samples. The sediments from other two creeks are affected by bank eroded material in addition to discharged sediments, and had larger inert fractions.

Overall, smaller and larger sediment particles from the three urban creeks were found to have higher weight losses on heating compared to medium sized particles. In similar terms with thermal chromatography results, the smaller and larger particles were found to have higher concentrations of COD compared to the medium sized particles. The linear regression ANOVA P values (<0.05) indicated that the sediments weight loss

on heating is strongly related to their associated COD concentrations. These data were compared to the PAH concentrations data in the next chapter to identify statistically valid relationships between site conditions, sediment characteristics, and PAH concentrations.

CHAPTER VII

PAHs CONCENTRATIONS ON SEDIMENT PARTICLES

Sediment samples collected from the three creeks were fractionated based on particle sizes. In addition, large organic material (LOM) (mostly pieces of leafs and grass clippings) were separated from the largest sieve size ($> 2800\mu\text{m}$) for separate analyses. The fractionated particles were subjected to TD/GC/MS for PAH analyses. A total of thirteen selected PAHs were analyzed in all the sample fractions. Resultant PAH concentrations were statistically examined to understand the effect of source areas and selected sediment characteristics on the measured concentrations.

The observed PAH concentrations for the different sediment particle sizes and associated standard deviations are shown in Tables C.1 through C.39. Figures C.14 through C.26 are box and whisker plots of the PAH concentrations associated with the different sediment fractions. As expected, there were large variations in the measured PAH concentrations. The PAH concentrations were therefore tested for their normality for each site and size range using probability plots and Anderson Darling statistical tests. These plots are shown as Figures C.1 through C.13. Other than a few cases (whose P value < 0.05), most of the PAH concentration groups were found to be normally distributed.

7.1 Testing the Concentrations for Variability

A Two-Way ANOVA analysis was conducted for each individual analyte to test the variability of the concentrations based on particle sizes, sediment location, and their interaction. The ANOVA analysis results are summarized in Table 7.1. This analysis shows that the particle size affects the concentration of analytes (low P value). Other than naphthalene, fluorene, phenanthrene and indeno(1,2,3-cd)pyrene, all the other PAH analytes were also found to be affected by the location of sediment samples. The interaction of particle size and sediment location were found to significantly affect the concentrations of phenanthrene, fluranthene, pyrene, benzo(a)anthracene, chrysene, benzo(a)pyrene, and dibenz(a,h)anthracene.

Table 7.1 Two-Way ANOVA P Values for Analyte Concentrations

PAH	P Value		
	Size	Location	Size*Location
Naphthalene	0.000	0.088	0.116
Fluorene	0.000	0.721	0.481
Phenanthrene	0.000	0.389	0.043
Anthracene	0.000	0.032	0.821
Fluranthene	0.000	0.000	0.000
Pyrene	0.000	0.000	0.000
Benzo(a)anthracene	0.000	0.005	0.002
Chrysene	0.000	0.004	0.000
Benzo(b)flouranthrene	0.000	0.002	0.254
Benzo(a)pyrene	0.004	0.032	0.022
Indeno(1,2,3-cd)pyrene	0.000	0.284	0.250
Dibenz(a,h)anthracene	0.000	0.019	0.002
Benzo(ghi)perylene	0.000	0.041	0.493

7.1.1 Comparing the Concentrations at the Three Creeks

One Way ANOVA analysis of the analyte concentrations for the sediment particle sizes from the three creeks showed that some of the analytes had significant difference in

their concentrations between sediment locations. The analysis results are summarized in Table 7.2. The significantly different sediment locations for each analyte and size range were identified using normal probability plots (having 95% confidence intervals) of the concentrations. The probability plots 25th and 75th percentile ranges were used to visually identify overlapping distributions or separate distributions. If the probability plot distributions for the three creeks were found to be all distinctly separate from each other, the one with the higher and the one with the lower concentrations were noted on the table. If only one site was distinct from the others on the probability plots, then that site was also noted, including if it was higher or lower than the others. In addition, box and whisker plots comparing analyte concentrations for each size range for each of the three creeks are shown in Figures C.27 through C.143.

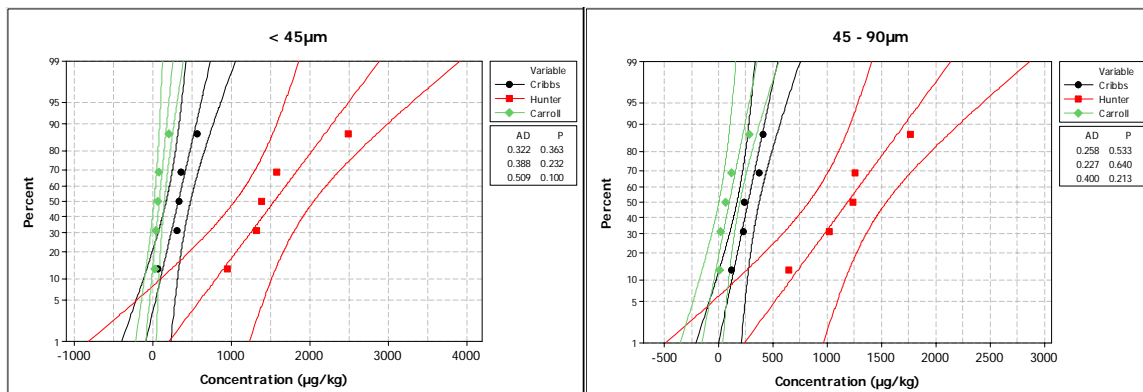


Figure 7.1 Probability plots of pyrene concentrations (for < 45 μm all creeks were different, for 45 - 90 μm Hunter Creek was higher than others)

There were more significant differences between the creek locations for the smaller particle sizes (<45 and 45 – 90 μm) than for the other sizes. A few PAHs had differences for the 90-180 μm size range, but only fluoranthene had differences for many

of the larger particle size ranges. Indeno(1,2,3-cd)pyrene and dibenz(a,h)anthracene did not have any significant differences between the locations for any of the particle size ranges. Hunter's Creek was noted as being the most common creek with higher PAH concentrations, most likely due to the obvious hydrocarbon contamination from the creek-side businesses.

Table 7.2. One Way Location ANOVA Results Comparing Analyte Concentrations by Particle Sizes

PAH	ANOVA P Values (95 C.I) by Particle Sizes (µm)								
	< 45	45 - 90	90 – 180	180 - 355	355 - 710	710 – 1400	1400 - 2800	> 2800 (w/o LOM)	LOM
Naphthalene	0.189	0.238	0.039 (Hunter, Low)	0.463	0.859	0.345	0.249	0.547	0.167
Fluorene	0.382	0.020 (Hunter, High)	0.572	0.616	0.594	0.744	0.449	0.151	0.447
Phenanthrene	0.002 (Cribbs,Low)	0.002 (Cribbs, Low)	0.360	0.281	0.310	0.312	0.248	0.846	0.014
Anthracene	0.374	0.010 (Carroll's, Low)	0.030 (Carroll's, Low)	0.304	0.232	0.215	0.113	0.379	0.748
Fluoranthene	0.001 (Hunter, High)	0.000 (Hunter, High)	0.001(ALL) (Carroll's, Low) (Hunter, High)	0.019 (Hunter, High)	0.036 (Hunter, High)	0.033 (Carroll's, Low)	0.029 (Carroll's, Low)	0.189	0.330
Pyrene	0.000 (All) (Carroll's, Low) (Hunter, High)	0.000 (Hunter, High)	0.040 (Hunter, High)	0.131	0.260	0.352	0.411	0.203	0.622
Benzo(a) anthracene	0.000 (All) (Carroll's, Low) (Hunter, High)	0.044 (All) (Carroll's, Low) (Hunter, High)	0.168	0.260	0.209	0.889	0.604	0.444	0.123

Continuation of above table

PAH	ANOVA P Values (95 C.I) by Particle Sizes (μm)								
	< 45	45 - 90	90 - 180	180 - 355	355 - 710	710 - 1400	1400 - 2800	> 2800 (w/o LOM)	LOM
Chrysene	0.000 (Hunter, High)	0.028 (Hunter, High)	0.201	0.080	0.106	0.266	0.718	0.475	0.071
Benzo(b)fluoranthrene	0.010 (Carroll's, Low)	0.011 (Hunter, High)	0.156	0.091	0.352	0.001	0.145	0.309	0.722
Benzo(a)pyrene	0.021 (Hunter, High)	0.155	0.721	0.098	0.898	0.123	0.165	0.009	0.921
Indeno(1,2,3-cd)pyrene	0.716	0.428	0.098	0.549	0.098	0.705	0.273	0.367	0.306
Dibenz(a,h)anthracene	0.062	0.043	0.620	0.251	0.387	0.177	0.194	0.255	0.216
Benzo(ghi)perylene	0.024 (Cribbs, High)	0.086	0.692	0.186	0.443	0.842	0.585	0.437	0.350

Many of the PAHs had a coefficient of variation (COV, or the ratio of the standard deviation to the average value) of 0.5 to 0.75. With 5 samples in each category, Figure 7.2 shows that this sampling effort can detect differences of about 100%, or greater (the average value of one set would have to be twice, or larger, than the average value from the other set). For some PAHs, the COV was smaller, at about 0.3. In that case, differences of about 40% could be detected. If differences as small as 25% are to be detected, and the COV is 0.75, then more than 100 sample pairs would be needed, clearly an unusually large sampling and analytical effort. For the purposes of this research, differences in average PAH concentrations between groups in the range of 40 to 100% are suitable, with a confidence of 95% and a power of 80%. When subgroups were not determined to be significantly different, they can be combined, resulting in larger sample numbers in each group, and increasing the sensitivity of the tests.

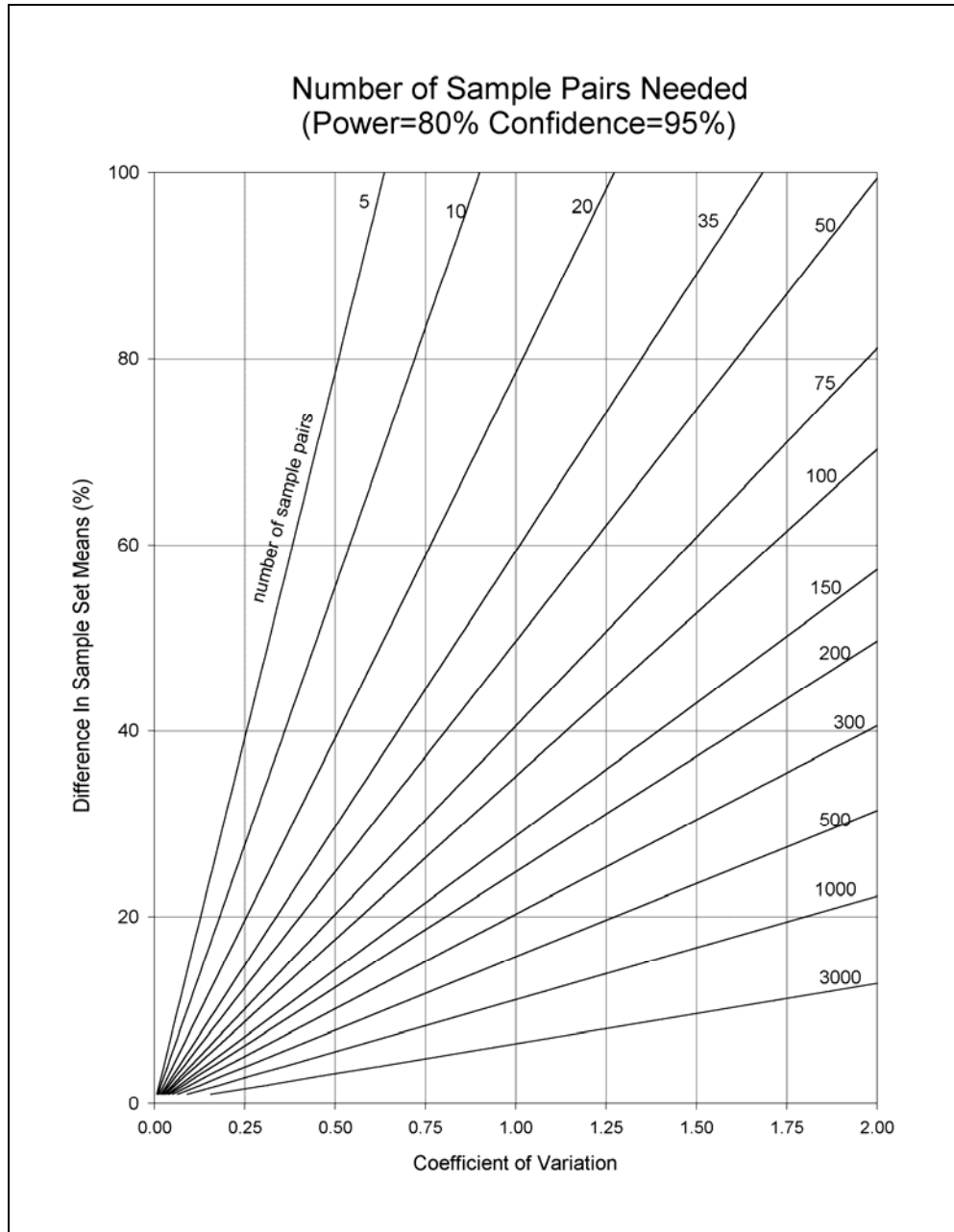


Figure 7.2 Sample Effort Needed for Paired Testing (Power of 80% and Confidence of 95%) (Burton and Pitt 2002)

7.1.2 Comparing PAH Concentrations for Different Particle Size Ranges

To check the effect of particle sizes on associated PAHs concentrations one-way

ANOVA analyses were conducted on individual analyte concentrations associated with different particle sizes at each sediment location. All of the PAHs, at all three creeks had significant differences in concentrations by particle size, with the exceptions of naphthalene at Cribbs Mill Creek, benzo(a)pyrene, indeno(1,2,3-cd)pyrene, benzo(ghi)perylene at Hunter Creek and benzo(ghi)perylene at Carroll's Creek (Table 7.3). Cluster analyses were performed on the PAH concentrations to see the similarities between the analyte concentrations for the different particle sizes at each creek site. The cluster dendograms are shown in Figures 143 through 146. The summary tables for the cluster groupings are shown on Tables 7.4 through 7.6. The particle size groups having similarity levels less than 75% were categorized into single groups. For Cribbs Mill Creek, for most of the analytes, there were two groups of concentrations by particle sizes. In almost all the cases, the large-sized LOM fraction was found to be a separate group from all the other sizes. In few cases, the larger sizes (710 – 1400 μm and 1400 – 2800 μm) along with LOM, formed a single group separate from the other particle sizes. At Hunter Creek, the large-sized LOM fraction still occurred as a separate group for most of the analytes, while in some cases, the smaller sized fractions were grouped with the LOM fraction. It was again mostly the large-sized LOM fraction which was separated as a single group and all the other sizes were placed in another single group for Carroll's Creek.

The box and whisker plots of the concentrations by size for all the analytes and creeks individually are shown in Figures C.1 through C.39. These plots do not include the large-sized LOM fraction and better indicate the PAH concentration variations for the particle sizes in their absence. In most cases, the large-sized LOM was present in only

very small amounts, so the other particle sizes are more significant from an overall mass perspective. As an example, Hunter's Creek, with a history of contamination of hydrocarbons from creek-side business, shows obviously higher concentrations than the other creeks for a number of PAHs (including naphthalene, fluorene, fluoranthene, pyrene, benzo(a)anthracene, chrysene, and benzo(b)fluoranthene), especially for the smaller particles sizes. Cribbs Mill Creek and Carroll's Creek appear to be more even in concentrations for different particle sizes, while Cribbs Mill Creek has generally higher PAH concentrations than Carroll's Creek. The Cribbs Mill Creek sampling location was in a long concrete channel having no opportunity for bank erosion material affecting the sediment concentrations, and the concrete lining had obvious algae levels that could have preferentially sorbed PAHs.

Table 7.3. One Way ANOVA P Values for PAHs Concentration by Particle Size

PAH	P Value (95 C.I.)		
	Cribbs Mill Creek	Hunter Creek	Carroll's Creek
Naphthalene	0.324	0.000	0.000
Fluorene	0.000	0.000	0.000
Phenanthrene	0.000	0.000	0.000
Anthracene	0.000	0.000	0.000
Fluoranthene	0.000	0.000	0.000
Pyrene	0.000	0.000	0.000
Benzo(a)anthracene	0.000	0.000	0.000
Chrysene	0.000	0.001	0.000
Benzo(b)fluoranthrene	0.000	0.011	0.000
Benzo(a)pyrene	0.039	0.060	0.000
Indeno(1,2,3-cd)pyrene	0.002	0.437	0.000
Dibenz(a,h)anthracene	0.024	0.010	0.000
Benzo(ghi)perylene	0.004	0.118	0.565

Table 7.4 Summary of Cluster groups for Cribbs Mill Creek Sediments (at similarity levels greater than 75%)

PAH	Naphthalene			Fluorene		Phenanthrene		
Groups by Size Range (µm)	LOM	710 - 1400, 1400 - 2800	Others	LOM	Others	LOM	Others	
Groups by Size Range (µm)	Anthracene			Fluoranthene		Pyrene		
	LOM	710 - 1400, 1400 - 2800	Others	LOM	Others	LOM	Others	
Groups by Size Range	Benzo(b)fluoranthene		Benzo(a)anthracene		Chrysene		Benzo(ghi)perylene	
	LOM, > 2800 (w/o LOM), 1400 - 2800	Others	LOM	Others	LOM	Others	LOM	Others
PAH	Benzo(a)pyrene		Indeno(1,2,3-cd)pyrene			Benz(a,h)anthracene		
Groups by Size Range (µm)	LOM, 1400 – 2800	Others	LOM, 1400 - 2800, 90 - 180, <45	All others are different from each other		LOM	1400 - 2800	Others

Table 7.5 Summary of Cluster groups for Hunter Creek Sediments (at similarity levels greater than 75%)

PAH	Naphthalene		Fluorene			Phenanthrene				
Groups by Size Range (µm)	LOM	Others	LOM	90-180, 180 – 355, 355 – 710, 710 – 1400, > 2800 (w/o LOM)	All others different from each other	LOM	< 45, 45 - 90	Others		
PAH	Anthracene		Fluoranthene				Pyrene			
Groups by Size Range (µm)	LOM	Others	< 45	45 - 90, LOM	90 - 180	Others	LOM	< 45, 45 - 90	90 - 180	Others

PAH	Benzo(b)fluoranthene			Benzo(a)anthracene			Chrysene				Benzo(ghi)perylene		
Groups by Size Range	LOM	< 45, 45 - 90, 90 - 180	Others	LOM	< 45, 45 - 90	Others	LOM, < 45, 45 - 90	90 - 180	180 - 355, 355 - 710, 1400 - 2800	710 - 1400	LOM	< 45	Others
PAH	Benzo(a)pyrene				Indeno(1,2,3-cd)pyrene			Benz(a,h)anthracene					
Groups by Size Range (µm)	LOM	45 - 90, < 45	1410 - 2800	Others	< 45, 45 - 90, >2800	180 - 355, 355 - 710	All others are different from each other		180 - 355, 355 - 710, 710 - 1400, > 2800		All others different from each other		

Table 7.6 Summary of Cluster groups for Carroll's Creek Sediments (at similarity levels greater than 75%)

PAH	Naphthalene			Fluorene			Phenanthrene		
Groups by Size Range (µm)	LOM	Others		LOM	Others		LOM	Others	
PAH	Anthracene			Fluoranthene			Pyrene		
Groups by Size Range (µm)	LOM	Others		LOM	Others			LOM	Others
PAH	Benzo(b)fluoranthene		Benzo(a)anthracene		Chrysene		Benzo(ghi)perylene		
Groups by Size Range	LOM	Others	LOM	Others	LOM	Others	LOM	90 - 180	Others
PAH	Benzo(a)pyrene			Indeno(1,2,3-cd)pyrene		Benz(a,h)anthracene			
Groups by Size Range (µm)	< 45, 710 - 1400, 1400 - 2800, >2800	45 - 90, 355 - 710	All others are different from each other		45 - 90, 180 - 355, 355 - 710, 710 - 1400, 1400 - 2800, >2800	All others are different from each other		LOM	Others

7.2 Relationships between COD and PAH Concentrations

Statistical analyses were conducted to test the possible relationship between COD and PAHs concentration associated with sediment particles, as the earlier fugacity calculations indicated an important relationship between these parameters. As described in chapter VI, each of the sediment size fractions from each site were also analyzed for COD concentrations. The ratios of PAH concentration to COD concentration for each sample were calculated, and are shown on Tables C.40 through C.42. Particle size and location were two variables that were examined using two-way ANOVA analyses to identify significant grouping of these concentration ratios. The analysis results are shown in Table 7.7. From this ANOVA analysis, ratios for most of the analytes were found to be significantly different based on the size or location, with only three PAHs having significant interaction terms. The large number of significant effects implies that the COD does not have a constant effect on the PAH concentrations.

Table 7.7 Two-Way ANOVA Analysis Results for PAH to COD Concentration Ratios

PAH	2 Way ANOVA P Value		
	Size	Location	Size*Location
Naphthalene	0.255	0.194	0.405
Fluorene	0.019	0.000	0.693
Phenanthrene	0.012	0.061	0.055
Anthracene	0.054	0.000	0.053
Fluranthene	0.061	0.000	0.051
Pyrene	0.017	0.000	0.027
Benzo(a)anthracene	0.014	0.801	0.057
Chrysene	0.003	0.001	0.038
Benzo(b)flouranthrene	0.003	0.078	0.470
Benzo(a)pyrene	0.000	0.002	0.239
Indeno(1,2,3-cd)pyrene	0.056	0.002	0.063
Dibenz(a,h)anthracene	0.000	0.000	0.012
Benzo(ghi)perylene	0.079	0.082	0.229

Regression analyses examining the relationships between COD and PAH concentrations was also conducted for each particle size and site for each PAH. The analysis results are shown in Tables C.43 through C.45. In slightly more than half of the cases, the response factor (the slope term) was found to be significant ($P < 0.05$); out of a total of 351 cases tested (9 different sizes, 13 analytes and 3 creeks) 193 cases were found to have significant response factors (55% of the total cases). However, when only examining the large-sized LOM fraction, the results were more obvious; out of a total of 39 conditions (13 PAHs and 3 creeks), 35 cases, or 90%, showed significant first-order polynomial relationships between COD and associated PAH concentrations. The TD/GC/MS analytical results found that the large-size LOM fractions had higher concentrations of PAHs compared to other particle sizes. Also, the large-size LOM fractions were also found to have higher concentrations of COD than the other sizes. This indicates that COD (and therefore organic fraction) may influence the sediment PAH concentrations.

7.3 Summary

PAH analyses were conducted on size fractionated sediment particles from three urban creeks in the Tuscaloosa/Northport, AL, area. The observed concentrations of each analyte showed less variability within each size range compared to the variability between most of the creek locations and for many of the different size ranges. The observed PAH concentrations were also normally distributed within each particle size group. Two-way ANOVA analyses of the data showed that the differences in the

observed concentration of analytes were found to be significant for many of the comparisons between locations and particle size. With few exceptions, PAH concentrations at the three locations were found to be different. One-way ANOVA analyses and normal probability plots were used to identify which sites were different from each other. For each individual analyte, one-way ANOVA and cluster analyses were used to identify the significantly different size fraction groups for each creek. Two-way ANOVA analyses examined the ratios of PAH to COD concentrations. Regression analyses of COD vs. the PAH concentrations did not show any consistent relationship. However, about 90% of the cases showed significant relationships when just the large-sized LOM fractions were considered alone, showing a strong relationship between COD and PAH concentrations when the organic content was high.

CHAPTER VIII

CONCLUSIONS

As discussed in chapter II, PAH contamination poses a threat to the environment due to their toxic and carcinogenic effects (USEPA 1997, CA EPA 1990a and 1990b, ATSDR 1995), thus necessitating effective treatment methods when they are present in problematic quantities. Understanding the distribution of contaminants between the water and sediment phases is important when selecting the best treatment approach. Because of their low solubility and high Log K_{OC} values, most of the PAHs in aquatic systems are mainly associated with suspended particles. Field observations have also shown that the main fate of PAHs in the aquatic environment is controlled by their association with the particulate matter (Pitt et al. 1999, Hwang et al. 2005).

Chapter III outlined the research hypotheses and the experimental design. Sediment samples were collected from three different creeks that were affected by different historical sources. The samples were all separated into different particle size groups for analyses.

Modeling partitioning of the PAHs and comparing the predictions with actual field observations from prior research was shown in chapter IV. The fugacity models, even though they predicted that the majority of the PAHs would be associated with particulates, were found to under-predict the particulate-bound fraction of the PAHs.

Chapter V presented the development of the TD/GC/MS analytical method and its performance when analyzing NIST standard sediments for PAH contamination. The method was found to be sensitive, with good recoveries. The method is relatively rapid and requires no organic solvents. However, sulfite interference needs to be controlled by the addition of a small amount of copper in the sample, and the samples may require freeze drying to prevent ice plugging in capillary column. In addition, small amounts of particulate sample enter the GC and caused contamination of the MSD, requiring more frequent instrument maintenance.

Analysis and results of particle size distribution, COD and material composition of sediments were discussed in Chapter VI. There was a strong correlation between the COD values and the fraction associated with leaves and grass clippings. The total combustible fractions of the samples were very small, with the exception of the large-sized large organic matter (LOM) that was separately analyzed. Most of the creek sediments were found in the intermediate particle ranges of several hundred micrometers, and very little of the LOM was found in the sediments.

Measured PAH concentrations for each of the samples separated by particle size, and the associated statistical analyses of the data, were shown in the chapter VII. ANOVA and supporting cluster analyses and exploratory data analyses identified which sample groups were significantly different from the other groups. The commercial site that had a history of hydrocarbon contamination generally had higher PAH concentrations, especially for the smaller particle sizes, than the samples from the other two creeks. The creek with historical SSO contamination did not have elevated organic or PAH concentrations, while the concrete-lined channel had frequent higher PAH values,

likely due to the absence of bank erosion material diluting the sediment discharged, and the elevated organic content associated with algae.

The following sections of this chapter will discuss the conclusions of the proposed hypothesis of the research work.

8.1 Hypothesis 1 Findings

The hypothesis 1 '*PAHs are strongly associated with particulate matter and variations in key characteristics of the sediment affect these associations*' was tested in two parts. For first part of the hypothesis, as discussed in chapter IV, fugacity level I partitioning calculations were performed for the PAHs in a hypothetical environmental system. This modeling approach indicated that except for the low molecular weight PAHs (naphthalene, fluorene, phenanthrene, and anthracene), all the other studied PAHs were predominantly partitioned with the sediment phase. The model predictions also indicated that the PAHs with Log (K_{OW}) or Log (K_{OC}) values greater than about 4.5 were mostly partitioned with the sediment phase, compared to other phases. The particulate and filterable PAH stormwater concentration data from prior field observations were compared to modeled values. The analytes were mostly associated with the particulate solids in the field samples. The high molecular weight PAHs had a greater portion associated with the particulates than the low molecular weight PAHs.

To test the second part of the hypothesis, sediment characteristics (particle sizes, sediment COD and material composition of the sediment) were measured and studied. All the analytical results of the sediment characteristics studied were presented in chapter VI. Overall, all characteristics studied showed similar trends, the smaller and larger

particles were found to have relatively higher values compared to the intermediate sized particles. A strong linear relation was seen between the calculated CODs and combustible material associated with the each particle size. A two-way ANOVA analyses showed that the concentrations of these analytes varied according to particle sizes. One-Way ANOVA analyses of concentrations of PAHs for each particle size (presented in chapter) for each creek separately also showed significant differences in analytes concentration, with the exceptions of naphthalene at Cribbs Mill Creek, benzo(a)pyrene, indeno(1,2,3-cd)pyrene, benzo(ghi)perylene at Hunter Creek and benzo(ghi)perylene at Carroll's Creek. Cluster analyses of the PAH concentrations for the different particle sizes showed that for most cases examined, the LOM fraction was found to be separate (having much higher concentrations) from all other sizes. When examining the other particle sizes (besides the large-sized LOM), Hunter Creek sediments were much greater than the other creeks, especially for the smaller particle sizes. PAH concentrations for the other two creeks were more inconsistent by particle size.

To test the relationship of sediment COD and PAH concentrations, a two-way ANOVA analyses was conducted on their concentration ratios. Particle sizes and locations were used to examine the effects of these variables on the observed ratios. There were many analytes which showed significant difference in the ratios, indicating no constant relationship of COD on the PAH concentrations associated with the sediment. Linear regressions of COD to PAH concentrations on each particle size for each creek separately showed a significant response factor (slope term) for slightly more than half the cases tested. When the large-sized LOM samples alone were considered, the

showed about 90% of the conditions had significant slope terms, indicating strong linear relations between COD and PAH concentrations, at least for high COD values.

Overall, testing the hypothesis 1 through fugacity modeling and reviews of available data, strongly demonstrated that the PAHs preferentially associate with solid particles compared with other phases in aquatic systems. Hence, the first part of hypothesis 1 can be accepted. Particle sizes categories also affect the concentrations of PAHs for some conditions, especially the high PAH concentrations found in the large-sized LOM fraction. The COD and the combustible fraction of the sediments were found to have no consistent effect on the PAH concentrations, except for the large-sized LOM material. The large variability of the observed PAH concentrations require additional sample to observe significant effects of COD on PAH concentrations for the samples having smaller organic material content. Therefore, the acceptance or rejection of the second part of the hypothesis is variable; large organic matter fractions of some samples affected the PAH concentrations, while smaller organic matter fractions did not indicate a clear relationship.

8.2 Hypothesis 2 Findings

The hypothesis 2 '*Sediment affected by historical events, such as contamination by sewage overflows or runoff from automobile service areas, will have higher concentrations of PAHs compared to non-affected sediment*' was tested by collecting analyzing sediment samples from three creeks. As described in chapter III, the sediments at Cribbs Mill Creek, Hunter Creek and Carroll's creeks were mainly affected by runoff

from residential, commercial and residential areas, respectively. The sediment at Carroll's Creek also had a past history of sewage contamination due to SSOs.

Two-way ANOVA analyses of the PAH concentrations considered particle size and location as variables. These tests indicated that other than naphthalene, fluorene, phenanthrene and indeno(1,2,3-cd)pyrene, all the other PAH analytes were affected by the location of the sediment samples. One-way ANOVA of the concentrations on different particles comparing the locations showed that for most of the analytes there were more significant differences between the creek locations for the smaller particle sizes (<45 and 45 – 90 μm) than for the other sizes. Using probability plots and other graphical analyses, Hunter Creek was found to have significantly higher concentrations than the other creeks, especially for the small particle sizes. Hunter Creek sediment had a history of contamination of hydrocarbons from creek-side businesses that caused the increased PAH concentrations. In contrast to the hypothesis, Cribbs Mill Creek generally had higher PAH concentrations than the sewage contaminated Carroll's Creek sediments. This may be due to the long time since the Carroll's Creek sediments were affected by the SSOs and that the Cribbs Mill Creek sampling location was in a long concrete channel. The channel had no bank erosion material affecting the sediment concentrations, and the concrete lining had obvious algae levels that could have preferentially sorbed PAHs. In addition, the contaminated sediment at Carroll's Creek either was flushed from the contamination site, or the contaminated sediment may be buried below the surface sampling depth.

Overall, hypothesis 2 can be partially accepted as location was a significant factor for most (but not all) of the analytes tested and for some (but not all) of the particle sizes.

The PAH concentrations in the Hunter Creek sediments were higher than the sediments from other creeks. Also, the concentration of PAH and other analytes for the sediments historically contaminated by sewage overflows at Carroll's Creek were actually found to be lower compared to sediments from the other two creeks, likely reflecting the transient nature of the contamination. As showed by the power analyses, for observed COVs in the data sets, larger numbers of samples are required to detect the smaller differences in the PAH concentrations.

REFERENCES

- Alexander M. Biodegradation and bioremediation. 2nd ed. San Diego Academic Press; 1999.
- Aryal, R.K., Furumai.H., Nakajima.F., Boller.M. Dynamic behavior of fractional suspended solids and particle bound polycyclic hydrocarbons in highway runoff. *Water Research* 39, 5126 – 5134. 2005.
- Atlas, R.M., Philp.J. *Applied Microbial Solutions for Real-World Environmental Cleanup*. ASM press, Washington, DC. 2005.
- Barbara, J.M., Van Metre, P.C., and Wilson, T.W. Concentration of Polycyclic Aromatic Hydrocarbons (PAHs) and Major and Trace Elements in Simulated Rainfall Runoff from Parking Lots. Austin, Texas. 2003.
- Bechman Coulter. Multisizer 3 Operator's Manual. 2001.
- Boehm, P.D., Farrington, J.W. Aspects of the polycyclic aromatic hydrocarbon geochemistry of the recent sediments in the Georges bank region. *Environmental Science and Technology* 18, 840-845. 1984.
- Boethling, R.S., Mackay,D. *Handbook of Property Estimation Methods for Chemicals*. Lewis Publishers, Boca Raton Washington DC. 2000.
- Box, G.E.P., Hunter, W.G. and Hunter, J.S. *Statistics for Experimenters*. John Wiley and Sons. New York. 1978
- Burton, G.A. and R. Pitt. *Handbook for Evaluating Stormwater Runoff Effects, A Tool Box of Procedures and Methods to Assist Watershed Managers*. CRC/Lewis Publishers, New York. 2002.
- Cheung, K.C., Leung, H.M., Kong, K.Y., and Wong, M.H. Residual levels of DDTs and PAHs in freshwater and marine fish from Hong Kong markets and their health risk assessment. *Chemosphere*. Volume 66, PP. 460 – 468. 2006.
- Chiou, C.T., Peters, L.J., and D.W. Schmedding, D.W. Partition equilibria of nonionic organic compounds between soil organic matter and water. *Environmental*

- Science and Technology*. 17(4), PP.227-231. 1983.
- Clark, C.D., De Bruyn, W.J., Jackie Ting, Scholle, W. Solution medium effects on the photochemical degradation of pyrene in water. *Journal of Photochemistry and Photobiology A: Chemistry*. No. of Pages 7.
- Countyway, R.E., Dickhut, R.M., Canuel, E.A. Polycyclic aromatic hydrocarbon (PAH) distributions and associations with organic matter in surface waters of the York River, VA Estuary. *Organic Geochemistry*. Vol. 34, pp. 209-224, 2003.
- Hambrick, G., Delaune, R., and Patrick, W. 1980. Effects of estuarine sediment pH and oxidation-reduction potential on microbial hydrocarbon degradation. *Applied Environmental Microbiology*. 40. 365 -369.
- Hemond, H.F., Fechner-Levy, E.J. *Chemical Fate and Transport in the Environment*. Second edition, Academic Press, California, USA. 2000.
- Heitkamp, M., Franklin, W., and Cerniglia, C. 1988. Microbial Metabolism of Polycyclic Aromatic Hydrocarbons: Isolation and Characterization of a Pyrene Degrading Bacterium. *Applied Environmental Microbiology*, 54. 2549 -2555.
- House, L.B., R.J. Waschbusch, and P.E. Hughes. *Water Quality of an Urban Wet Detention Pond in Madison, Wisconsin, 1987-1988*. U. S. Geological Survey, in cooperation with the Wisconsin Department of Natural Resources. USGS Open File Report 93-172, 1993.
- Hwang, H.M., Foster, G.D. Characterization of polycyclic aromatic hydrocarbons in urban stormwater runoff flowing into the tidal Anacostia River. *Environmental Pollution* 140, 416-426. 2006.
- Karickhoff, S.W. Semi-empirical estimation of sorption of hydrophobic pollutants on natural sediments and soils. *Chemosphere* 10(8):833-846. 1981.
- Kuklick, J.R., Sivertsen, S.K., Sander, M., Scott, I.S. Factors influencing polycyclic aromatic hydrocarbon distribution in South Carolina estuarine sediments. *Journal of experimental marine biology and ecology*. Vol. 213, pp. 13 – 29, 1997.
- Lyman, W.J., Reehl, W.F., and Rosenblatt, D.H. *Handbook of Chemical Property Estimation Methods*. McGraw-Hill, New York. 1982.
- Mackay, D., Shiu, W.Y., Ma, K.C. *Illustrated Handbook of Physical-Chemical Properties and Environmental Fate for Organic Chemicals*. Volume II, Lewis Publishers. 1992.
- McCready, S., Slee, D. J., Birch, G.F., Taylor, S.E. The distribution of polycyclic aromatic hydrocarbons in surficial sediments of Sydney Harbour, Australia. *Marine*

pollution bulletin, Vol. 40, No.11, pp.99-9-1006, 2000.

- Morquecho ,R. E. *Pollutant Associations With Particulates In Stormwater*. PhD Dissertation, University of Alabama, AL. 2005.
- Ollivon. D., Blanchoud. H., Motelay-Massei. A., Garban. B. Atmospheric deposition of PAHs to an urban site, Paris, France. *Atmospheric Environment*, 36, 2891 – 2900. 2002.
- Parmer, K. D. *Photo Biodegradation of Pyrene and benzo(a)pyrene in a Model of the near Surface Environment*. PhD Dissertation, University of Alabama at Birmingham, AL 1993.
- Pitt, R.E., R. Field. M. Lalor, and M. Brown. Urban Stormwater Toxic Pollutants: Assessment, Sources, and Treatability. *Water Environment Research* 67 (3), 260-275. 1995.
- Pitt, R.E., R. Field, M. Lalor, and M. Brown. Urban Stormwater Toxic Pollutants: Assessment, Sources, and Treatability. *Water Environment Research*. Vol. 67, No. 3, pp. 260-275. May/June 1995.
- Pitt, R. “Unique Features of the Source Loading and Management Model (SLAMM).” In: *Advances in Modeling the Management of Stormwater Impacts, Volume 6*. (Edited by W. James). Computational Hydraulics International, Guelph, Ontario and Lewis Publishers/CRC Press. Pp. 13 – 37. 1997.
- Pitt, R., Roberson, B., Barron, P., Ayyoubi, A., and Clark, S. *Stormwater treatment at critical areas: The multi-chambered treatment train (MCTT)*. U.S. Environmental Protection Agency, Water Supply and Water Resource Division. National Risk Management Research Laboratory. EPA 600/R-99/017.Cincinnati,OH. 1999.
- Pitt. R. S. Clark, J. Lantrip, and J. Day. *Telecommunication Manhole Water and Sediment Study*. Bellcore, Inc. (now Telcordia), Special Report SR-3841. Morriston, NJ. With further support from NYNEX, BellSouth, Bell Atlantic, GTE, SNET, Pacific Bell, US West, Ameritech and AT&T. *Vol. 1: Evaluation of Field Test Kits* (483 pgs); *Vol. 2: Water and Sediment Characteristics* (1290 pgs); *Vol. 3: Discharge Evaluation Report* (218 pgs); *Vol. 4: Treatment of Pumped Water* (104 pgs). December 1998.
- Ray, H. MSCE. *Street Dirt as a Phosphorus Source in Urban Stormwater* (published thesis). Department of Civil and Environmental Engineering, University of Alabama at Birmingham. 1997.
- Rockne KJ, Shor LM, Young LY, Taghon GL, Kosson DS (2002). “Distributed sequestration and release of PAHs in weathered sediment: The role of sediment

- structure and organic carbon properties”, Environ. Sci. Technol. 36. 2636-2644.
- Rushton, B. *Broadway Outfall Stormwater Retrofit Project, Monitoring CDS Unit and Constructed Pond*. South Florida Water Management District and City of Temple Terrace. Project Number W241. Final Report. Brooksville, FL. 2006.
- Sherrill, T., and Saylor., 1980. Phenanthrene biodegradation in fresh environments. *Applied Environmental Microbiology*. 39, 172 – 178.
- SIS AutoDesorb™ Operation Manual, Autodesorb Model 2000. (available from Scientific Instrument Services, Inc. Ringoes, NJ).
- Standard Methods for the Examination of Water and Wastewater*. 21st Edition. American public health Association, Washington, Dc 20001-3710. 2005
- SW-846 On-line. Test Methods, U.S. Environmental Protection Agency. (Available at <http://www.epa.gov/epaoswer/hazwaste/test/main.htm>).
- Synder, S., Vaderford, B., Pearson, R., Quinones., Yoon, Y. Analytical Methods Used to Measure Endocrine Disrupting Compounds in Water. *Practice periodical of Hazardous, Toxic, and Radioactive Waste Management*. ASCE, October 2003.
- Terzi. E., Samara.C. Dry deposition of polycyclic aromatic hydrocarbons in urban and rural sites of Western Greece. *Atmospheric Environment* Vol 39, 6261-6270. 2005.
- Toxicological profile for Polycyclic Aromatic Hydrocarbons (PAHs). Agency for Toxic Substances and Disease registry, Atlanta, GA. August 1995. (Available at: <http://www.atsdr.cdc.gov/toxprofiles/tp69.html#bookmark03>).
- USEPA, 200b. National Water Quality Inventory (EPA-841-R-00-01). United States Environmental Protection Agency, Washington, DC.
- Van Metre, P.C., Mahler, B.J., Furlong, E.T. Urban Sprawl Leaves Its PAH Signature. *Environmental Science & Technology* Vol. 34 No.19, 4064-4070. 2000.
- Webber. D. B. Dryfall: An important constituent of atmospheric hydrocarbon deposition. *Org. Geochem*, Vol. 9, No. 2, 57-62. 1986.
- Zhou, J.L., Fileman, T.W., Evans, S., Donkin, P., Llewellyn, C., Readman, J.W., Mantoura, R.F., Rowland, S.J. Fluoranthene and Pyrene in the Suspended Particulate Matter and Surface Sediments of the Humber Estuary, UK. *Marine Pollution Bulletin*, Vol.36, No.8, PP. 587-597, 1998.

APPENDIX A

PROPERTIES AND FATE MODELING OF PAHs

Table A.1 Model Predicted Portioning of Benzo(a)anthracene with 2⁴ Factorial Design Variables

Factor Value				Amount of Analyte Partitioned Into		
A	B	C	D	Air	Water	Suspended Solids
+	+	+	+	1.4E-15	2.5E-09	5.0E-08
+	+	+	-	2.2E-14	3.9E-08	1.4E-08
+	+	-	+	2.2E-14	3.8E-08	1.5E-08
+	+	-	-	2.7E-14	4.8E-08	4.8E-09
+	-	+	+	4.8E-17	8.4E-11	1.7E-09
+	-	+	-	1.7E-16	2.9E-10	1.5E-09
+	-	-	+	7.2E-16	1.3E-09	5.0E-10
+	-	-	-	9.1E-16	1.6E-09	1.6E-10
-	+	+	+	1.1E-14	2.1E-09	5.0E-08
-	+	+	-	3.8E-14	7.6E-09	4.5E-08
-	+	-	+	1.8E-13	3.6E-08	1.7E-08
-	+	-	-	2.3E-13	4.7E-08	5.5E-09
-	-	+	+	3.5E-16	7.1E-11	1.7E-09
-	-	+	-	1.3E-15	2.5E-10	1.5E-09
-	-	-	+	5.9E-15	1.2E-09	5.6E-10
-	-	-	-	7.8E-15	1.6E-09	1.8E-10

Table A.2 Calculated Effects of Factors and their Interactions on the Associations of Benzo(a)anthracene with Different Media

Factors/ Interactions	Effect		
	Air	Water	Suspended Solids
A	-2.3E-14	4.3E-09	-4.3E-09
B	8.4E-14	3.7E-08	2.4E-08
C	-6.4E-14	-2.6E-08	1.5E-08
D	-1.4E-14	-8.1E-09	8.1E-09
AB	-2.0E-14	4.3E-09	-4.3E-09
AC	1.0E-14	3.6E-09	-3.6E-09
AD	2.1E-14	-3.7E-09	3.7E-09
BC	-6.0E-14	-2.5E-08	1.4E-08
BD	-1.3E-14	-7.8E-09	7.8E-09
CD	1.9E-15	-2.5E-09	2.5E-09
ABC	2.6E-14	3.6E-09	-3.6E-09
ABD	6.8E-15	-3.7E-09	3.7E-09
ACD	-5.6E-15	-4.0E-09	4.0E-09
BCD	1.6E-15	-2.6E-09	2.6E-09
ABCD	-5.3E-15	-4.0E-09	4.0E-09

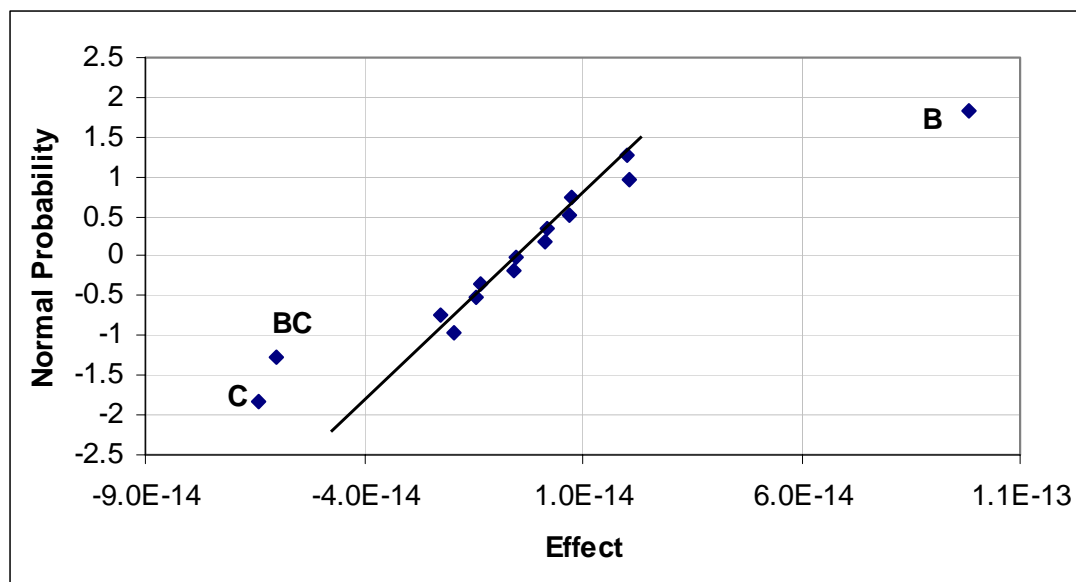


Figure A.1 Probability plot of effects of partitioning of benzo(a)anthracene with air

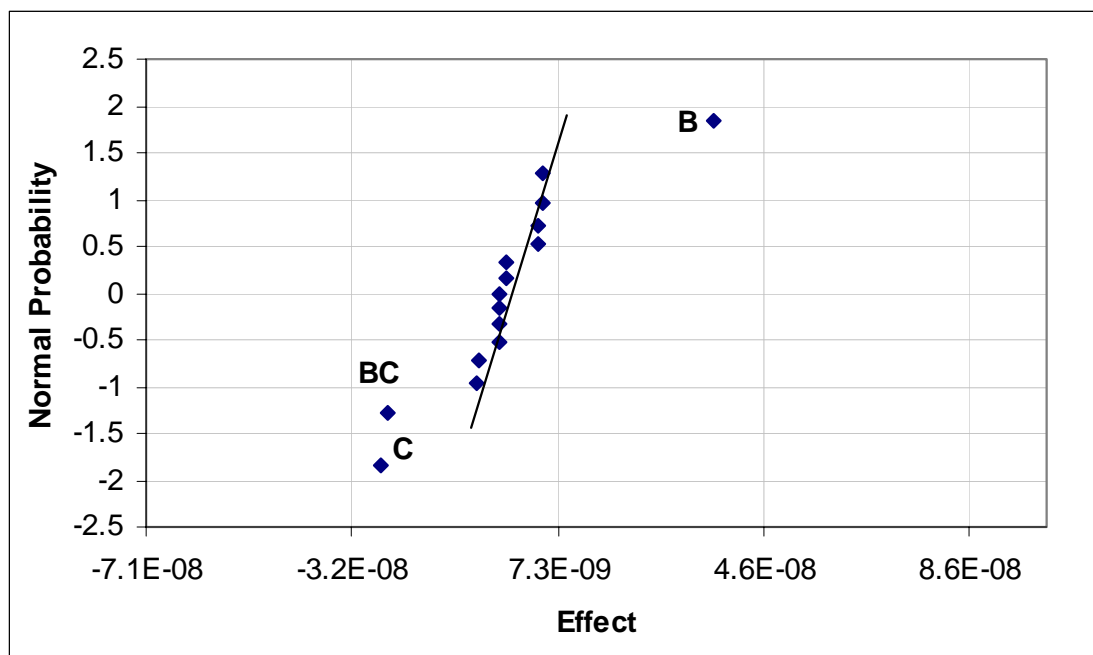


Figure A.2 Probability plot of effects of partitioning of benzo(a)anthracene with water

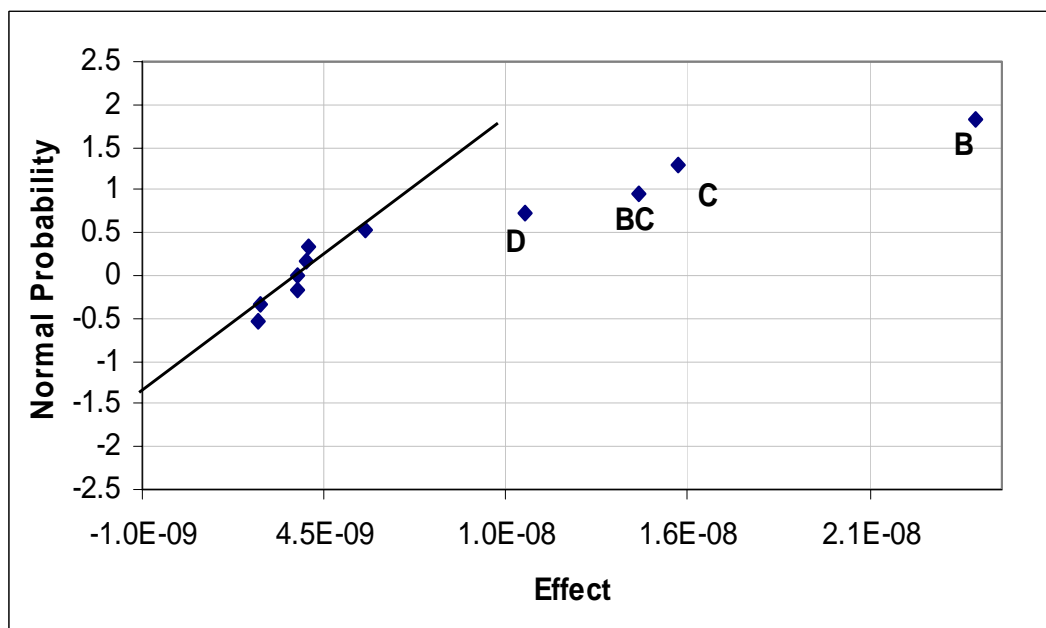


Figure A.3 Probability plot of effects of partitioning of benzo(a)anthracene with suspended solids

Table A.3. Model Predicted Portioning of Chrysene with 2⁴ Factorial Design Variables

Factor Value				Amount of Analyte Partitioned Into		
A	B	C	D	Air	Water	Suspended Solids
+	+	+	+	8.5E-13	5.3E-08	5.3E-12
+	+	+	-	6.3E-13	3.9E-08	1.4E-08
+	+	-	+	6.1E-13	3.8E-08	1.5E-08
+	+	-	-	7.8E-13	4.8E-08	4.8E-09
+	-	+	+	1.4E-15	8.4E-11	1.7E-09
+	-	+	-	4.7E-15	2.9E-10	1.5E-09
+	-	-	+	2.0E-14	1.3E-09	5.0E-10
+	-	-	-	2.6E-14	1.6E-09	1.6E-10
-	+	+	+	1.9E-14	2.1E-09	5.0E-08
-	+	+	-	6.7E-14	7.6E-09	4.5E-08
-	+	-	+	3.1E-13	3.6E-08	1.7E-08
-	+	-	-	4.1E-13	4.7E-08	5.5E-09
-	-	+	+	6.3E-16	7.1E-11	1.7E-09
-	-	+	-	2.2E-15	2.5E-10	1.5E-09
-	-	-	+	1.0E-14	1.2E-09	5.6E-10
-	-	-	-	1.4E-14	1.6E-09	1.8E-10

Table A.4 Calculated Effects of Factors and their Interactions on the Associations of Chrysene with Different Media

Factors/ Interactions	Effect		
	Air	Water	Suspended Solids
A	1.3E-13	1.1E-08	-1.1E-08
B	4.5E-13	3.3E-08	3.8E-08
C	-1.0E-13	-2.0E-08	2.0E-08
D	-1.3E-14	-1.8E-09	5.8E-09
AB	1.3E-13	1.1E-08	-1.1E-08
AC	9.0E-14	9.9E-09	-9.9E-09
AD	2.5E-14	2.5E-09	-2.5E-09
BC	-8.0E-14	-9.8E-09	9.8E-09
BD	-9.6E-15	-1.5E-09	1.5E-10
CD	5.5E-14	3.8E-09	-2.8E-09
ABC	9.5E-14	9.9E-09	-9.9E-09
ABD	2.6E-14	2.5E-09	-2.5E-09
ACD	4.2E-14	2.3E-09	-2.3E-09
BCD	5.4E-14	3.7E-09	-3.7E-09
ABCD	4.2E-14	2.3E-09	-2.3E-09

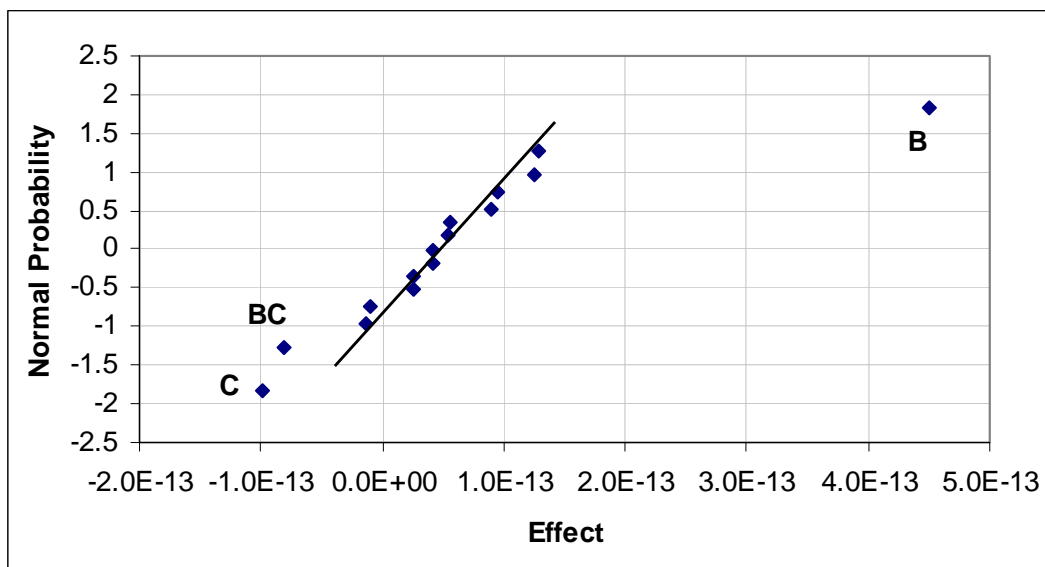


Figure A.4 Probability plot of effects of partitioning of chrysene with air

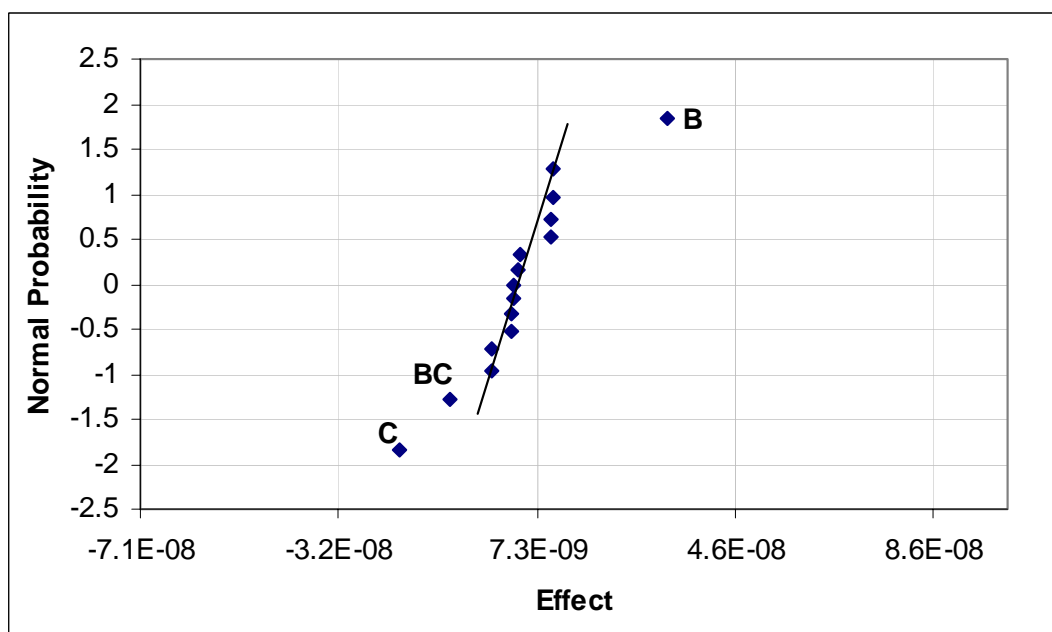


Figure A.5 Probability plot of effects of partitioning of chrysene with water

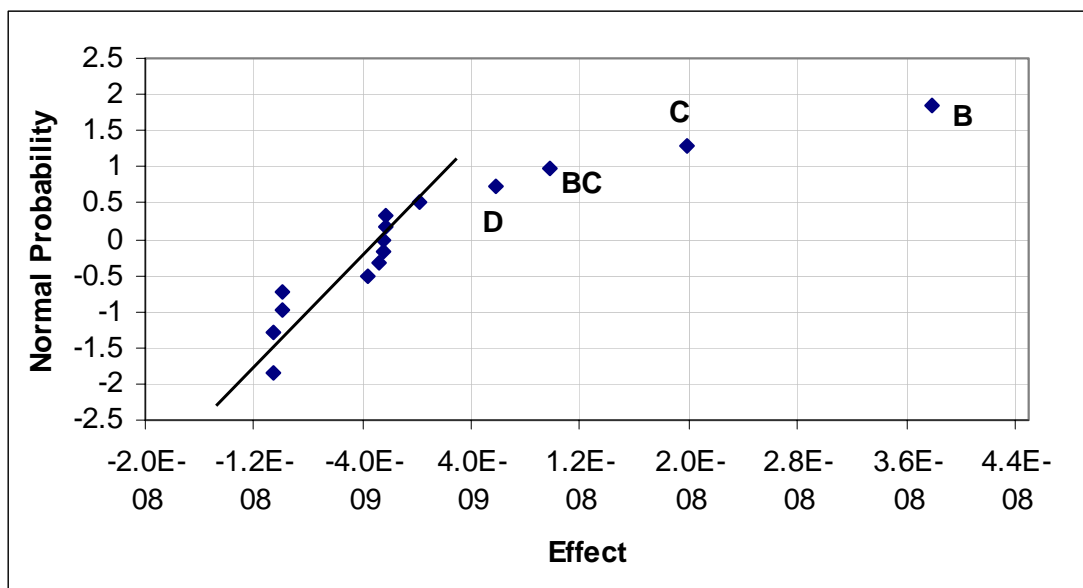
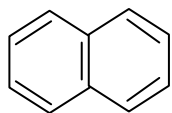
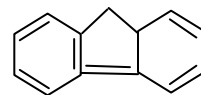


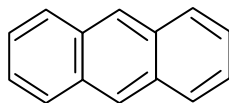
Figure A.6 Probability plot of effects of partitioning of chrysene with suspended solids



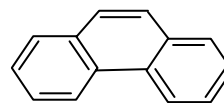
Naphthalene



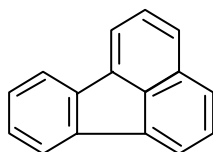
Fluorene



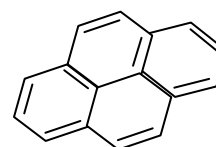
Anthracene



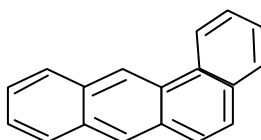
Phenanthrene



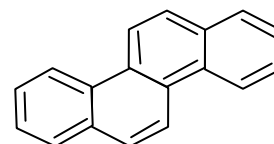
Fluoranthene



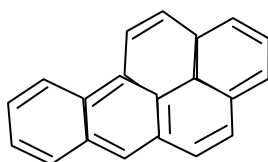
Pyrene



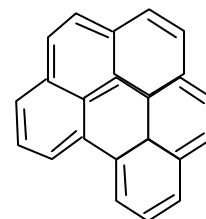
Benz(a)anthracene



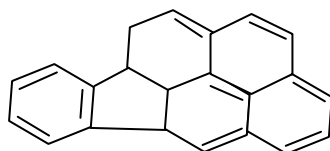
Chrysene



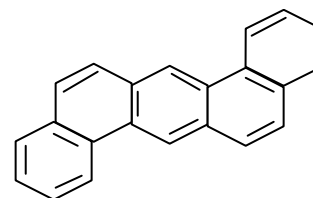
Benz(a)pyrene



Benz(ghi)perylene



Indeno(1,2,3-cd)pyrene



Dibenzo(ah)anthracene

Figure A.7 Structures of selected PAHs

Table A.5 Physical Chemical Properties of PAHs (Source: ATSDR, 1995)

PAH	Molecular Formula	Molecular Weight	Water Solubility (mg/L)	Log(K _{ow})	Log (K _{oc})	Vapor Pressure (mm Hg)	Henry's Law Constant (atm-m ³ /mol)
Naphthalene	C ₁₀ H ₈	128.16	30	3.25	3.20	8.2x10 ⁻¹ at 25 °C	4.5x10 ⁻³
Fluorene	C ₁₃ H ₁₀	166.20	1.68 – 1.98	4.18	3.86	3.2x10 ⁻⁴ at 20°C	1.0x10 ⁻⁴
Phenanthrene	C ₁₄ H ₁₀	178.2	1.2	4.45	4.15	6.8x10 ⁻⁴ at 25°C	2.56x10 ⁻⁵
Anthracene	C ₁₄ H ₁₀	178.20	0.076	4.07	4.15	1.7x10 ⁻⁵ at 25°C	1.77x10 ⁻⁵
Fluranthene	C ₁₆ H ₁₀	202.26	0.20 – 0.26	4.90	4.58	5.0x10 ⁻⁶ at 25°C	6.5x10 ⁻⁶
Pyrene	C ₁₆ H ₁₀	202.3	0.077	4.88	4.58	2.5x10 ⁻⁸ at 25°C	1.14x10 ⁻⁵
Benzo(a)anthracene	C ₁₈ H ₁₂	228.29	0.01	5.61	5.3	2.2x10 ⁻⁸ at 20oC	1x10 ⁻⁶
Chrysene	C ₁₈ H ₁₂	228.3	2.8x10 ⁻³	5.16	5.3	6.3x10 ⁻⁷ at 25°C	1.05x10 ⁻⁶
Benzo(b)flouranthrene	C ₂₀ H ₁₂	252.3	0.0012	6.04	5.74	5.0x10 ⁻⁷ at 20 – 25°C	1.22x10 ⁻⁵
Benzo(a)pyrene	C ₂₀ H ₁₂	252.3	0.0023	6.06	6.74	5.6x10 ⁻⁹ at 25°C	4.9x10 ⁻⁷
Indeno(1,2,3-cd)pyrene	C ₂₂ H ₁₂	276.30	0.062	6.58	6.20	-10 ⁻¹¹ – 10 ⁻⁶ at 20°C	6.95x10 ⁻⁸
Dibenz(a,h)anthracene	C ₂₂ H ₁₄	278.35	5x10 ⁻⁴	6.84	6.52	1x10 ⁻¹⁰ at 20°C	7.3x10 ⁻⁸
Benzo(ghi)perylene	C ₂₂ H ₁₂	276.34	2.6x10 ⁻⁴	6.5	6.2	1.03x10 ⁻¹⁰ at 25°C	1.44x10 ⁻⁷

APPENDIX B

THERMAL DESORPTION ANALYTICAL METHOD DEVELOPMENT

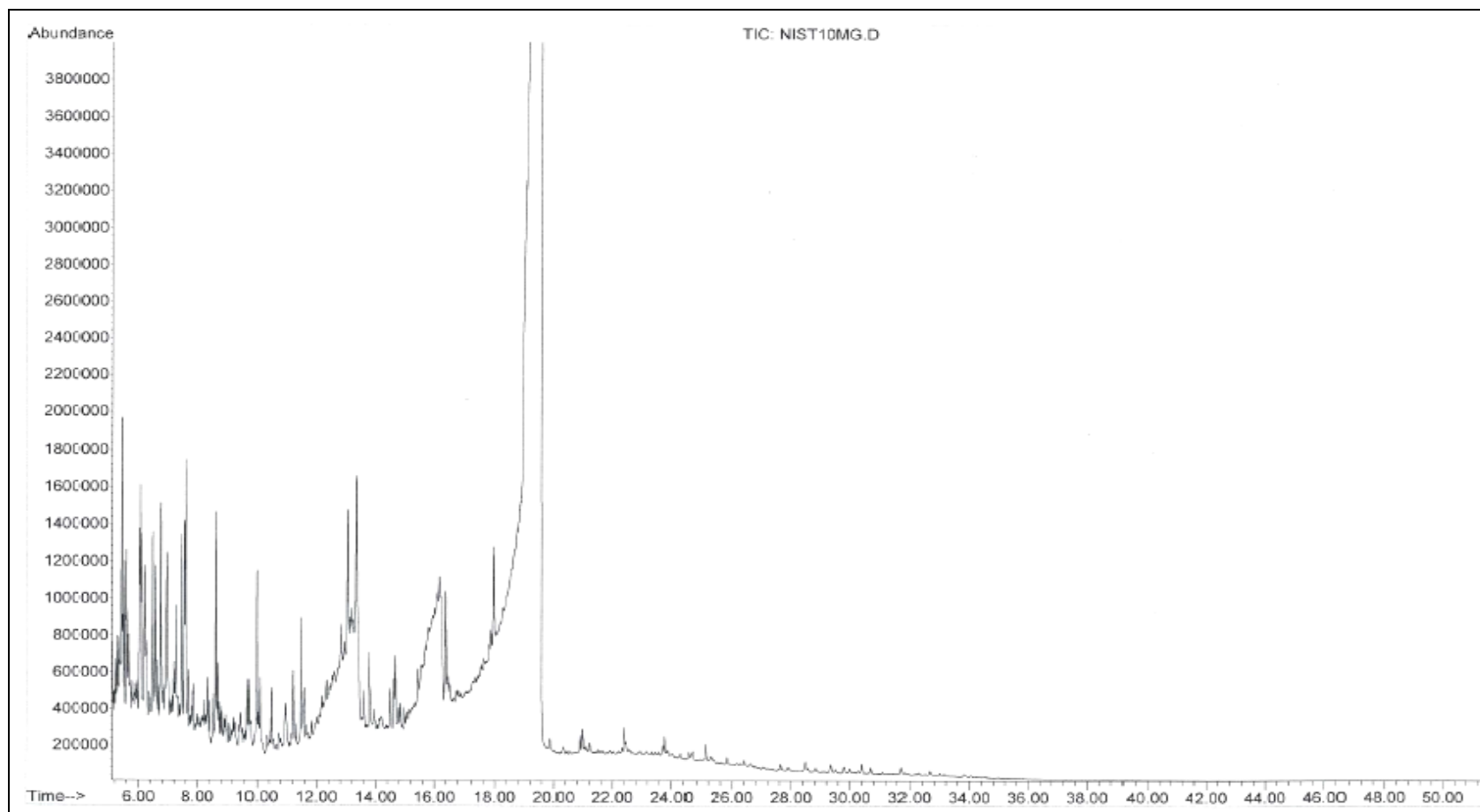


Figure B.1 Chromatogram of NIST standard with dominant peaks of sulfur compounds

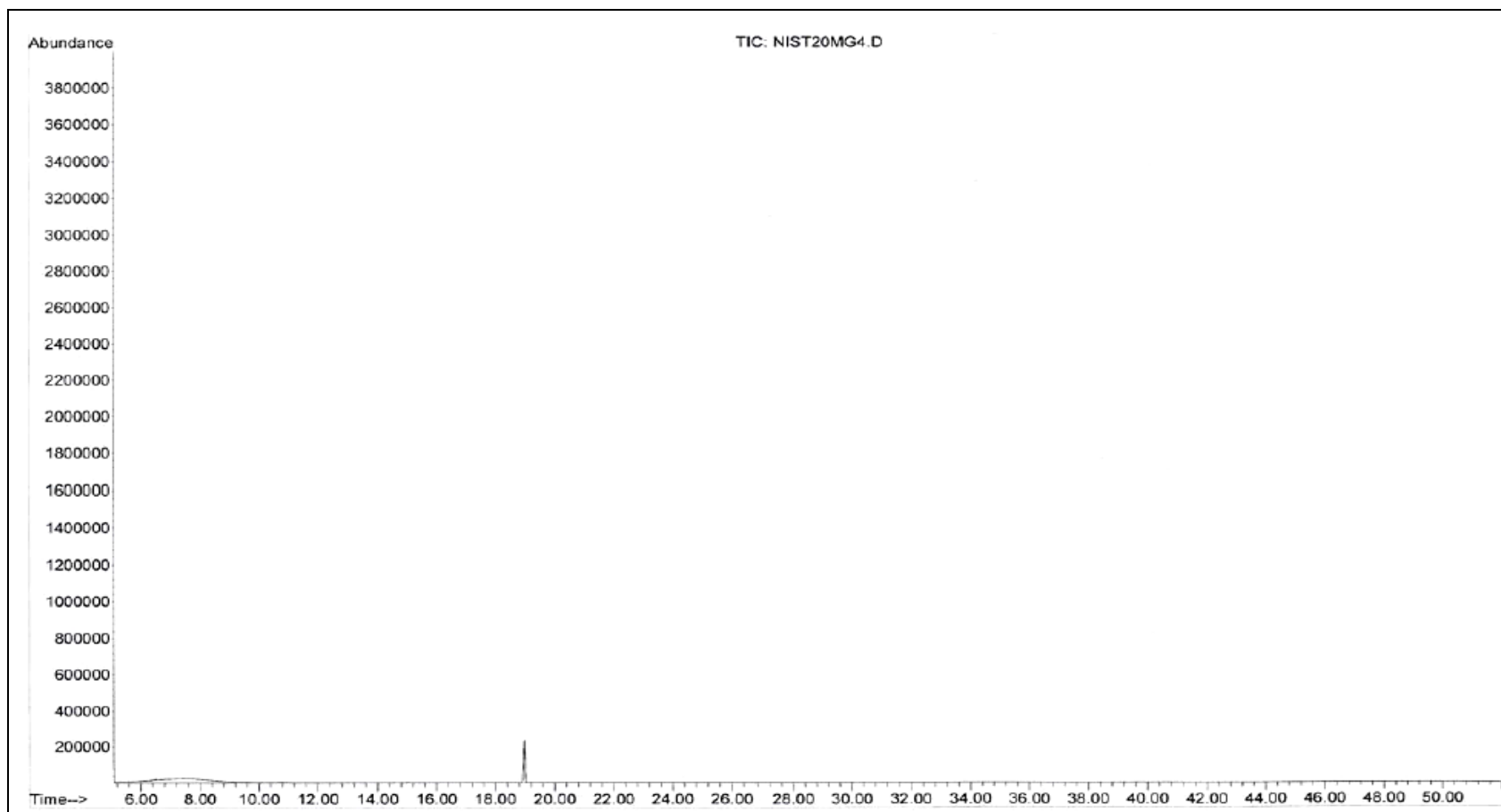


Figure B.2 Chromatogram of NIST standard with ice plugging problem.

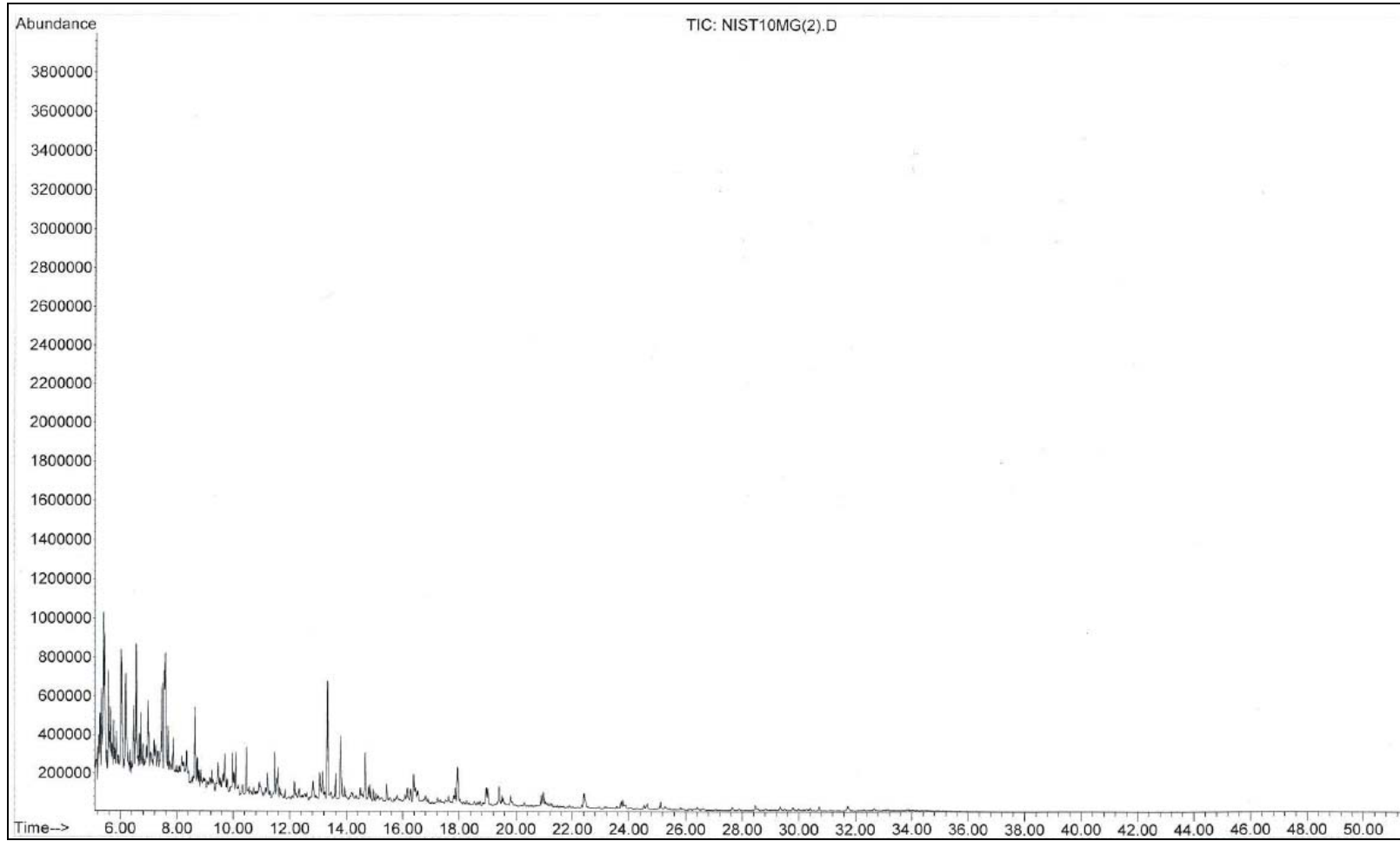


Figure B.3 Chromatogram of freeze dried NIST standard with copper

Table B.1. NIST Certified Weights and Method Calculated Weights of PAH Analytes in the Standard Sediment

PAH	Technique	Amount (ng) of Analyte in Corresponding Weight (mg) of NIST Standard Sample							
		3	6	10	20	30	40	50	60
Naphthalene	NIST	2.54	5.09	8.48	16.96	25.44	33.92	42.4	50.88
	TD/GC/MS	4.48	13.37	18.37	28.36	39.77	51.96	58.16	66.85
Fluorene	NIST	0.26	0.51	0.85	1.7	2.55	3.4	4.25	5.1
	TD/GC/MS	1.38	2.27	3.15	3.8	4.47	5.69	8.43	9.19
Phenanthrene	NIST	1.22	2.44	4.06	8.12	12.18	16.24	20.3	24.36
	TD/GC/MS	3.49	7.12	7.49	12.32	16.47	19.09	21.35	23.74
Anthracene	NIST	0.55	1.1	1.84	3.68	5.52	7.36	9.2	11.04
	TD/GC/MS	Nd	nd	3.5	4.88	5.91	6.47	7.08	7.44
Fluranthene	NIST	1.95	3.91	6.51	13.02	19.53	26.04	32.55	39.06
	TD/GC/MS	1.41	3.65	4.3	6.17	8.34	10.02	12.7	14.4
Pyrene	NIST	1.74	3.49	5.81	11.62	17.43	23.24	29.05	34.86
	TD/GC/MS	6.13	9.25	11.62	13.94	16.73	18.27	20.75	21.13
Benzo(a)anthracene	NIST	1.01	2.01	3.35	6.7	10.05	13.4	16.75	20.1
	TD/GC/MS	nd	2.37	2.02	3.32	4.14	4.96	5.35	5.9
Chrysene	NIST	0.87	1.75	2.91	5.82	8.73	11.64	14.55	17.46
	TD/GC/MS	nd	1.52	2.13	2.88	3.99	4.62	5.1	5.42
Benzo(b)flouranthrene	NIST	1.36	2.72	4.53	9.06	13.59	18.12	22.65	27.18
	TD/GC/MS	nd	4.03	5.14	5.63	6.27	7.6	8.68	10.2
Benzo(a)pyrene	NIST	1.07	2.15	3.58	7.16	10.74	14.32	17.9	21.48
	TD/GC/MS	nd	nd	5.49	6.16	7.28	9.06	10.91	12.75
Indeno(1,2,3-cd)pyrene	NIST	1.02	2.05	3.41	6.82	10.23	13.64	17.05	20.46
	TD/GC/MS	nd	nd	1.23	1.47	2.48	4.59	5.04	7.28
Dibenz(a,h)anthracene	NIST	0.16	0.32	0.54	1.08	1.62	2.16	2.7	3.24
	TD/GC/MS	nd	nd	Nd	nd	nd	0.46	0.79	1.87
Benzo(ghi)perylene	NIST	0.92	1.84	3.07	6.14	9.21	12.28	15.35	18.42
	TD/GC/MS	nd	nd	1.71	2.04	3.16	4.34	6.13	7.02

nd: peak area not calculated; too low

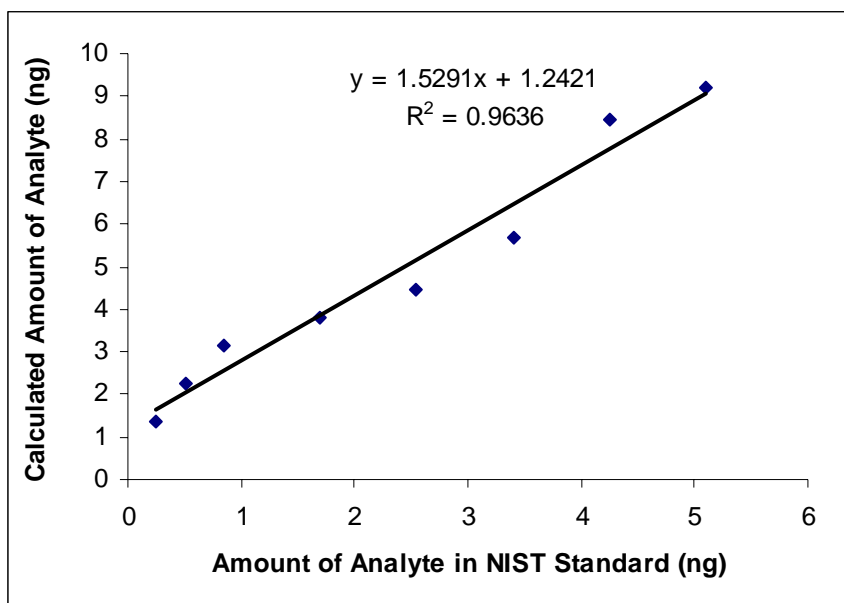


Figure B.4 Relation between fluorene weights in NIST standards and method calculated weights

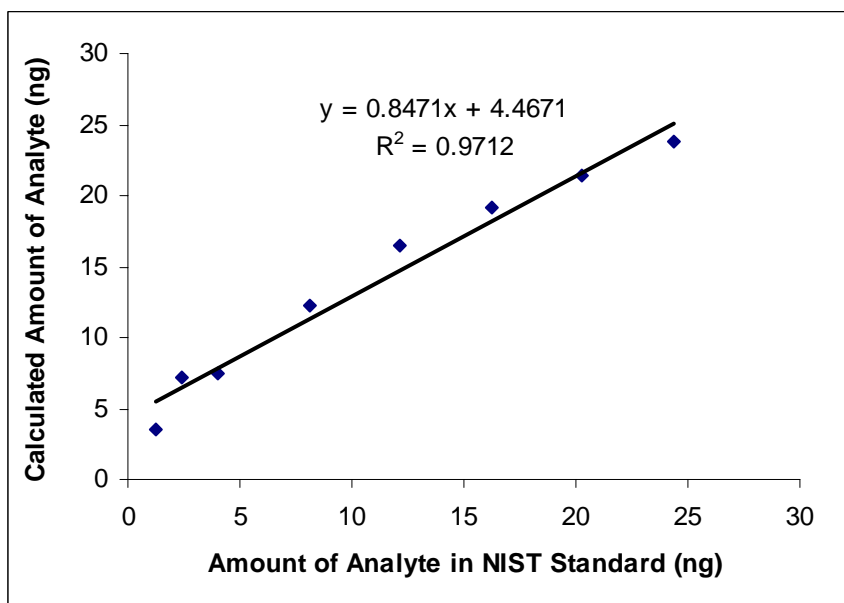


Figure B.5 Relation between phenanthrene weights in NIST standards and method calculated weights

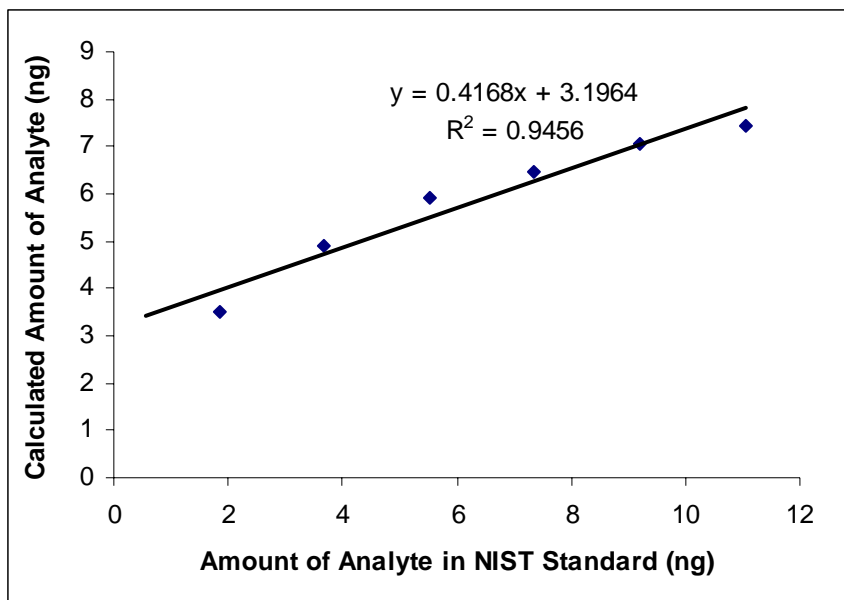


Figure B.6 Relation between anthracene weights in NIST standards and method calculated weights

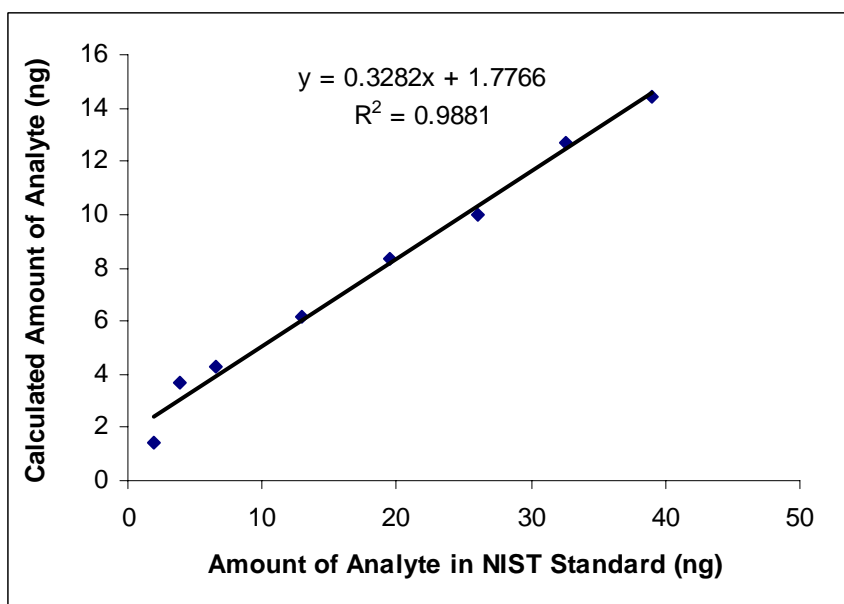


Figure B.7 Relation between fluranthene weights in NIST standards and method calculated weights

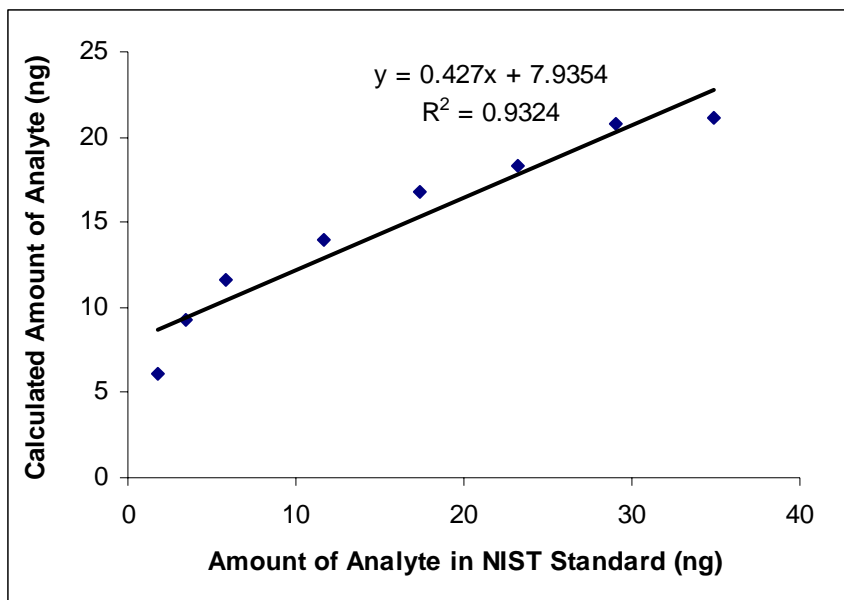


Figure B.8 Relation between pyrene weights in NIST standards and method calculated weights

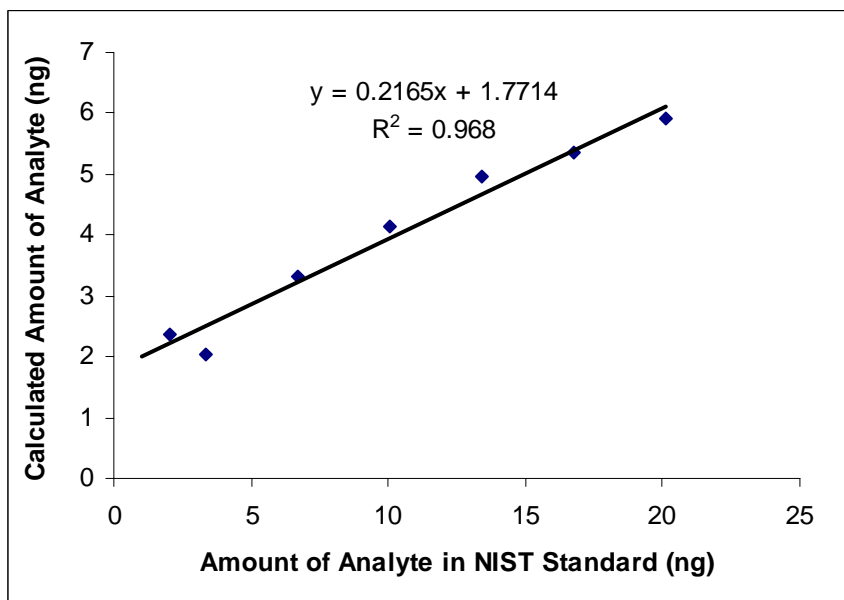


Figure B.9 Relation between benzo(a)anthracene weights in NIST standards and method calculated weights

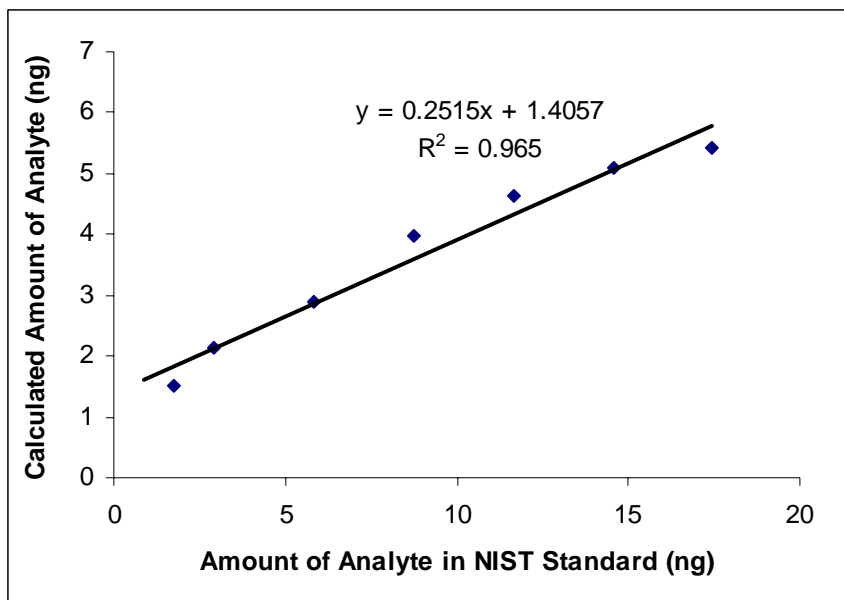


Figure B.10 Relation between chrysene weights in NIST standards and method calculated weights

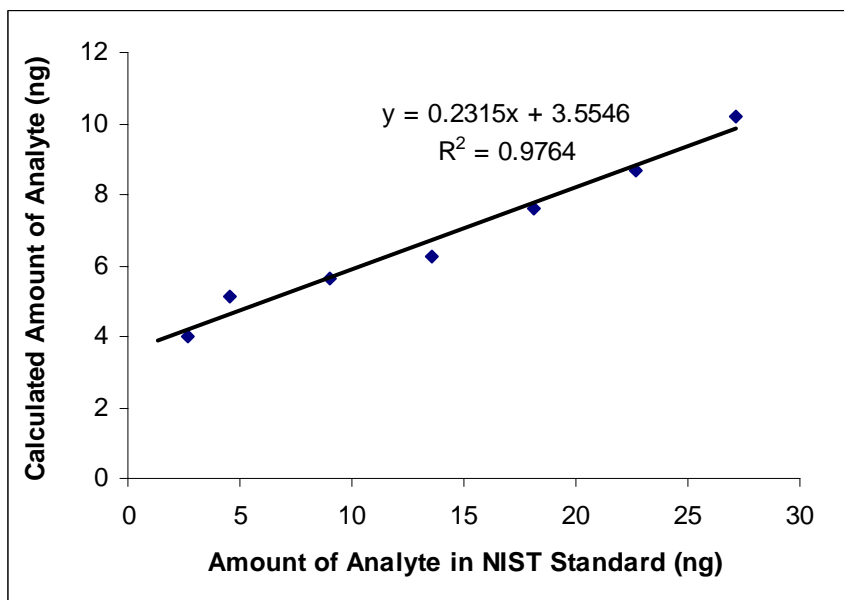


Figure B.11 Relation between benzo(b)fluoranthene weights in NIST standards and method calculated weights

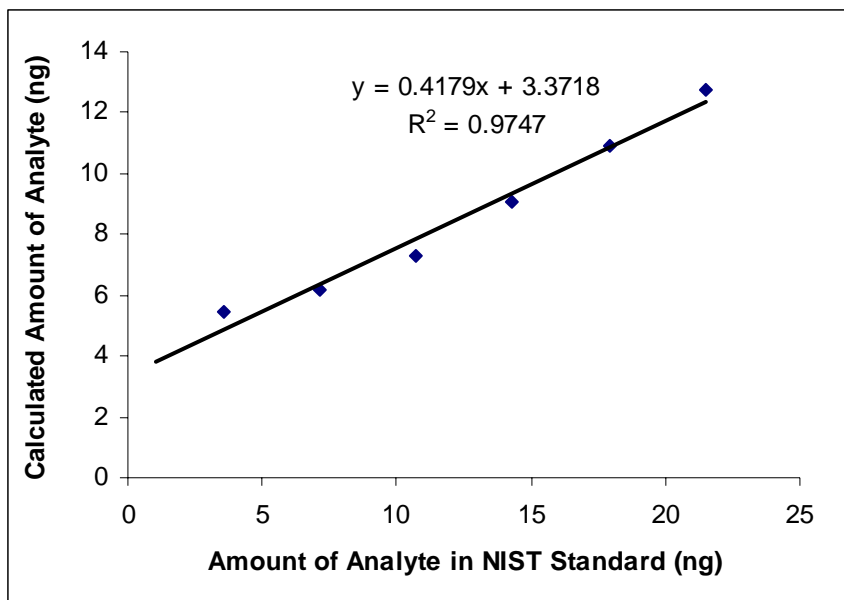


Figure B.12 Relation between benzo(a)pyrene weights in NIST standards and method calculated weights

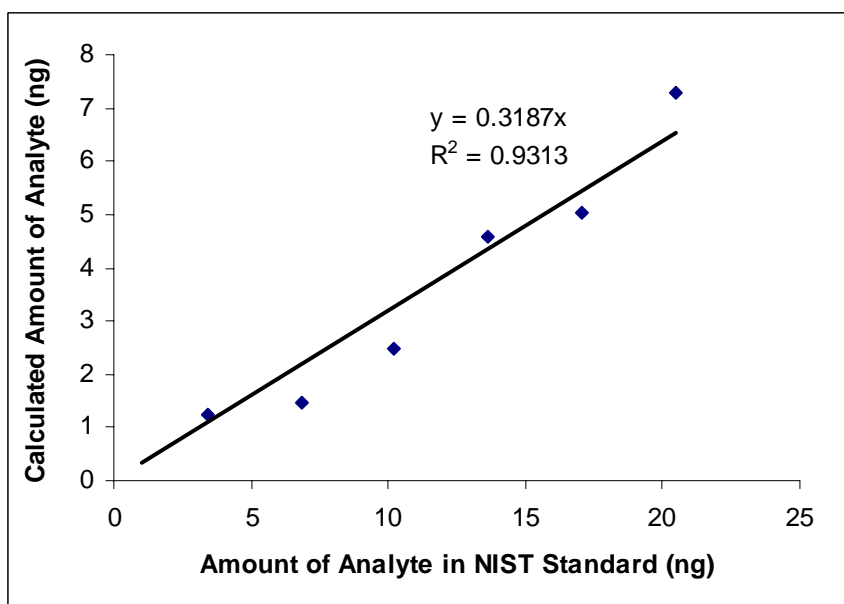


Figure B.13 Relation between indeno(1,2,3-cd)pyrene weights in NIST standards and method calculated weights

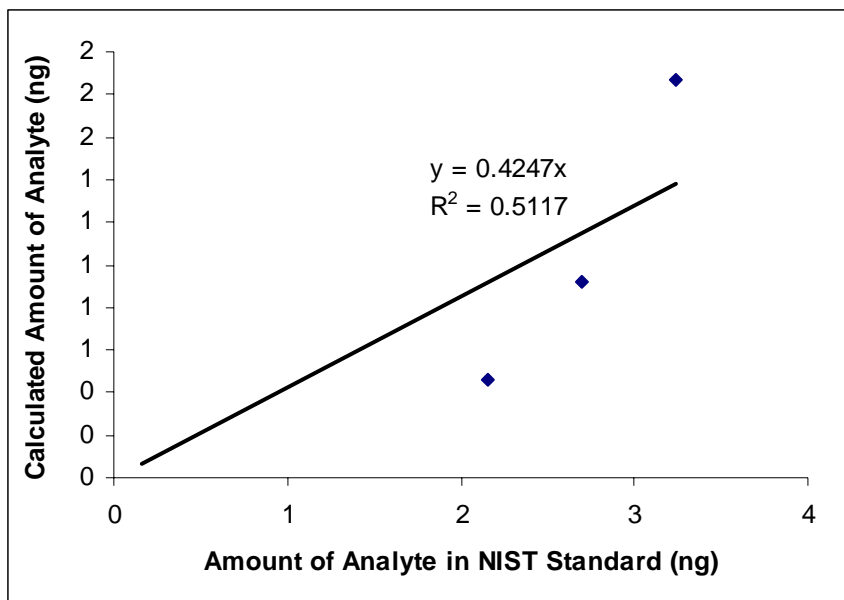


Figure B.14 Relation between dibenz(a,h)anthracene weights in standards and method calculated weights

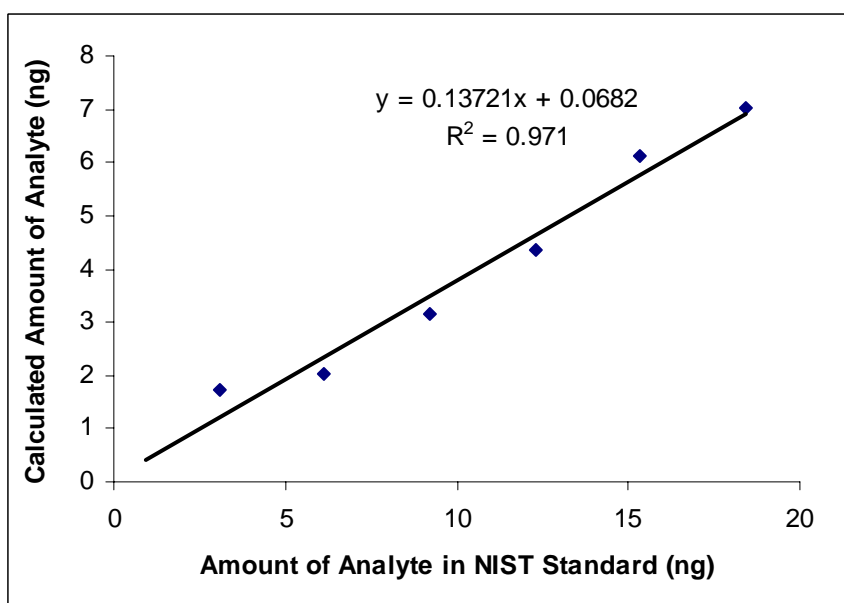


Figure B.15 Relation between benzo(ghi)perylene weights in NIST standards and method calculated weights

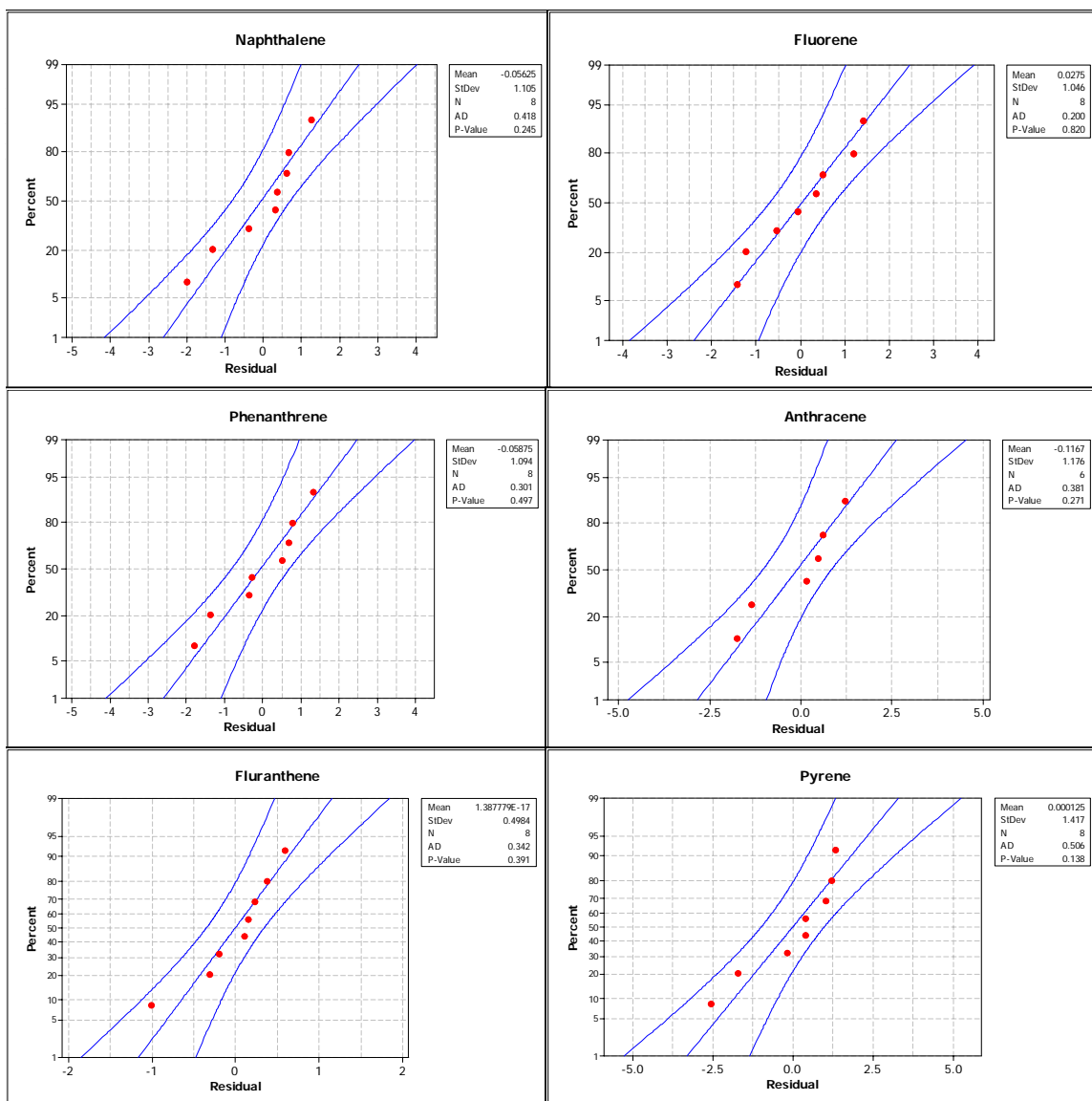


Figure B.16 Residual Plots of method response for naphthalene, fluorene, phenanthrene, anthracene, fluranthene, pyrene in NIST sediment standard

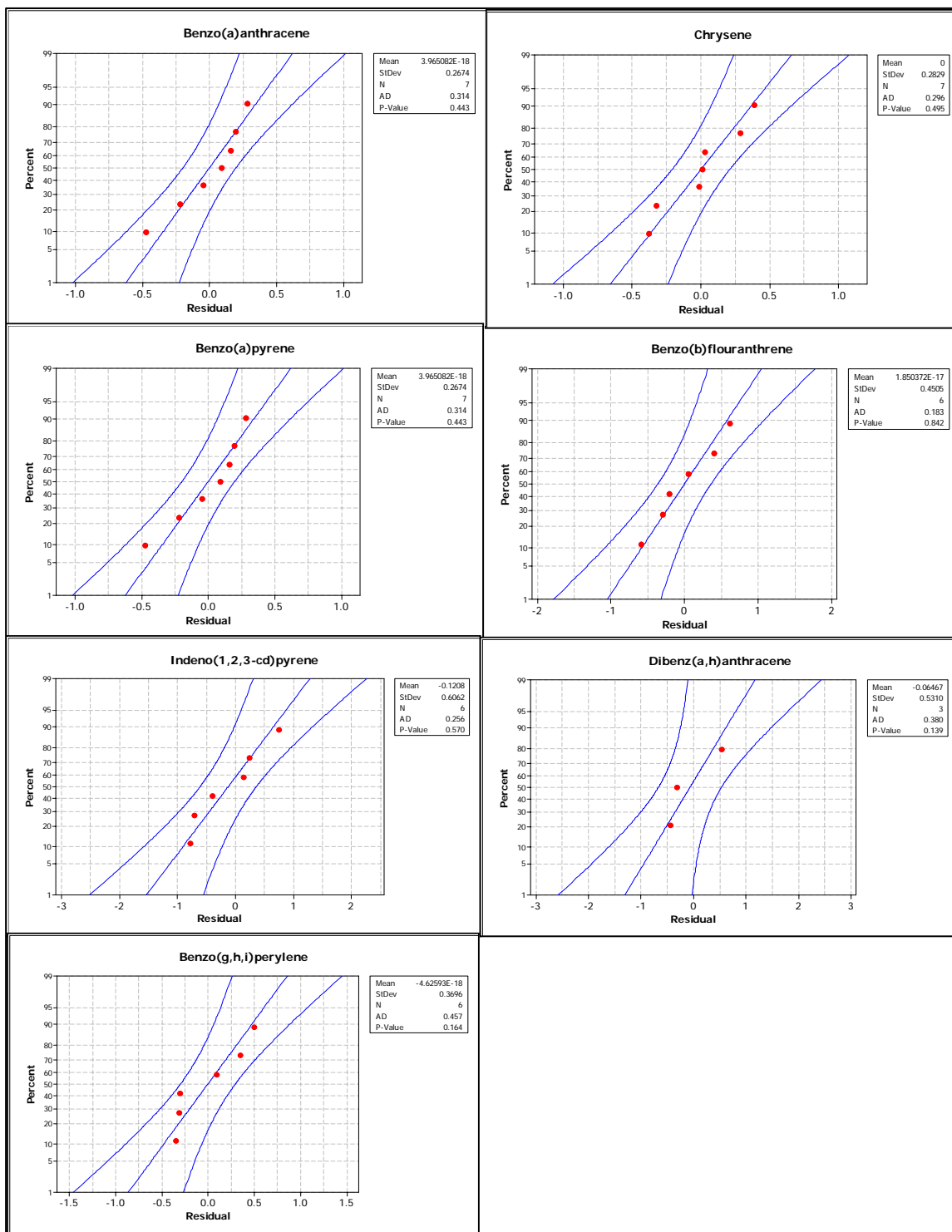


Figure B.17 Residual Plots of method response for benzo(a)anthracene, chrysene, benzo(a)pyrene, beno(b)flouranthene, indeno(1,2,3-cd)pyrene, dibenz(a,h)anthracene, benzo(g,h,i)perylene in NIST sediment standard

Table B.2 Calculated Concentrations of Analytes in Coarser 710 - 1400 μ m Sediment Composite Sample and in Corresponding Grinded Sample

PAH	Concentration in Coarser Composite Sample (μ g/kg)					Concentration in Grinded Composite Sample (μ g/kg)				
	Run 1	Run2	Run3	Average	Standard Deviation	Run 1	Run2	Run3	Average	Standard Deviation
Naphthalene	2074	861	1469	1468	606	1035	670	223	643	406
Fluorene	4361	3167	2966	3498	754	2783	1702	1714	2066	621
Phenanthrene	1631	951	732	1105	469	1135	890	824	950	164
Anthracene	1716	2349	921	1662	715	2372	1038	1018	1476	776
Fluoranthene	2185	1971	784	1647	755	1943	1154	1406	1501	403
Pyrene	2202	2290	966	1819	740	1802	1284	1398	1495	272
Benzo(a)anthracene	3772	3137	1773	2894	1021	1545	1206	716	1155	417
Chrysene	1500	2449	990	1646	741	1693	965	641	1099	539
Benzo(b)flouranthrene	19540	3046	1099	7895	10132	1514	2247	987	1583	633
Benzo(a)pyrene	10890	9423	3621	7978	3844	3298	5094	3462	3951	993
Indeno(1,2,3-cd)pyrene	17319	7491	10717	11843	5010	2395	31767	41207	25123	20241
Dibenz(a,h)anthracene	40339	69502	16585	42142	26504	25229	95107	57497	59278	34973
Benzo(ghi)perylene	32533	30452	13415	25467	10489	22417	16877	10545	16613	5940

Table B.3 Calculated Concentrations of Analytes in Coarser 1400 - 2800 μ m Sediment Composite Sample and in Corresponding Grinded Sample

PAH	Concentration in Coarser Composite Sample (μ g/kg)					Concentration in Grinded Composite Sample (μ g/kg)				
	Run 1	Run2	Run3	Average	Standard Deviation	Run 1	Run2	Run3	Average	Standard Deviation
Naphthalene	211	95	152	153	58	652	352	217	407	222
Fluorene	1059	1658	1574	1430	324	4191	1834	2558	2861	1207
Phenanthrene	149	126	272	182	79	1235	512	654	801	383
Anthracene	652	345	824	607	243	2791	1054	851	1565	1066
Fluranthene	51	49	122	74	41	769	309	170	416	314
Pyrene	238	212	341	264	69	1057	596	459	704	313
Benzo(a)anthracene	181	293	224	233	57	1041	174	308	508	467
Chrysene	169	112	218	166	53	654	167	285	369	254
Benzo(b)flouranthrene	87	99	146	110	31	722	61	130	304	363
Benzo(a)pyrene	290	332	497	373	109	959	223	498	560	372
Indeno(1,2,3-cd)pyrene	9	17	32	19	11	11	5	73	30	38
Dibenz(a,h)anthracene	8	16	32	19	12	330	4	79	138	171
Benzo(ghi)perylene	284	355	250	296	53	570	281	202	351	193

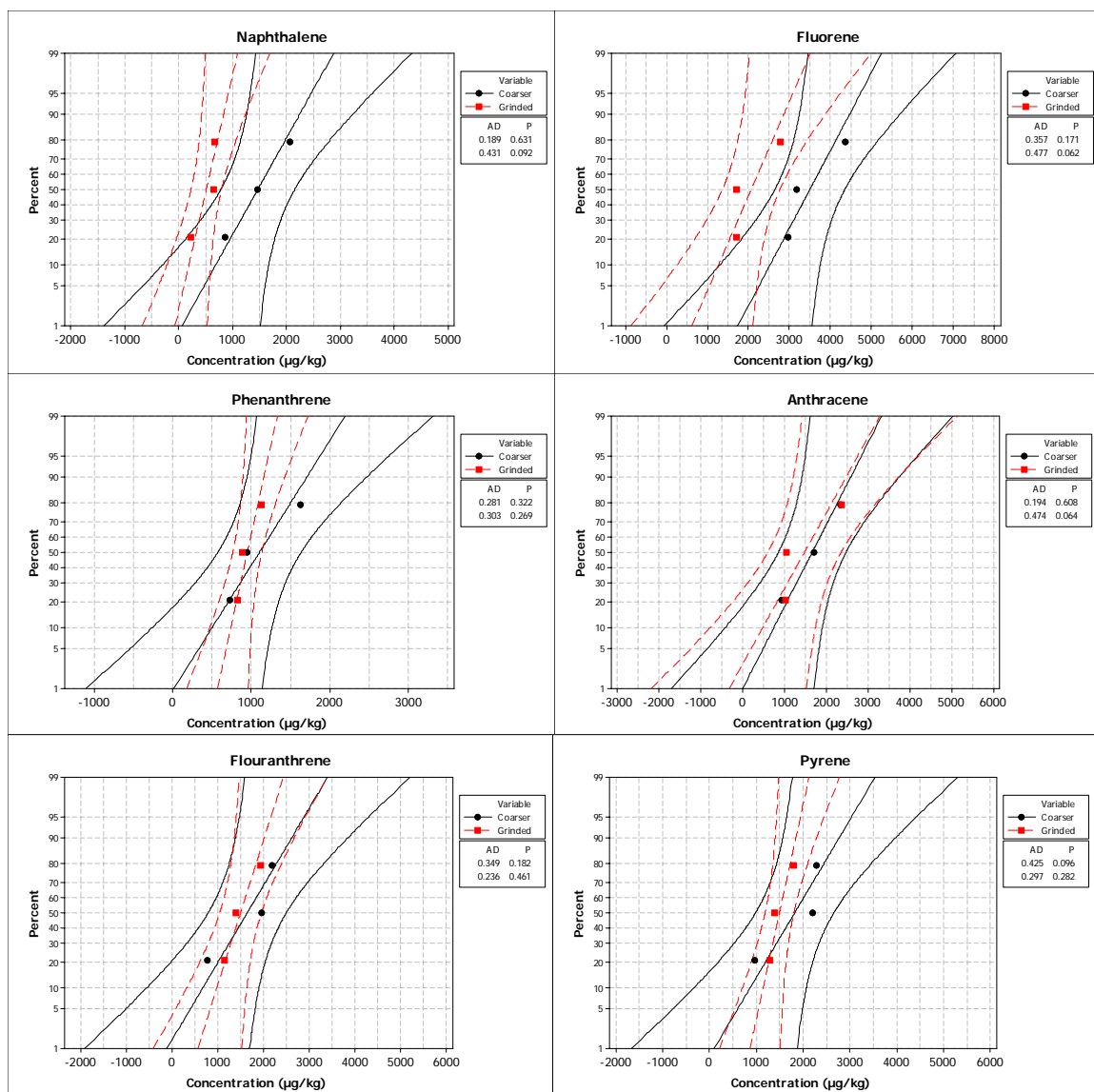


Figure B.18 Normal probability plots for concentrations of naphthalene, fluorene, phenanthrene, anthracene, flouranthrene, pyrene in 710 - 14000µm size composite sample

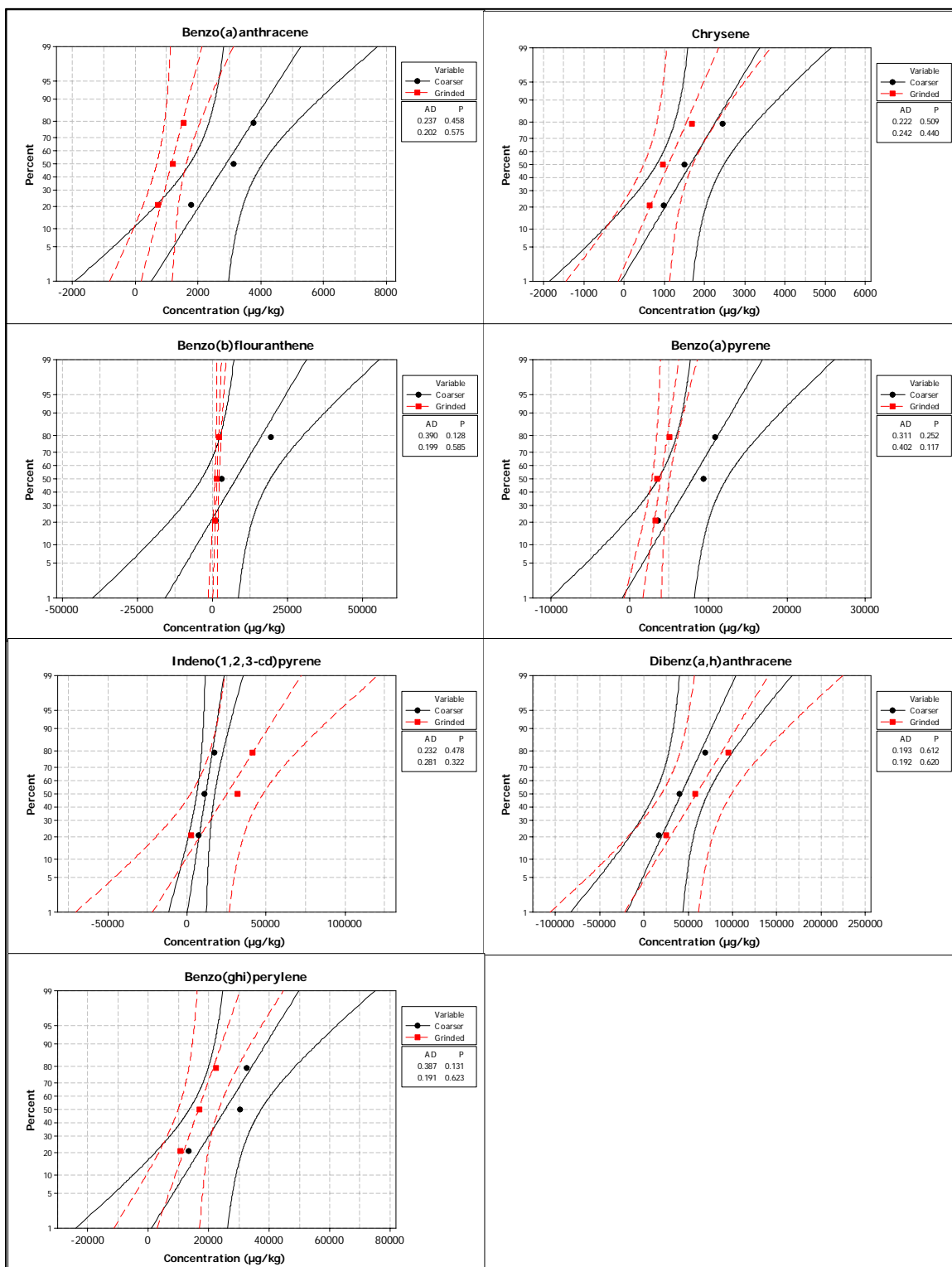


Figure B.19 Normal probability plots for for benzo(a)anthracene, chrysene, benzo(a)pyrene, beno(b)flouranthene, indeno(1,2,3-cd)pyrene, dibenz(a,h)anthracene, benzo(ghi)perylene in 710 - 1400µm size composite sample

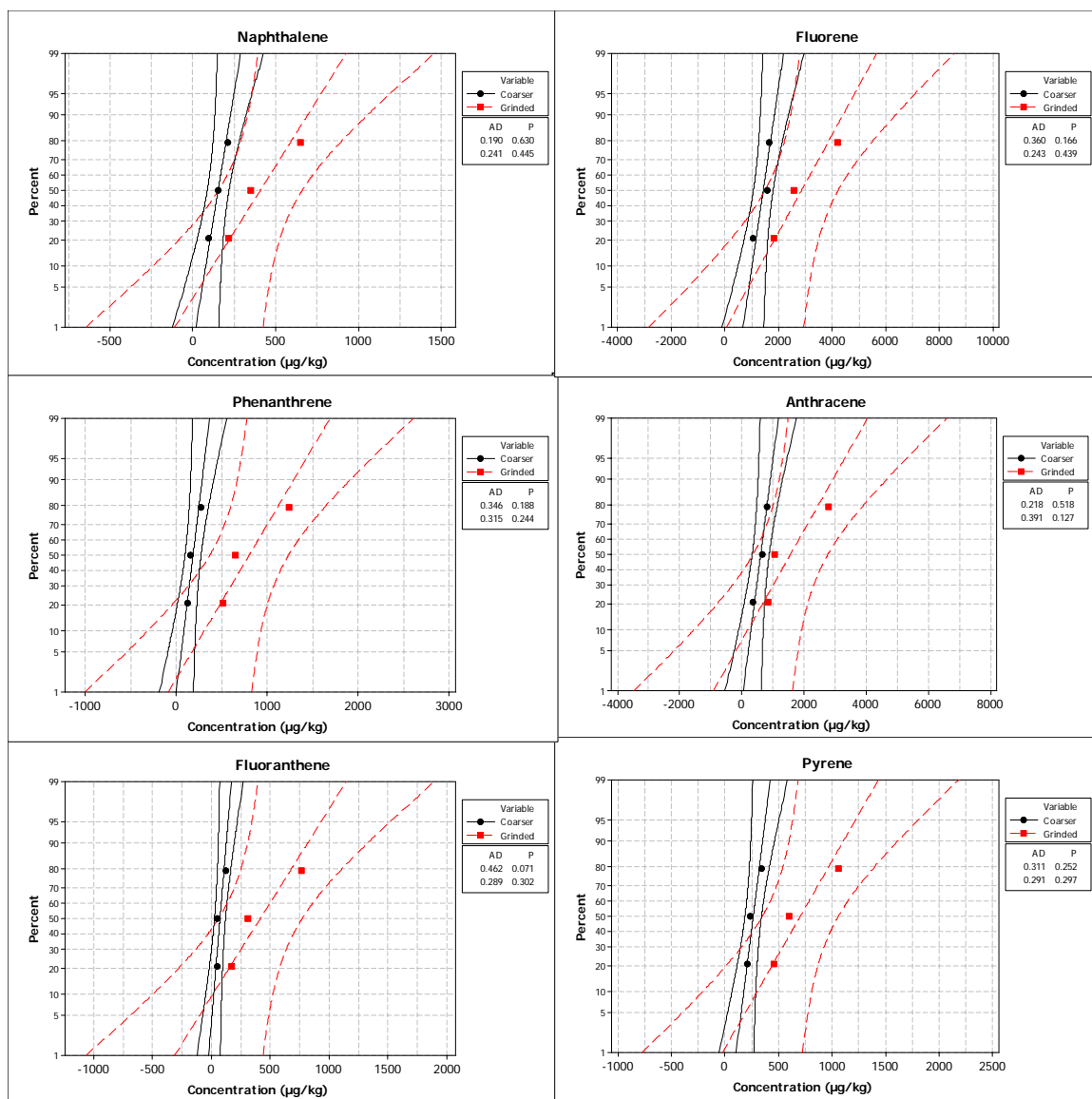


Figure B.20 Normal probability plots for concentrations of naphthalene, fluorene, phenanthrene, anthracene, fluoranthene, pyrene in 1400 - 2800µm size composite sample

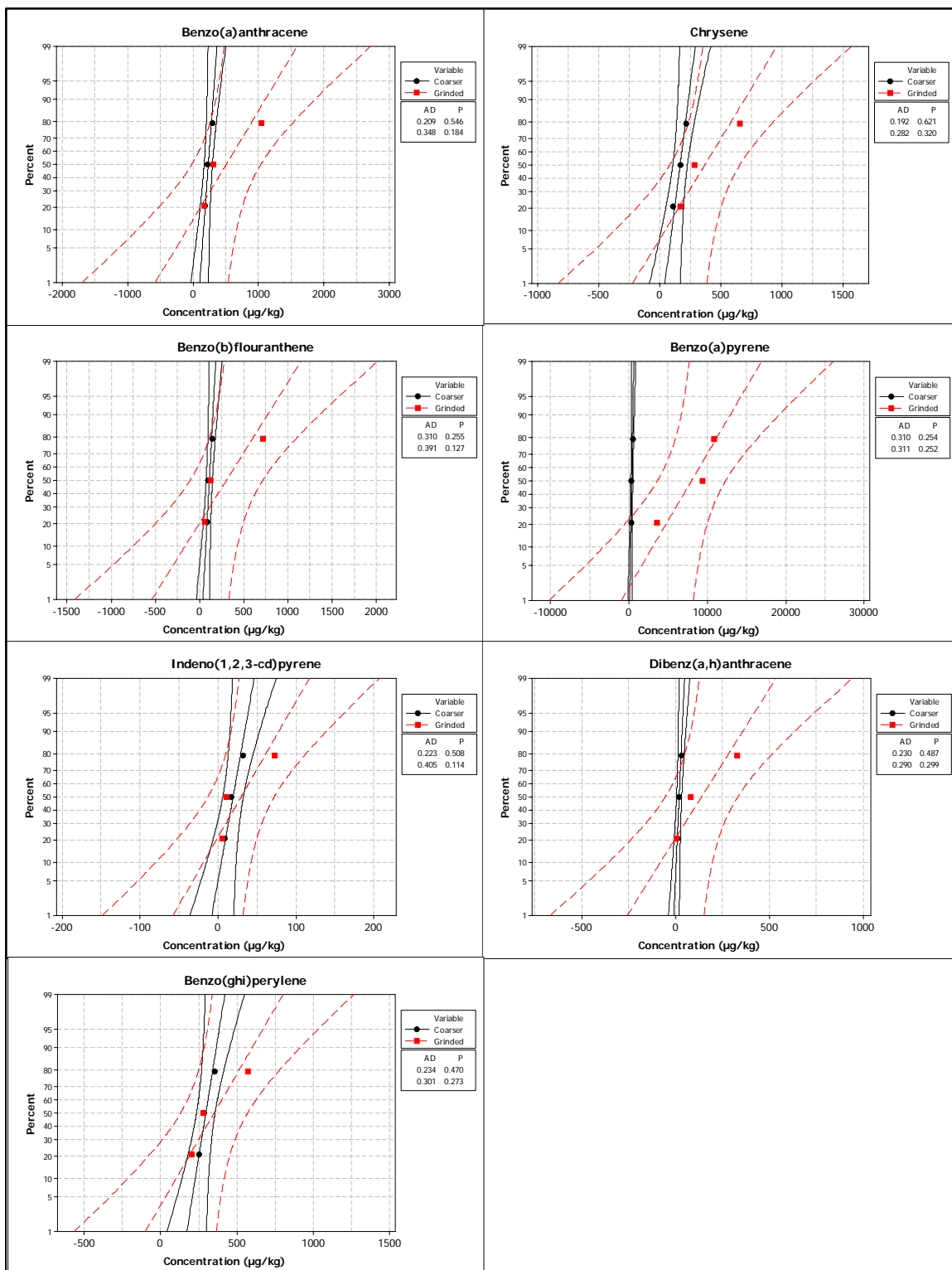


Figure B.21 Normal probability plots for for benzo(a)anthracene, chrysene, benzo(a)pyrene, Benzo(b)flouranthene, Indeno(1,2,3-cd)pyrene, dibenz(a,h)anthracene, benzo(ghi)perylene in 1400 - 2800µm size composite sample

APPENDIX C

STATISTICAL ANALYSES OF THE DATA

Table C.1 Observed Concentrations of Naphthalene at Cribbs Mill Creek

Size Range (µm)	Concentration (µg/kg), Sample Number					Mean Concentration (µg/kg)	Standard Deviation
	3/28	8/18	9/9	9/26	10/9		
< 45	189	92	1045	568	283	436	384
45 - 90	101	59	466	486	216	266	200
90 - 180	59	101	683	681	281	361	305
180 - 355	62	61	176	252	125	135	81
355 - 710	37	87	362	103	75	133	130
710 - 1400	156	113	8126	824	365	1917	3483
1400 - 2800	102	87	7973	1866	685	2143	3338
> 2800 (w/o LOM)	84	99	153	259	147	149	69
> 2800 (LOM)	1057	1895	4584	2015	1656	2241	1361

w/o LOM = with LOM removed LOM = Large organic matter

Table C.2 Observed Concentrations of Fluorene at Cribbs Mill Creek

Size Range (µm)	Concentration (µg/kg), Sample Number					Mean Concentration (µg/kg)	Standard Deviation
	3/28	8/18	9/9	9/26	10/9		
< 45	56	89	26	685	256	223	273
45 - 90	67	35	54	212	111	96	71
90 - 180	25	81	567	329	307	262	217
180 - 355	59	52	15	521	199	169	209
355 - 710	48	41	541	105	231	193	209
710 - 1400	61	58	458	149	223	190	165
1400 - 2800	108	101	389	565	354	303	198
> 2800 (w/o LOM)	49	251	159	255	154	174	85
> 2800 (LOM)	1903	2057	3289	1204	2132	2117	751

w/o LOM = with LOM removed LOM = Large organic matter

Table C.3 Observed Concentrations of Phenanthrene at Cribbs Mill Creek

Size Range (μm)	Concentration ($\mu\text{g}/\text{kg}$), Sample Number					Mean Concentration ($\mu\text{g}/\text{kg}$)	Standard Deviation
	3/28	8/18	9/9	9/26	10/9		
< 45	256	98	27	189	105	135	89
45 - 90	206	40	86	78	68	96	64
90 - 180	167	ND	53	167	110	124	55
180 - 355	ND	52	12	111	58	58	41
355 - 710	ND	28	56	97	60	60	28
710 - 1400	392	42	41	166	83	145	147
1400 - 2800	941	15	276	247	179	332	355
> 2800 (w/o LOM)	124	611	18	98	242	219	234
> 2800 (LOM)	1980	2304	5821	953	3026	2817	1838

w/o LOM = with LOM removed LOM = Large organic matter

Table C.4 Observed Concentrations of Anthracene at Cribbs Mill Creek

Size Range (μm)	Concentration ($\mu\text{g}/\text{kg}$), Sample Number					Mean Concentration ($\mu\text{g}/\text{kg}$)	Standard Deviation
	3/28	8/18	9/9	9/26	10/9		
< 45	223	125	178	593	298	283	184
45 - 90	193	65	309	402	259	246	126
90 - 180	53	20	105	442	189	162	169
180 - 355	ND	33	18	202	84	84	83
355 - 710	132	31	262	684	326	287	250
710 - 1400	603	73	832	525	477	502	276
1400 - 2800	2480	53	1035	632	573	955	921
> 2800 (w/o LOM)	321	126	69	429	208	231	146
> 2800 (LOM)	2540	4215	853	1621	2230	2292	1254

w/o LOM = with LOM removed LOM = Large organic matter

Table C.5 Observed Concentrations of Fluoranthene at Cribbs Mill Creek

Size Range (μm)	Concentration ($\mu\text{g}/\text{kg}$), Sample Number					Mean Concentration ($\mu\text{g}/\text{kg}$)	Standard Deviation
	3/28	8/18	9/9	9/26	10/9		
< 45	332	290	44	302	222	238	116
45 – 90	441	399	67	325	302	307	145
90 – 180	245	243	43	208	177	183	83
180 – 355	141	159	43	127	114	117	44
355 – 710	138	160	133	139	143	143	10
710 – 1400	398	278	149	301	275	280	89
1400 – 2800	366	269	291	542	308	355	110
> 2800 (w/o LOM)	240	105	20	211	122	140	88
> 2800 (LOM)	2240	1092	3059	1092	2238	1944	847

w/o LOM = with LOM removed LOM = Large organic matter

Table C.6 Observed Concentrations of Pyrene at Cribbs Mill Creek

Size Range (μm)	Concentration ($\mu\text{g}/\text{kg}$), Sample Number					Mean Concentration ($\mu\text{g}/\text{kg}$)	Standard Deviation
	3/28	8/18	9/9	9/26	10/9		
< 45	313	363	66	562	330	327	177
45 - 90	405	226	116	369	237	271	117
90 - 180	178	95	71	543	236	225	190
180 - 355	117	60	99	215	125	123	57
355 - 710	98	69	40	289	133	126	98
710 - 1400	272	90	214	312	205	219	84
1400 - 2800	261	159	111	386	219	227	105
> 2800 (w/o LOM)	527	321	50	198	190	257	179
> 2800 (LOM)	2240	2654	922	2923	2166	2181	769

w/o LOM = with LOM removed LOM = Large organic matter

Table C.7 Observed Concentrations of Benzo(a)anthracene at Cribbs Mill Creek

Size Range (μm)	Concentration ($\mu\text{g}/\text{kg}$), Sample Number					Mean Concentration ($\mu\text{g}/\text{kg}$)	Standard Deviation
	3/28	8/18	9/9	9/26	10/9		
< 45	270	89	179	689	350	315	231
45 - 90	321	53	205	522	299	280	172
90 - 180	179	12	330	755	315	318	276
180 - 355	93	40	185	629	254	240	233
355 - 710	97	15	206	511	208	207	188
710 - 1400	185	22	419	173	127	185	146
1400 - 2800	171	25	933	393	196	344	355
> 2800 (w/o LOM)	350	72	29	218	1547	443	630
> 2800 (LOM)	4350	2537	1260	3202	3313	2932	1138

w/o LOM = with LOM removed LOM = Large organic matter

Table C.8 Observed Concentrations of Chrysene at Cribbs Mill Creek

Size Range (μm)	Concentration ($\mu\text{g}/\text{kg}$), Sample Number					Mean Concentration ($\mu\text{g}/\text{kg}$)	Standard Deviation
	3/28	8/18	9/9	9/26	10/9		
< 45	418	108	96	568	361	310	205
45 - 90	507	43	147	922	525	429	349
90 - 180	307	30	249	664	407	331	231
180 - 355	162	49	142	356	220	186	113
355 - 710	158	37	176	383	239	199	126
710 - 1400	350	42	424	142	305	253	157
1400 - 2800	313	56	833	136	427	353	305
> 2800 (w/o LOM)	310	134	15	142	156	151	105
> 2800 (LOM)	3010	2936	3016	1353	1788	2420	792

w/o LOM = with LOM removed LOM = Large organic matter

Table C.9 Observed Concentrations of Benzo(b)fluoranthrene at Cribbs Mill Creek

Size Range (μm)	Concentration ($\mu\text{g}/\text{kg}$), Sample Number					Mean Concentration ($\mu\text{g}/\text{kg}$)	Standard Deviation
	3/28	8/18	9/9	9/26	10/9		
< 45	1010	686	216	496	574	597	289
45 - 90	105	119	205	562	291	257	187
90 - 180	593	62	252	268	371	309	194
180 - 355	2600	626	108	252	987	915	1002
355 - 710	320	103	167	322	270	236	98
710 - 1400	741	414	613	468	607	569	129
1400 - 2800	735	114	1323	236	765	635	483
> 2800 (w/o LOM)	532	455	36	163	1530	543	588
> 2800 (LOM)	4390	3522	1040	1633	1869	2491	1405

w/o LOM = with LOM removed LOM = Large organic matter

Table C.10 Observed Concentrations of Benzo(a)pyrene at Cribbs Mill Creek

Size Range (μm)	Concentration ($\mu\text{g}/\text{kg}$), Sample Number					Mean Concentration ($\mu\text{g}/\text{kg}$)	Standard Deviation
	3/28	8/18	9/9	9/26	10/9		
< 45	665	693	212	924	610	621	258
45 - 90	882	510	324	598	663	596	205
90 - 180	512	515	749	995	674	689	199
180 - 355	1970	289	233	570	943	801	711
355 - 710	159	664	242	430	445	388	197
710 - 1400	269	549	2086	435	1023	872	734
1400 - 2800	345	910	8132	294	3112	2559	3321
> 2800 (w/o LOM)	850	687	857	239	594	645	253
> 2800 (LOM)	4650	2109	3013	1099	2074	2589	1336

w/o LOM = with LOM removed LOM = Large organic matter

Table C.11 Observed Concentrations of Indeno(1,2,3-cd)pyrene at Cribbs Mill Creek

Size Range (μm)	Concentration ($\mu\text{g}/\text{kg}$), Sample Number					Mean Concentration ($\mu\text{g}/\text{kg}$)	Standard Deviation
	3/28	8/18	9/9	9/26	10/9		
< 45	732	562	420	854	668	647	165
45 - 90	281	393	992	470	581	543	273
90 - 180	374	312	1752	2406	1511	1271	908
180 - 355	131	130	588	427	382	332	199
355 - 710	219	356	786	360	455	435	213
710 - 1400	269	287	1308	376	651	578	436
1400 - 2800	261	550	3563	283	1369	1205	1393
> 2800 (w/o LOM)	534	144	98	211	610	320	235
> 2800 (LOM)	1520	956	3563	1956	2717	2142	1022

w/o LOM = with LOM removed LOM = Large organic matter

Table C.12 Observed Concentrations of Dibenz(a,h)anthracene at Cribbs Mill Creek

Size Range (μm)	Concentration ($\mu\text{g}/\text{kg}$), Sample Number					Mean Concentration ($\mu\text{g}/\text{kg}$)	Standard Deviation
	3/28	8/18	9/9	9/26	10/9		
< 45	114	413	901	953	656	607	350
45 - 90	40	358	1266	562	623	570	451
90 - 180	50	412	1460	1051	854	765	550
180 - 355	23	257	623	623	423	390	256
355 - 710	32	301	715	699	482	446	287
710 - 1400	ND	227	1344	1398	1371	1085	572
1400 - 2800	559	448	4941	351	1950	1650	1952
> 2800 (w/o LOM)	720	148	68	492	427	371	265
> 2800 (LOM)	720	3022	1533	2533	1964	1954	891

w/o LOM = with LOM removed LOM = Large organic matter

Table C.13 Observed Concentrations of Benzo(ghi)perylene at Cribbs Mill Creek

Size Range (μm)	Concentration ($\mu\text{g}/\text{kg}$), Sample Number					Mean Concentration ($\mu\text{g}/\text{kg}$)	Standard Deviation
	3/28	8/18	9/9	9/26	10/9		
< 45	548	167	990	453	389	509	303
45 - 90	153	86	474	622	287	324	223
90 - 180	236	153	1346	269	219	444	506
180 - 355	84	129	151	182	132	136	36
355 - 710	135	69	ND	193	132	132	50
710 - 1400	190	62	386	1997	750	677	782
1400 - 2800	313	107	1027	683	368	499	360
> 2800 (w/o LOM)	588	147	562	365	500	433	181
> 2800 (LOM)	988	1238	798	3521	2658	1841	1190

w/o LOM = with LOM removed LOM = Large organic matter

Table C.14 Observed Concentration of Naphthalene at Hunter Creek

Size Range (μm)	Concentration ($\mu\text{g}/\text{kg}$), Sample Number					Mean Concentration ($\mu\text{g}/\text{kg}$)	Standard Deviation
	8/18	9/9	9/26	10/9	10/21		
< 45	11	178	192	74	195	130	83
45 - 90	27	98	186	109	59	96	60
90 - 180	21	172	87	4	68	70	66
180 - 355	15	281	57	9	26	78	115
355 - 710	27	63	254	94	44	97	92
710 - 1400	31	20	157	236	519	193	204
1400 - 2800	78	102	551	351	106	238	207
> 2800 (w/o LOM)	82	5	72	168	147	95	65
> 2800 (LOM)	1723	2150	5413	8667	2311	4053	2967

w/o LOM = with LOM removed LOM = Large organic matter

Table C.15 Observed Concentration of Fluorene at Hunter Creek

Size Range (μm)	Concentration ($\mu\text{g}/\text{kg}$), Sample Number					Mean Concentration ($\mu\text{g}/\text{kg}$)	Standard Deviation
	8/18	9/9	9/26	10/9	10/21		
< 45	107	542	93	198	1090	406	424
45 - 90	103	367	292	264	521	310	153
90 - 180	160	562	123	34	417	259	221
180 - 355	80	53	40	32	197	80	68
355 - 710	114	63	NA	14	245	109	99
710 - 1400	20	305	60	38	407	166	178
1400 - 2800	178	410	616	515	183	380	196
> 2800 (w/o LOM)	79	89	214	126	217	145	67
> 2800 (LOM)	2900	1435	986	297	1075	1339	965

w/o LOM = with LOM removed LOM = Large organic matter

Table C.16 Observed Concentration of Phenanthrene at Hunter Creek

Size Range (μm)	Concentration ($\mu\text{g}/\text{kg}$), Sample Number					Mean Concentration ($\mu\text{g}/\text{kg}$)	Standard Deviation
	8/18	9/9	9/26	10/9	10/21		
< 45	772	529	351	249	926	566	283
45 - 90	395	372	351	259	799	435	210
90 - 180	34	503	59	39	457	218	239
180 - 355	131	238	ND	9	241	155	110
355 - 710	248	162	55	27	260	150	107
710 - 1400	42	333	105	46	422	190	176
1400 - 2800	107	412	146	106	101	174	134
> 2800 (w/o LOM)	137	34	128	153	322	155	104
> 2800 (LOM)	2748	874	1400	925	479	1285	881

w/o LOM = with LOM removed LOM = Large organic matter

Table C.17 Observed Concentration of Anthracene at Hunter Creek

Size Range (μm)	Concentration ($\mu\text{g}/\text{kg}$), Sample Number					Mean Concentration ($\mu\text{g}/\text{kg}$)	Standard Deviation
	8/18	9/9	9/26	10/9	10/21		
< 45	58	708	125	320	1599	562	632
45 - 90	54	543	651	515	949	542	323
90 - 180	424	712	52	612	570	474	257
180 - 355	16	432	86	ND	456	248	229
355 - 710	55	342	19	136	306	172	146
710 - 1400	132	900	27	ND	637	424	414
1400 - 2800	83	309	214	152	566	265	188
> 2800 (w/o LOM)	103	200	313	178	613	281	200
> 2800 (LOM)	3502	2189	3141	2150	1594	2515	783

w/o LOM = with LOM removed LOM = Large organic matter

Table C.18 Observed Concentration of Fluranthene at Hunter Creek

Size Range (μm)	Concentration ($\mu\text{g}/\text{kg}$), Sample Number					Mean Concentration ($\mu\text{g}/\text{kg}$)	Standard Deviation
	8/18	9/9	9/26	10/9	10/21		
< 45	701	1256	1324	2935	2066	1656	864
45 - 90	1385	582	1521	2605	1352	1489	724
90 - 180	409	1122	846	323	1109	762	379
180 - 355	701	712	124	56	561	431	318
355 - 710	1294	633	201	79	506	543	476
710 - 1400	917	462	248	69	469	433	317
1400 - 2800	517	612	82	56	171	287	259
> 2800 (w/o LOM)	712	303	60	142	321	308	251
> 2800 (LOM)	1893	650	1543	620	638	1069	605

w/o LOM = with LOM removed LOM = Large organic matter

Table C.19 Observed Concentrations of Pyrene at Hunter Creek

Size Range (μm)	Concentration ($\mu\text{g}/\text{kg}$), Sample Number					Mean Concentration ($\mu\text{g}/\text{kg}$)	Standard Deviation
	8/18	9/9	9/26	10/9	10/21		
< 45	1382	958	1324	1582	2495	1548	575
45 - 90	647	1022	1241	1770	1261	1188	408
90 - 180	2097	957	286	81	1154	915	798
180 - 355	340	563	58	25	522	302	252
355 - 710	1636	218	86	20	480	488	665
710 - 1400	330	271	124	33	612	274	222
1400 - 2800	216	328	119	31	403	220	151
> 2800 (w/o LOM)	270	74	161	41	129	135	89
> 2800 (LOM)	2987	1594	1875	748	1298	1700	832

w/o LOM = with LOM removed LOM = Large organic matter

Table C.20 Observed Concentrations of Benzo(a)anthracene at Hunter Creek

Size Range (μm)	Concentration ($\mu\text{g}/\text{kg}$), Sample Number					Mean Concentration ($\mu\text{g}/\text{kg}$)	Standard Deviation
	8/18	9/9	9/26	10/9	10/21		
< 45	80	722	1622	1208	1826	1092	706
45 - 90	85	428	508	1411	1879	862	750
90 - 180	184	801	ND	11	677	418	380
180 - 355	263	390	39	22	291	201	163
355 - 710	862	287	27	175	460	362	321
710 - 1400	22	352	43	156	296	174	148
1400 - 2800	62	628	99	167	502	292	256
> 2800 (w/o LOM)	109	21	107	159	263	132	89
> 2800 (LOM)	2613	1180	2415	729	1526	1693	804

w/o LOM = with LOM removed LOM = Large organic matter

Table C.21 Observed Concentrations of Chrysene at Hunter Creek

Size Range (μm)	Concentration ($\mu\text{g}/\text{kg}$), Sample Number					Mean Concentration ($\mu\text{g}/\text{kg}$)	Standard Deviation
	8/18	9/9	9/26	10/9	10/21		
< 45	210	1257	924	1591	2095	1215	709
45 - 90	186	1033	2354	1815	681	1214	871
90 - 180	518	1303	58	226	820	585	495
180 - 355	596	632	95	34	381	348	276
355 - 710	1037	589	51	190	505	475	384
710 - 1400	40	169	315	151	269	189	108
1400 - 2800	108	633	84	268	469	312	236
> 2800 (w/o LOM)	88	41	47	142	338	131	123
> 2800 (LOM)	1823	553	985	1462	1259	1217	480

w/o LOM = with LOM removed LOM = Large organic matter

Table C.22 Observed Concentrations of Benzo(b)flourantrene at Hunter Creek

Size Range (μm)	Concentration ($\mu\text{g}/\text{kg}$), Sample Number					Mean Concentration ($\mu\text{g}/\text{kg}$)	Standard Deviation
	8/18	9/9	9/26	10/9	10/21		
< 45	109	1551	859	1307	1418	1049	586
45 - 90	69	875	1102	1626	1883	1111	708
90 - 180	77	1505	856	168	479	617	582
180 - 355	113	521	124	22	466	249	227
355 - 710	50	313	514	111	479	294	210
710 - 1400	204	285	413	62	671	327	231
1400 - 2800	152	154	241	64	835	289	311
> 2800 (w/o LOM)	204	81	77	244	637	249	229
> 2800 (LOM)	1524	870	745	940	4642	1744	1647

w/o LOM = with LOM removed LOM = Large organic matter

Table C.23 Observed Concentrations of Benzo(a)pyrene at Hunter Creek

Size Range (μm)	Concentration ($\mu\text{g}/\text{kg}$), Sample Number					Mean Concentration ($\mu\text{g}/\text{kg}$)	Standard Deviation
	8/18	9/9	9/26	10/9	10/21		
< 45	675	2331	5421	7803	1514	3549	2979
45 - 90	401	782	2015	12311	2935	3689	4923
90 - 180	495	894	206	650	381	525	262
180 - 355	410	901	26	214	347	380	326
355 - 710	284	452	NA	45	524	326	213
710 - 1400	585	182	285	127	772	390	277
1400 - 2800	936	544	142	70	1055	550	448
> 2800 (w/o LOM)	431	279	144	100	544	300	188
> 2800 (LOM)	1023	1501	953	610	7556	2329	2939

w/o LOM = with LOM removed LOM = Large organic matter

Table C.24 Observed Concentrations of Indeno(1,2,3-cd)pyrene at Hunter Creek

Size Range (μm)	Concentration ($\mu\text{g}/\text{kg}$), Sample Number					Mean Concentration ($\mu\text{g}/\text{kg}$)	Standard Deviation
	8/18	9/9	9/26	10/9	10/21		
< 45	420	255	1622	1935	493	945	773
45 - 90	276	125	1985	1570	627	917	820
90 - 180	234	972	125	256	109	339	359
180 - 355	184	322	ND	128	342	244	105
355 - 710	344	302	514	158	531	370	156
710 - 1400	492	80	100	216	3020	782	1262
1400 - 2800	626	403	317	209	1751	661	628
> 2800 (w/o LOM)	126	57	315	1723	624	569	682
> 2800 (LOM)	1203	588	542	2403	1505	1248	764

w/o LOM = with LOM removed LOM = Large organic matter

Table C.25 Observed Concentrations of Dibenz(a,h)anthracene at Hunter Creek

Size Range (μm)	Concentration ($\mu\text{g}/\text{kg}$), Sample Number					Mean Concentration ($\mu\text{g}/\text{kg}$)	Standard Deviation
	8/18	9/9	9/26	10/9	10/21		
< 45	333	1962	4876	6448	433	2810	2739
45 - 90	217	918	2541	3630	925	1646	1399
90 - 180	183	1264	259	533	108	469	472
180 - 355	138	726	154	30	432	296	283
355 - 710	299	523	214	128	713	375	239
710 - 1400	412	431	512	206	939	500	270
1400 - 2800	488	625	112	220	1549	599	569
> 2800 (w/o LOM)	312	69	309	356	524	314	163
> 2800 (LOM)	1724	1385	679	802	864	1091	445

w/o LOM = with LOM removed LOM = Large organic matter

Table C.26 Observed Concentrations of Benzo(ghi)perylene at Hunter Creek

Size Range (μm)	Concentration ($\mu\text{g}/\text{kg}$), Sample Number					Mean Concentration ($\mu\text{g}/\text{kg}$)	Standard Deviation
	8/18	9/9	9/26	10/9	10/21		
< 45	96	1390	2016	2247	894	1329	870
45 - 90	62	978	525	803	1683	810	598
90 - 180	59	1165	558	ND	176	490	498
180 - 355	43	782	57	ND	617	375	381
355 - 710	49	328	224	172	364	228	126
710 - 1400	67	734	219	173	1318	502	524
1400 - 2800	124	523	242	117	972	396	362
> 2800 (w/o LOM)	53	147	836	162	646	369	349
> 2800 (LOM)	1073	4222	1400	2092	7102	3178	2513

w/o LOM = with LOM removed LOM = Large organic matter

Table C.27 Observed Concentrations of Naphthalene at Crroll's Creek

Size Range (μm)	Concentration ($\mu\text{g}/\text{kg}$), Sample Number					Mean Concentration ($\mu\text{g}/\text{kg}$)	Standard Deviation
	8/18	9/9	9/26	10/9	10/21		
< 45	22	561	95	102	217	199	214
45 - 90	81	425	157	30	165	171	152
90 - 180	163	11	5	15	102	59	71
180 - 355	15	157	31	55	93	70	57
355 - 710	101	65	464	27	58	143	181
710 - 1400	99	31	782	16	379	261	326
1400 - 2800	107	759	102	215	286	294	271
> 2800 (w/o LOM)	27	183	36	169	231	129	92
> 2800 (LOM)	1702	672	1819	3029	863	1617	936

w/o LOM = with LOM removed LOM = Large organic matter

Table C.28 Observed Concentration of Fluorene at Carroll's Creek

Size Range (μm)	Concentration ($\mu\text{g}/\text{kg}$), Sample Number					Mean Concentration ($\mu\text{g}/\text{kg}$)	Standard Deviation
	8/18	9/9	9/26	10/9	10/21		
< 45	27	175	228	169	121	144	76
45 - 90	184	113	147	266	102	163	66
90 - 180	252	ND	32	99	162	137	94
180 - 355	78	31	101	301	121	126	103
355 - 710	207	11	68	186	69	108	84
710 - 1400	313	ND	307	141	216	244	82
1400 - 2800	224	119	152	187	301	197	70
> 2800 (w/o LOM)	364	723	210	180	169	329	234
> 2800 (LOM)	1263	3621	687	2106	1623	1860	1113

w/o LOM = with LOM removed LOM = Large organic matter

Table C.29 Observed Concentration of Phenanthrene at Carroll's Creek

Size Range (μm)	Concentration ($\mu\text{g}/\text{kg}$), Sample Number					Mean Concentration ($\mu\text{g}/\text{kg}$)	Standard Deviation
	8/18	9/9	9/26	10/9	10/21		
< 45	7	63	8	260	125	92	105
45 - 90	30	64	4	236	96	86	91
90 - 180	44	37	ND	69	81	58	21
180 - 355	17	45	3	241	38	69	98
355 - 710	82	23	178	216	54	111	83
710 - 1400	38	49	33	84	81	57	24
1400 - 2800	92	138	9	124	72	87	51
> 2800 (w/o LOM)	56	172	166	466	98	192	161
> 2800 (LOM)	1253	3802	627	1732	2183	1920	1200

w/o LOM = with LOM removed LOM = Large organic matter

Table C.30 Observed Concentrations of Anthracene at Carroll's Creek

Size Range (μm)	Concentration ($\mu\text{g}/\text{kg}$), Sample Number					Mean Concentration ($\mu\text{g}/\text{kg}$)	Standard Deviation
	8/18	9/9	9/26	10/9	10/21		
< 45	113	104	88	524	261	218	185
45 - 90	115	55	44	69	99	77	30
90 - 180	39	ND	ND	105	64	69	33
180 - 355	102	77	50	290	132	130	94
355 - 710	62	22	53	241	59	87	88
710 - 1400	67	ND	26	317	144	138	128
1400 - 2800	127	231	128	564	231	256	180
> 2800 (w/o LOM)	48	113	163	284	109	144	88
> 2800 (LOM)	1430	2987	627	1027	3724	1959	1332

w/o LOM = with LOM removed LOM = Large organic matter

Table C.31 Observed Concentrations of Fluranthene at Carroll's Creek

Size Range (µm)	Concentration (µg/kg), Sample Number					Mean Concentration (µg/kg)	Standard Deviation
	8/18	9/9	9/26	10/9	10/21		
< 45	60	37	66	154	106	85	46
45 - 90	41	39	28	104	182	79	65
90 - 180	59	63	34	88	213	91	71
180 - 355	18	15	31	137	99	60	55
355 - 710	43	21	53	100	71	58	30
710 - 1400	29	27	61	50	162	66	56
1400 - 2800	93	48	43	99	63	69	26
> 2800 (w/o LOM)	103	69	61	285	121	128	91
> 2800 (LOM)	1026	624	2102	3281	712	1549	1133

w/o LOM = with LOM removed LOM = Large organic matter

Table C.32 Observed Concentrations of Pyrene at Carroll's Creek

Size Range (µm)	Concentration (µg/kg), Sample Number					Mean Concentration (µg/kg)	Standard Deviation
	8/18	9/9	9/26	10/9	10/21		
< 45	21	43	65	211	79	84	75
45 - 90	10	16	67	279	120	99	110
90 - 180	19	21	60	237	153	98	95
180 - 355	31	32	60	249	130	101	92
355 - 710	17	101	82	231	103	107	78
710 - 1400	31	87	49	184	301	130	112
1400 - 2800	51	73	51	202	278	131	104
> 2800 (w/o LOM)	41	71	121	207	182	125	71
> 2800 (LOM)	3120	872	3604	2892	927	2283	1289

w/o LOM = with LOM removed LOM = Large organic matter

Table C.33 Observed Concentrations of Benzo(a)anthracene at Carroll's Creek

Size Range (μm)	Concentration ($\mu\text{g}/\text{kg}$), Sample Number					Mean Concentration ($\mu\text{g}/\text{kg}$)	Standard Deviation
	8/18	9/9	9/26	10/9	10/21		
< 45	33	179	42	131	99	97	61
45 - 90	16	203	21	47	132	84	81
90 - 180	48	22	10	63	219	72	84
180 - 355	43	66	16	110	98	67	39
355 - 710	13	116	152	128	112	104	53
710 - 1400	65	41	99	124	382	142	138
1400 - 2800	99	234	23	223	312	178	115
> 2800 (w/o LOM)	194	452	224	323	110	261	132
> 2800 (LOM)	1782	2039	589	3026	1902	1868	868

w/o LOM = with LOM removed LOM = Large organic matter

Table C.34 Observed Concentrations of Chrysene at Carroll's Creek

Size Range (μm)	Concentration ($\mu\text{g}/\text{kg}$), Sample Number					Mean Concentration ($\mu\text{g}/\text{kg}$)	Standard Deviation
	8/18	9/9	9/26	10/9	10/21		
< 45	72	155	34	631	342	247	246
45 - 90	28	67	19	279	423	163	180
90 - 180	41	13	12	553	240	172	234
180 - 355	68	46	12	104	132	72	47
355 - 710	22	101	131	268	200	144	94
710 - 1400	89	ND	24	160	178	113	71
1400 - 2800	48	196	21	538	312	223	212
> 2800 (w/o LOM)	89	362	60	429	214	231	163
> 2800 (LOM)	1862	2973	894	969	2262	1792	881

w/o LOM = with LOM removed matter LOM = Large organic matter

Table C.35 Observed Concentrations of Benzo(b)flourantrene at Carroll's Creek

Size Range (μm)	Concentration ($\mu\text{g}/\text{kg}$), Sample Number					Mean Concentration ($\mu\text{g}/\text{kg}$)	Standard Deviation
	8/18	9/9	9/26	10/9	10/21		
< 45	20	134	27	343	217	148	136
45 - 90	23	84	20	573	217	184	232
90 - 180	322	23	179	125	98	150	111
180 - 355	16	43	20	38	92	42	30
355 - 710	44	124	62	213	318	152	114
710 - 1400	21	25	18	61	129	51	47
1400 - 2800	162	206	6	314	313	200	127
> 2800 (w/o LOM)	179	178	90	315	216	196	81
> 2800 (LOM)	1027	2712	638	4023	3102	2301	1429

w/o LOM = with LOM removed LOM = Large organic matter

Table C.36 Observed Concentrations of Benzo(a)pyrene at Carroll's Creek

Size Range (μm)	Concentration ($\mu\text{g}/\text{kg}$), Sample Number					Mean Concentration ($\mu\text{g}/\text{kg}$)	Standard Deviation
	8/18	9/9	9/26	10/9	10/21		
< 45	473	180	93	231	289	253	142
45 - 90	431	82	72	536	313	287	207
90 - 180	1049	14	1951	228	612	771	769
180 - 355	303	39	104	31	123	120	110
355 - 710	481	ND	54	635	146	329	274
710 - 1400	340	ND	3	240	128	178	145
1400 - 2800	637	194	6	189	214	248	233
> 2800 (w/o LOM)	263	205	127	295	261	230	66
> 2800 (LOM)	1526	3027	3627	453	1729	2073	1262

w/o LOM = with LOM removed LOM = Large organic matter

Table C.37 Observed Concentrations of Indeno(1,2,3-cd)pyrene at Carroll's Creek

Size Range (μm)	Concentration ($\mu\text{g}/\text{kg}$), Sample Number					Mean Concentration ($\mu\text{g}/\text{kg}$)	Standard Deviation
	8/18	9/9	9/26	10/9	10/21		
< 45	245	216	1494	1302	587	769	596
45 - 90	159	ND	739	672	321	473	278
90 - 180	821	ND	2167	1555	587	1282	719
180 - 355	118	76	603	33	152	197	232
355 - 710	265	211	341	32	101	190	125
710 - 1400	114	ND	120	614	421	317	244
1400 - 2800	158	184	43	562	305	251	198
> 2800 (w/o LOM)	312	237	102	43	211	181	108
> 2800 (LOM)	1672	672	2134	3273	1903	1931	935

w/o LOM = with LOM removed LOM = Large organic matter

Table C.38 Observed Concentrations of Dibenz(a,h)anthracene at Carroll's Creek

Size Range (μm)	Concentration ($\mu\text{g}/\text{kg}$), Sample Number					Mean Concentration ($\mu\text{g}/\text{kg}$)	Standard Deviation
	8/18	9/9	9/26	10/9	10/21		
< 45	204	266	463	655	321	382	180
45 - 90	130	160	93	142	204	146	41
90 - 180	690	54	1838	856	512	790	658
180 - 355	91	110	97	115	291	141	84
355 - 710	214	191	402	114	301	245	111
710 - 1400	96	63	ND	1248	682	522	561
1400 - 2800	165	132	44	623	321	257	228
> 2800 (w/o LOM)	158	146	128	146	289	173	65
> 2800 (LOM)	1700	982	1110	673	2692	1432	797

w/o LOM = with LOM removed LOM = Large organic matter

Table C.39 Observed Concentrations of Benzo(ghi)perylene at Carroll's Creek

Size Range (μm)	Concentration ($\mu\text{g}/\text{kg}$), Sample Number					Mean Concentration ($\mu\text{g}/\text{kg}$)	Standard Deviation
	8/18	9/9	9/26	10/9	10/21		
< 45	56	172	522	371	261	277	180
45 - 90	132	ND	95	425	190	210	148
90 - 180	164	195	623	2578	528	818	1004
180 - 355	39	123	98	43	301	121	107
355 - 710	62	ND	365	50	112	147	148
710 - 1400	59	ND	263	1006	492	455	408
1400 - 2800	112	331	175	523	321	293	160
> 2800 (w/o LOM)	172	237	326	171	302	242	72
> 2800 (LOM)	1527	2386	3027	982	524	1689	1020

w/o LOM = with LOM removed LOM = Large organic matter

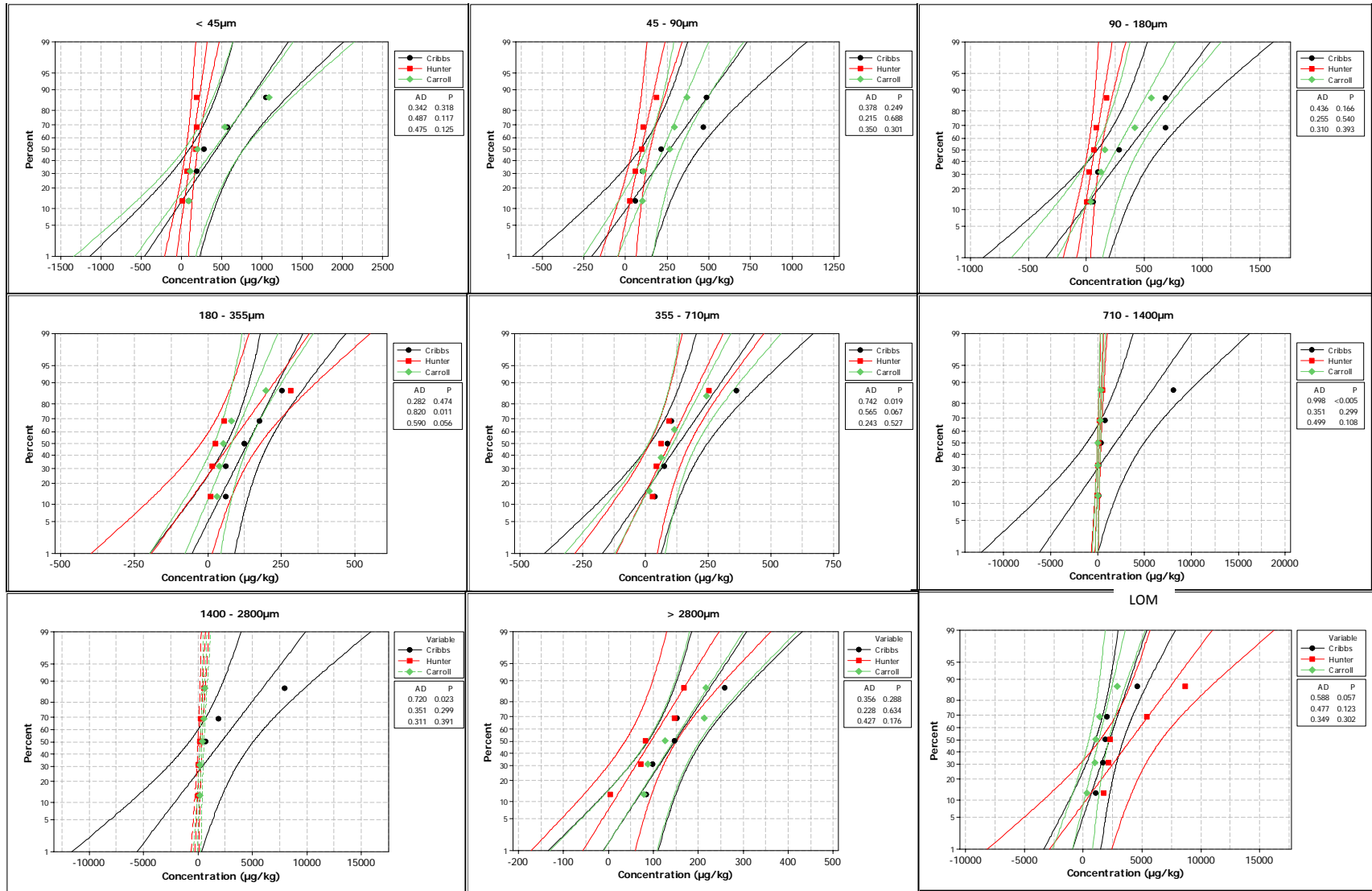


Figure C.1 Probability plots for naphthalene concentrations

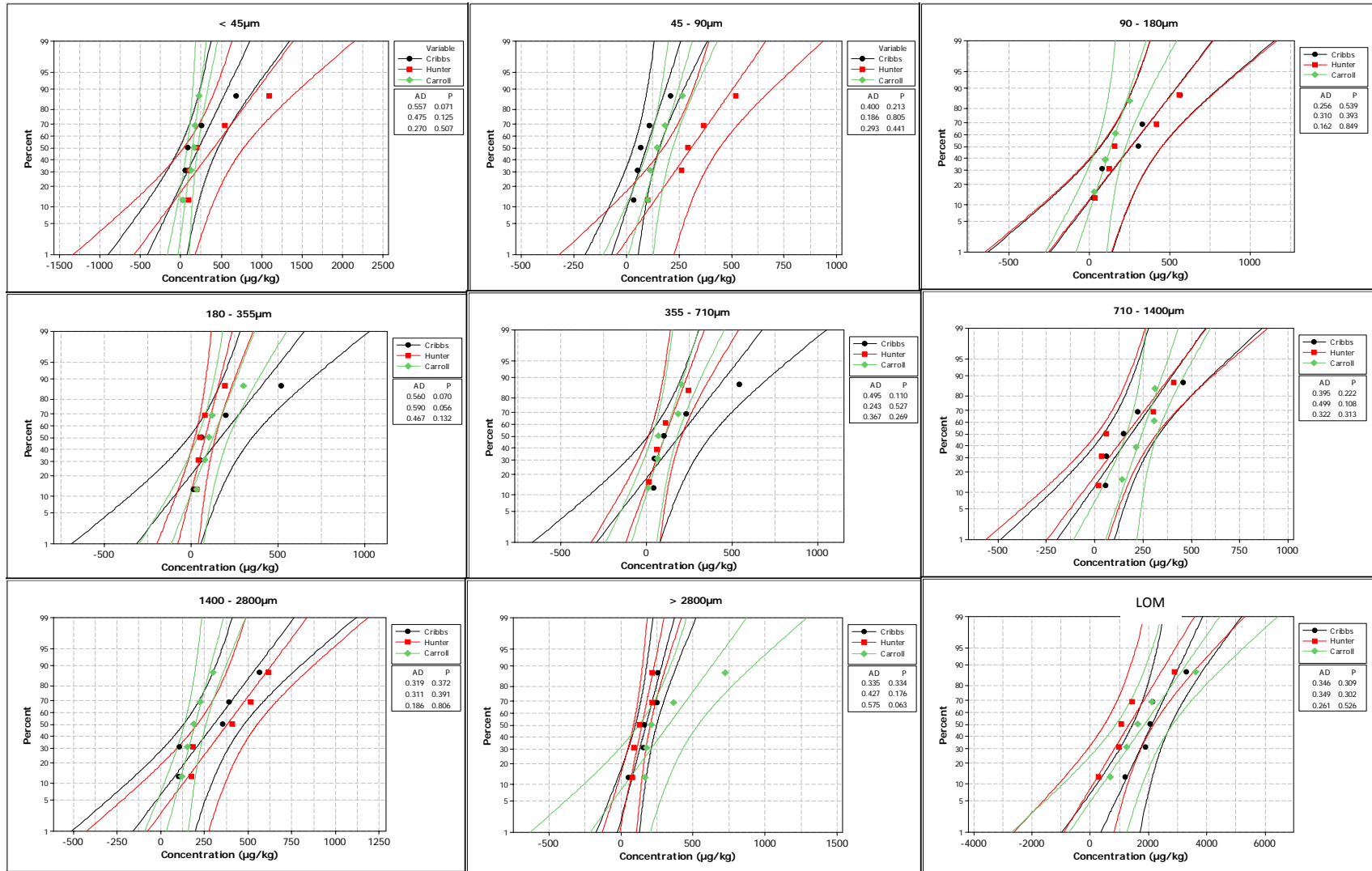


Figure C.2 Probability plots for fluorene concentrations

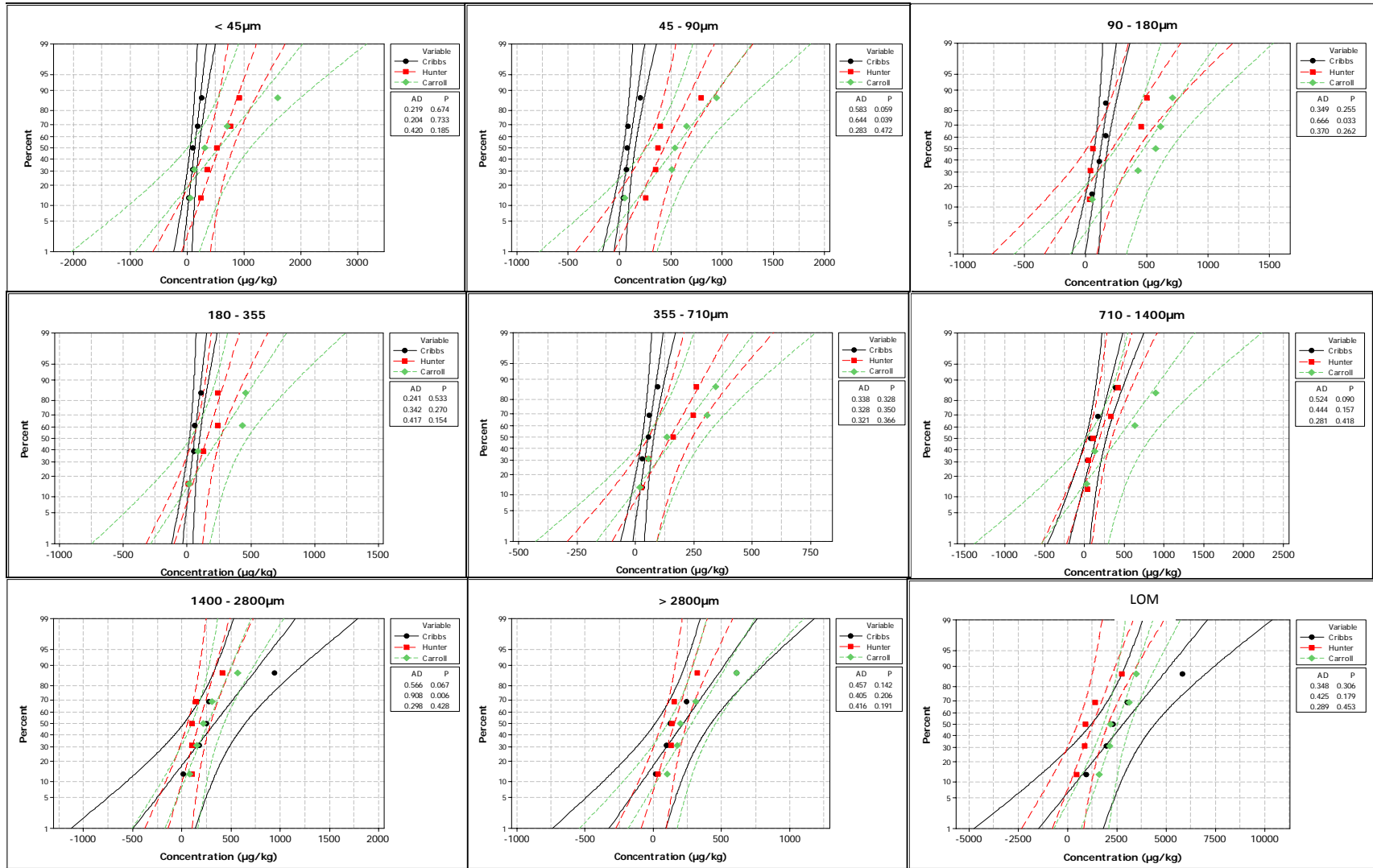


Figure C.3 Probability plots for phenanthrene concentrations

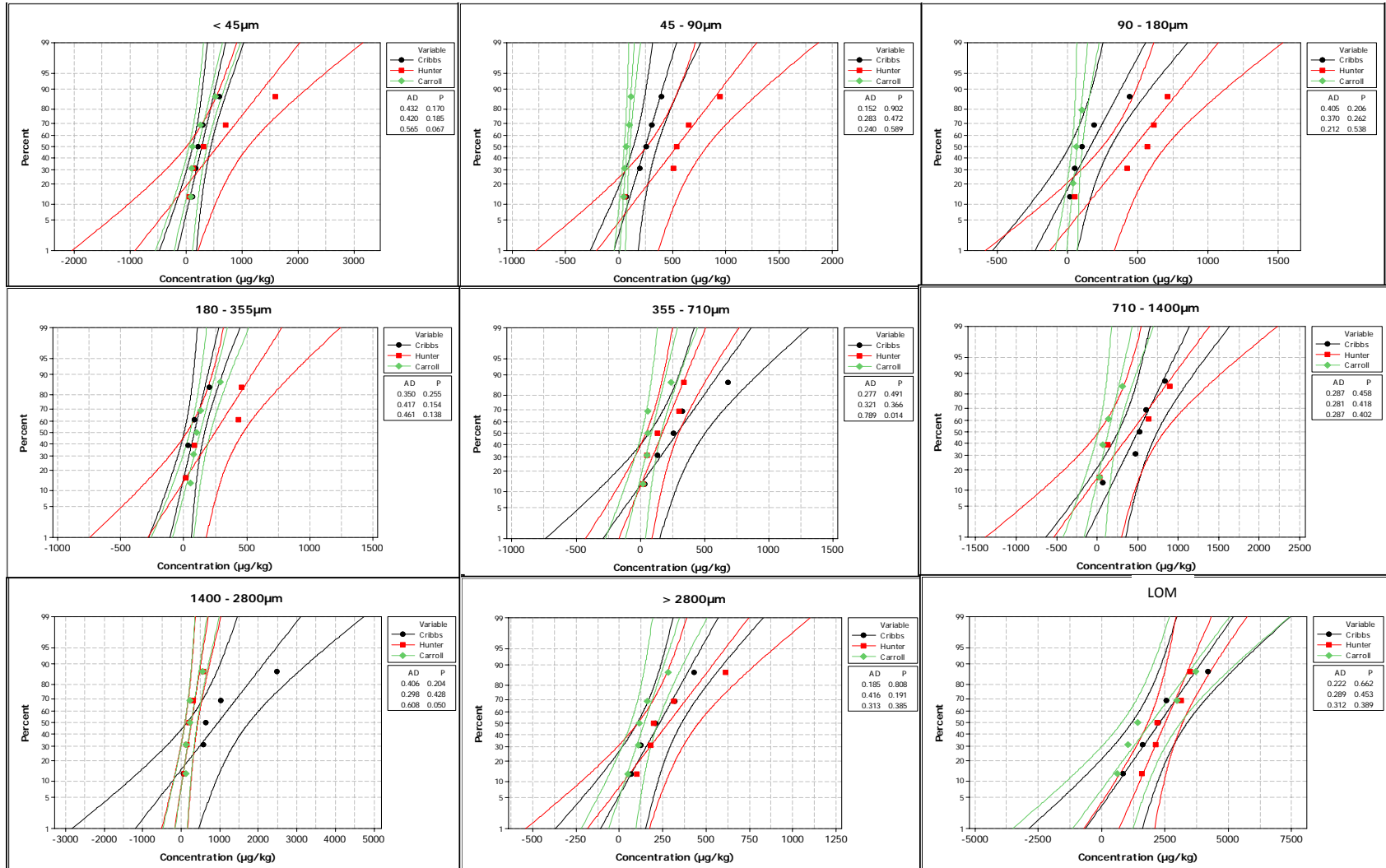


Figure C.4 Probability plots for anthracene concentrations

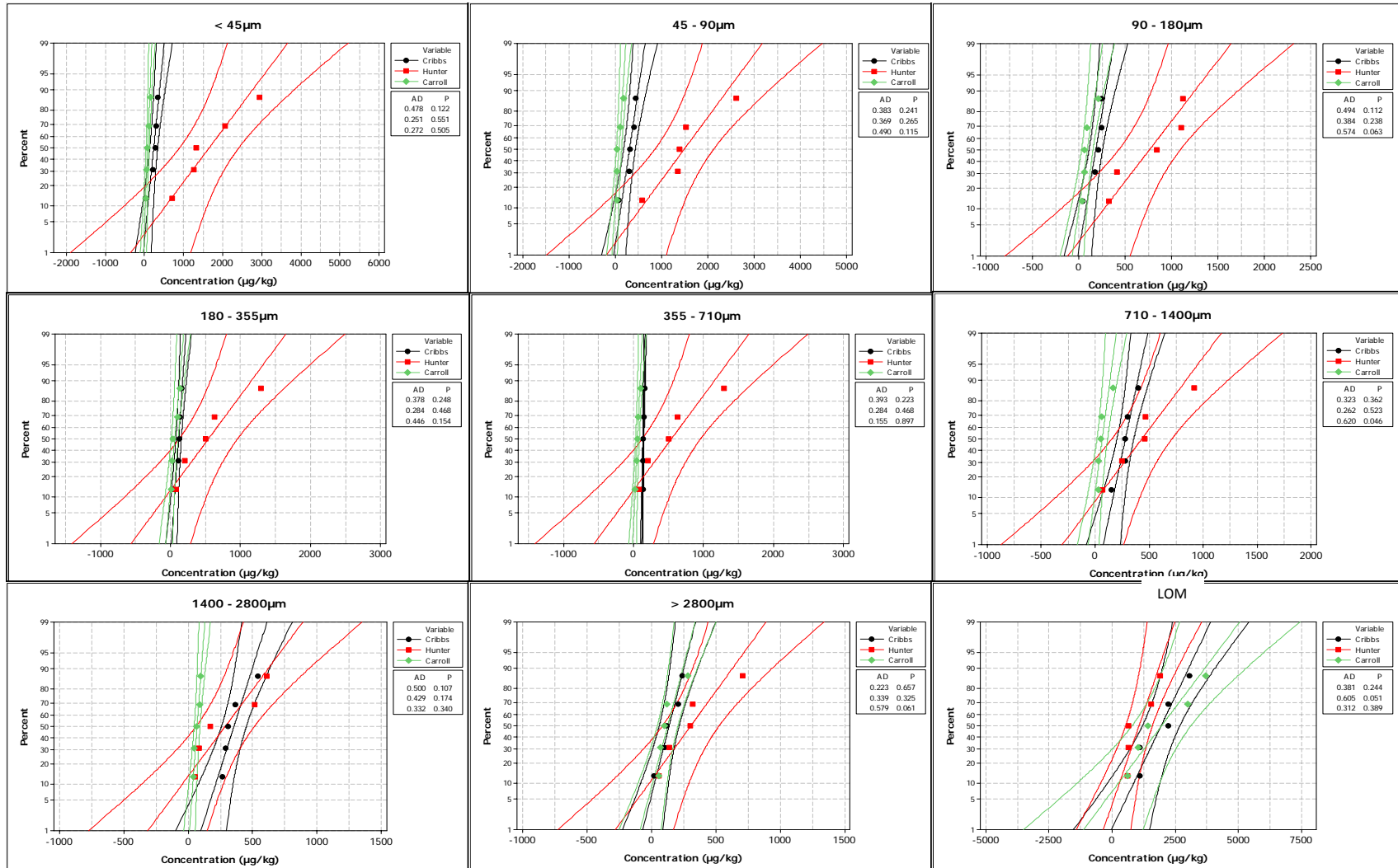


Figure C.5 Probability plots for fluranthene concentrations

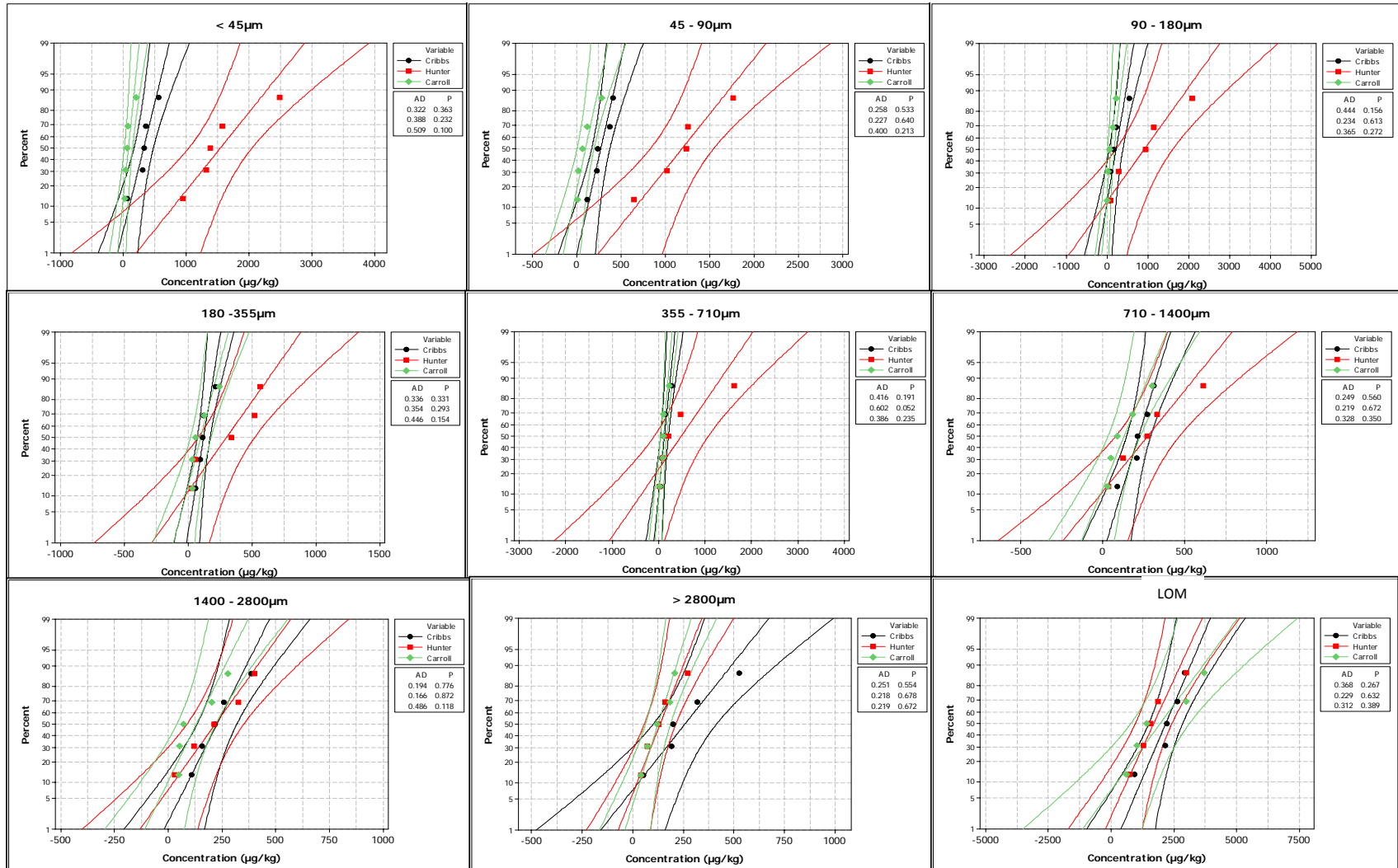


Figure C.6 Probability plots for pyrene concentrations

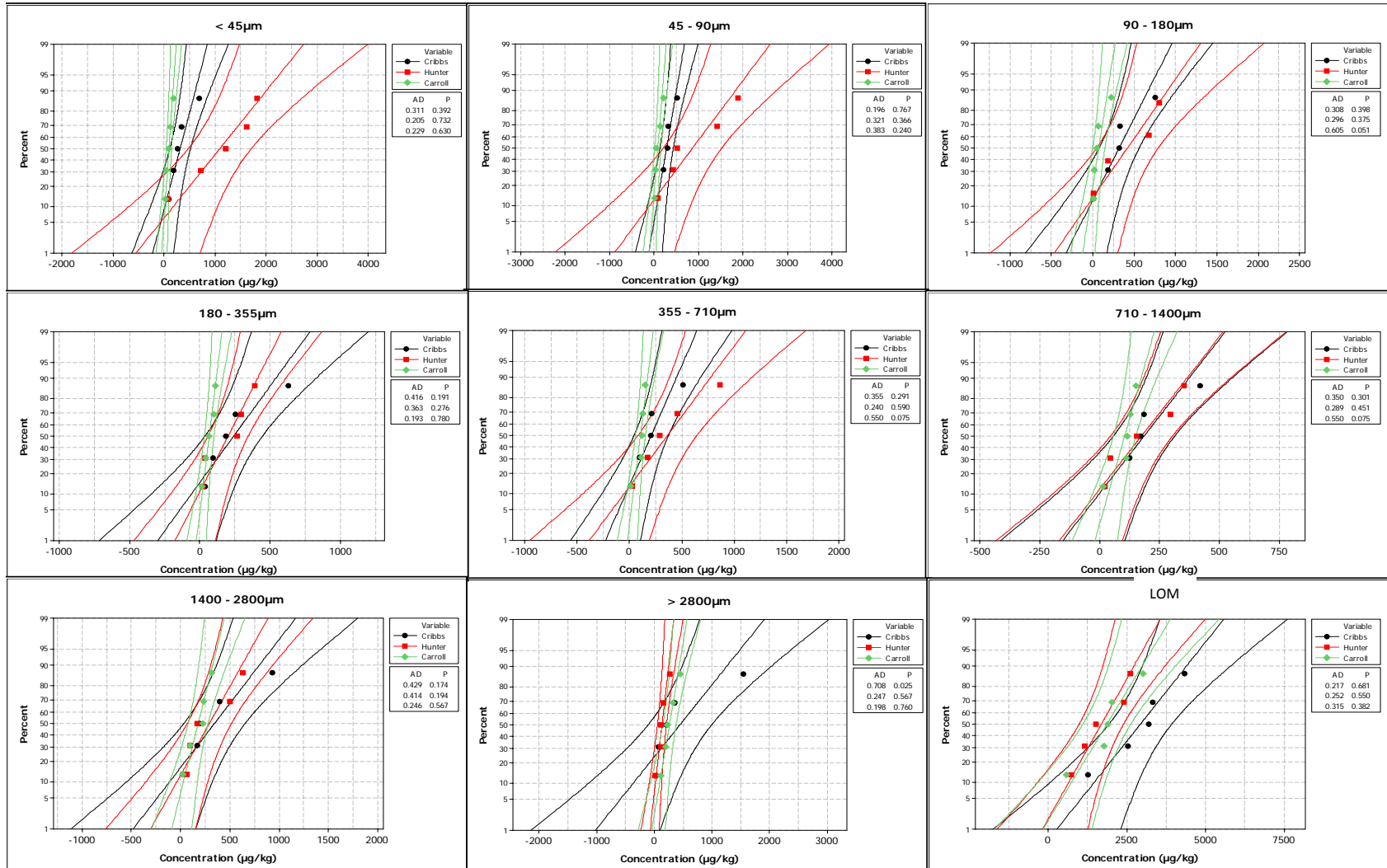


Figure C.7 Probability plots for benzo(a)anthracene concentrations

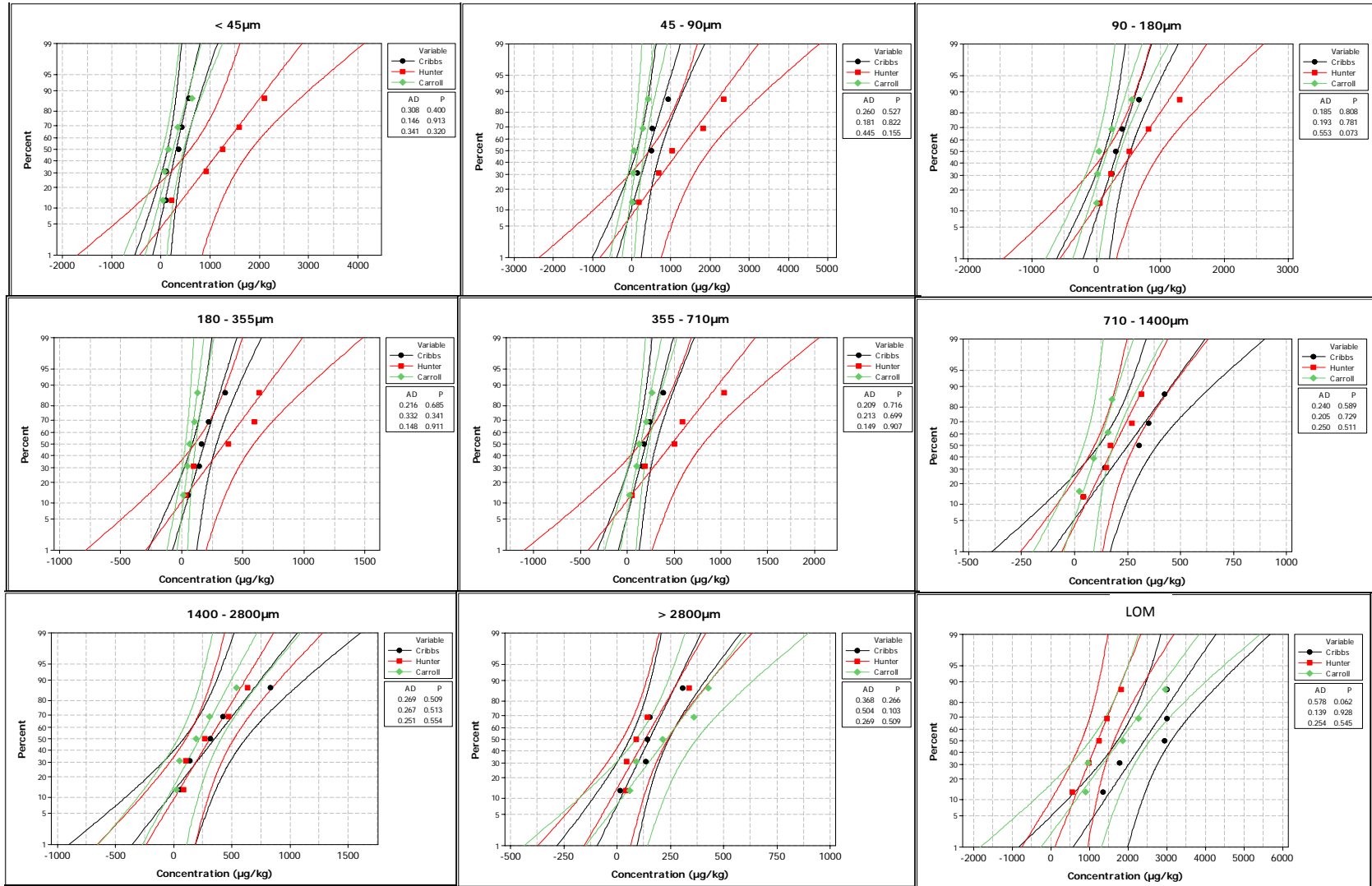


Figure C.8 Probability plots for chrysenes concentrations

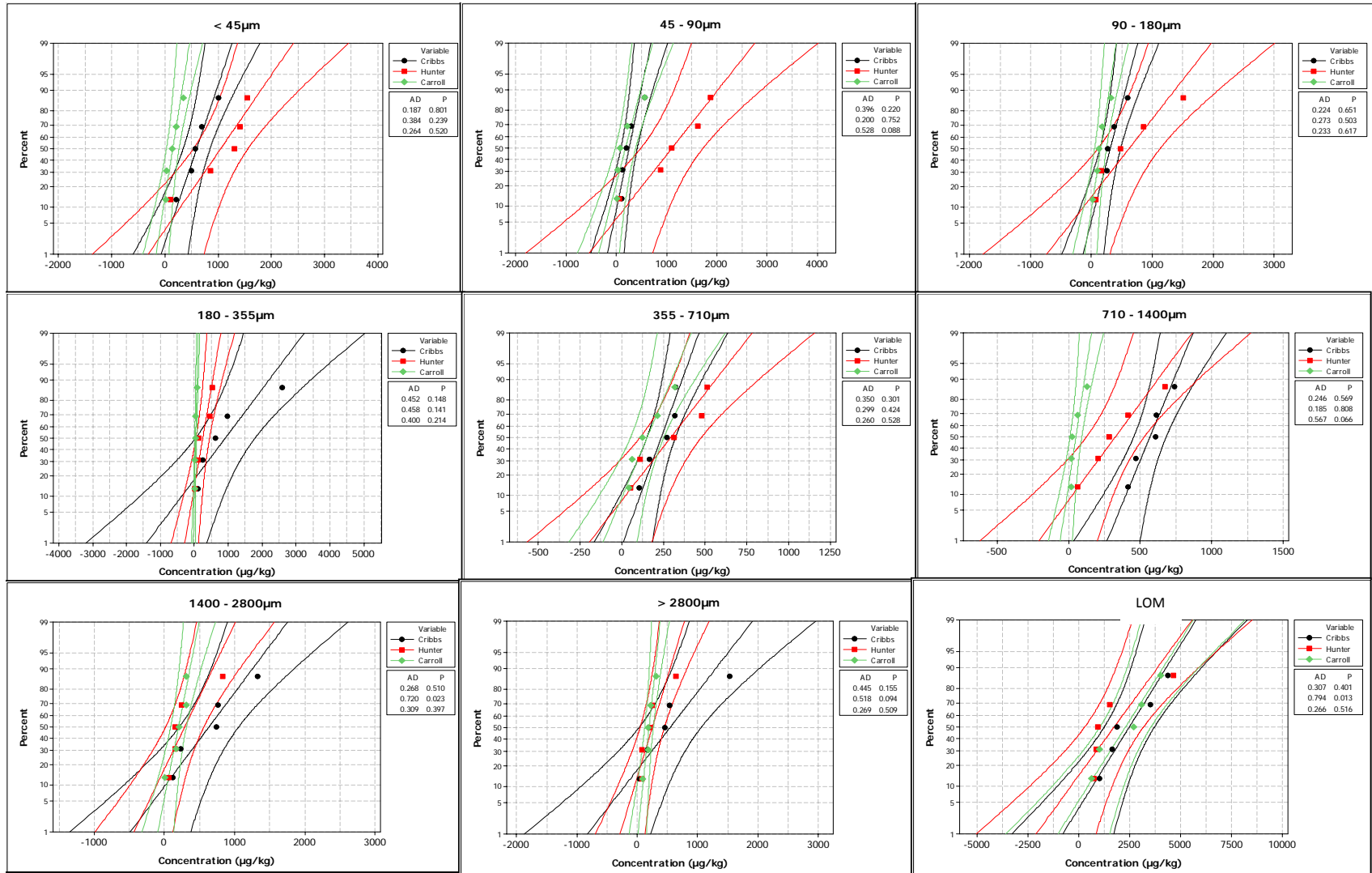


Figure C.9 Probability plots for benzo(b)fluoranthrene concentrations

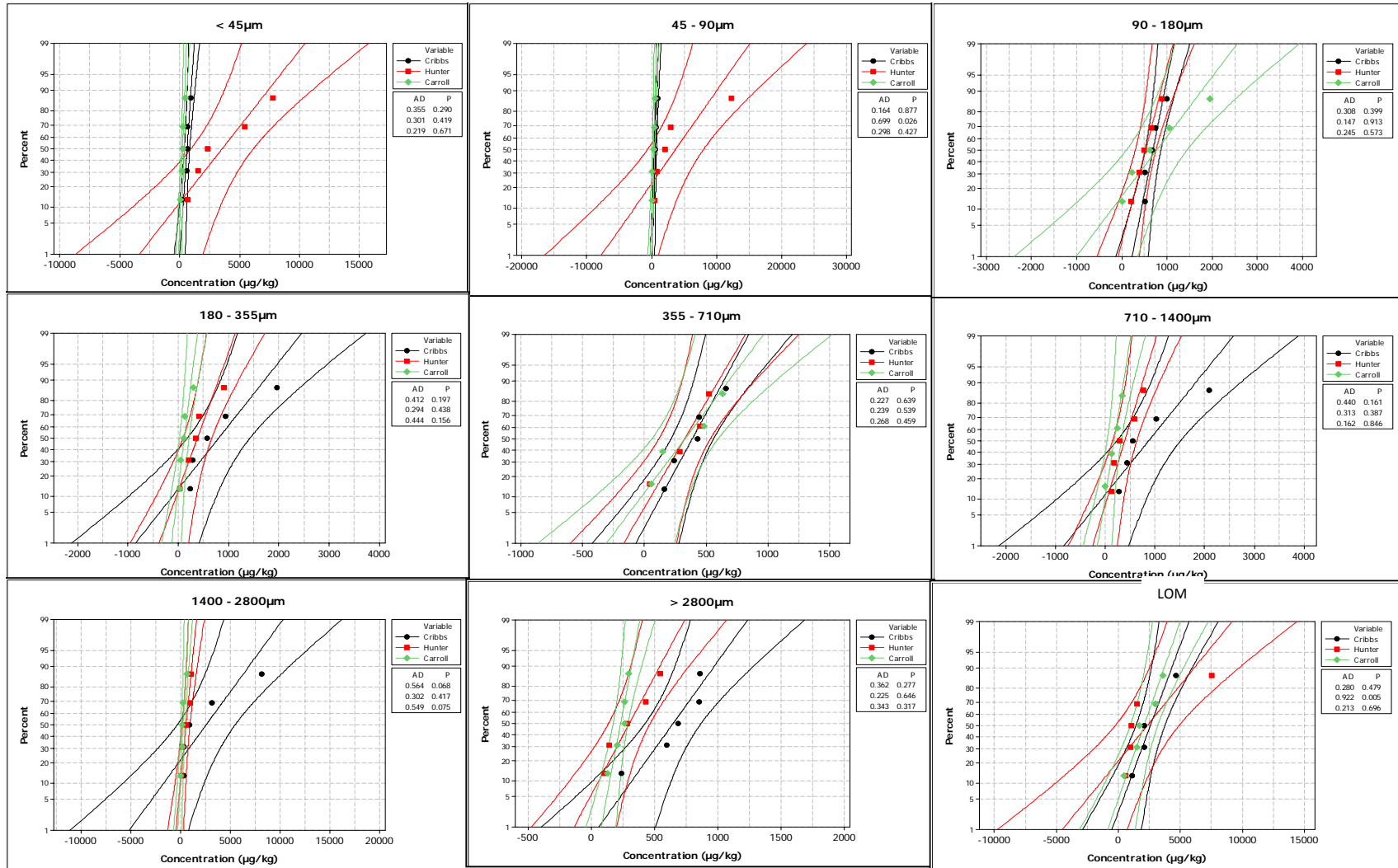


Figure C.10 Probability plots for benzo(a)pyrene concentrations

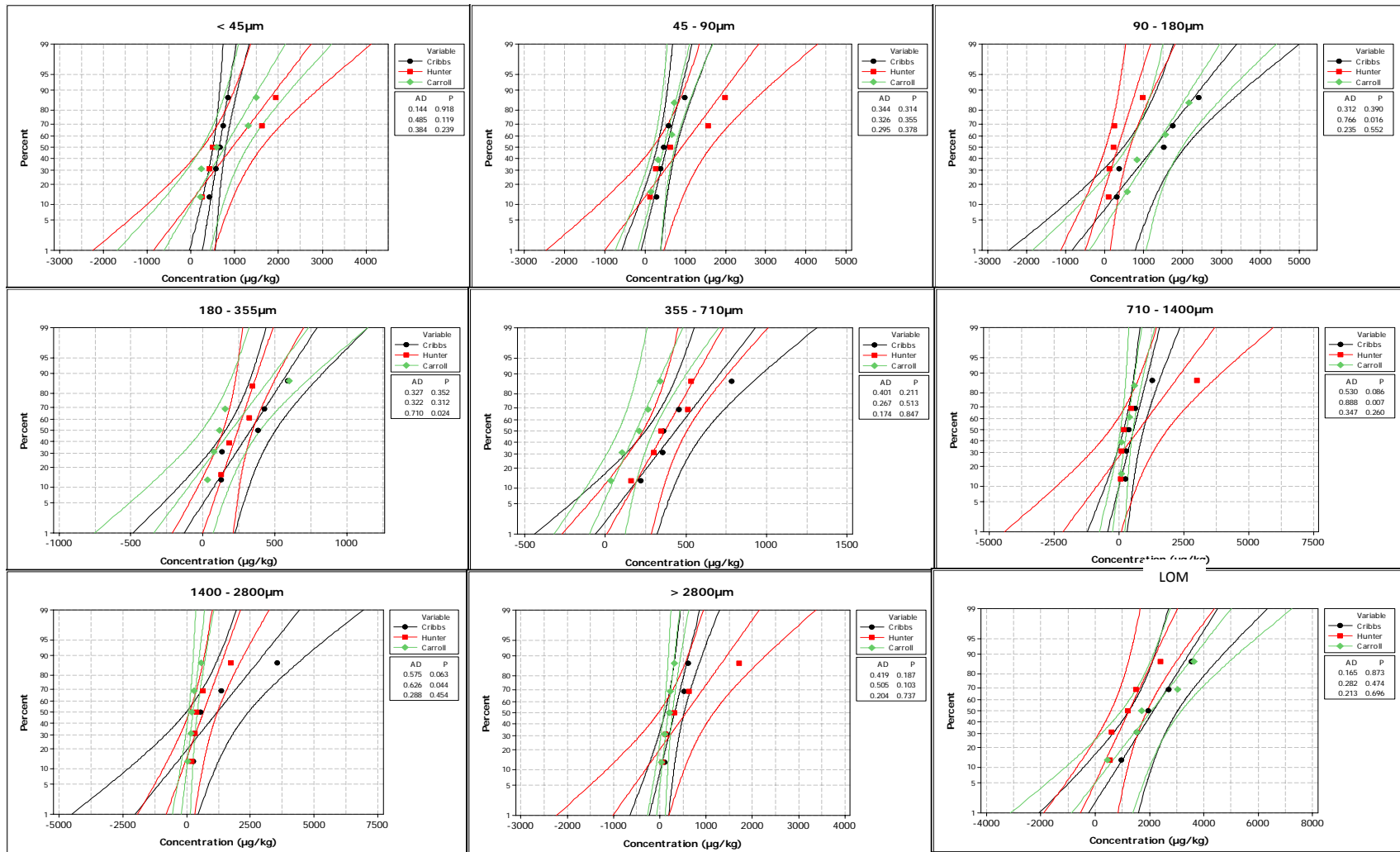


Figure C.11 Probability plots for indeno(1,2,3-cd)pyrene concentrations

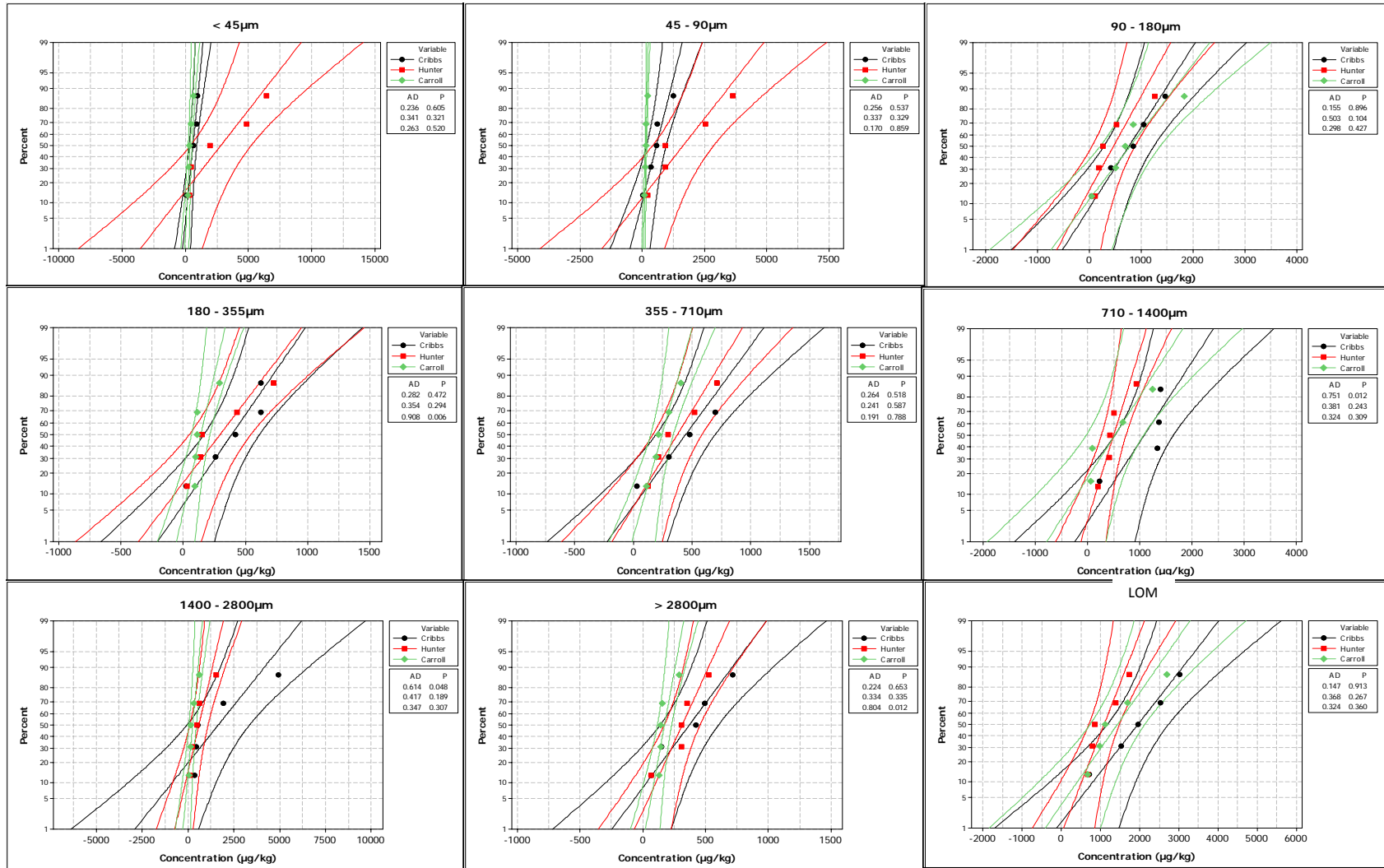


Figure C.12 Probability plots for dibenz(a,h)anthracene concentrations

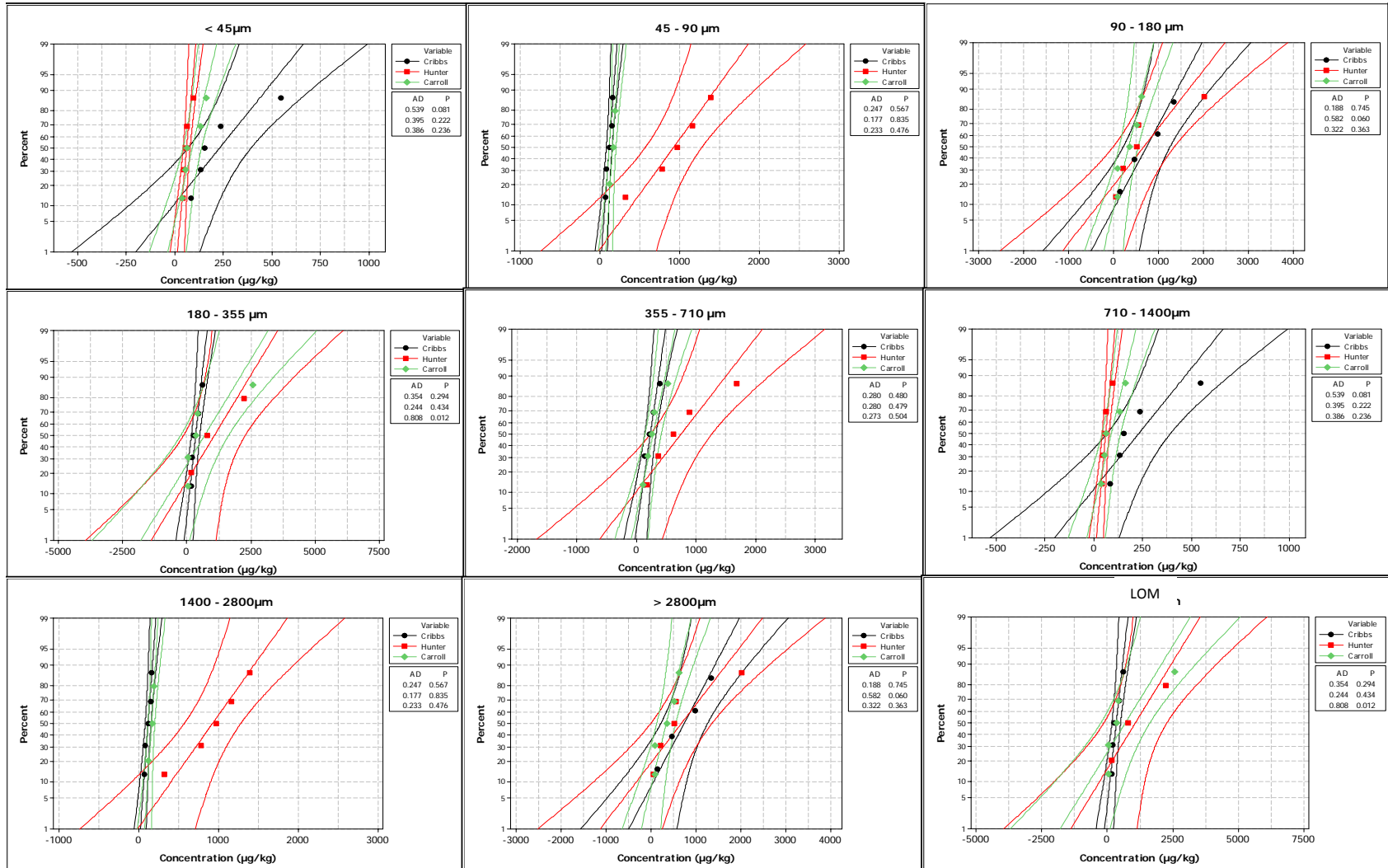


Figure C.13 Probability plots for benzo(ghi)perylene concentrations

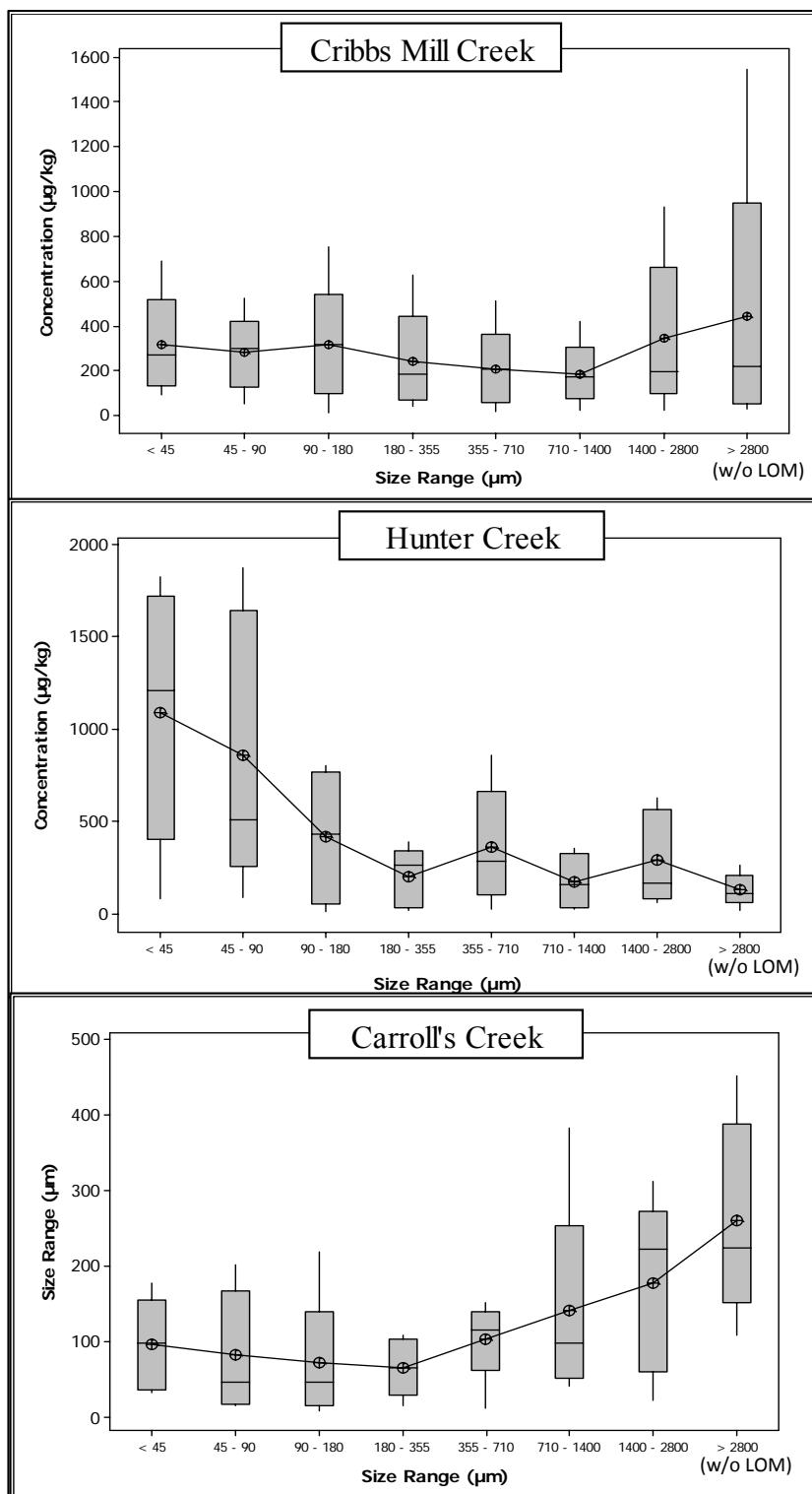


Figure C.14 Box Whisker plots for concentrations of naphthalene by particle size

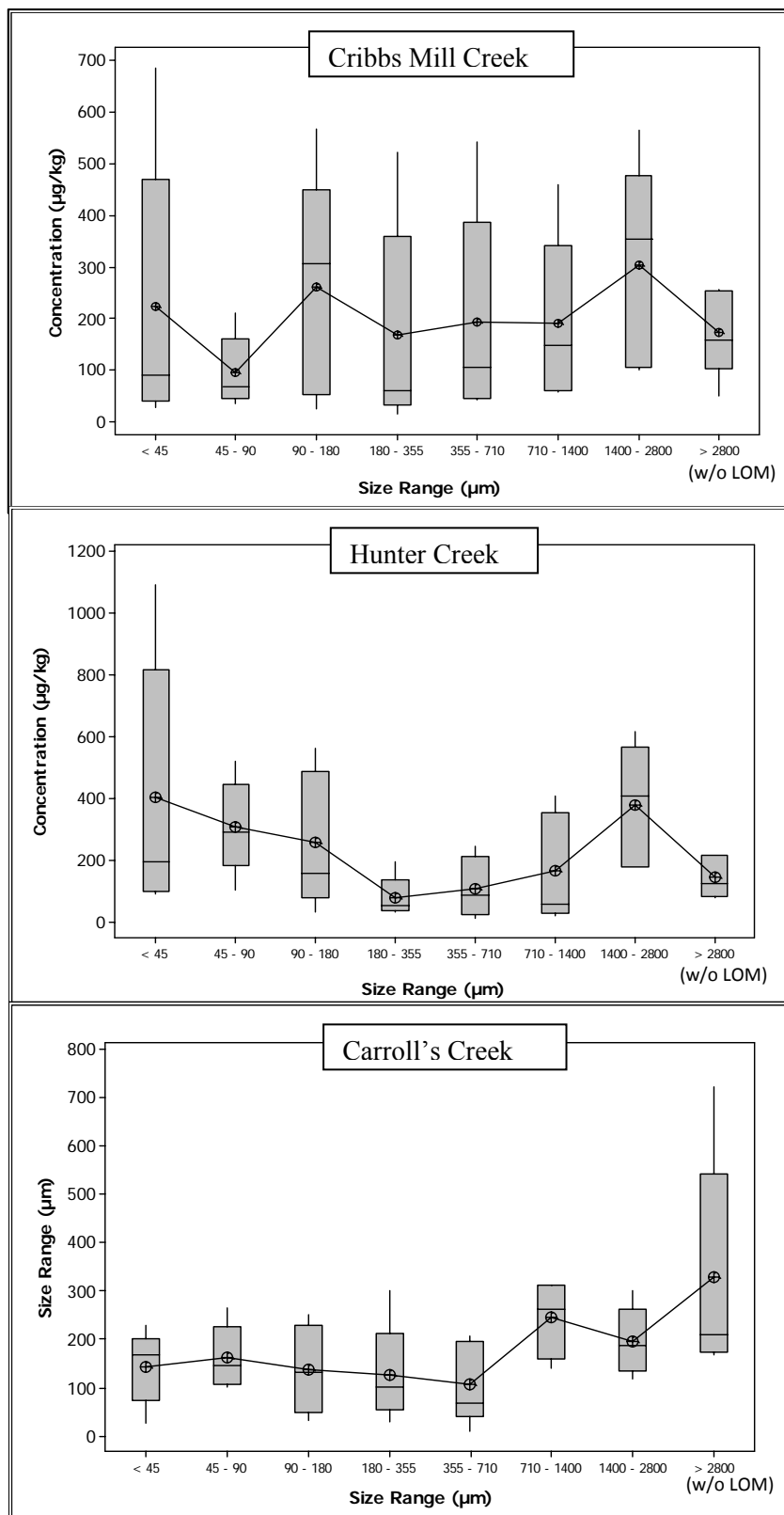


Figure C.15 Box Whisker plots for concentrations of fluorene by particle size

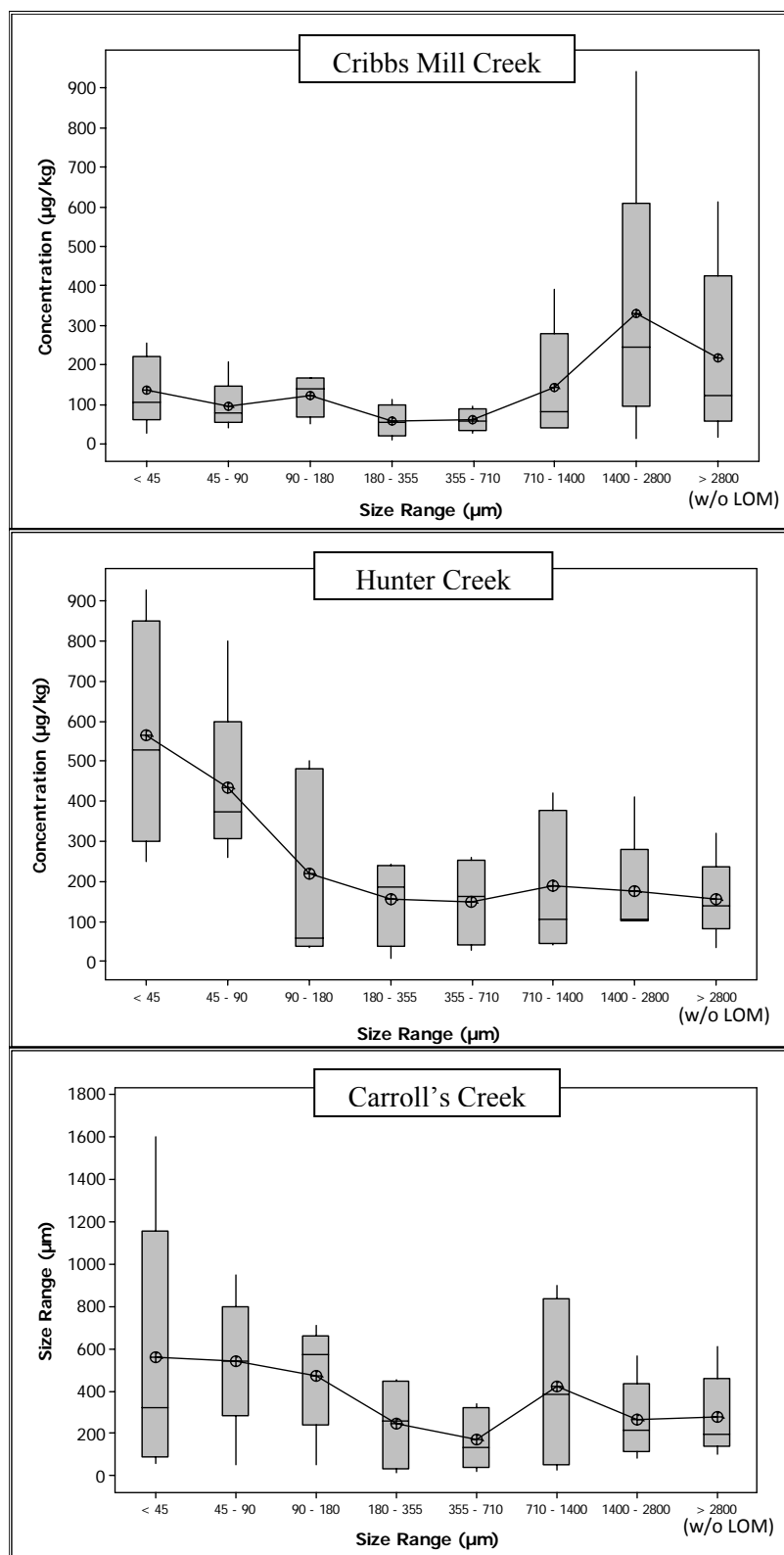


Figure C.16 Box Whisker plots for concentrations of phenanthrene by particle size

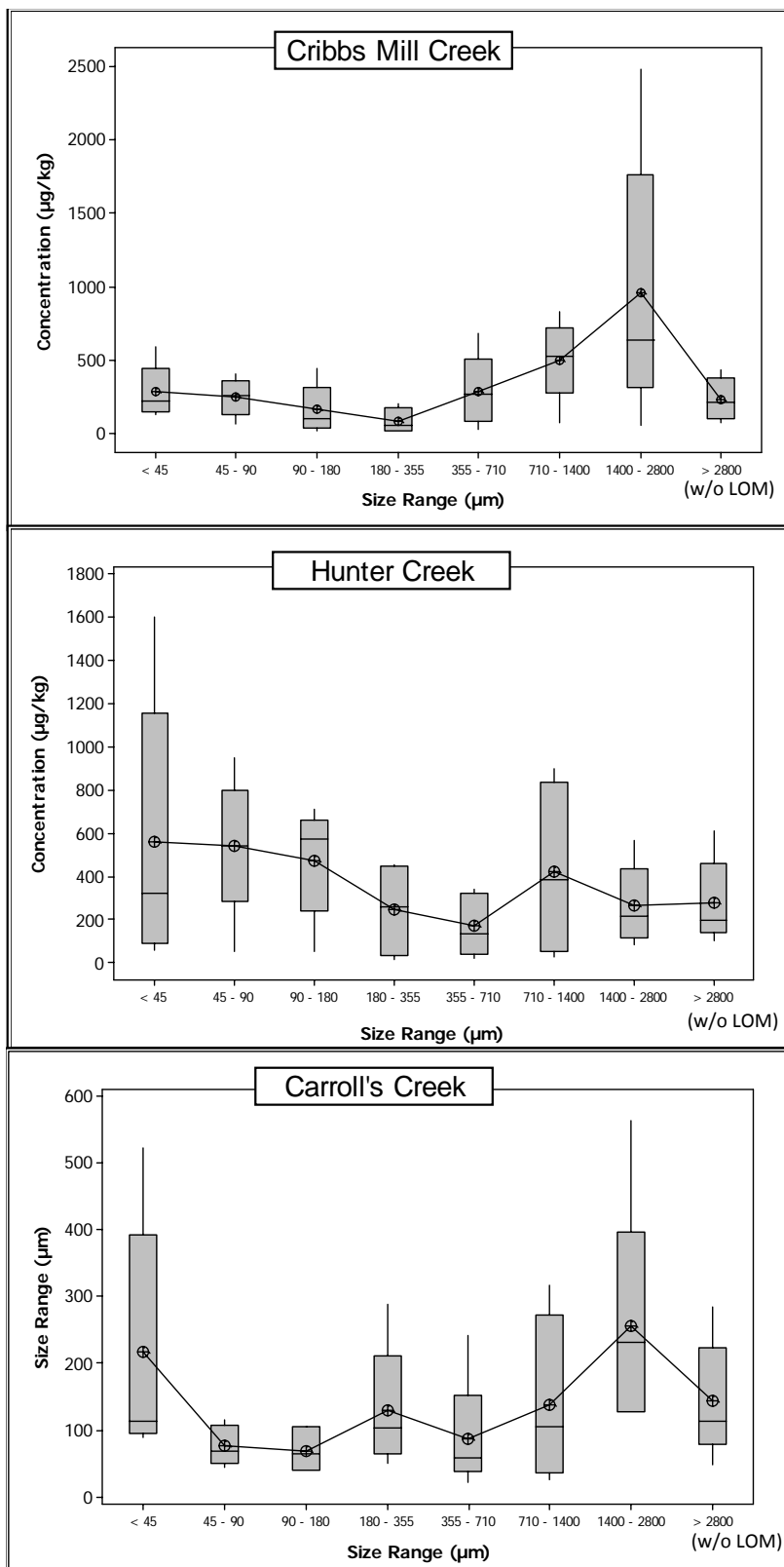


Figure C.17 Box Whisker plots for concentrations of anthracene by particle size

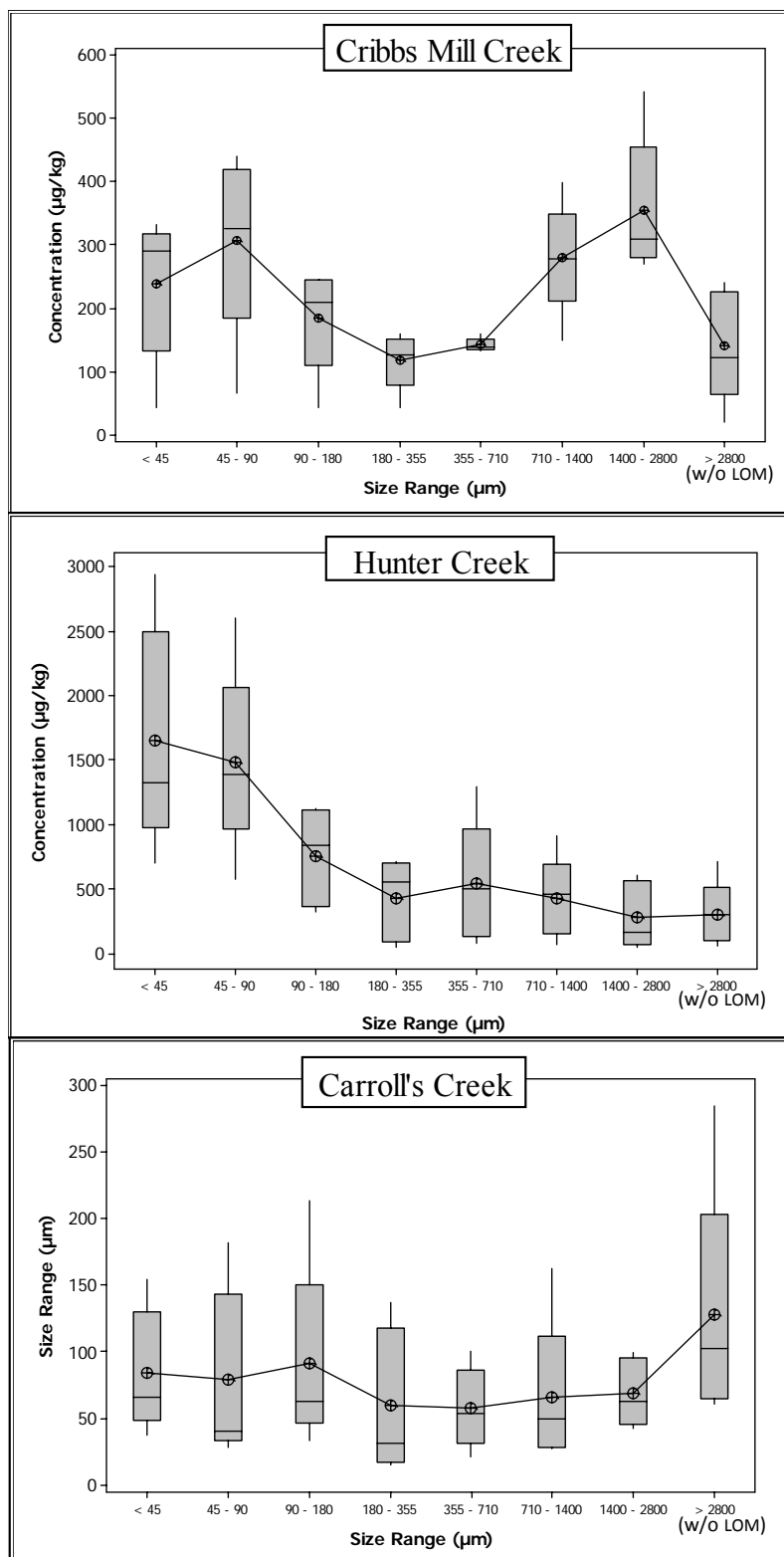


Figure C.18 Box Whisker plots for concentrations of fluoranthene by particle size

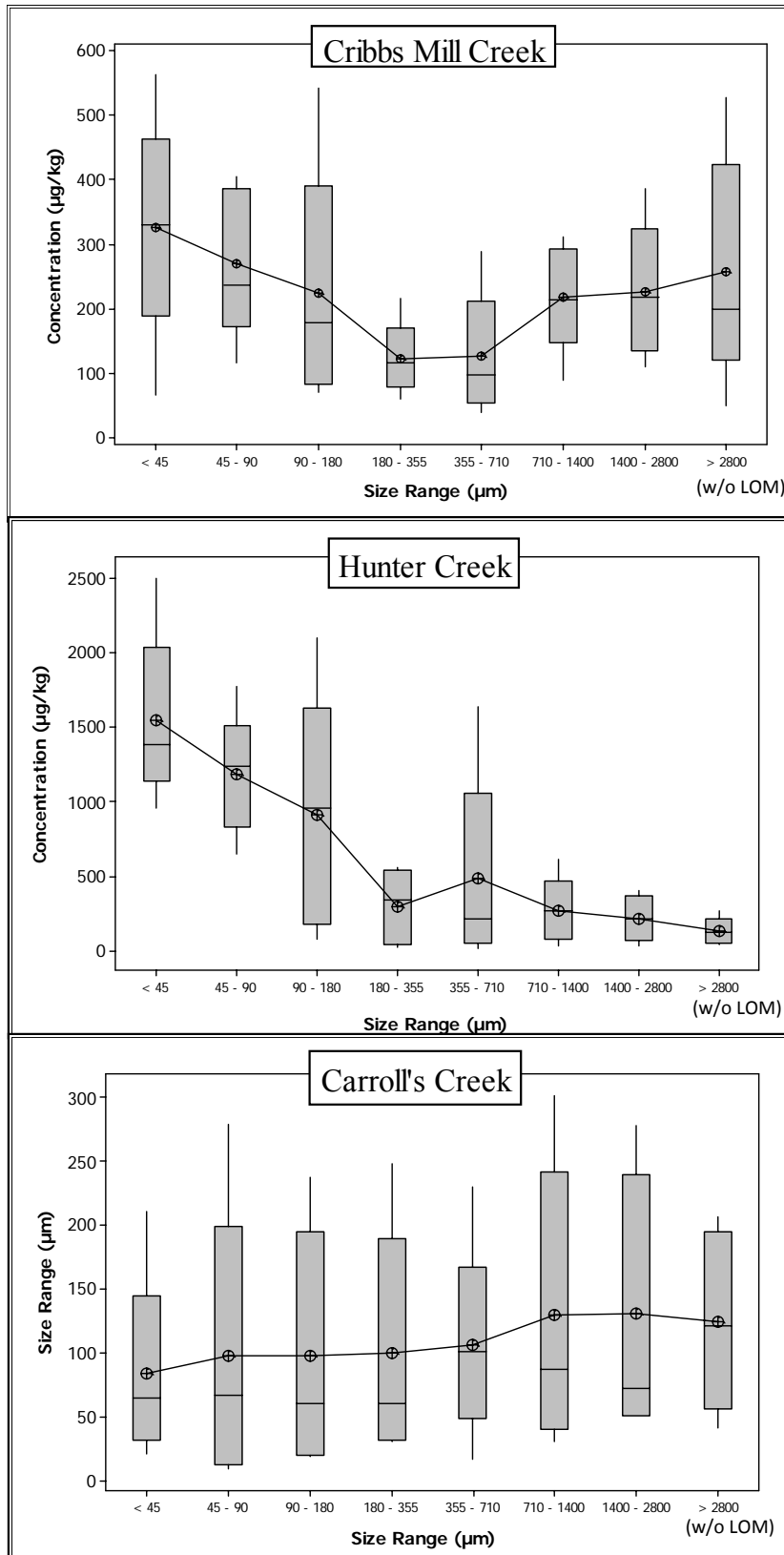


Figure C.19 Box Whisker plots for concentrations of pyrene by particle size

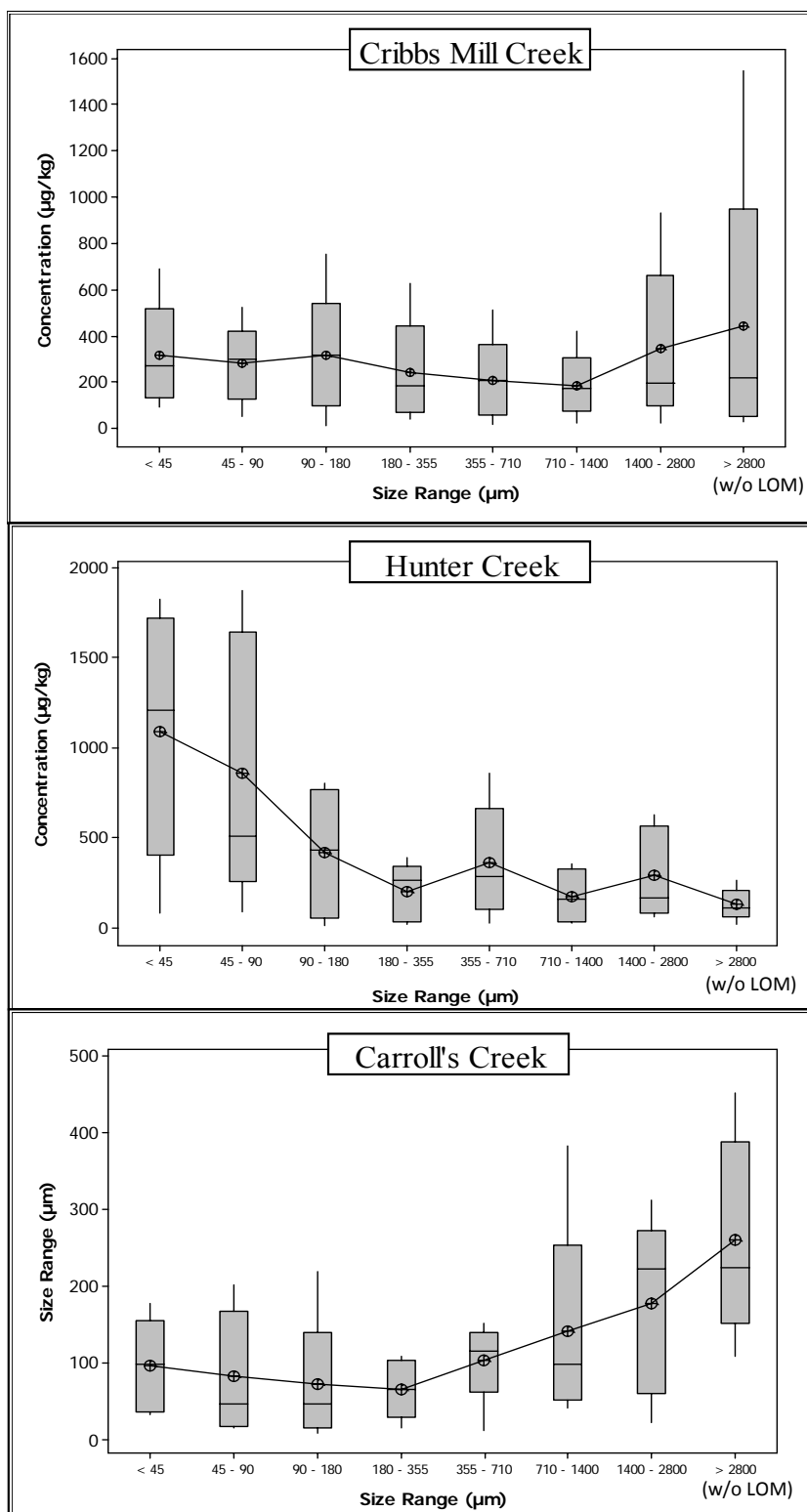


Figure C.20 Box Whisker plots for concentrations of benzo(a)anthracene by particle size

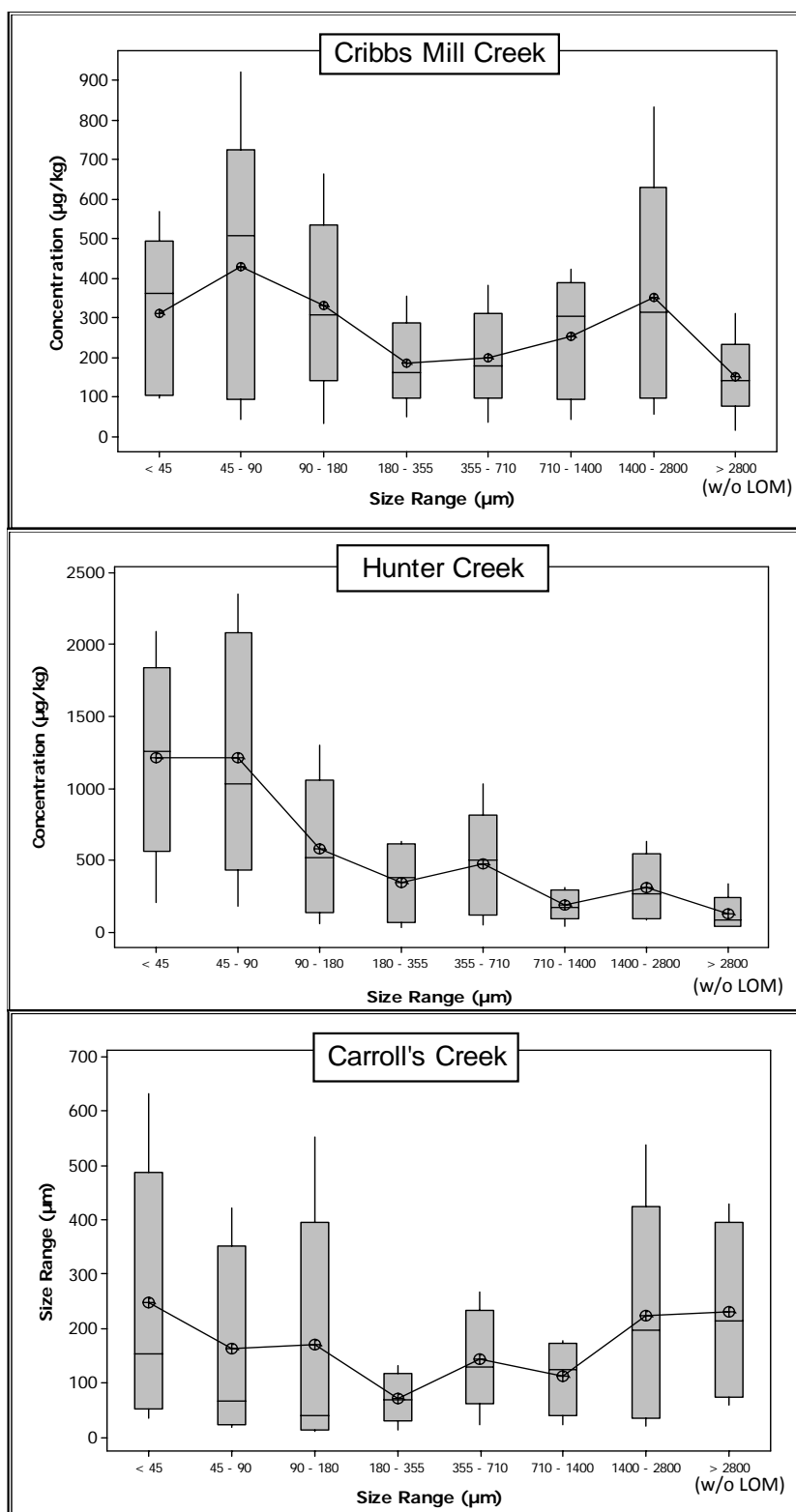


Figure C.21 Box Whisker plots for concentrations of chrysene by particle size

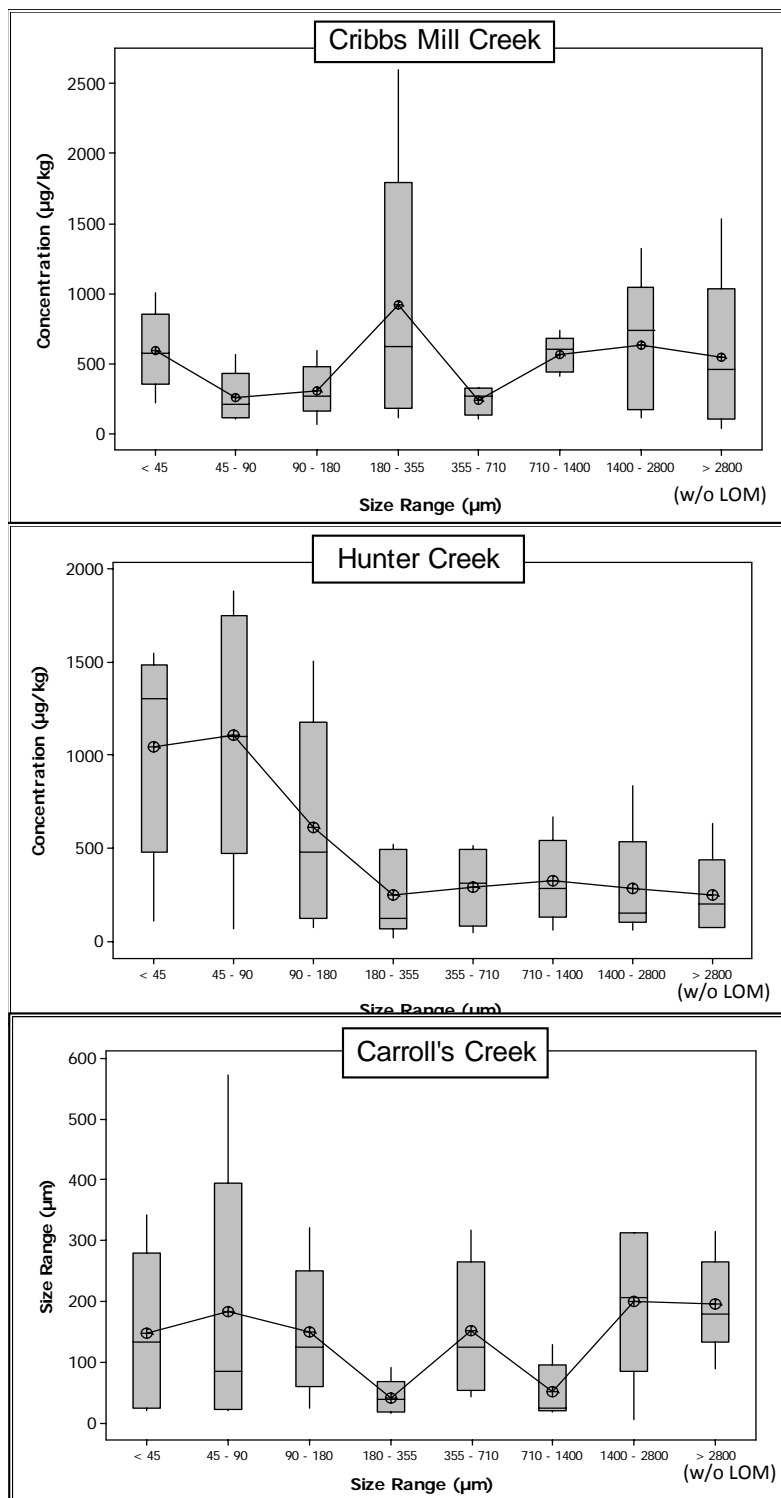


Figure C.22 Box Whisker plots for concentrations of benzo(b)fluoranthene particle size

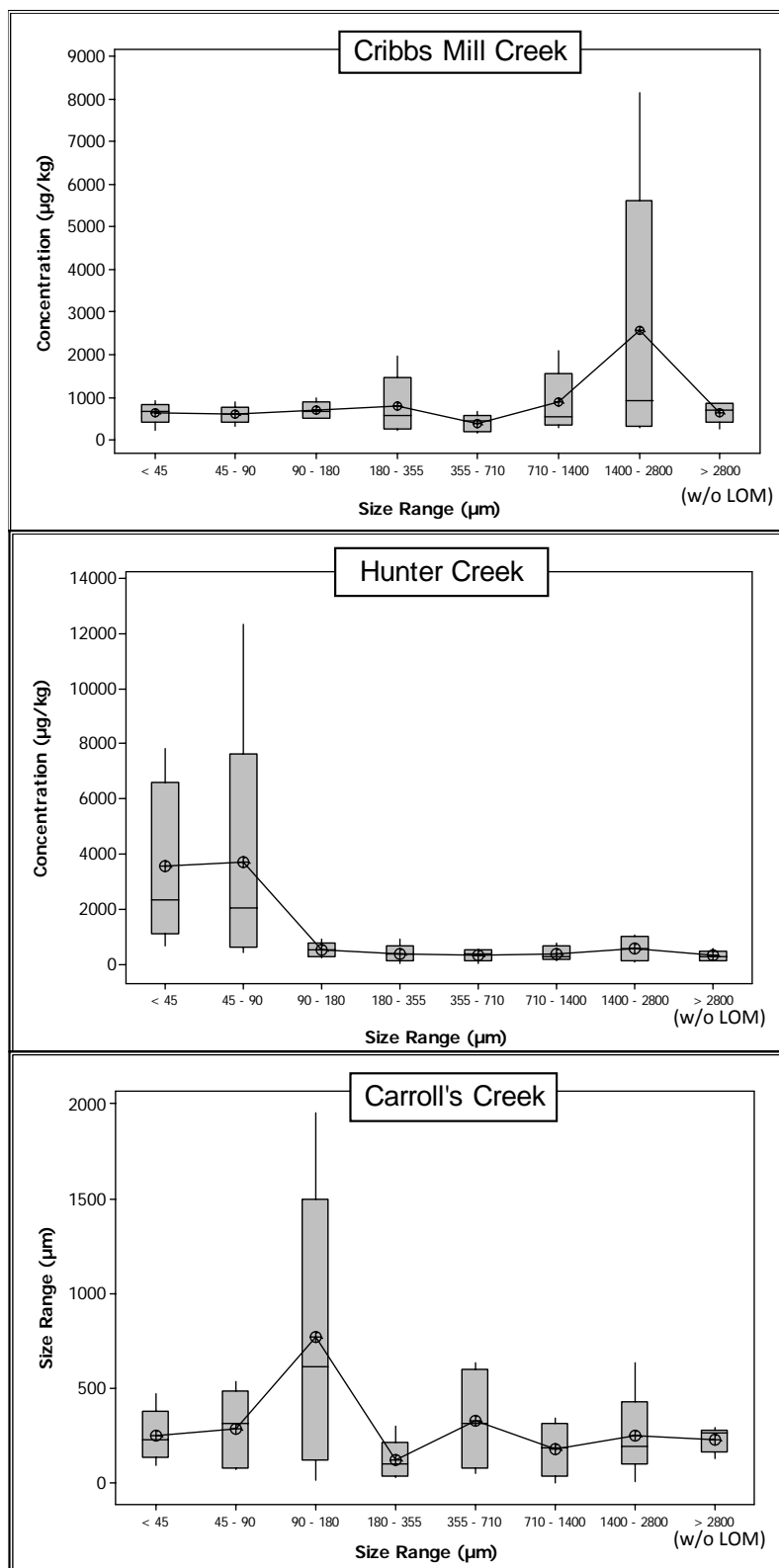


Figure C.23 Box Whisker plots for concentrations of benzo(a)pyrene particle size

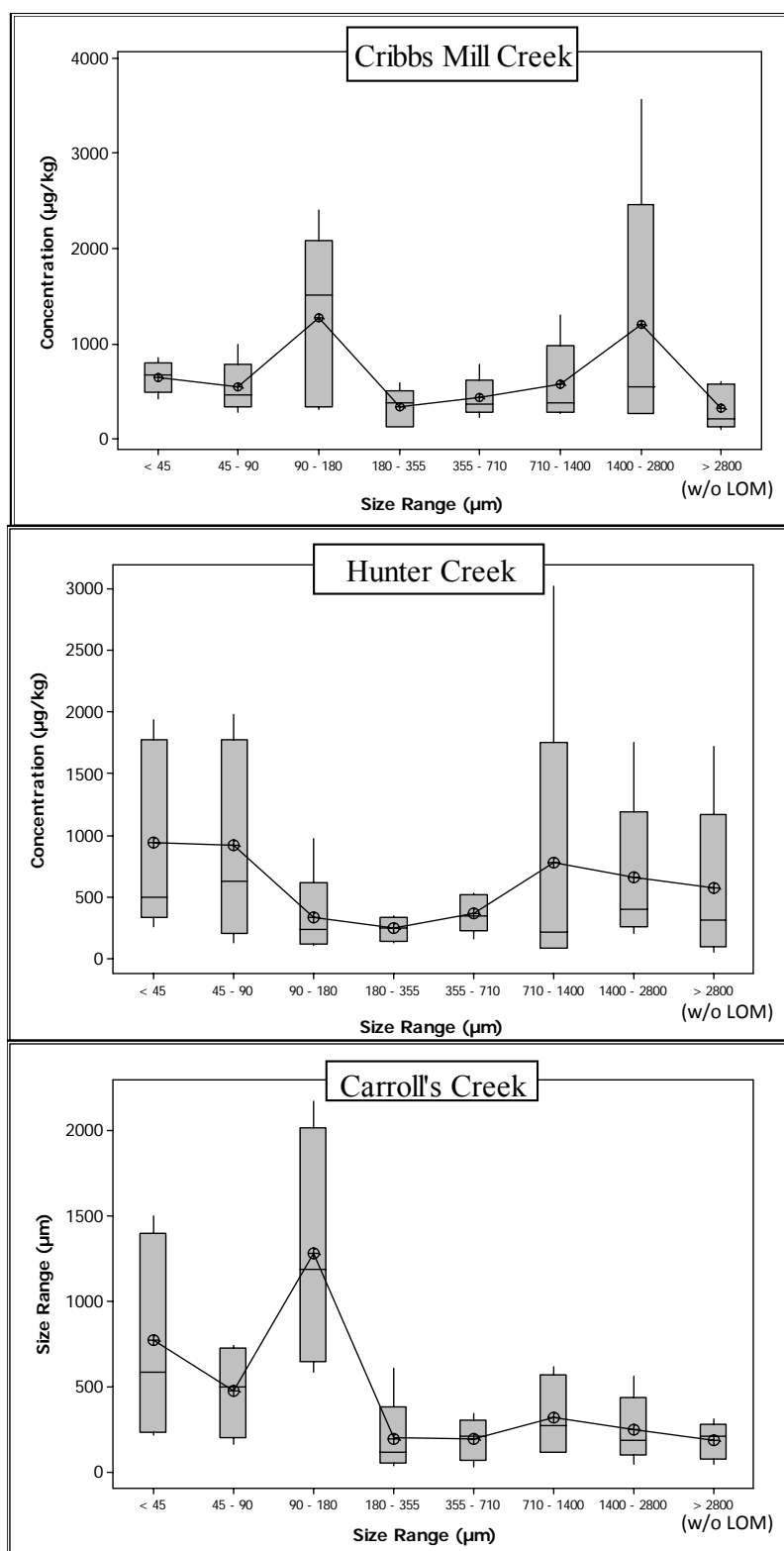


Figure C.24 Box Whisker plots for concentrations of indeno(1,2,3-cd)pyrene by particle size

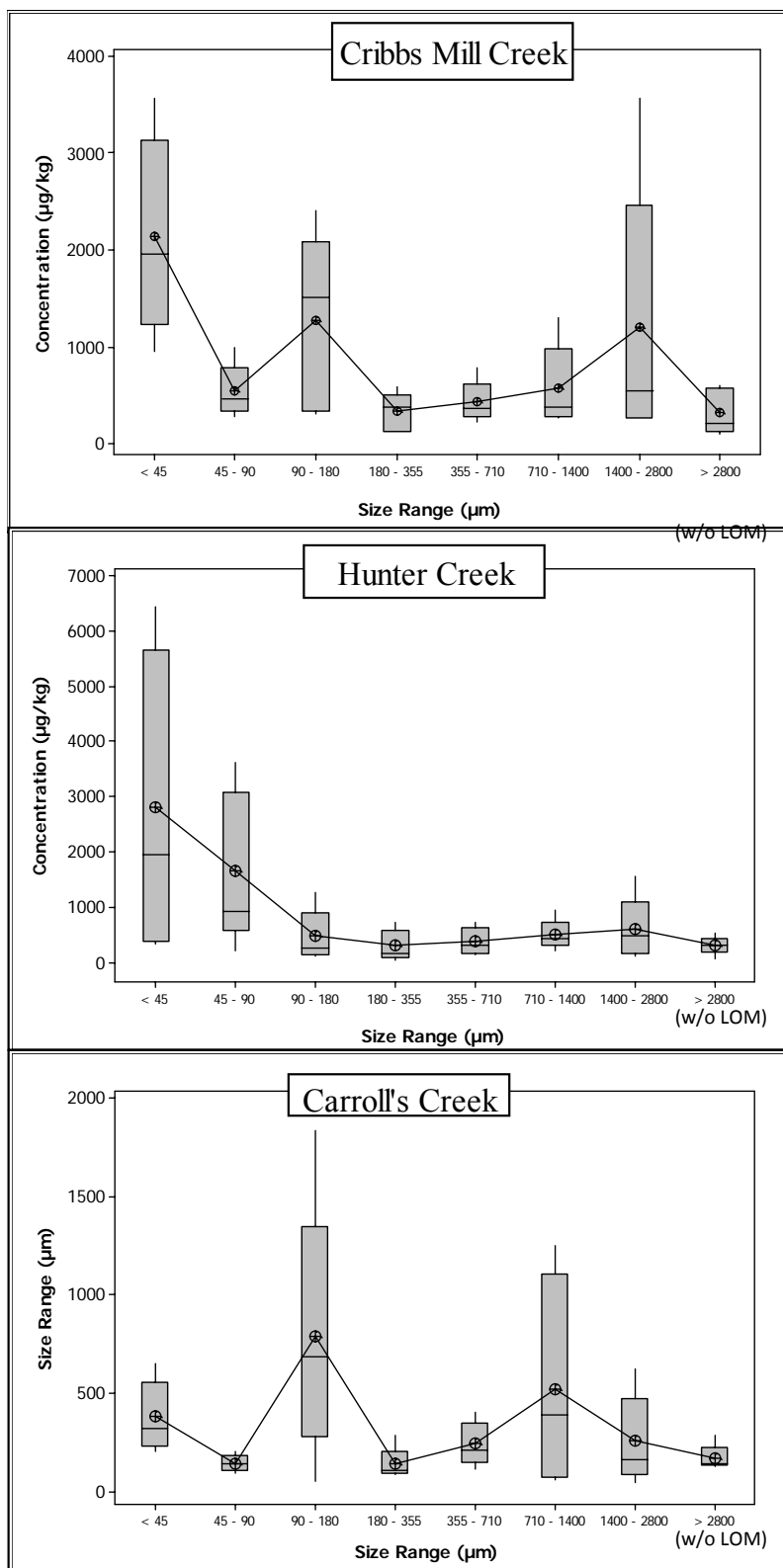


Figure 25 Box Whisker plots for concentrations of dibenz(a,h)anthracene by particle size

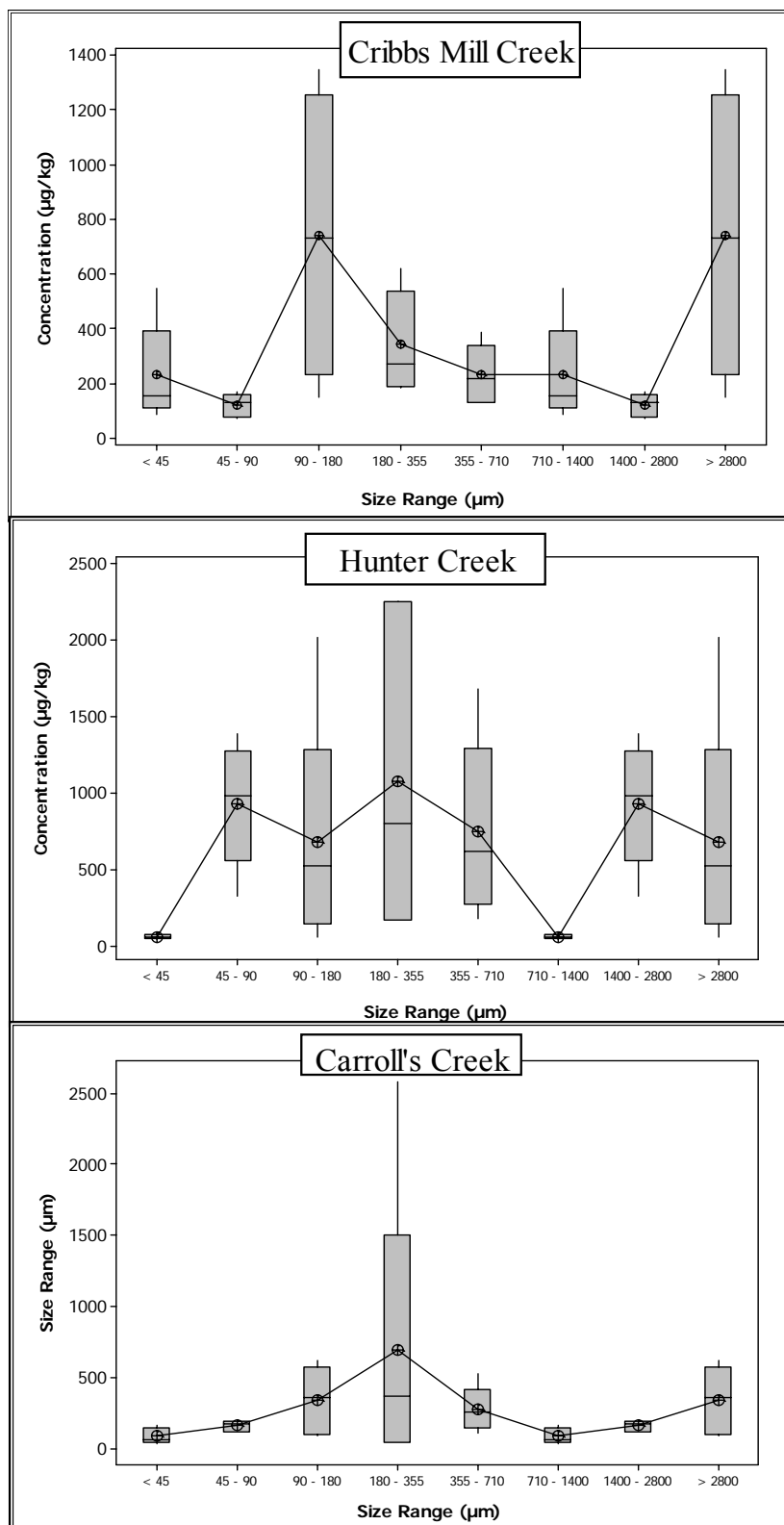


Figure C.26 Box Whisker plots for concentrations of benzo(ghi)perylene by particle size

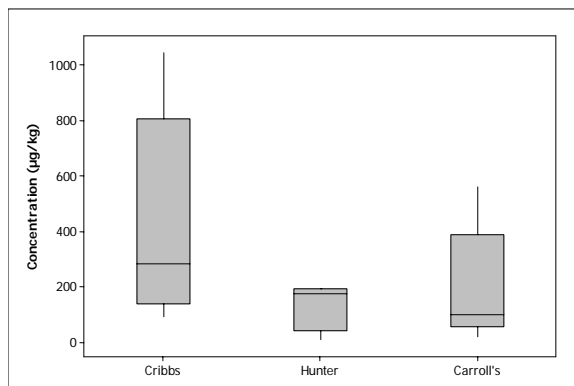


Figure C.27 Box Box Whisker lot for naphthalene concentration with particle size range $< 45\mu\text{m}$

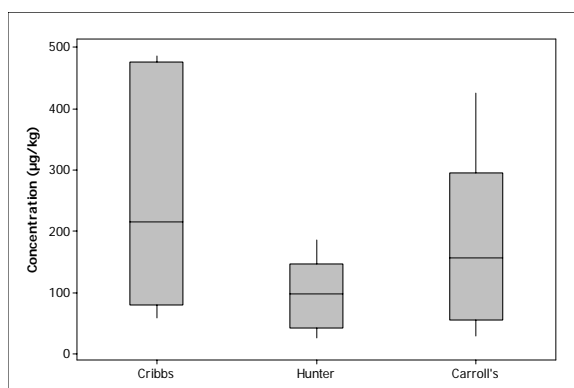


Figure C.28 Box Whisker lot for naphthalene concentration with particle size range $45 - 90\mu\text{m}$

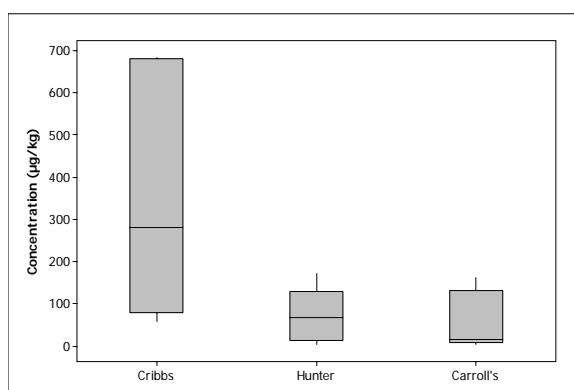


Figure C.29 Box Box Whisker lot for naphthalene concentration with particle size range $90 - 180\mu\text{m}$

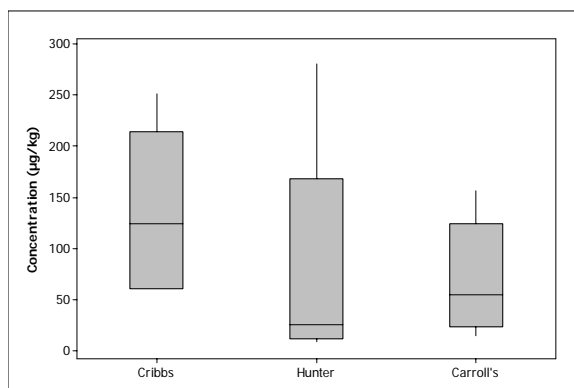


Figure C.30 Box Whisker lot for naphthalene concentration with particle size range 180 – 355µm

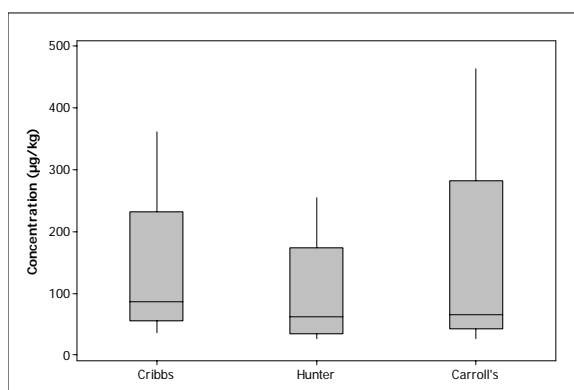


Figure C.31 Box Whisker lot for naphthalene concentration with particle size range 355 – 710µm

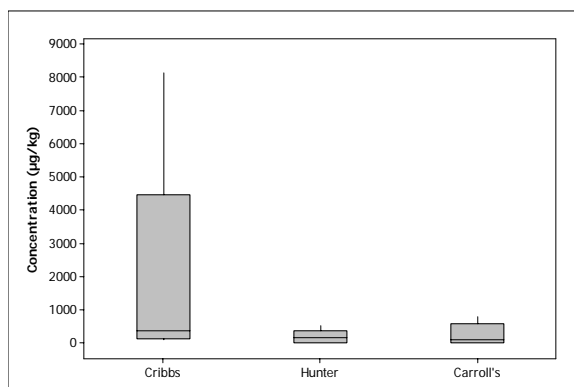


Figure C.32 Box Box Whisker lot for naphthalene concentration with particle size range 710 – 1400µm

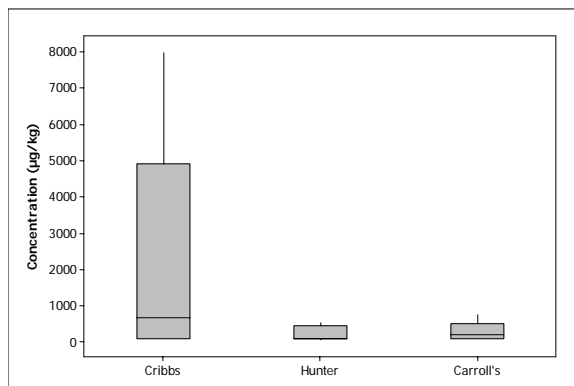


Figure C.33 Box Whisker lot for naphthalene concentration with particle size range 1400 – 2800µm

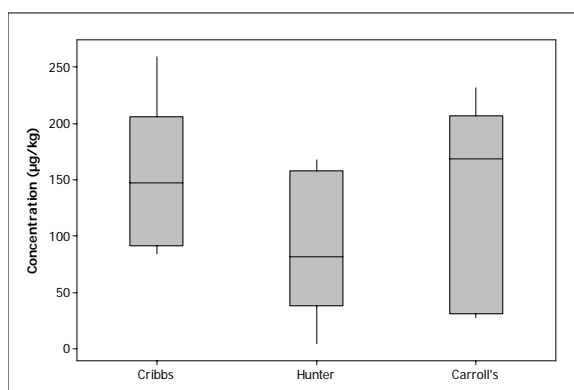


Figure C.34 Box Whisker lot for naphthalene concentration with particle size range > 2800µm

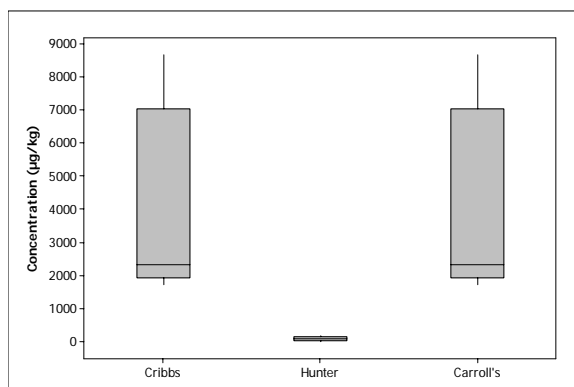


Figure C.35 Box Whisker lot for naphthalene concentration with LOM

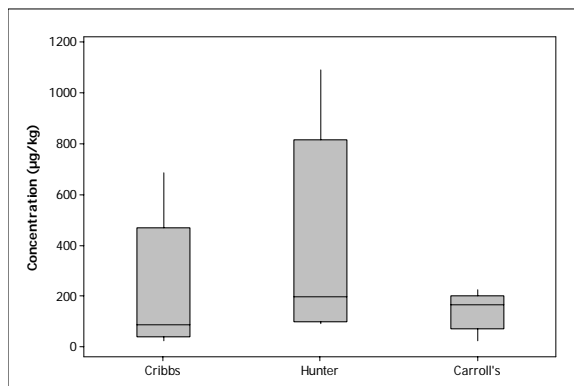


Figure C.36 Box and Whisker Plot for fluorene concentration on particle size range < 45µm

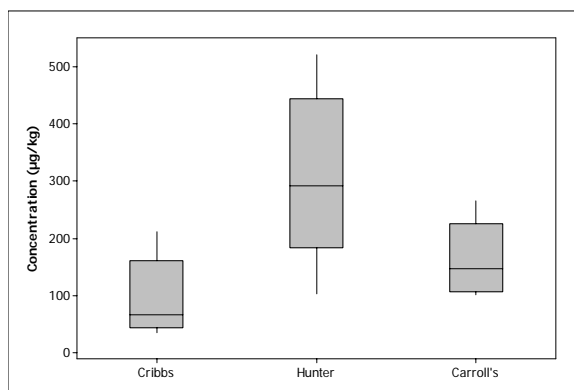


Figure C.37 Box and Whisker Plot for fluorene concentration on particle size range 45 - 90µm

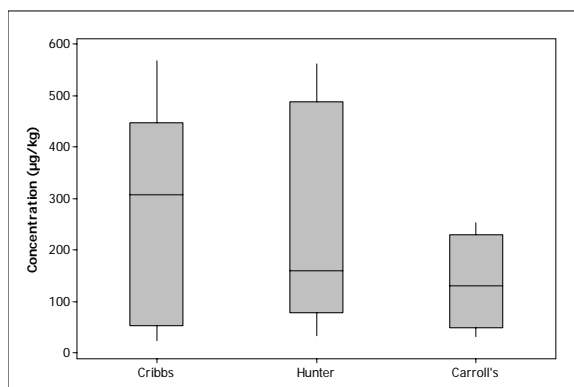


Figure C.38 Box and Whisker Plot for fluorene concentration on particle size range 90 - 180µm

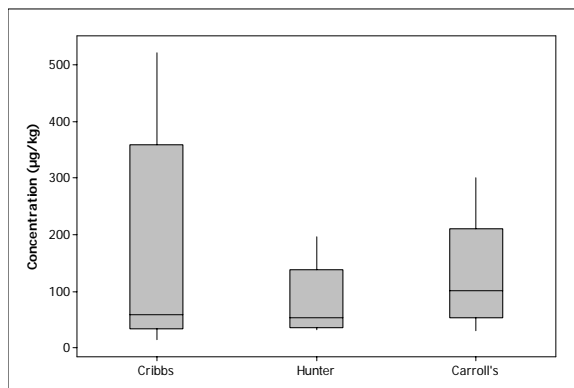


Figure C.39 Box Box Whisker Plot for fluorene concentration on particle size range 180 - 355 μ m

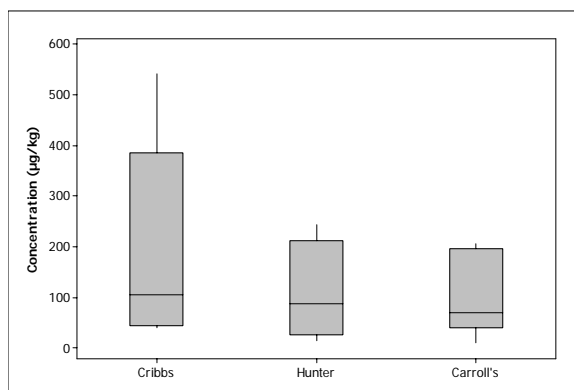


Figure C.40 Box Whisker Plot for fluorene concentration on particle size range 355 - 710 μ m

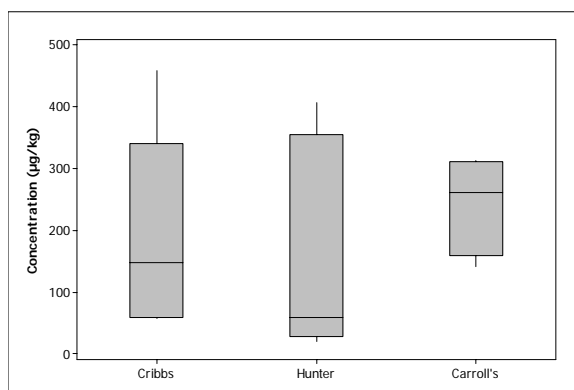


Figure C.41 Box Box Whisker Plot for fluorene concentration on particle size range 710 - 1400 μ m

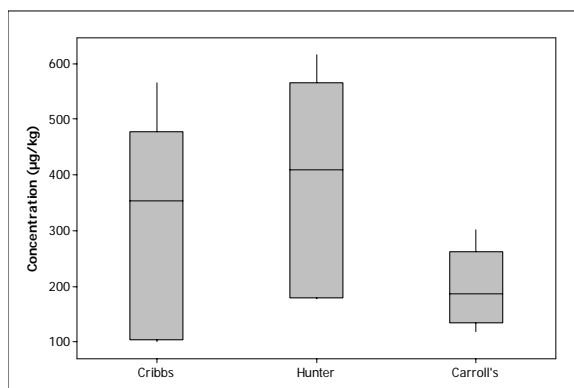


Figure C.42 Box Whisker Plot for fluorene concentration on particle size range 1400 - 2800µm

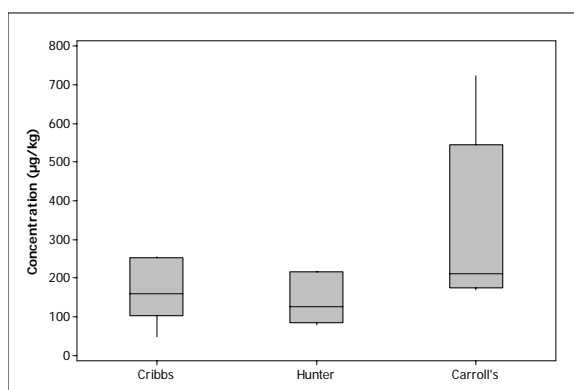


Figure C.43 Box Whisker Plot for fluorene concentration on particle size range > 2800µm

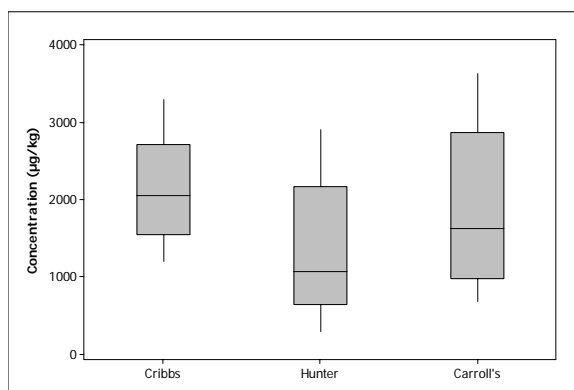


Figure C.44 Box Whisker Plot for fluorene concentration on LOM

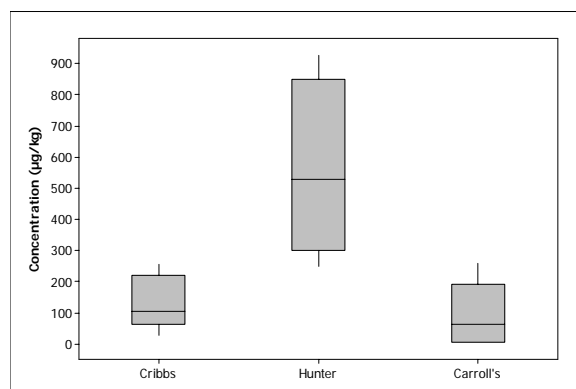


Figure C.45 Box Whisker Plot for Phenanthrene Concentration on Particle Size Range < 45µm

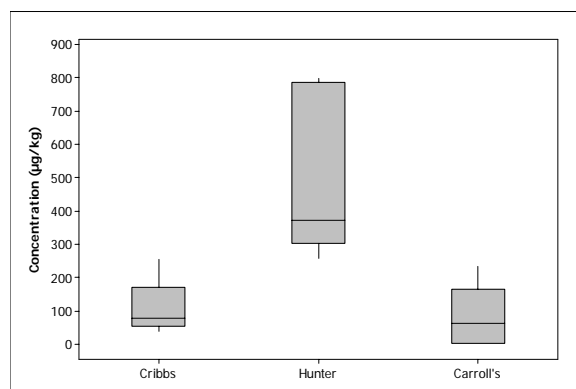


Figure C.46 Box Whisker plot for phenanthrene concentration on particle size range 45 - 90µm

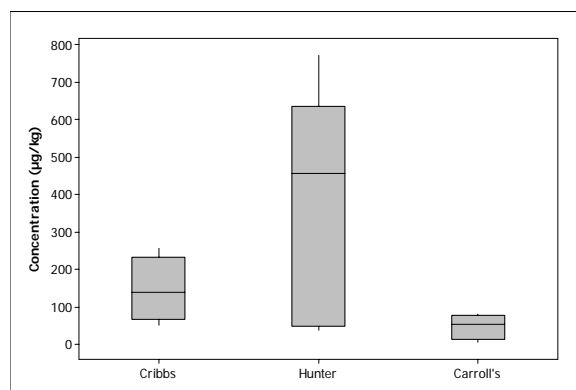


Figure C.47 Box Whisker plot for phenanthrene concentration on particle size range 90 - 180µm

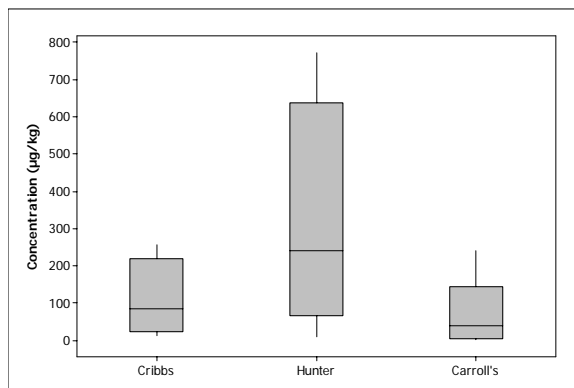


Figure C.48 Box Whisker plot for phenanthrene concentration on particle size range 180 - 355µm

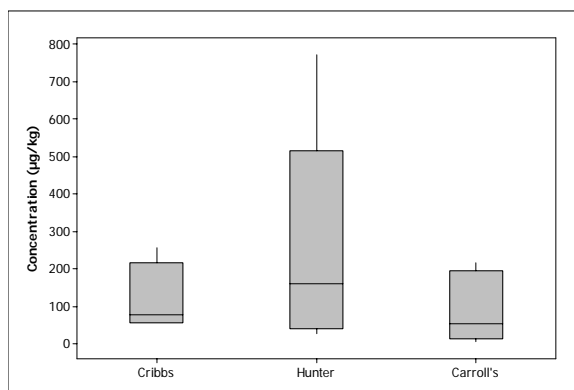


Figure C.49 Box Box Whisker plot for phenanthrene concentration on particle size range 355 - 710µm

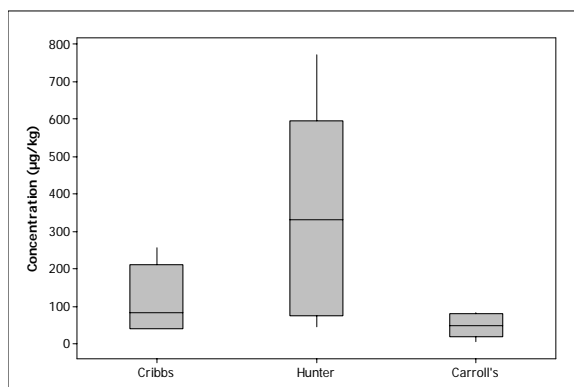


Figure C.50 Box Whisker plot for phenanthrene concentration on particle size range 710 - 1400µm

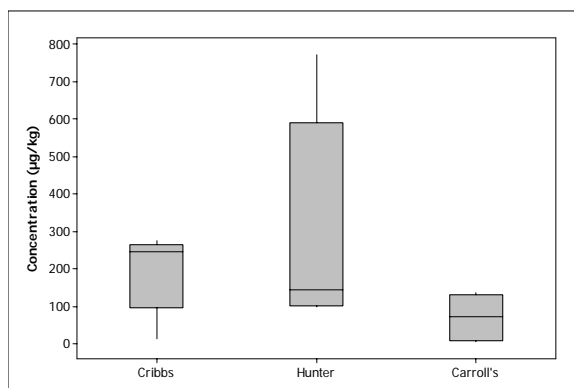


Figure C.51 Box Whisker plot for phenanthrene concentration on particle size range 1400 - 2800 μm

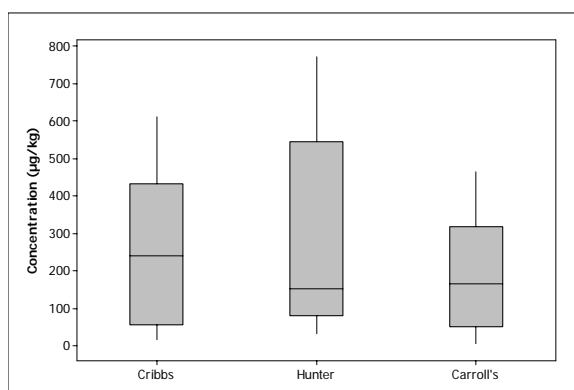


Figure C.52 Box Whisker plot for phenanthrene concentration on particle size range > 2800 μm (w/o LOM)

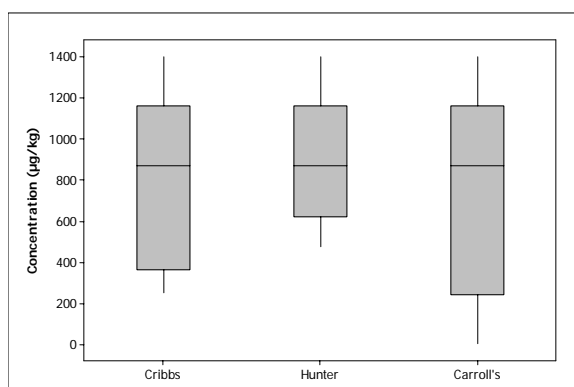


Figure C.53 Box Whisker plot for phenanthrene concentration on LOM

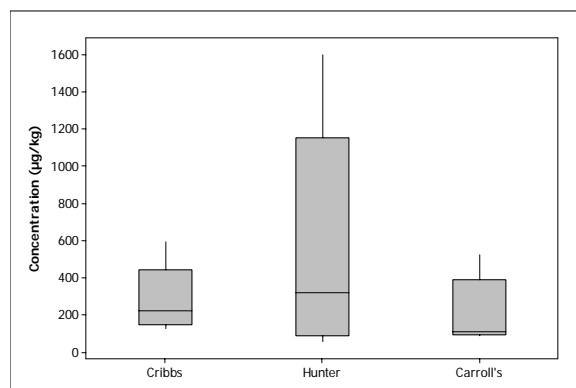


Figure C.54 Box Whisker plot for anthracene concentration on particle size range < 45µm

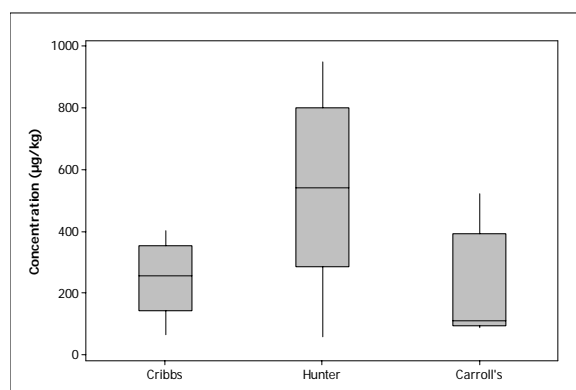


Figure C.55 Box Whisker plot for anthracene concentration on particle size range 45 - 90µm

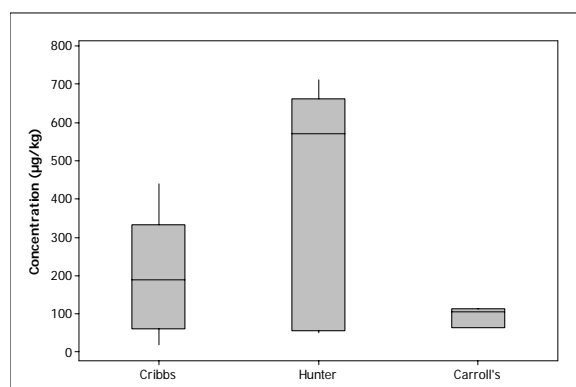


Figure C.56 Box Whisker plot for anthracene concentration on particle size range 90 - 180µm

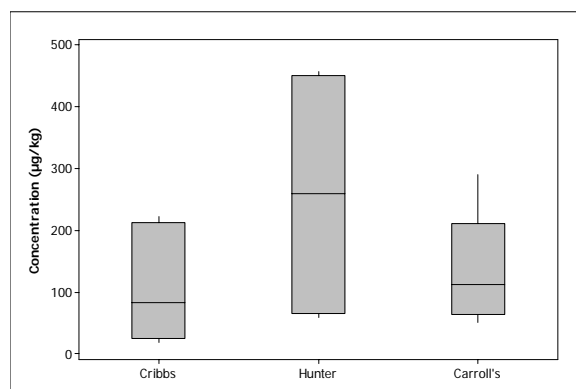


Figure C.57 Whisker plot for anthracene concentration on particle size range 180 - 355µm

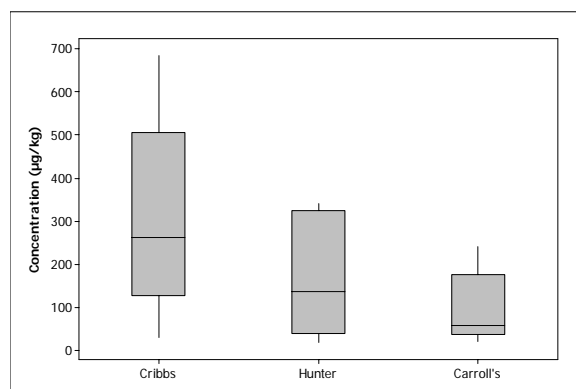


Figure C.58 Whisker plot for anthracene concentration on particle size range 355 - 710µm

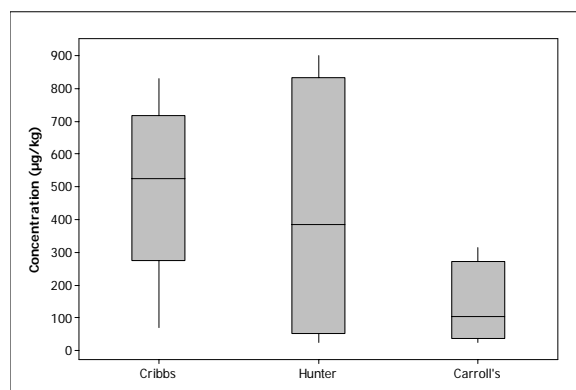


Figure C.59 Whisker plot for anthracene concentration on particle size range 710 - 1400µm

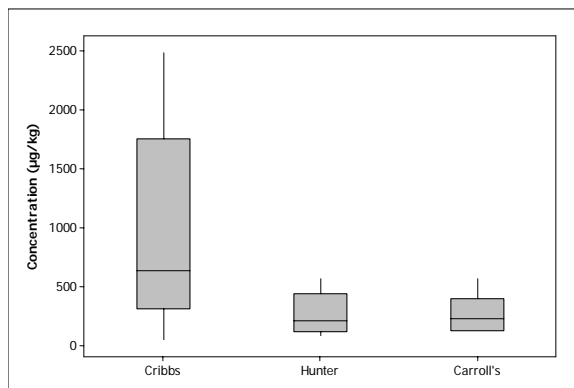


Figure C.60 Whisker plot for anthracene concentration on particle size range 1400 - 2800µm

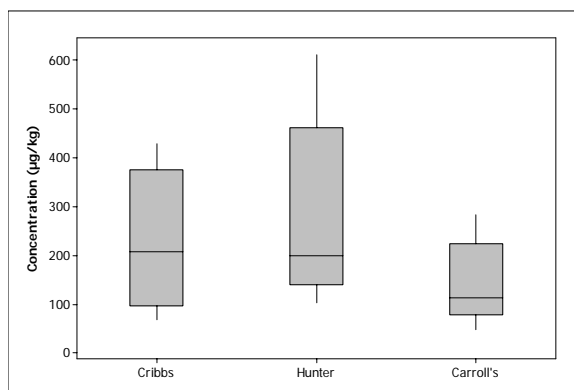


Figure C.61 Whisker plot for anthracene concentration on particle size range > 2800µm (w/o LOM)

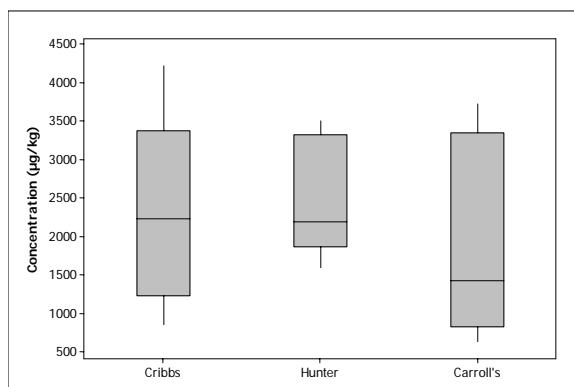


Figure C.62 Box Whisker plot for anthracene concentration with LOM

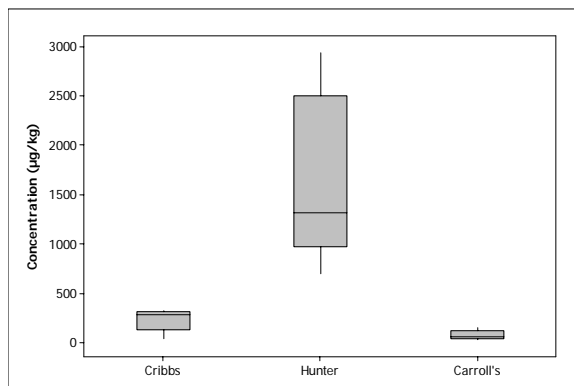


Figure C.63 Box Whisker plot for fluoranthene Concentration on particle size range < 45µm

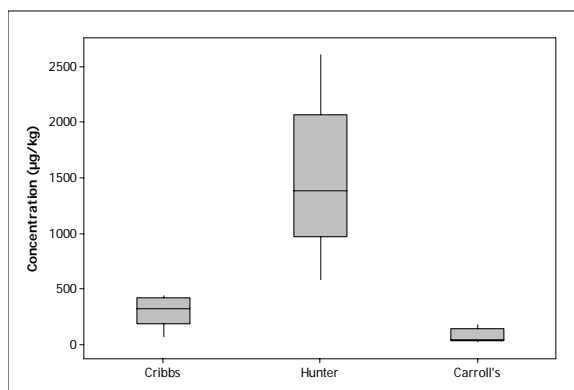


Figure C.64 Box Whisker plot for fluoranthene Concentration on particle size range 45 - 90µm

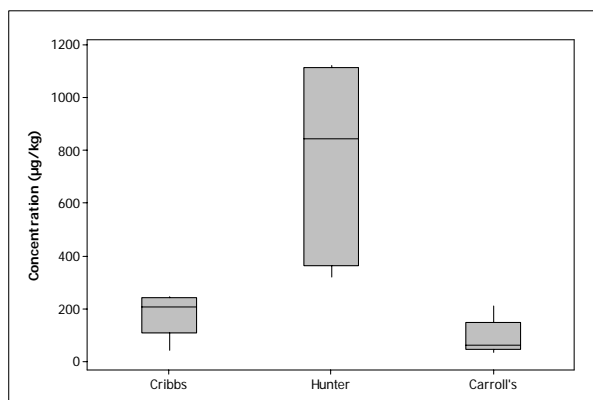


Figure C.65 Whisker plot for fluoranthene Concentration on particle size range 90 - 180µm

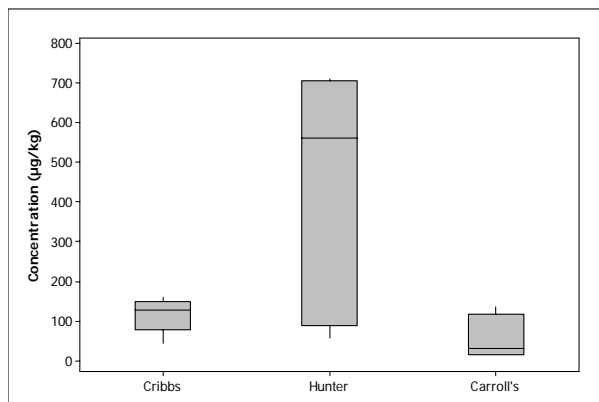


Figure C.66 Whisker plot for fluoranthene Concentration on particle size range 180 - 355µm

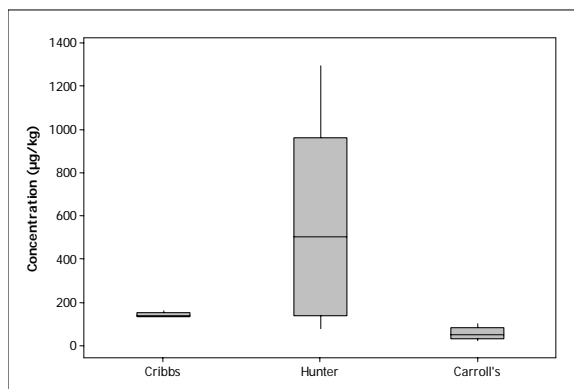


Figure C.67 Whisker plot for fluoranthene Concentration on particle size range 355 - 710µm

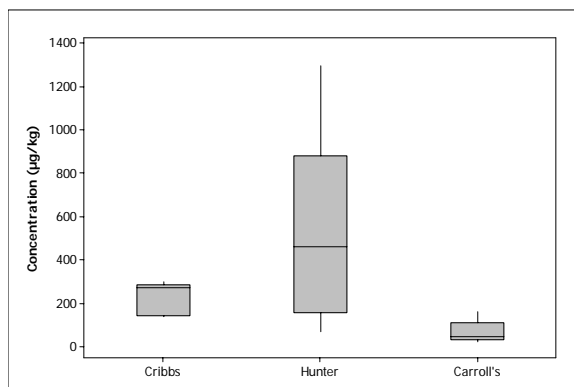


Figure C.68 Box Whisker plot for fluoranthene Concentration on particle size range 710 - 1400µm

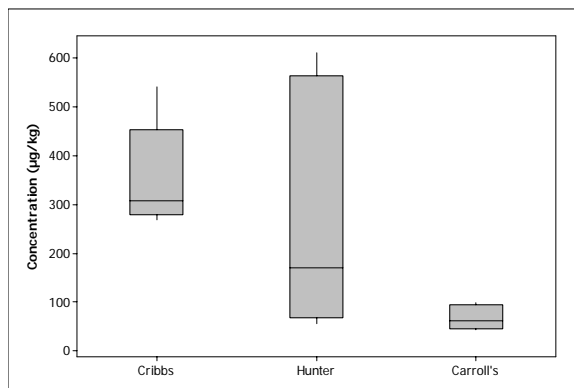


Figure C.69 Whisker plot for fluoranthene Concentration on particle size range 1400 - 2800µm

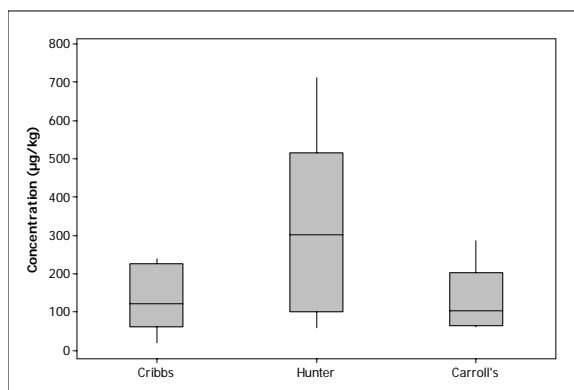


Figure C.70 Box Whisker plot for fluoranthene Concentration on particle size range > 2800µm (w/o LOM)

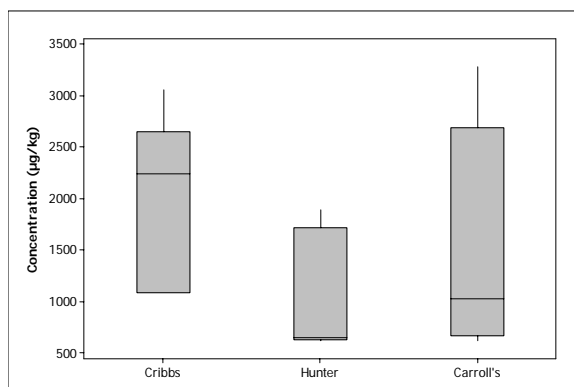


Figure C.71 Box Whisker plot for fluoranthene concentration with LOM

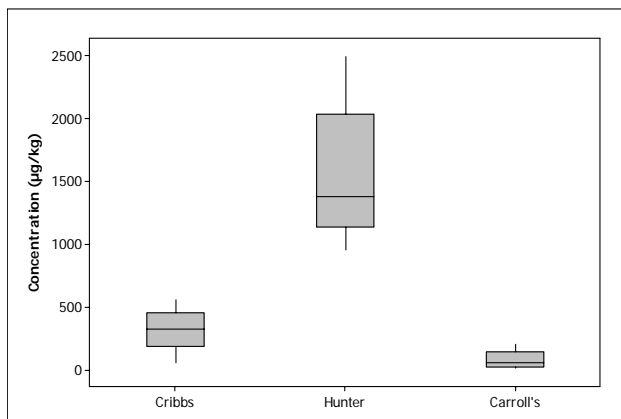


Figure C.72 Box Whisker plot for pyrene concentration with particle size range < 45µm

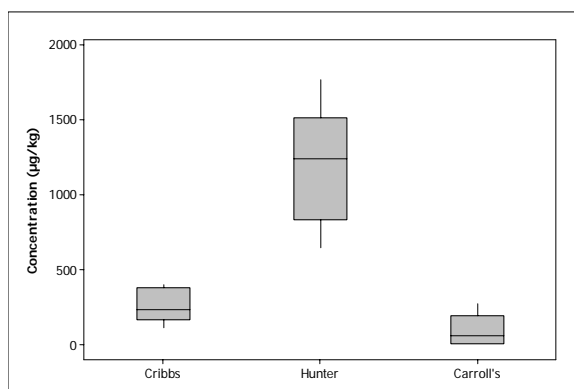


Figure C.73 Whisker plot for pyrene concentration with particle size range 45 - 90µm

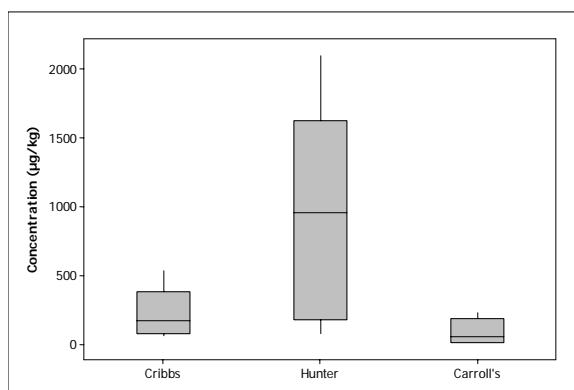


Figure C.74 Whisker plot for pyrene concentration with particle size range 90 - 180µm

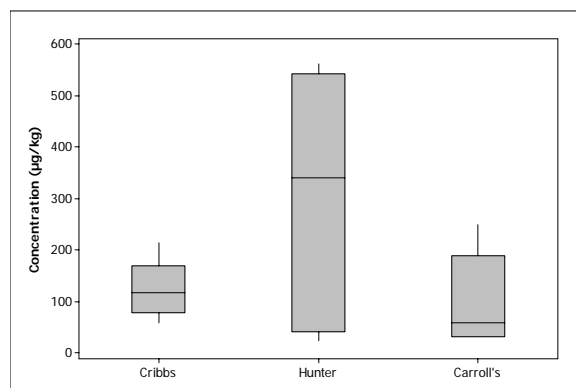


Figure C.75 Box Whisker plot for pyrene concentration with particle size range 180 - 355µm

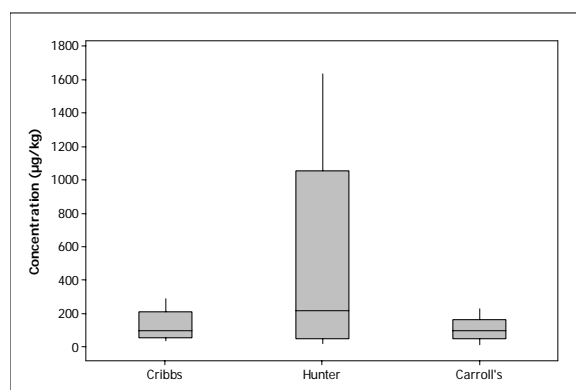


Figure C.76 Box Box Whisker plot for pyrene concentration with particle size range 355 - 710µm

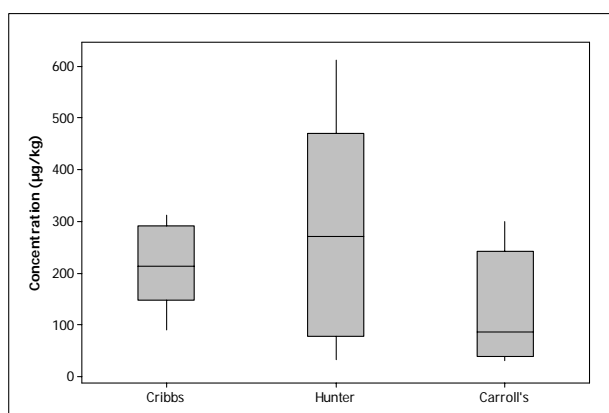


Figure C.77 Box Whisker plot for pyrene concentration with particle size range 710 - 1400µm

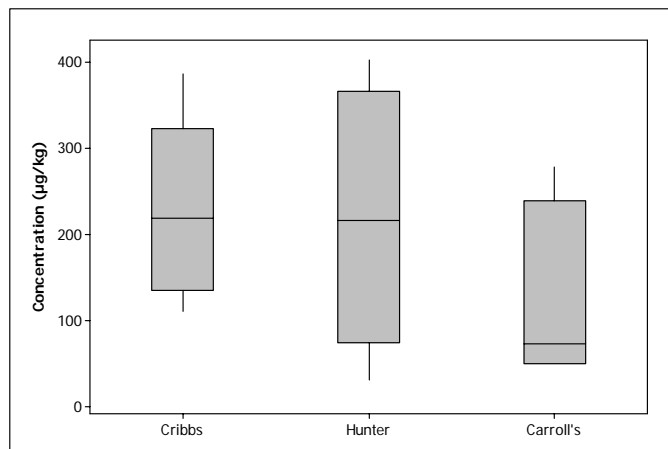


Figure C.78 Box Whisker plot for pyrene concentration with particle size range 1400 - 2800µm

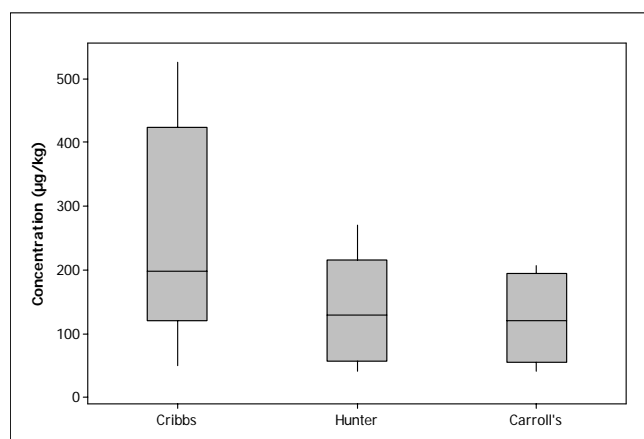


Figure C.79 Box Whisker plot for pyrene concentration with particle size range > 2800µm

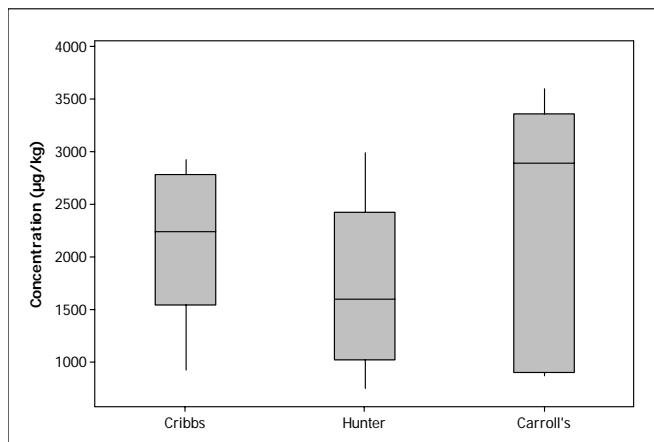


Figure C.80 Box Whisker plot for pyrene concentration with LOM

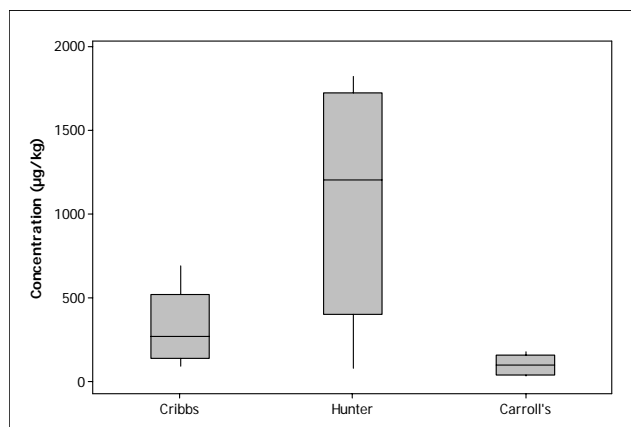


Figure C.81 Box Whisker plot for benzo(a)anthracene concentration with particle size range < 45µm

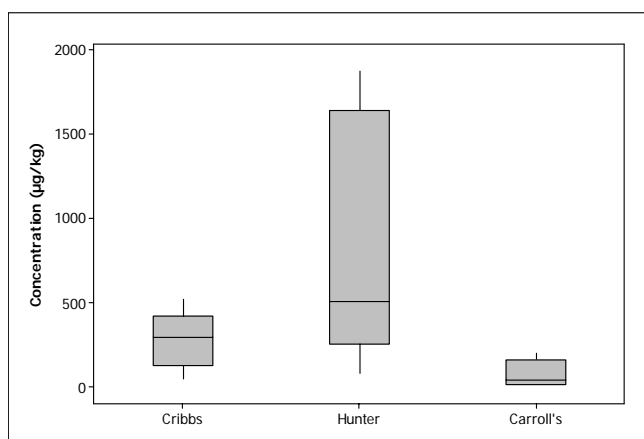


Figure C.82 Box Whisker plot for benzo(a)anthracene concentration with particle size range 45 - 90µm

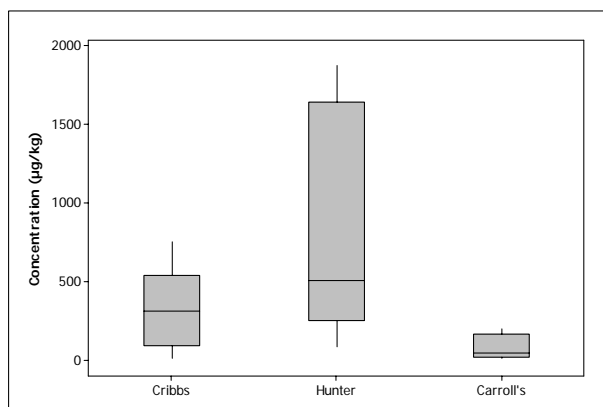


Figure C.83 Box Whisker plot for benzo(a)anthracene concentration with particle size range 90 - 180µm

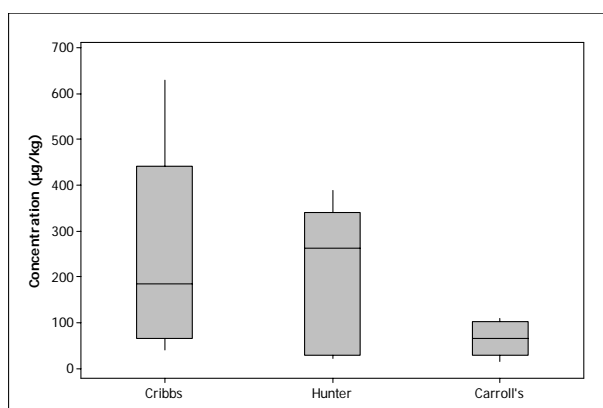


Figure C.84 Box Whisker plot for benzo(a)anthracene concentration with particle size range 180 - 355µm

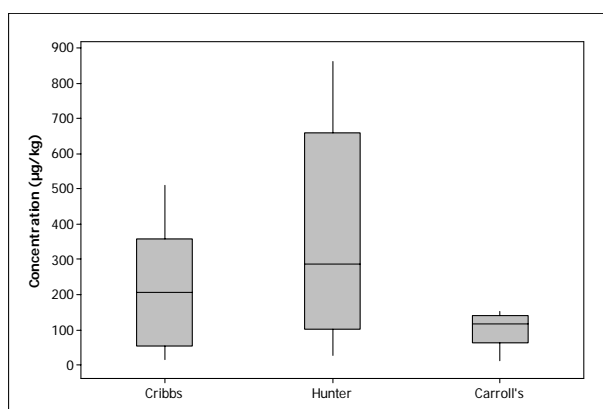


Figure C.85 Box Whisker plot for benzo(a)anthracene concentration with particle size range 355 - 710µm

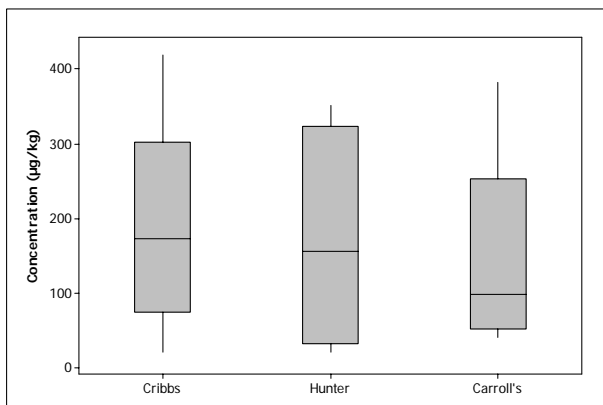


Figure C.86 Box and Whisker plot for benzo(a)anthracene concentration with particle size range 710 - 1400 μm

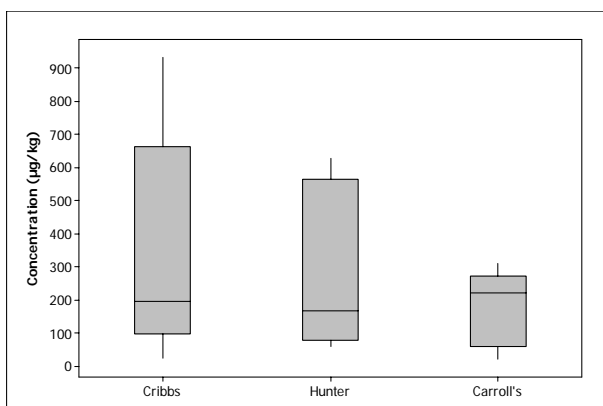


Figure C.87 Box and Whisker plot for benzo(a)anthracene concentration with particle size range 1400 - 2800 μm

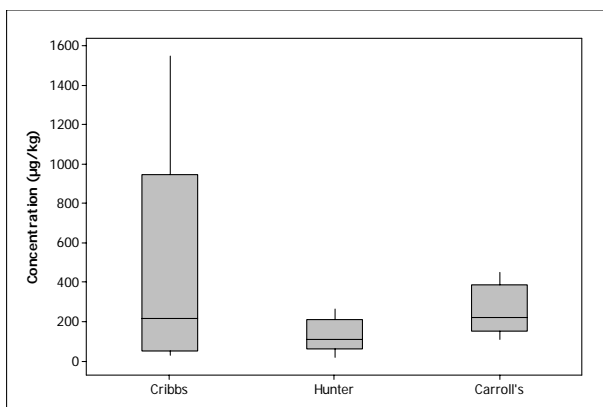


Figure C.88 Box and Whisker plot for benzo(a)anthracene concentration with particle size range > 2800 μm (w/o LOM)

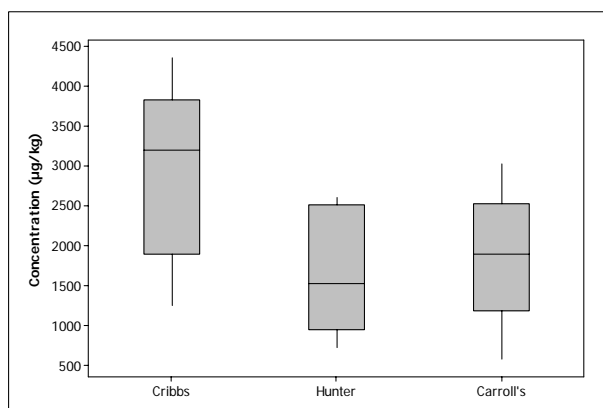


Figure C.89 Box Whisker plot for benzo(a)anthracene concentration with LOM

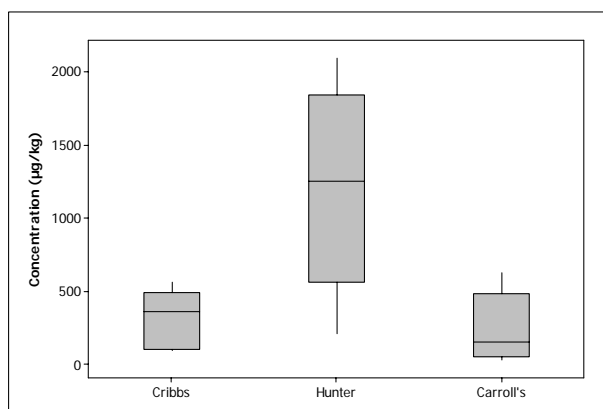


Figure C.90 Box Whisker plot for chrysene concentration with particle size range < 45µm

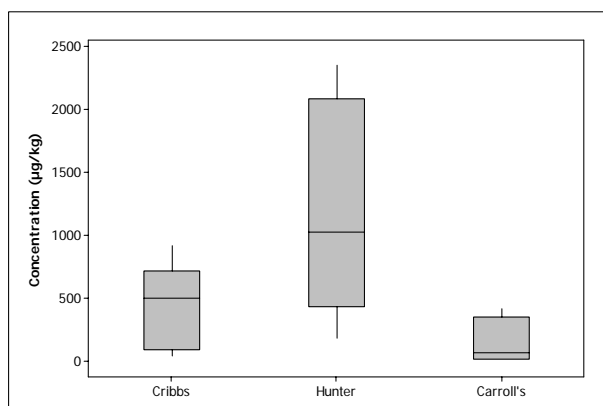


Figure C.91 Box Whisker plot for chrysene concentration with particle size range 45 - 90µm

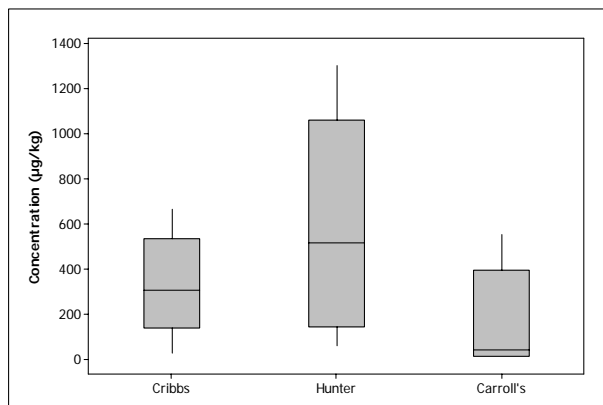


Figure C.92 Box Whisker plot for chrysene concentration with particle size range 90 - 180µm

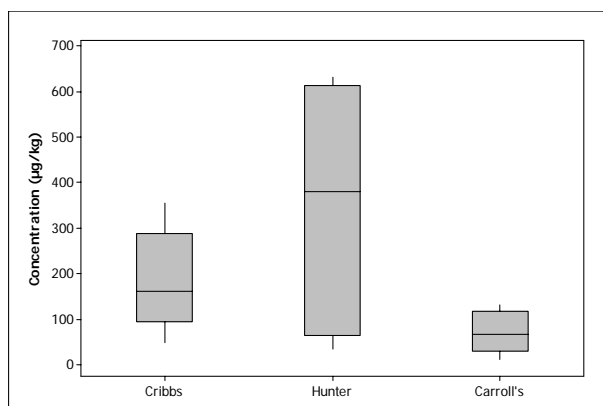


Figure C.93 Box Whisker plot for chrysene concentration with particle size range 180 - 355µm

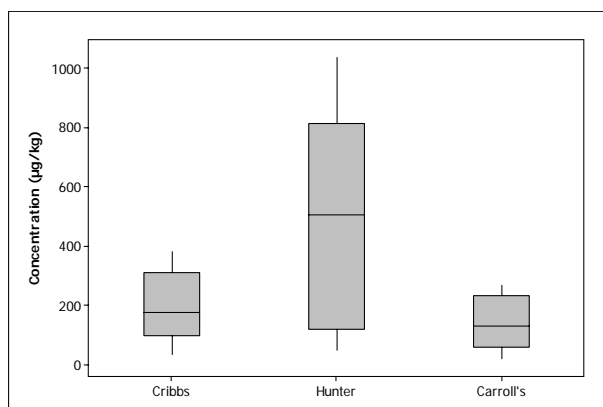


Figure C.94 Box Whisker plot for chrysene concentration with particle size range 355 - 710µm

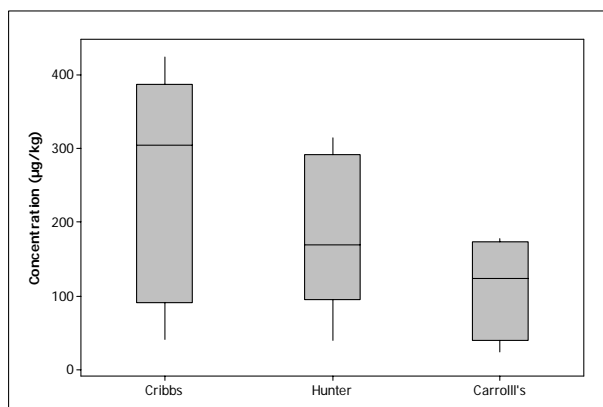


Figure C.95 Box Whisker plot for chrysene concentration with particle size range 710 - 1400µm

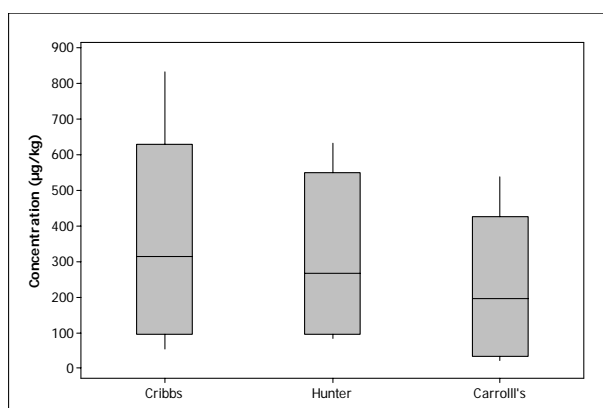


Figure C.96 Box Whisker plot for chrysene concentration with particle size range 1400 - 2800µm

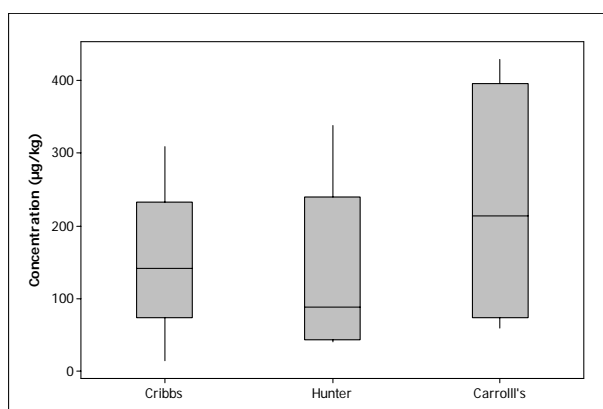


Figure C.97 Box Whisker plot for chrysene concentration with particle size range > 2800µm (w/o LOM)

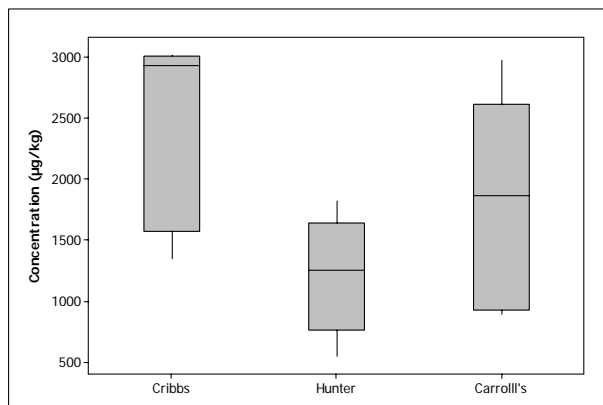


Figure C.98 Box Whisker plot for Chrysene concentration with LOM

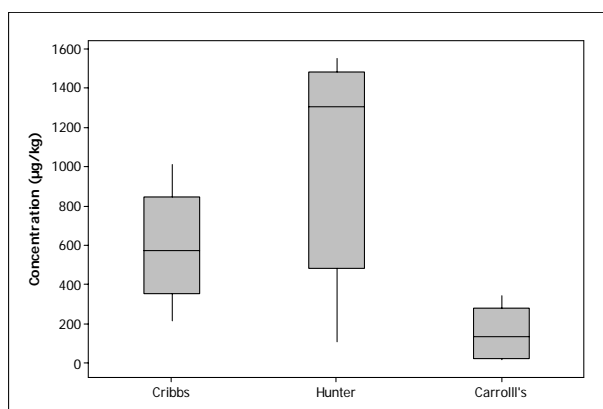


Figure C.99 Box Whisker plot for Benzo(b)fluoranthrene concentration with particle size range < 45µm

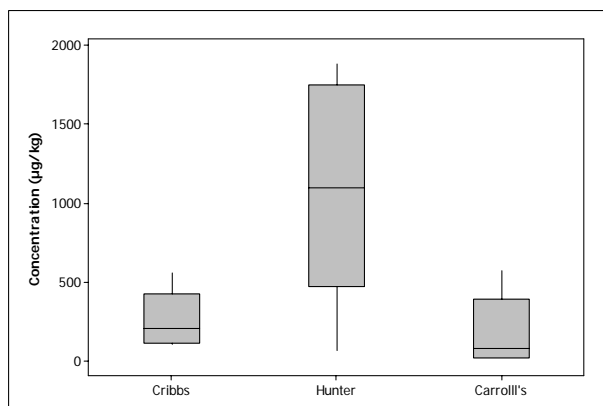


Figure C.100 Box Whisker plot for Benzo(b)fluoranthrene concentration with particle size range 45 - 90µm

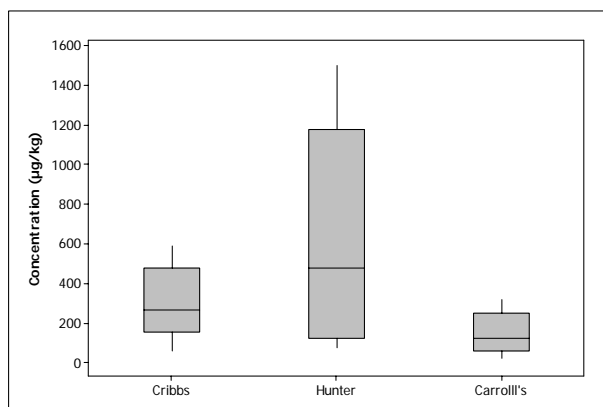


Figure C.101 Box Whisker plot for Benzo(b)fluoranthrene concentration with particle size range 90 - 180µm

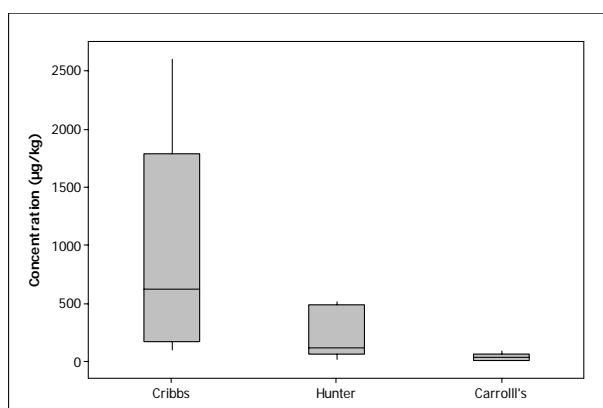


Figure C.102 Box Whisker plot for Benzo(b)fluoranthrene concentration with particle size range 180 - 355µm

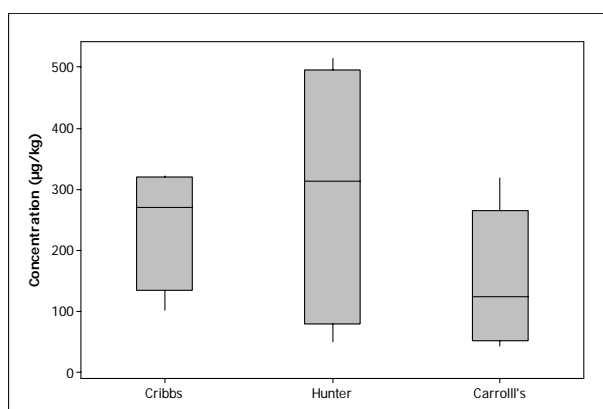


Figure C.103 Box Whisker plot for Benzo(b)fluoranthrene concentration with particle size range 355 - 710µm

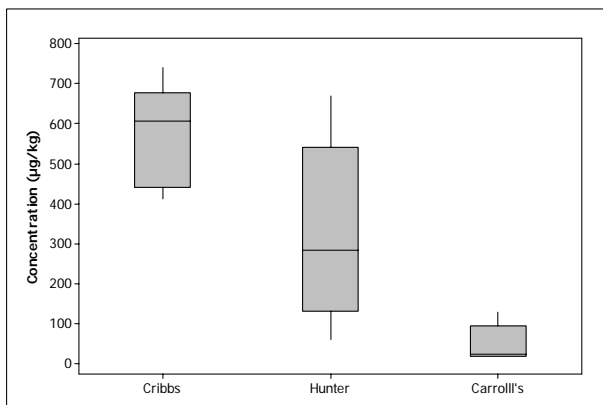


Figure C.104 Box Whisker plot for Benzo(b)fluoranthrene concentration with particle size range 710 - 1400µm

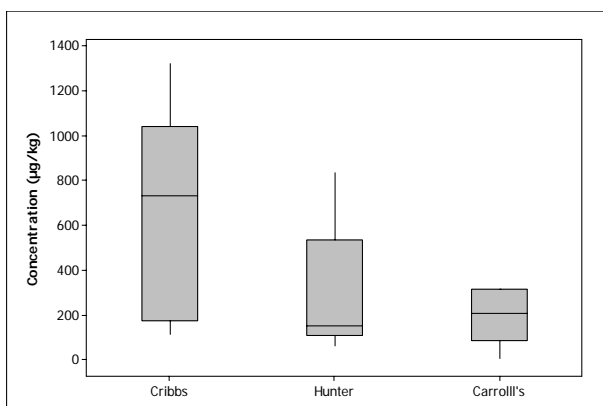


Figure C.105 Box Whisker plot for Benzo(b)fluoranthrene concentration with particle size range 1400 - 2800µm

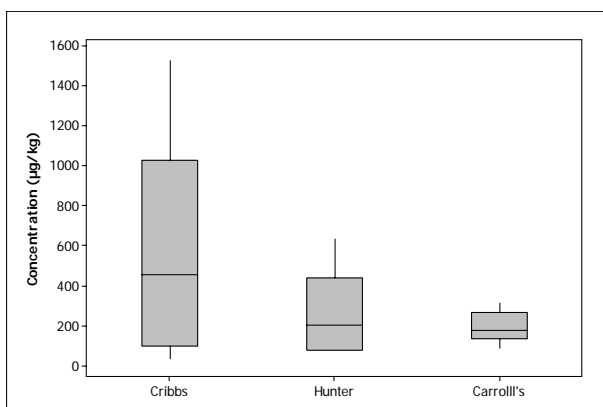


Figure C.106 Box Whisker plot for Benzo(b)fluoranthrene concentration with particle size range < 2800µm (w/o LOM)

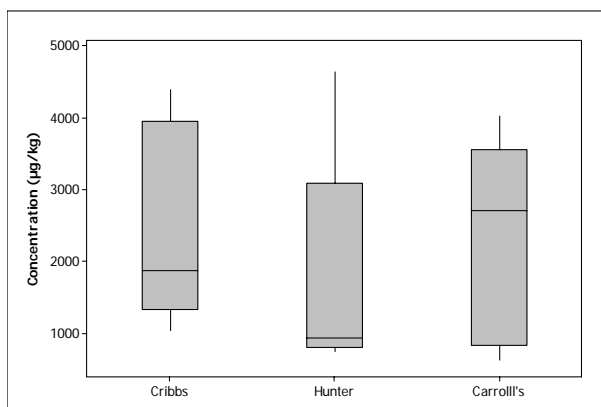


Figure C.107 Box Whisker plot for benzo(b)fluoranthrene concentration with LOM

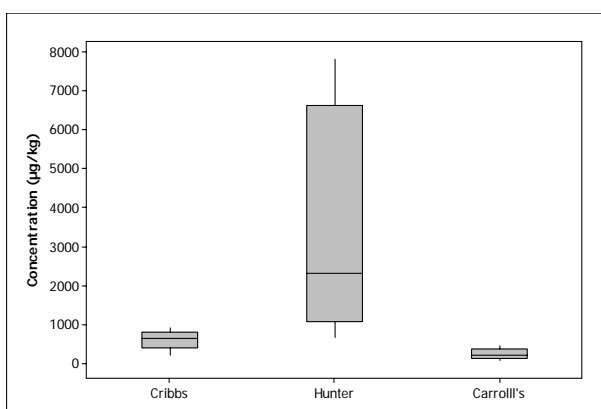


Figure C.108 Box Whisker plot for benzo(a)pyrene concentration on particle size range < 45µm

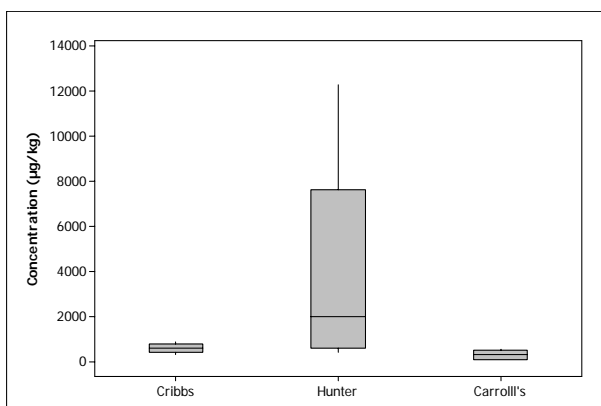


Figure C.109 Whisker plot for benzo(a)pyrene concentration with particle size range 45 - 90µm

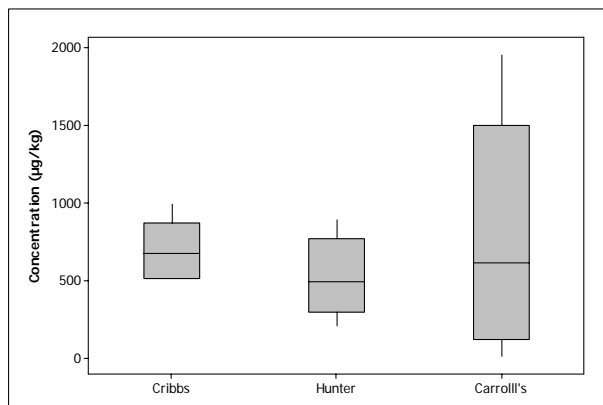


Figure C.110 Whisker plot for benzo(a)pyrene concentration with particle size range 90 - 180µm

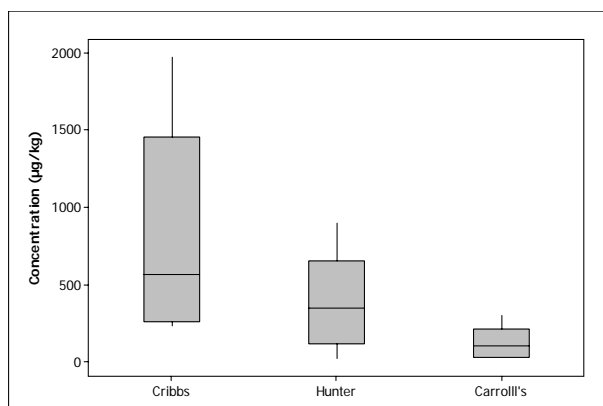


Figure C.111 Whisker plot for benzo(a)pyrene concentration with particle size range 180 - 355µm

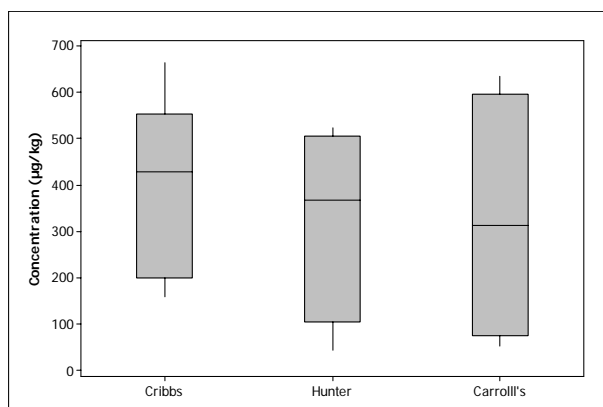


Figure C.112 Whisker plot for benzo(a)pyrene concentration with particle size range 355 - 710µm

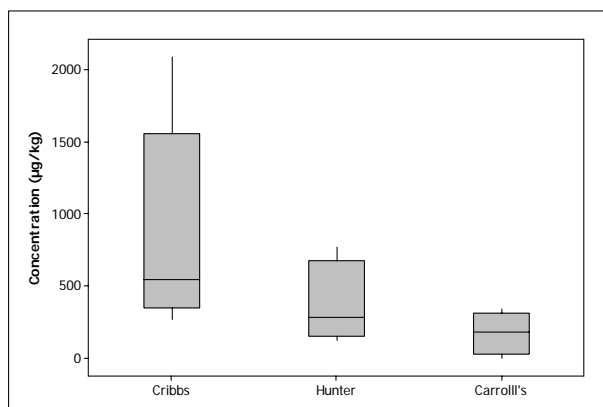


Figure C.113 Whisker plot for benzo(a)pyrene concentration with particle size range 710 - 1400µm

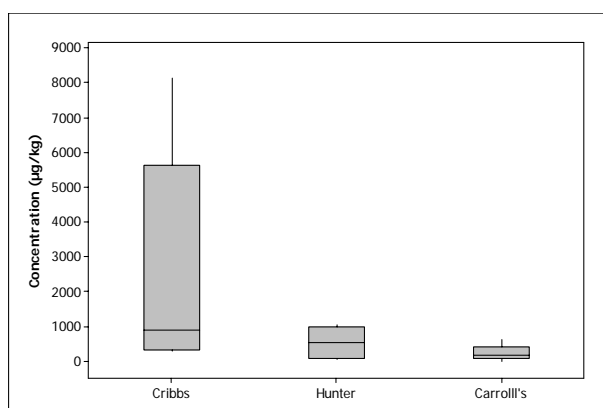


Figure C.114 Whisker plot for benzo(a)pyrene concentration with particle size range 1400 - 2800µm

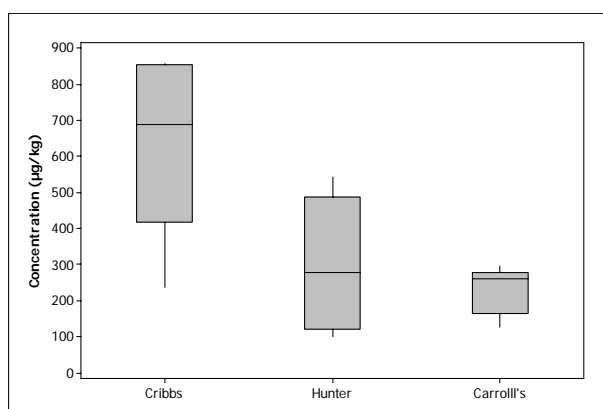


Figure C.115 Whisker plot for benzo(a)pyrene concentration with particle size range > 2800µm (w/o LOM)

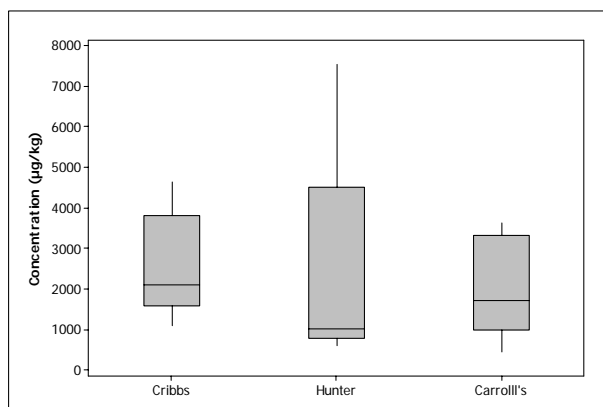


Figure C.116 Box Whisker plot for benzo(a)pyrene concentration with LOM

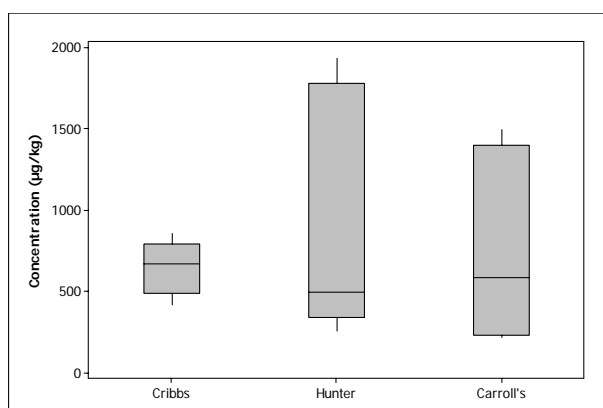


Figure C.117 Box Whisker plot for indeno(1,2,3-cd)pyrene concentration with particle size range < 45µm

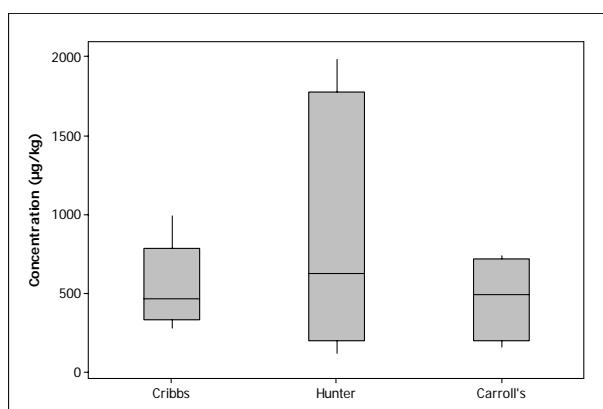


Figure C.118 Box Whisker plot for indeno(1,2,3-cd)pyrene concentration with particle size range 45 - 90µm

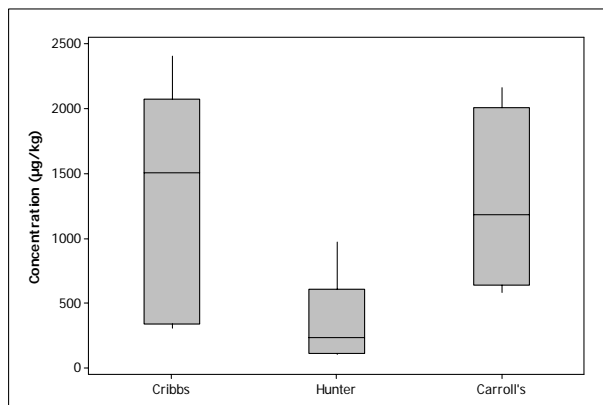


Figure C.119 Box Whisker plot for indeno(1,2,3-cd)pyrene concentration with particle size range 90 - 180µm

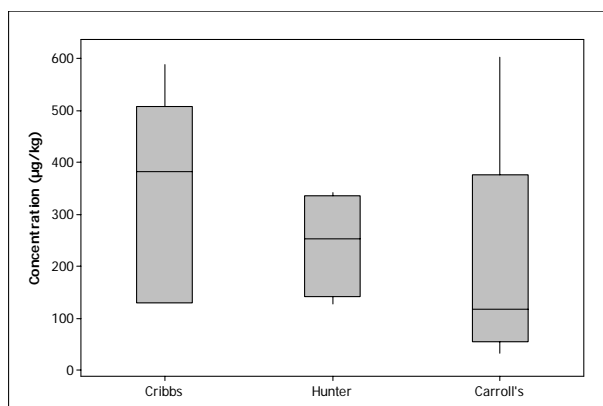


Figure C.120 Box Whisker plot for indeno(1,2,3-cd)pyrene concentration with particle size range 180 - 355µm

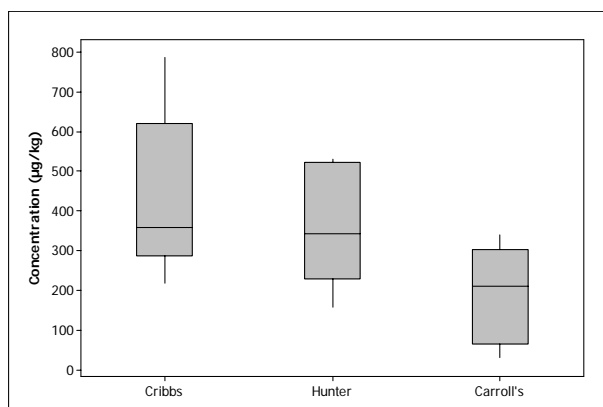


Figure C.121 Box Whisker plot for indeno(1,2,3-cd)pyrene concentration with particle size range 355 - 710µm

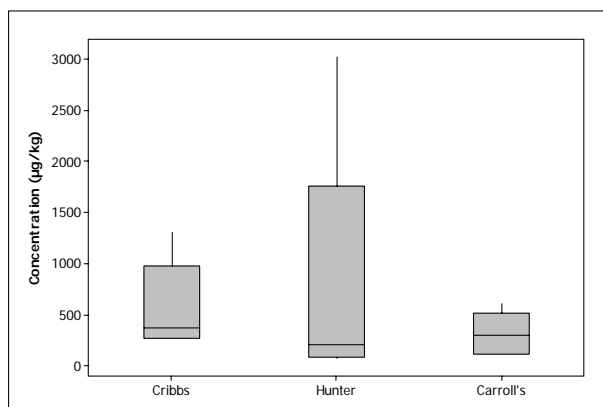


Figure C.122 Box Whisker plot for indeno(1,2,3-cd)pyrene concentration with particle size range 710 - 1400µm

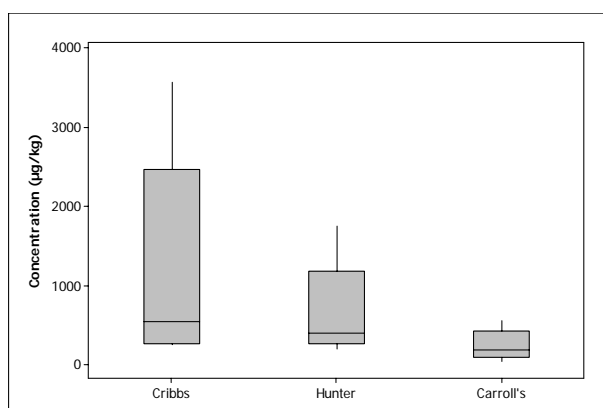


Figure C.123 Box Whisker plot for indeno(1,2,3-cd)pyrene concentration with particle size range 1400 - 2800µm

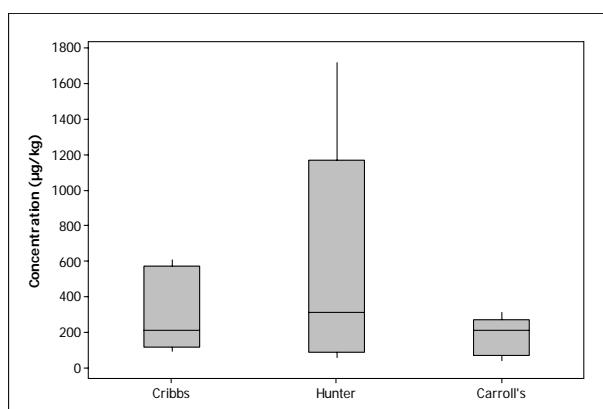


Figure C.124 Box Whisker plot for indeno(1,2,3-cd)pyrene concentration with particle size range > 2800µm (w/o LOM)

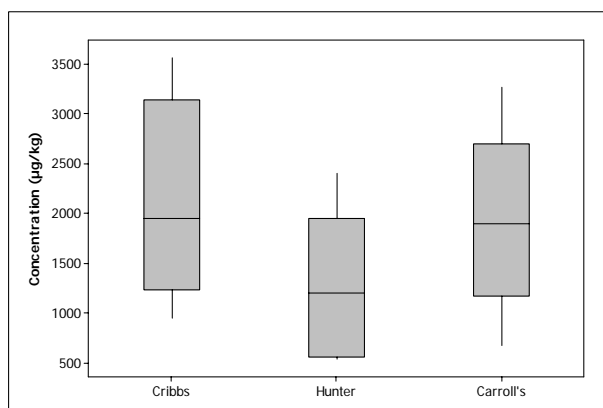


Figure C.125 Box Whisker plot for indeno(1,2,3-cd)pyrene concentration with LOM

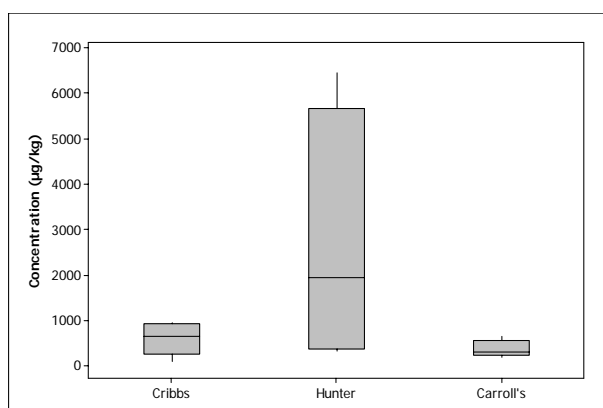


Figure C.126 Box Whisker plot for dibenz(a,h)anthracene concentration with particle size range < 45µm

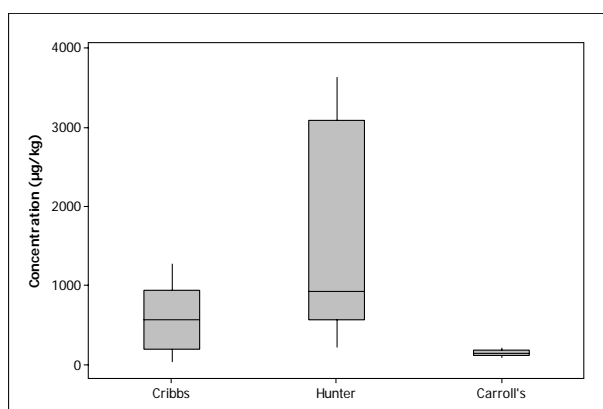


Figure C.127 Box Whisker plot for dibenz(a,h)anthracene concentration with particle size range 45 - 90µm

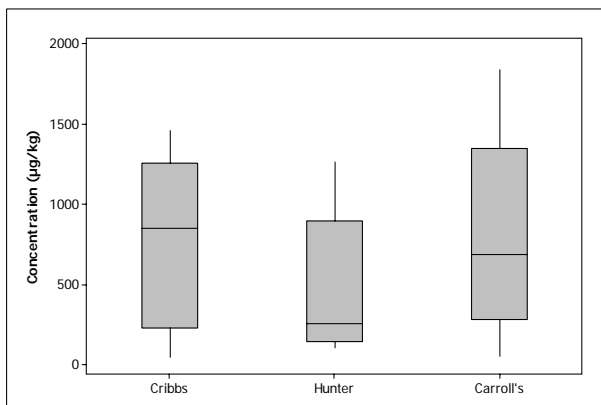


Figure C.128 Box Whisker plot for dibenz(a,h)anthracene concentration with particle size range 90 - 180µm

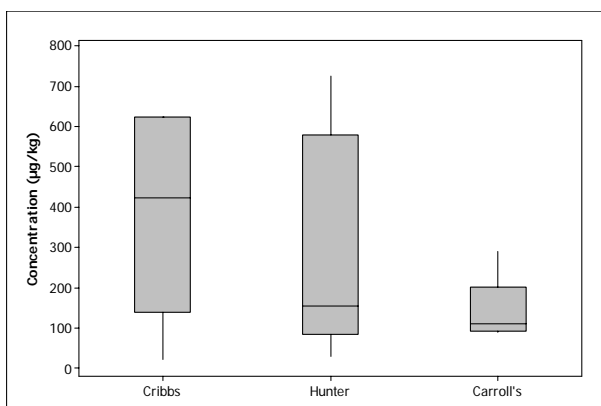


Figure C.129 Box Whisker plot for dibenz(a,h)anthracene concentration with particle size range 180 - 355µm

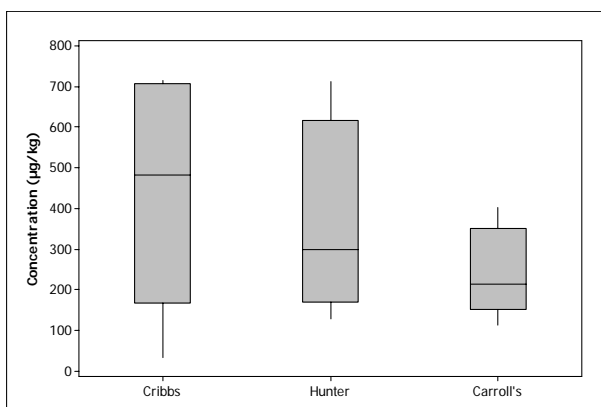


Figure C.130 Box Whisker plot for dibenz(a,h)anthracene concentration with particle size range 355 - 710µm

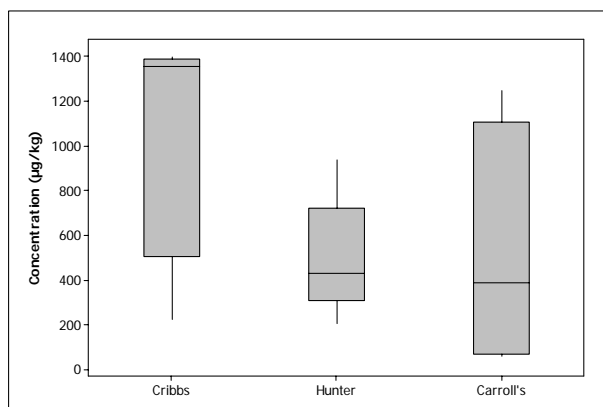


Figure C.131 Box Whisker plot for dibenz(a,h)anthracene concentration with particle size range 710 - 1400um

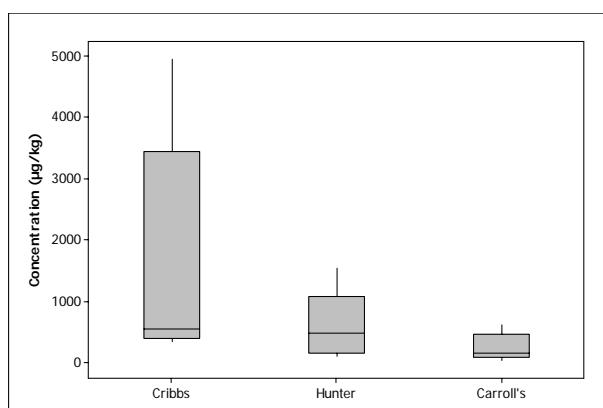


Figure C.132 Box Whisker plot for dibenz(a,h)anthracene concentration with particle size range 1400 - 2800um

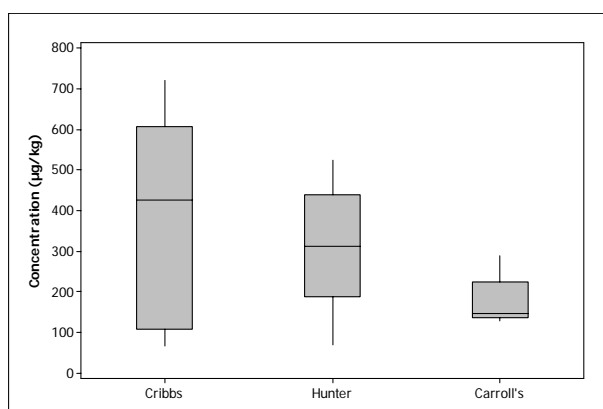


Figure C.133 Box Whisker plot for dibenz(a,h)anthracene concentration with particle size range > 2800um (w/o LOM)

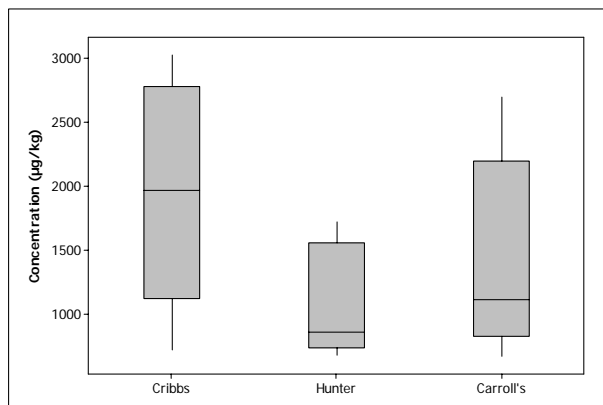


Figure C.134 Box Whisker plot for dibenz(a,h)anthracene concentration with LOM

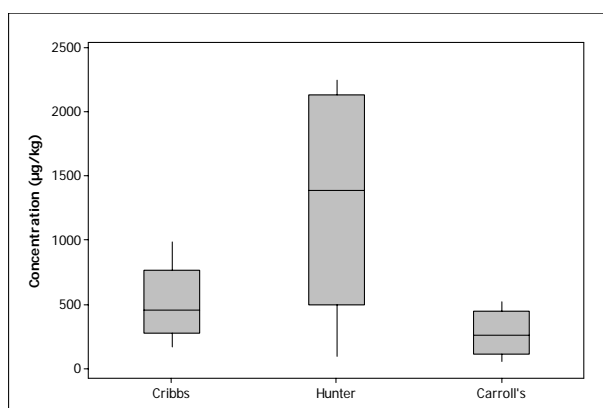


Figure C.135 Box Whisker plot for Benzo(ghi)perylene concentration with particle size range < 45µm

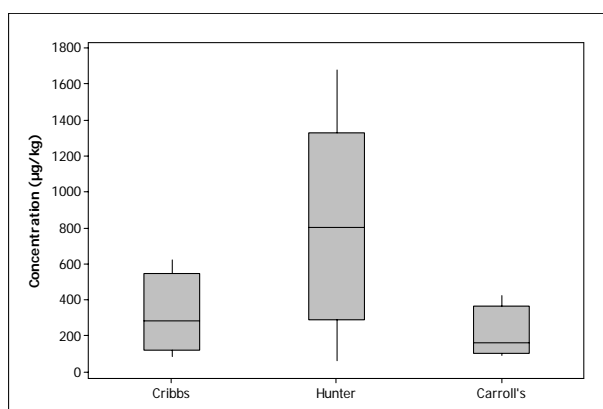


Figure C.136 Box Whisker plot for Benzo(ghi)perylene concentration with particle size range 45 - 90µm

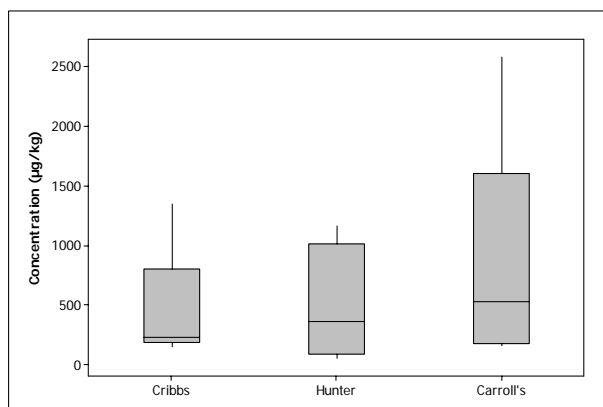


Figure C.137 Box Whisker plot for benzo(ghi)perylene concentration with particle size range 90 - 180 μm

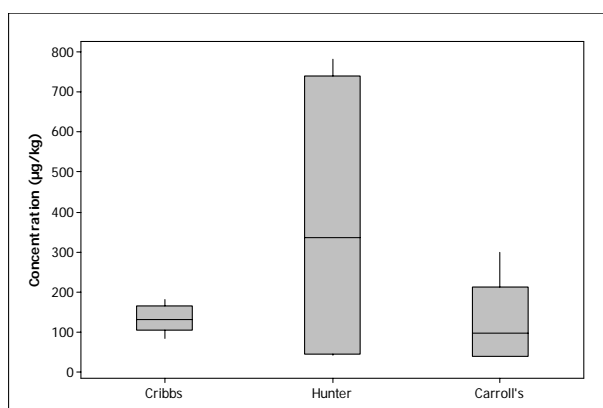


Figure C.138 Box Whisker plot for benzo(ghi)perylene concentration with particle size range 180 - 355 μm

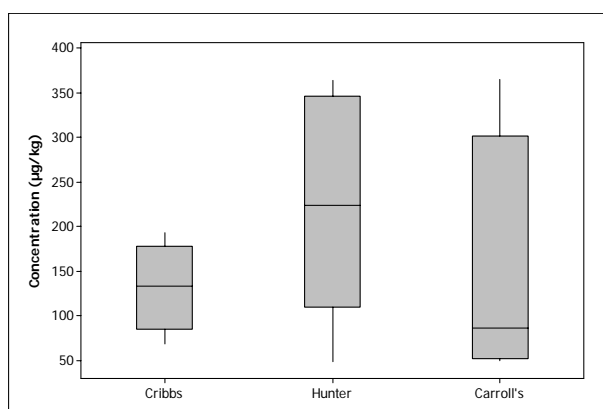


Figure C.139 Box Whisker plot for benzo(ghi)perylene concentration with particle size range 355 - 710 μm

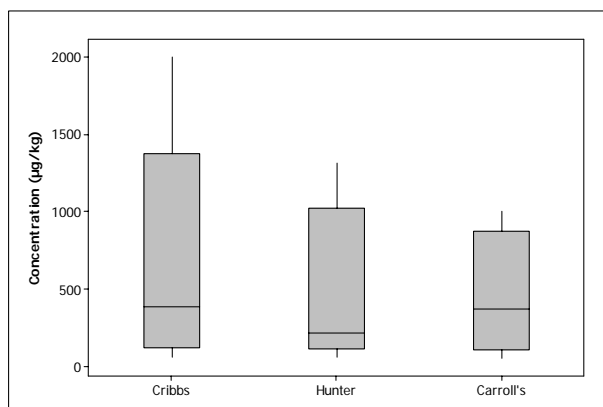


Figure C.140 Box Whisker plot for benzo(ghi)perylene concentration with particle size range 710 - 1400um

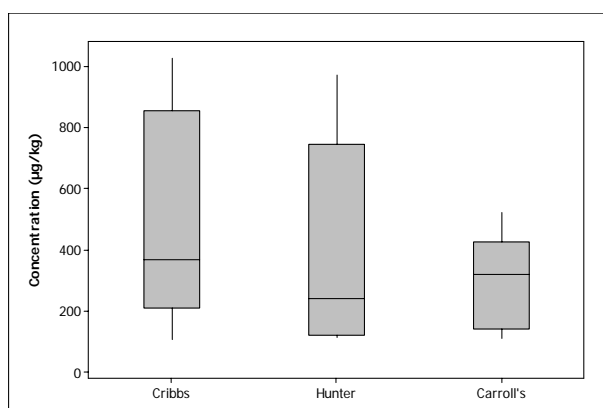


Figure C.141 Box Whisker plot for benzo(ghi)perylene concentration with particle size range 1400 - 2800um

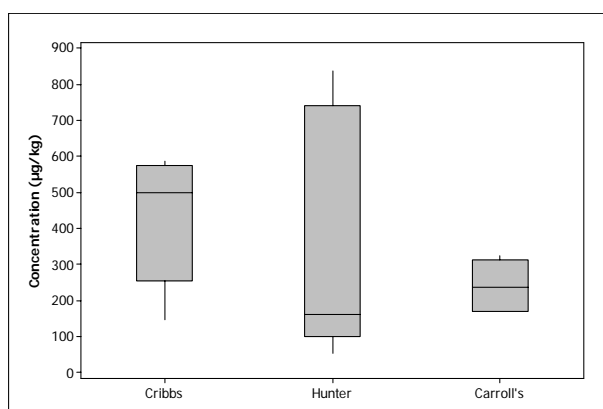


Figure C.142 Box Whisker plot for benzo(ghi)perylene concentration with particle size range > 2800um (w/o LOM)

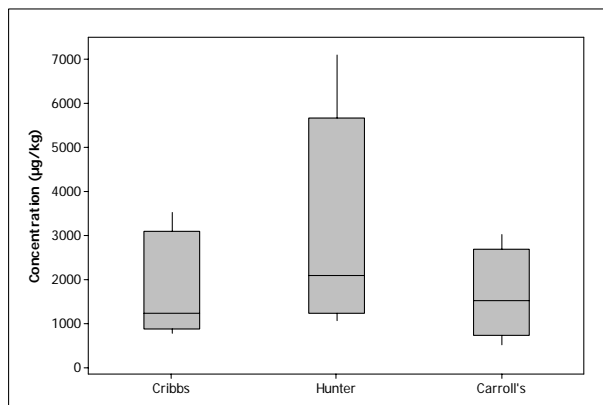


Figure C.143 Box Whisker plot for Benzo(ghi)perylene concentration with LOM

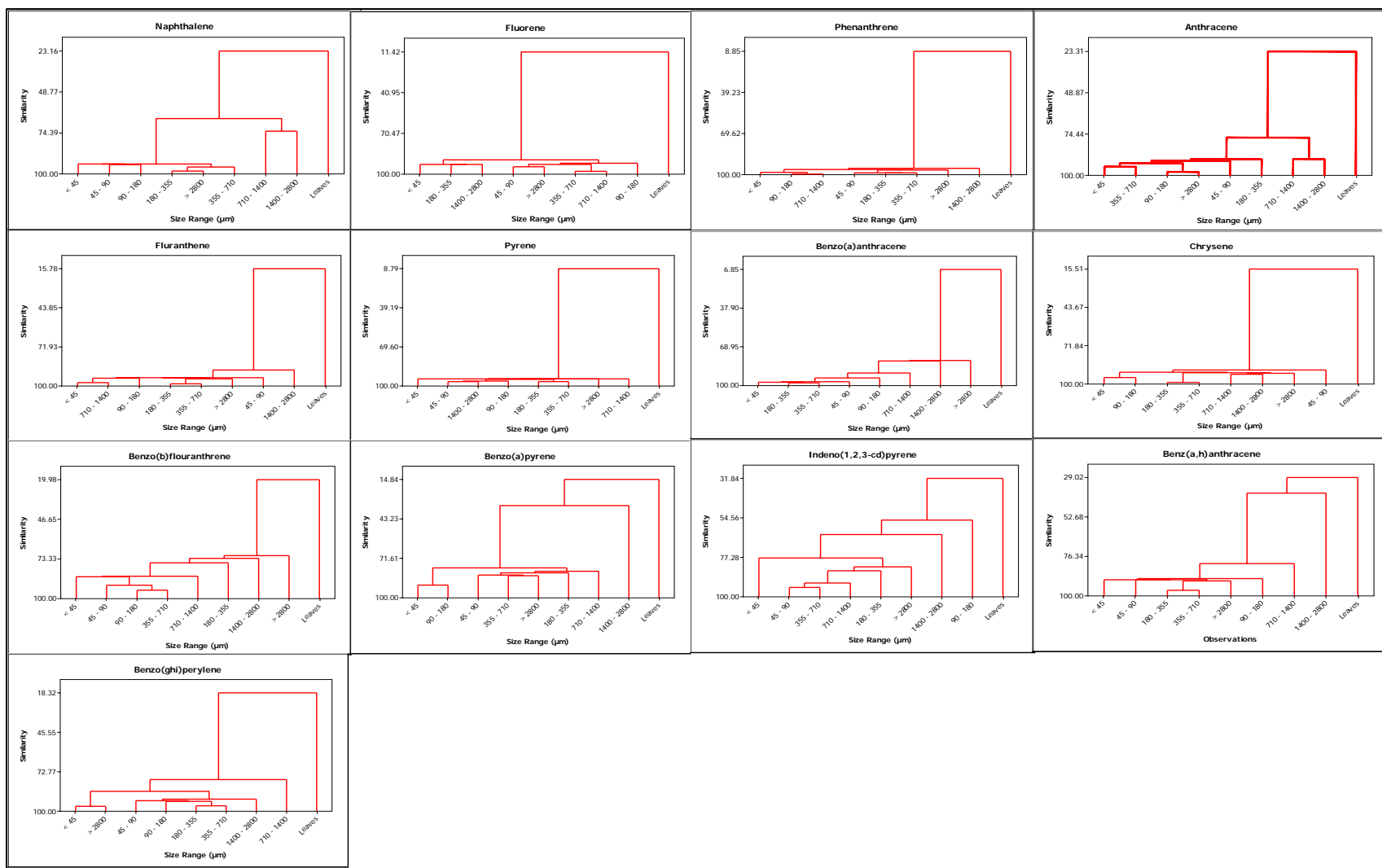


Figure C.144 Cluster analyses of PAHs concentration by particle size for Cribbs Mill Creek

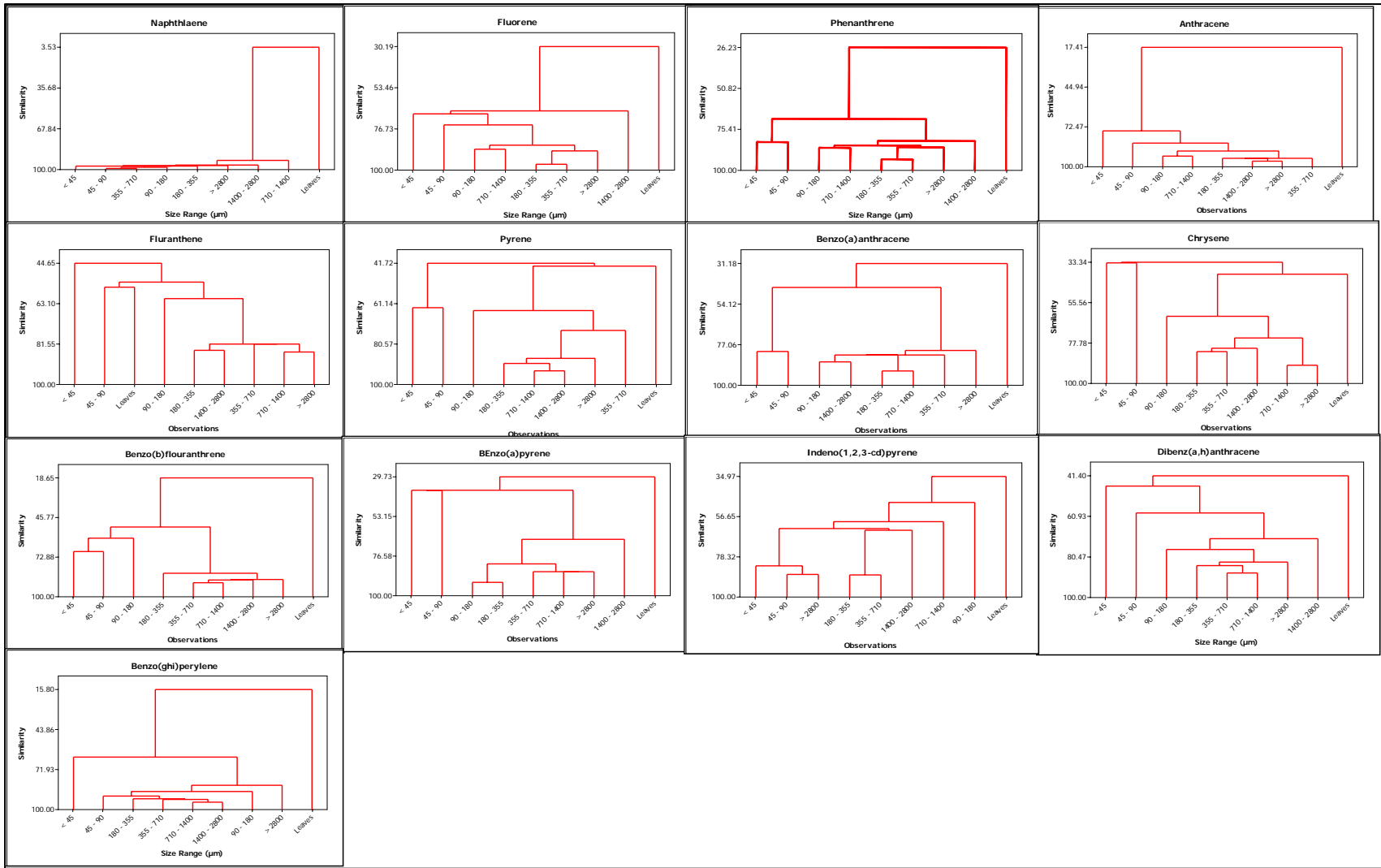


Figure C.145 Cluster Analyses of PAHs concentration by particle size for Hunter Creek

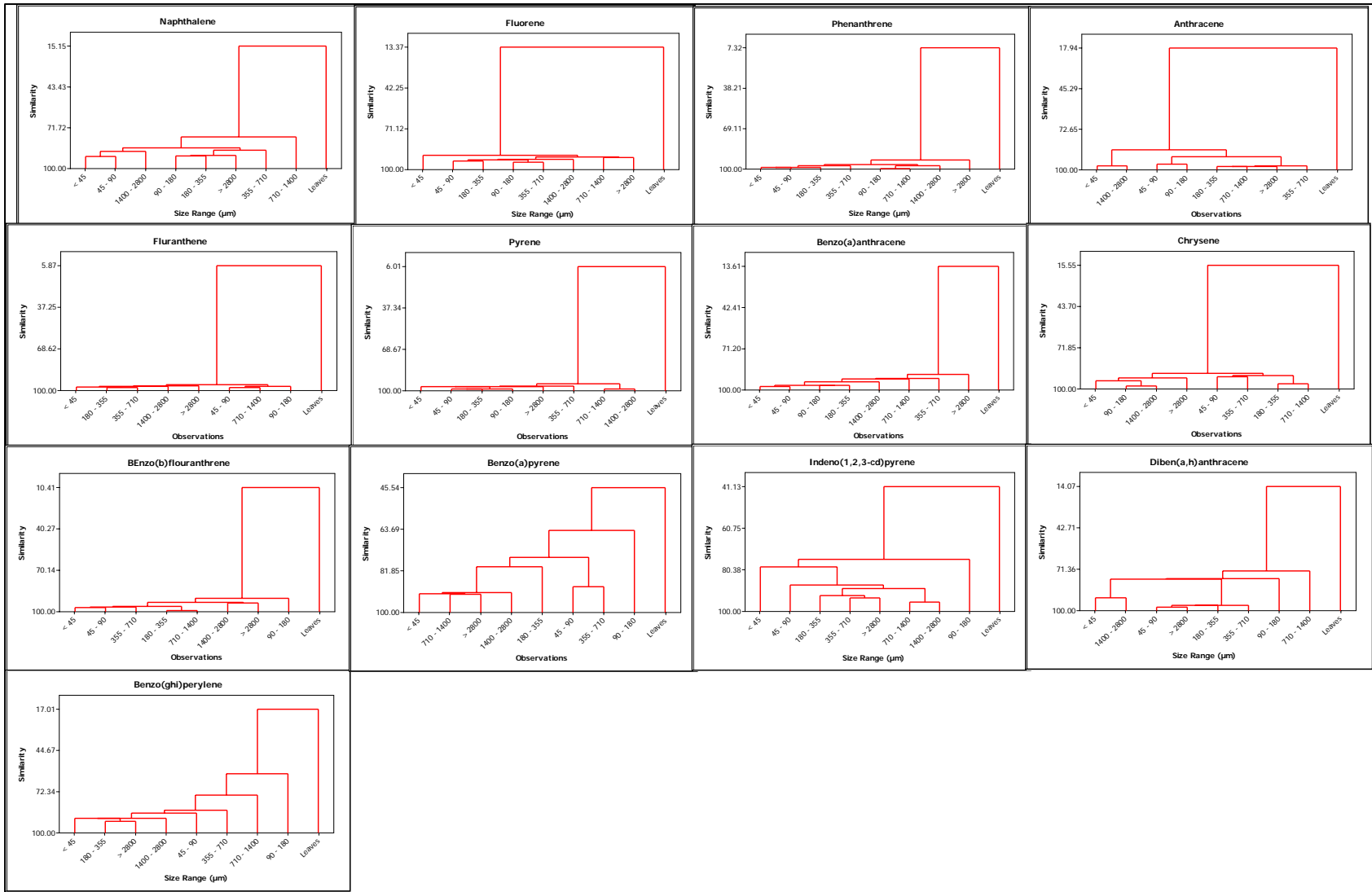


Figure C.146 Cluster analyses of PAHs concentration by particle size for Carroll's Creek

Table C.40 Ratios of Concentrations over CODs ($\mu\text{g}/\text{gm}$) for Cribbs Mill Creek

Size Range (μm)	Naphthalene	Fluorene	Phenanthrene	Anthracene	Fluoranthene	Pyrene	Benzo(a)anthracene
<45	3.6E-03	1.1E-03	4.9E-03	4.3E-03	6.3E-03	6.0E-03	5.2E-03
<45	4.6E-04	4.4E-04	4.9E-04	6.2E-04	1.4E-03	1.8E-03	4.4E-04
<45	1.2E-02	3.0E-04	3.1E-04	2.0E-03	5.0E-04	7.6E-04	2.1E-03
<45	4.5E-03	5.4E-03	1.5E-03	4.7E-03	2.4E-03	4.4E-03	5.4E-03
<45	2.1E-03	1.9E-03	7.8E-04	2.2E-03	1.6E-03	2.4E-03	2.6E-03
45 – 90	3.1E-03	2.1E-03	6.3E-03	5.9E-03	1.4E-02	1.2E-02	9.9E-03
45 – 90	4.0E-04	2.4E-04	2.7E-04	4.4E-04	2.7E-03	1.5E-03	3.6E-04
45 – 90	1.0E-02	1.2E-03	1.9E-03	6.8E-03	1.5E-03	2.5E-03	4.5E-03
45 – 90	3.9E-03	1.7E-03	6.3E-04	3.2E-03	2.6E-03	3.0E-03	4.2E-03
45 – 90	1.7E-03	8.8E-04	5.4E-04	2.1E-03	2.4E-03	1.9E-03	2.4E-03
90 – 180	4.5E-03	1.9E-03	1.3E-02	4.0E-03	1.9E-02	1.3E-02	1.4E-02
90 – 180	1.4E-03	1.1E-03	NA	2.8E-04	3.4E-03	1.3E-03	1.6E-04
90 – 180	2.0E-02	1.6E-02	1.5E-03	3.0E-03	1.2E-03	2.0E-03	9.5E-03
90 – 180	1.2E-02	6.0E-03	3.0E-03	8.0E-03	3.8E-03	9.8E-03	1.4E-02
90 – 180	5.5E-03	6.0E-03	2.2E-03	3.7E-03	3.5E-03	4.6E-03	6.2E-03
180 – 355	8.6E-03	8.3E-03	0.0E+00	0.0E+00	2.0E-02	1.6E-02	1.3E-02
180 – 355	8.1E-04	6.9E-04	6.8E-04	4.3E-04	2.1E-03	7.9E-04	5.2E-04
180 – 355	6.4E-03	5.5E-04	4.3E-04	6.6E-04	1.6E-03	3.6E-03	6.7E-03
180 – 355	6.1E-03	1.3E-02	2.7E-03	4.9E-03	3.1E-03	5.2E-03	1.5E-02
180 – 355	2.2E-03	3.6E-03	1.0E-03	1.5E-03	2.1E-03	2.2E-03	4.6E-03
355 – 710	8.1E-04	1.1E-03	0.0E+00	2.9E-03	3.0E-03	2.2E-03	2.1E-03
355 – 710	6.7E-04	3.2E-04	2.2E-04	2.4E-04	1.2E-03	5.4E-04	1.2E-04
355 – 710	5.5E-03	8.2E-03	8.5E-04	4.0E-03	2.0E-03	6.1E-04	3.1E-03
355 – 710	3.5E-03	3.6E-03	3.3E-03	2.4E-02	4.8E-03	1.0E-02	1.8E-02
355 – 710	2.6E-03	8.0E-03	2.1E-03	1.1E-02	4.9E-03	4.6E-03	7.1E-03

Continuation of above Table

Size Range (μm)	Naphthalene	Fluorene	Phenanthrene	Anthracene	Fluranthene	Pyrene	Benzo(a) anthracene
710 – 1400	1.6E-03	6.4E-04	4.1E-03	6.3E-03	4.2E-03	2.9E-03	1.9E-03
710 – 1400	7.3E-04	3.7E-04	2.7E-04	4.7E-04	1.8E-03	5.8E-04	1.4E-04
710 – 1400	6.1E-02	3.4E-03	3.1E-04	6.3E-03	1.1E-03	1.6E-03	3.2E-03
710 – 1400	2.0E-02	3.5E-03	3.9E-03	1.3E-02	7.2E-03	7.4E-03	4.1E-03
710 – 1400	2.4E-03	1.5E-03	5.5E-04	3.2E-03	1.8E-03	1.4E-03	8.4E-04
1400 – 2800	7.5E-04	8.0E-04	6.9E-03	1.8E-02	2.7E-03	1.9E-03	1.3E-03
1400 – 2800	7.5E-04	8.0E-04	6.9E-03	1.8E-02	2.7E-03	1.9E-03	1.3E-03
1400 – 2800	6.9E-04	8.0E-04	1.2E-04	4.2E-04	2.1E-03	1.3E-03	2.0E-04
1400 – 2800	5.3E-02	2.6E-03	1.8E-03	6.9E-03	1.9E-03	7.4E-04	6.2E-03
1400 – 2800	1.6E-02	4.7E-03	2.1E-03	5.3E-03	4.5E-03	3.2E-03	3.3E-03
>2800	5.4E-04	3.2E-04	7.9E-04	2.1E-03	1.5E-03	3.4E-03	2.2E-03
>2800	5.4E-04	3.2E-04	7.9E-04	2.1E-03	1.5E-03	3.4E-03	2.2E-03
>2800	7.4E-04	1.9E-03	4.6E-03	9.4E-04	7.9E-04	2.4E-03	5.4E-04
>2800	9.5E-04	9.8E-04	1.1E-04	4.3E-04	1.2E-04	3.1E-04	1.8E-04
>2800	2.4E-03	2.3E-03	8.9E-04	3.9E-03	1.9E-03	1.8E-03	2.0E-03
LOM	9.1E-04	1.6E-03	1.7E-03	2.2E-03	1.9E-03	1.9E-03	3.8E-03
LOM	9.1E-04	1.6E-03	1.7E-03	2.2E-03	1.9E-03	1.9E-03	3.8E-03
LOM	9.4E-04	1.0E-03	1.1E-03	2.1E-03	5.4E-04	1.3E-03	1.3E-03
LOM	2.4E-03	1.7E-03	3.0E-03	4.4E-04	1.6E-03	4.7E-04	6.5E-04
LOM	1.1E-03	6.4E-04	5.1E-04	8.7E-04	5.8E-04	1.6E-03	1.7E-03
LOM	1.5E-03	2.0E-03	2.8E-03	2.1E-03	2.1E-03	2.0E-03	3.1E-03

Continuation of above Table

Size Range (μm)	Chrysene	Benzo(b) fluoranthrene	Benzo(a) pyrene	Indeno(1,2,3-cd) pyrene	Dibenz(a,h) anthracene	Benzo(ghi) perylene
<45	8.0E-03	1.9E-02	1.3E-02	1.4E-02	2.2E-03	1.0E-02
<45	5.4E-04	3.4E-03	3.4E-03	2.8E-03	2.1E-03	8.3E-04
<45	1.1E-03	2.5E-03	2.4E-03	4.8E-03	1.0E-02	1.1E-02
<45	4.5E-03	3.9E-03	7.3E-03	6.7E-03	7.5E-03	3.6E-03
<45	2.7E-03	4.3E-03	4.5E-03	5.0E-03	4.9E-03	2.9E-03
45 – 90	1.6E-02	3.2E-03	2.7E-02	8.6E-03	1.2E-03	4.7E-03
45 – 90	2.9E-04	8.1E-04	3.5E-03	2.7E-03	2.4E-03	5.9E-04
45 – 90	3.2E-03	4.5E-03	7.1E-03	2.2E-02	2.8E-02	1.0E-02
45 – 90	7.4E-03	4.5E-03	4.8E-03	3.8E-03	4.5E-03	5.0E-03
45 – 90	4.2E-03	2.3E-03	5.3E-03	4.6E-03	4.9E-03	2.3E-03
90 – 180	2.3E-02	4.5E-02	3.9E-02	2.8E-02	3.8E-03	1.8E-02
90 – 180	4.3E-04	8.7E-04	7.2E-03	4.4E-03	5.8E-03	2.1E-03
90 – 180	7.2E-03	7.2E-03	2.2E-02	5.0E-02	4.2E-02	3.9E-02
90 – 180	1.2E-02	4.9E-03	1.8E-02	4.4E-02	1.9E-02	4.9E-03
90 – 180	8.0E-03	7.3E-03	1.3E-02	3.0E-02	1.7E-02	4.3E-03
180 – 355	2.3E-02	3.6E-01	2.8E-01	1.8E-02	3.2E-03	1.2E-02
180 – 355	6.5E-04	8.2E-03	3.8E-03	1.7E-03	3.4E-03	1.7E-03
180 – 355	5.2E-03	3.9E-03	8.5E-03	2.1E-02	2.3E-02	5.5E-03
180 – 355	8.6E-03	6.1E-03	1.4E-02	1.0E-02	1.5E-02	4.4E-03
180 – 355	3.9E-03	1.8E-02	1.7E-02	6.8E-03	7.6E-03	2.4E-03
355 – 710	3.5E-03	7.1E-03	3.5E-03	4.8E-03	7.1E-04	3.0E-03
355 – 710	2.9E-04	8.0E-04	5.1E-03	2.8E-03	2.3E-03	5.4E-04
355 – 710	2.7E-03	2.5E-03	3.7E-03	1.2E-02	1.1E-02	0.0E+00
355 – 710	1.3E-02	1.1E-02	1.5E-02	1.2E-02	2.4E-02	6.6E-03
355 – 710	8.2E-03	9.3E-03	1.5E-02	1.6E-02	1.7E-02	4.5E-03

Continuation of above Table

Size Range (µm)	Chrysene	Benzo(b) flouranthrene	Benzo(a) pyrene	Indeno(1,2,3-cd) pyrene	Dibenz(a,h) anthracene	Benzo(ghi) perylene
710 - 1400	3.7E-03	7.8E-03	2.8E-03	2.8E-03	0.0E+00	2.0E-03
710 - 1400	2.7E-04	2.7E-03	3.5E-03	1.9E-03	1.5E-03	4.0E-04
710 - 1400	3.2E-03	4.6E-03	1.6E-02	9.8E-03	1.0E-02	2.9E-03
710 - 1400	3.4E-03	1.1E-02	1.0E-02	8.9E-03	3.3E-02	4.8E-02
710 - 1400	2.0E-03	4.0E-03	6.8E-03	4.3E-03	9.1E-03	5.0E-03
1400 - 2800	2.3E-03	5.4E-03	2.5E-03	1.9E-03	4.1E-03	2.3E-03
1400 - 2800	2.3E-03	5.4E-03	2.5E-03	1.9E-03	4.1E-03	2.3E-03
1400 - 2800	4.4E-04	9.0E-04	7.2E-03	4.3E-03	3.5E-03	8.4E-04
1400 - 2800	5.6E-03	8.8E-03	5.4E-02	2.4E-02	3.3E-02	6.8E-03
1400 - 2800	1.1E-03	2.0E-03	2.5E-03	2.4E-03	2.9E-03	5.7E-03
>2800	2.0E-03	3.4E-03	5.4E-03	3.4E-03	4.6E-03	3.8E-03
>2800	2.0E-03	3.4E-03	5.4E-03	3.4E-03	4.6E-03	3.8E-03
>2800	1.0E-03	3.4E-03	5.1E-03	1.1E-03	1.1E-03	1.1E-03
>2800	9.4E-05	2.2E-04	5.3E-03	6.1E-04	4.2E-04	3.5E-03
>2800	1.3E-03	1.5E-03	2.2E-03	1.9E-03	4.5E-03	3.3E-03
LOM	2.6E-03	3.8E-03	4.0E-03	1.3E-03	6.2E-04	8.5E-04
LOM	2.6E-03	3.8E-03	4.0E-03	1.3E-03	6.2E-04	8.5E-04
LOM	1.5E-03	1.8E-03	1.0E-03	4.8E-04	1.5E-03	6.2E-04
LOM	1.5E-03	5.3E-04	1.5E-03	1.8E-03	7.9E-04	4.1E-04
LOM	7.2E-04	8.7E-04	5.9E-04	1.0E-03	1.4E-03	1.9E-03
LOM	1.7E-03	1.7E-03	1.9E-03	2.5E-03	1.8E-03	2.5E-03

Table C.41 Ratios of Concentrations over CODs ($\mu\text{g}/\text{gm}$) for Hunter Creek

Size Range (μm)	Naphthalene	Fluorene	Phenanthrene	Anthracene	Fluranthene	Pyrene	Benzo(a)anthracene
<45	1.5E-04	1.4E-03	1.0E-02	7.8E-04	9.3E-03	1.8E-02	1.1E-03
<45	4.6E-03	1.4E-02	1.4E-02	1.8E-02	3.2E-02	2.5E-02	1.9E-02
<45	4.4E-03	2.1E-03	8.0E-03	2.8E-03	3.0E-02	3.0E-02	1.2E-02
<45	1.1E-03	3.0E-03	3.8E-03	4.9E-03	4.5E-02	2.4E-02	9.6E-03
<45	3.7E-03	2.1E-02	1.8E-02	3.1E-02	4.0E-02	4.8E-02	3.5E-02
45 - 90	6.2E-04	2.4E-03	9.1E-03	1.2E-03	3.2E-02	1.5E-02	2.0E-03
45 - 90	3.5E-03	1.3E-02	1.3E-02	1.9E-02	2.1E-02	3.6E-02	1.5E-02
45 - 90	6.0E-03	9.4E-03	1.1E-02	2.1E-02	4.9E-02	4.0E-02	4.1E-03
45 - 90	1.3E-03	3.2E-03	3.1E-03	6.2E-03	3.1E-02	2.1E-02	9.7E-03
45 - 90	2.7E-03	2.4E-02	3.7E-02	4.4E-02	6.2E-02	5.8E-02	8.6E-02
90 - 180	1.6E-03	1.2E-02	2.6E-03	3.2E-02	3.1E-02	1.6E-01	1.4E-02
90 - 180	2.2E-02	7.2E-02	6.5E-02	9.2E-02	1.4E-01	1.2E-01	1.0E-01
90 - 180	8.6E-03	1.2E-02	5.9E-03	5.2E-03	8.4E-02	2.8E-02	0.0E+00
90 - 180	3.1E-04	2.4E-03	2.7E-03	4.3E-02	2.3E-02	5.7E-03	8.1E-04
90 - 180	8.6E-03	5.3E-02	5.8E-02	7.2E-02	1.4E-01	1.5E-01	4.1E-02
180 - 355	1.8E-02	9.3E-02	1.5E-01	1.9E-02	8.2E-01	4.0E-01	3.1E-01
180 - 355	8.3E-02	1.6E-02	7.1E-02	1.3E-01	2.1E-01	1.7E-01	1.2E-01
180 - 355	1.4E-02	9.9E-03	0.0E+00	2.2E-02	3.1E-02	1.5E-02	9.7E-03
180 - 355	2.1E-03	7.9E-03	2.2E-03	0.0E+00	1.4E-02	6.1E-03	5.3E-03
180 - 355	5.3E-03	4.1E-02	5.0E-02	9.4E-02	1.2E-01	1.1E-01	6.0E-02
355 - 710	5.9E-03	2.5E-02	5.4E-02	1.2E-02	2.8E-01	3.6E-01	1.4E-01
355 - 710	1.3E-02	1.3E-02	3.2E-02	6.8E-02	1.3E-01	4.4E-02	5.7E-02
355 - 710	3.9E-02	0.0E+00	8.3E-03	2.9E-03	3.1E-02	1.3E-02	4.1E-03
355 - 710	1.5E-02	2.3E-03	4.3E-03	2.2E-02	1.3E-02	3.3E-03	2.8E-02
355 - 710	3.6E-03	2.0E-02	2.1E-02	2.5E-02	4.1E-02	3.9E-02	8.2E-03

Continuation of above Table

710 - 1400	1.1E-03	7.0E-04	1.5E-03	4.6E-03	3.2E-02	1.1E-02	7.7E-04
710 - 1400	3.0E-04	4.6E-03	5.1E-03	1.4E-02	7.0E-03	4.1E-03	5.4E-03
710 - 1400	5.1E-03	1.9E-03	3.4E-03	8.8E-04	8.1E-03	4.1E-03	1.4E-03
710 - 1400	1.3E-02	2.0E-03	2.5E-03	0.0E+00	3.7E-03	1.8E-03	8.5E-03
710 - 1400	3.7E-03	2.9E-03	3.0E-03	4.5E-03	3.3E-03	4.3E-03	2.1E-03
1400 - 2800	7.2E-04	1.6E-03	9.8E-04	7.6E-04	4.7E-03	2.0E-03	5.7E-04
1400 - 2800	1.5E-03	5.9E-03	5.9E-03	4.4E-03	8.7E-03	4.7E-03	9.0E-03
1400 - 2800	6.0E-03	6.7E-03	1.6E-03	2.4E-03	9.0E-04	1.3E-03	1.1E-03
1400 - 2800	6.8E-02	9.9E-02	2.0E-02	2.9E-02	1.1E-02	6.0E-03	3.2E-02
1400 - 2800	6.0E-04	1.0E-03	5.7E-04	3.2E-03	9.7E-04	2.3E-03	2.8E-03
>2800	2.1E-03	2.0E-03	3.6E-03	2.7E-03	1.8E-02	7.0E-03	2.8E-03
>2800	9.7E-05	1.8E-03	6.9E-04	4.1E-03	6.2E-03	1.5E-03	4.3E-04
>2800	2.2E-02	6.5E-02	3.9E-02	9.5E-02	1.8E-02	4.9E-02	3.2E-02
>2800	3.6E-03	2.7E-03	3.3E-03	3.8E-03	3.0E-03	8.8E-04	3.4E-03
>2800	2.7E-03	4.0E-03	5.9E-03	1.1E-02	5.9E-03	2.4E-03	4.9E-03
LOM	1.4E-03	2.4E-03	2.3E-03	2.9E-03	1.6E-03	2.5E-03	2.2E-03
LOM	1.6E-03	1.1E-03	6.5E-04	1.6E-03	4.9E-04	1.2E-03	8.8E-04
LOM	3.9E-03	7.0E-04	1.0E-03	2.2E-03	1.1E-03	1.3E-03	1.7E-03
LOM	5.4E-03	1.9E-04	5.8E-04	1.3E-03	3.9E-04	4.7E-04	4.6E-04
LOM	1.3E-03	6.2E-04	2.8E-04	9.2E-04	3.7E-04	7.5E-04	8.8E-04

Continuation of above Table

Size Range (μm)	Chrysene	Benzo(b) fluoranthrene	Benzo(a) pyrene	Indeno(1,2,3-cd) pyrene	Dibenz(a,h) anthracene	Benzo(ghi) perylene
<45	2.8E-03	1.4E-03	9.0E-03	5.6E-03	4.4E-03	1.3E-03
<45	1.5E-02	1.5E-02	6.0E-02	6.6E-03	5.1E-02	3.6E-02
<45	2.1E-02	1.2E-02	1.2E-01	3.7E-02	1.1E-01	4.6E-02
<45	1.4E-02	1.3E-02	1.2E-01	3.0E-02	9.9E-02	3.4E-02
<45	2.5E-02	2.7E-02	2.9E-02	9.5E-03	8.3E-03	1.7E-02
45 - 90	4.3E-03	1.6E-03	9.2E-03	6.3E-03	5.0E-03	1.4E-03
45 - 90	3.7E-02	3.1E-02	2.8E-02	4.5E-03	3.3E-02	3.5E-02
45 - 90	4.2E-02	3.5E-02	6.5E-02	6.4E-02	8.1E-02	1.7E-02
45 - 90	1.1E-02	1.9E-02	1.5E-01	1.9E-02	4.3E-02	9.6E-03
45 - 90	2.4E-02	4.6E-02	1.3E-01	2.9E-02	4.2E-02	7.7E-02
90 - 180	3.6E-02	5.8E-03	3.7E-02	1.8E-02	1.4E-02	4.5E-03
90 - 180	7.5E-02	1.9E-01	1.1E-01	1.2E-01	1.6E-01	1.5E-01
90 - 180	5.8E-03	6.5E-02	2.0E-02	1.2E-02	2.6E-02	5.5E-02
90 - 180	1.6E-02	1.2E-02	4.6E-02	1.8E-02	3.8E-02	0.0E+00
90 - 180	2.8E-02	6.1E-02	4.8E-02	1.4E-02	1.4E-02	2.2E-02
180 - 355	3.3E-01	1.3E-01	4.8E-01	2.1E-01	1.6E-01	5.0E-02
180 - 355	1.0E-01	1.5E-01	2.7E-01	9.5E-02	2.1E-01	2.3E-01
180 - 355	2.4E-02	3.1E-02	6.6E-03	0.0E+00	3.9E-02	1.4E-02
180 - 355	8.3E-03	5.2E-03	5.2E-02	3.1E-02	7.4E-03	0.0E+00
180 - 355	4.4E-02	5.2E-02	7.1E-02	7.0E-02	8.9E-02	1.3E-01
355 - 710	5.7E-02	1.1E-02	6.2E-02	7.5E-02	6.5E-02	1.1E-02
355 - 710	4.3E-02	6.3E-02	9.0E-02	6.0E-02	1.0E-01	6.6E-02
355 - 710	7.8E-03	7.8E-02	0.0E+00	7.8E-02	3.2E-02	3.4E-02
355 - 710	3.0E-02	1.8E-02	7.1E-03	2.5E-02	2.1E-02	2.8E-02
355 - 710	1.6E-02	1.3E-02	4.3E-02	4.3E-02	5.8E-02	3.0E-02

Continuation of above Table

Size Range (µm)	Chrysene	Benzo(b) flouranthrene	Benzo(a) pyrene	Indeno(1,2,3-cd) pyrene	Dibenz(a,h) anthracene	Benzo(ghi) perylene
710 - 1400	4.0E+01	2.0E+02	5.8E+02	4.9E+02	4.1E+02	6.7E+01
710 - 1400	1.7E+02	2.9E+02	1.8E+02	8.0E+01	4.3E+02	7.3E+02
710 - 1400	2.9E+02	4.1E+02	2.8E+02	1.0E+02	5.1E+02	2.2E+02
710 - 1400	1.5E+02	6.2E+01	1.3E+02	2.2E+02	2.1E+02	1.7E+02
710 - 1400	9.9E+01	3.6E+02	7.7E+02	3.0E+03	9.4E+02	1.3E+03
1400 - 2800	1.1E+02	1.5E+02	9.4E+02	6.3E+02	4.9E+02	1.2E+02
1400 - 2800	3.0E+02	1.5E+02	5.4E+02	4.0E+02	6.3E+02	5.2E+02
1400 - 2800	8.4E+01	2.4E+02	1.4E+02	3.2E+02	1.1E+02	2.4E+02
1400 - 2800	1.2E+02	6.4E+01	7.0E+01	2.1E+02	2.2E+02	1.2E+02
1400 - 2800	2.1E+02	6.2E+02	1.1E+03	1.8E+03	1.5E+03	9.7E+02
>2800	8.8E+01	2.0E+02	4.3E+02	1.3E+02	3.1E+02	5.3E+01
>2800	4.1E+01	8.1E+01	2.8E+02	5.7E+01	6.9E+01	1.5E+02
>2800	4.7E+01	7.7E+01	1.4E+02	3.2E+02	3.1E+02	8.4E+02
>2800	1.4E+02	2.4E+02	1.0E+02	1.7E+03	3.6E+02	1.6E+02
>2800	1.3E+02	5.2E+02	5.4E+02	6.2E+02	5.2E+02	6.5E+02
LOM	1.8E+03	1.5E+03	1.0E+03	1.2E+03	1.7E+03	1.1E+03
LOM	5.5E+02	8.7E+02	1.5E+03	5.9E+02	1.4E+03	4.2E+03
LOM	9.9E+02	7.5E+02	9.5E+02	5.4E+02	6.8E+02	1.4E+03
LOM	1.5E+03	9.4E+02	6.1E+02	2.4E+03	8.0E+02	2.1E+03
LOM	1.3E+03	4.6E+03	7.6E+03	1.5E+03	8.6E+02	7.1E+03

Table C.42 Ratios of Concentrations over CODs ($\mu\text{g}/\text{gm}$) for Carroll's Creek

Size Range (μm)	Naphthalene	Fluorene	Phenanthrene	Anthracene	Fluranthene	Pyrene	Benzo(a)anthracene
<45	4.4E-04	5.4E-04	1.4E-04	2.3E-03	1.2E-03	4.2E-04	6.5E-04
<45	2.5E-02	7.8E-03	2.8E-03	4.6E-03	1.7E-03	1.9E-03	8.0E-03
<45	2.2E-03	5.3E-03	1.9E-04	2.0E-03	1.5E-03	1.5E-03	9.7E-04
<45	1.6E-03	2.6E-03	4.0E-03	8.0E-03	2.4E-03	3.2E-03	2.0E-03
<45	3.7E-03	2.1E-03	2.1E-03	4.4E-03	1.8E-03	1.3E-03	1.7E-03
45 – 90	2.5E-03	5.8E-03	9.4E-04	3.6E-03	1.3E-03	3.1E-04	4.9E-04
45 – 90	3.1E-02	8.2E-03	4.6E-03	4.0E-03	2.8E-03	1.2E-03	1.5E-02
45 – 90	6.7E-03	6.3E-03	1.5E-04	1.9E-03	1.2E-03	2.9E-03	8.9E-04
45 – 90	1.4E-03	1.3E-02	1.1E-02	3.3E-03	4.9E-03	1.3E-02	2.2E-03
45 – 90	5.2E-03	3.3E-03	3.1E-03	3.2E-03	5.8E-03	3.8E-03	4.2E-03
90 – 180	1.3E-02	1.9E-02	3.4E-03	3.0E-03	4.6E-03	1.5E-03	3.7E-03
90 – 180	9.4E-04	0.0E+00	3.2E-03	0.0E+00	5.4E-03	1.8E-03	1.9E-03
90 – 180	4.7E-04	3.0E-03	0.0E+00	0.0E+00	3.1E-03	5.6E-03	9.1E-04
90 – 180	1.3E-03	8.8E-03	6.1E-03	9.3E-03	7.8E-03	2.1E-02	5.6E-03
90 – 180	5.9E-03	9.4E-03	4.7E-03	3.7E-03	1.2E-02	8.8E-03	1.3E-02
180 – 355	8.7E-03	4.5E-02	9.9E-03	5.9E-02	1.0E-02	1.8E-02	2.5E-02
180 – 355	1.7E-02	3.3E-03	4.8E-03	8.2E-03	1.6E-03	3.4E-03	7.0E-03
180 – 355	2.8E-03	8.9E-03	2.4E-04	4.4E-03	2.7E-03	5.3E-03	1.4E-03
180 – 355	4.4E-03	2.4E-02	1.9E-02	2.3E-02	1.1E-02	2.0E-02	8.6E-03
180 – 355	5.7E-03	7.4E-03	2.3E-03	8.1E-03	6.0E-03	7.9E-03	6.0E-03
355 – 710	1.8E-03	3.6E-03	1.4E-03	1.1E-03	7.5E-04	2.9E-04	2.3E-04
355 – 710	1.9E-03	3.3E-04	6.9E-04	6.4E-04	6.1E-04	3.0E-03	3.4E-03
355 – 710	1.2E-02	1.8E-03	4.6E-03	1.4E-03	1.4E-03	2.1E-03	4.0E-03
355 – 710	6.4E-04	4.3E-03	5.0E-03	5.6E-03	2.3E-03	5.4E-03	3.0E-03
355 – 710	1.0E-03	1.2E-03	9.4E-04	1.0E-03	1.3E-03	1.8E-03	2.0E-03

Continuation of above Table

Size Range (µm)	Naphthalene	Fluorene	Phenanthrene	Anthracene	Fluranthene	Pyrene	Benzo(a)anthracene
710 - 1400	5.9E-04	1.9E-03	2.3E-04	4.0E-04	1.7E-04	1.9E-04	3.9E-04
710 - 1400	2.3E-04	0.0E+00	3.7E-04	0.0E+00	2.1E-04	6.6E-04	3.1E-04
710 - 1400	7.4E-03	2.9E-03	3.1E-04	2.4E-04	5.7E-04	4.6E-04	9.3E-04
710 - 1400	1.8E-04	1.5E-03	9.1E-04	3.5E-03	5.4E-04	2.0E-03	1.4E-03
710 - 1400	3.3E-03	1.9E-03	7.1E-04	1.2E-03	1.4E-03	2.6E-03	3.3E-03
1400 - 2800	1.2E-03	2.6E-03	1.1E-03	1.5E-03	1.1E-03	5.8E-04	1.1E-03
1400 - 2800	1.3E-02	2.0E-03	2.3E-03	3.9E-03	8.0E-04	1.2E-03	3.9E-03
1400 - 2800	6.1E-04	9.1E-04	5.2E-05	7.7E-04	2.6E-04	3.1E-04	1.4E-04
1400 - 2800	1.9E-03	1.7E-03	1.1E-03	5.1E-03	8.9E-04	1.8E-03	2.0E-03
1400 - 2800	2.6E-03	2.7E-03	6.5E-04	2.1E-03	5.7E-04	2.5E-03	2.8E-03
>2800	2.9E-04	3.9E-03	6.0E-04	5.2E-04	1.1E-03	4.4E-04	2.1E-03
>2800	1.7E-03	6.9E-03	1.6E-03	1.1E-03	6.6E-04	6.8E-04	4.3E-03
>2800	3.6E-04	2.1E-03	1.7E-03	1.7E-03	6.2E-04	1.2E-03	2.3E-03
>2800	2.2E-03	2.3E-03	6.1E-03	3.7E-03	3.7E-03	2.7E-03	4.2E-03
>2800	2.1E-03	1.5E-03	8.9E-04	9.9E-04	1.1E-03	1.7E-03	1.0E-03
LOM	1.1E-03	8.3E-04	8.2E-04	9.3E-04	6.7E-04	2.0E-03	1.2E-03
LOM	5.2E-04	2.8E-03	2.9E-03	2.3E-03	4.8E-04	6.8E-04	1.6E-03
LOM	1.8E-03	6.8E-04	6.2E-04	6.2E-04	2.1E-03	3.6E-03	5.8E-04
LOM	2.5E-03	1.8E-03	1.5E-03	8.6E-04	2.8E-03	2.4E-03	2.5E-03
LOM	6.6E-04	1.2E-03	1.7E-03	2.8E-03	5.4E-04	7.1E-04	1.5E-03

Continuation of above Table

Size Range (µm)	Chrysene	Benzo(b) flouranthrene	Benzo(a) pyrene	Indeno(1,2,3-cd) pyrene	Dibenz(a,h) anthracene	Benzo(ghi) perylene
<45	1.4E-03	4.1E-04	9.5E-03	4.9E-03	4.1E-03	1.1E-03
<45	6.9E-03	6.0E-03	8.0E-03	9.7E-03	1.2E-02	7.7E-03
<45	7.9E-04	6.2E-04	2.1E-03	3.5E-02	1.1E-02	1.2E-02
<45	9.7E-03	5.3E-03	3.6E-03	2.0E-02	1.0E-02	5.7E-03
<45	5.8E-03	3.7E-03	4.9E-03	1.0E-02	5.4E-03	4.4E-03
45 - 90	8.9E-04	7.3E-04	1.3E-02	5.0E-03	4.0E-03	4.1E-03
45 - 90	4.8E-03	6.1E-03	6.0E-03	0.0E+00	1.2E-02	0.0E+00
45 - 90	8.0E-04	8.7E-04	3.1E-03	3.1E-02	4.0E-03	4.0E-03
45 - 90	1.3E-02	2.7E-02	2.5E-02	3.2E-02	6.7E-03	2.0E-02
45 - 90	1.3E-02	6.9E-03	1.0E-02	1.0E-02	6.5E-03	6.0E-03
90 - 180	3.2E-03	2.5E-02	8.1E-02	6.3E-02	5.3E-02	1.3E-02
90 - 180	1.1E-03	2.0E-03	1.2E-03	0.0E+00	4.6E-03	1.7E-02
90 - 180	1.1E-03	1.6E-02	1.8E-01	2.0E-01	1.7E-01	5.7E-02
90 - 180	4.9E-02	1.1E-02	2.0E-02	1.4E-01	7.6E-02	2.3E-01
90 - 180	1.4E-02	5.7E-03	3.5E-02	3.4E-02	3.0E-02	3.1E-02
180 - 355	3.9E-02	9.0E-03	1.7E-01	6.8E-02	5.2E-02	2.2E-02
180 - 355	4.9E-03	4.6E-03	4.2E-03	8.1E-03	1.2E-02	1.3E-02
180 - 355	1.1E-03	1.8E-03	9.1E-03	5.3E-02	8.5E-03	8.6E-03
180 - 355	8.2E-03	3.0E-03	2.4E-03	2.6E-03	9.0E-03	3.4E-03
180 - 355	8.1E-03	5.6E-03	7.5E-03	9.3E-03	1.8E-02	1.8E-02
355 - 710	3.8E-04	7.7E-04	8.4E-03	4.6E-03	3.7E-03	1.1E-03
355 - 710	3.0E-03	3.7E-03	0.0E+00	6.2E-03	5.6E-03	0.0E+00
355 - 710	3.4E-03	1.6E-03	1.4E-03	8.9E-03	1.1E-02	9.5E-03
355 - 710	6.2E-03	5.0E-03	1.5E-02	7.3E-04	2.6E-03	1.2E-03
355 - 710	3.5E-03	5.6E-03	2.6E-03	1.8E-03	5.3E-03	2.0E-03

Continuation of above Table

Size Range (µm)	Chrysene	Benzo(b) flouranthrene	Benzo(a) pyrene	Indeno(1,2,3-cd) pyrene	Dibenz(a,h) anthracene	Benzo(ghi) perylene
710 - 1400	5.4E-04	1.3E-04	2.0E-03	6.8E-04	5.8E-04	3.5E-04
710 - 1400	0.0E+00	1.9E-04	0.0E+00	0.0E+00	4.8E-04	0.0E+00
710 - 1400	2.2E-04	1.7E-04	2.9E-05	1.1E-03	0.0E+00	2.5E-03
710 - 1400	1.7E-03	6.6E-04	2.6E-03	6.7E-03	1.4E-02	1.1E-02
710 - 1400	1.6E-03	1.1E-03	1.1E-03	3.7E-03	5.9E-03	4.3E-03
1400 - 2800	5.5E-04	1.9E-03	7.3E-03	1.8E-03	1.9E-03	1.3E-03
1400 - 2800	3.3E-03	3.4E-03	3.2E-03	3.1E-03	2.2E-03	5.5E-03
1400 - 2800	1.2E-04	3.6E-05	3.7E-05	2.6E-04	2.6E-04	1.0E-03
1400 - 2800	4.9E-03	2.8E-03	1.7E-03	5.1E-03	5.6E-03	4.7E-03
1400 - 2800	2.8E-03	2.8E-03	1.9E-03	2.8E-03	2.9E-03	2.9E-03
>2800	9.6E-04	1.9E-03	2.8E-03	3.3E-03	1.7E-03	1.8E-03
>2800	3.5E-03	1.7E-03	2.0E-03	2.3E-03	1.4E-03	2.3E-03
>2800	6.1E-04	9.1E-04	1.3E-03	1.0E-03	1.3E-03	3.3E-03
>2800	5.6E-03	4.1E-03	3.8E-03	5.5E-04	1.9E-03	2.2E-03
>2800	1.9E-03	2.0E-03	2.4E-03	1.9E-03	2.6E-03	2.7E-03
LOM	1.2E-03	6.7E-04	1.0E-03	1.1E-03	1.1E-03	1.0E-03
LOM	2.3E-03	2.1E-03	2.3E-03	5.2E-04	7.6E-04	1.8E-03
LOM	8.8E-04	6.3E-04	3.6E-03	2.1E-03	1.1E-03	3.0E-03
LOM	8.1E-04	3.4E-03	3.8E-04	2.8E-03	5.7E-04	8.3E-04
LOM	1.7E-03	2.4E-03	1.3E-03	1.5E-03	2.1E-03	4.0E-04

Table C.43 Analyte Concentration and COD Regression Analyses Results for Cribbs Mill Creek Sediments

Analyte	Size Range (µm)	R ²	Response Factor (Slope)	P Value	Size Range (µm)	R ²	Response Factor (Slope)	P Value
Naphthalene	< 45	0.402	2.70E-06	0.175	45 - 90	0.508	2.15E-06	0.111
Fluorene	< 45	0.45	1.70E-06	0.144	45 - 90	0.681	8.94E-07	0.042
Phenanthrene	< 45	0.52	8.67E-07	0.105	45 - 90	0.347	6.19E-07	0.218
Anthracene	< 45	0.615	1.97E-06	0.064	45 - 90	0.618	2.01E-06	0.063
Fluranthene	< 45	0.762	1.74E-06	0.023	45 - 90	0.766	2.75E-06	0.022
Pyrene	< 45	0.794	2.48E-06	0.017	45 - 90	0.689	2.27E-06	0.040
Benzo(a)anthracene	< 45	0.55	2.14E-06	0.091	45 - 90	0.593	2.32E-06	0.073
Chrysene	< 45	0.541	2.03E-06	0.095	45 - 90	0.562	3.75E-06	0.085
Benzo(b)flouranthrene	< 45	0.682	4.12E-06	0.042	45 - 90	0.715	2.44E-06	0.033
Benzo(a)pyrene	< 45	0.824	4.61E-06	0.012	45 - 90	0.701	4.92E-06	0.037
Indeno(1,2,3-cd)pyrene	< 45	0.797	4.54E-06	0.016	45 - 90	0.596	4.34E-06	0.071
Dibenz(a,h)anthracene	< 45	0.715	4.43E-06	0.033	45 - 90	0.495	4.63E-06	0.118
Benzo(ghi)perylene	< 45	0.471	3.04E-06	0.131	45 - 90	0.576	2.72E-06	0.080

Continuation of above Table

Analyte	Size Range (µm)	R ²	Response Factor (Slope)	P Value	Size Range (µm)	R ²	Response Factor (Slope)	P Value
Naphthalene	90 - 180	0.565	6.92E-06	0.084	180- 355	0.555	2.39E-06	0.088
Fluorene	90 - 180	0.553	4.94E-06	0.089	180 - 355	0.386	3.28E-06	0.187
Phenanthrene	90 - 180	0.723	2.32E-06	0.038	180- 355	0.643	1.74E-06	0.046
Anthracene	90 - 180	0.533	3.29E-06	0.099	180 - 355	0.720	3.75E-06	0.039
Fluranthene	90 - 180	0.765	3.52E-06	0.022	180- 355	0.772	2.27E-06	0.021
Pyrene	90 - 180	0.599	4.43E-06	0.070	180 - 355	0.565	2.10E-06	0.084
Benzo(a)anthracene	90 - 180	0.534	5.99E-06	0.098	180- 355	0.415	4.28E-06	0.167
Chrysene	90 - 180	0.565	5.98E-06	0.084	180 - 355	0.500	3.13E-06	0.115
Benzo(b)flouranthrene	90 - 180	0.393	4.53E-06	0.182	180- 355	0.193	1.18E-05	0.382
Benzo(a)pyrene	90 - 180	0.822	1.31E-05	0.012	180- 355	0.232	1.04E-05	0.329
Indeno(1,2,3-cd)pyrene	90 - 180	0.645	2.46E-05	0.049	180 - 355	0.537	5.78E-06	0.097
Dibenz(a,h)anthracene	90 - 180	0.664	1.51E-05	0.048	180- 355	0.636	7.55E-06	0.057
Benzo(ghi)perylene	90 - 180	0.31	7.19E-06	0.025	180- 355	0.782	2.58E-06	0.019

Continuation of above Table

Analyte	Size Range (µm)	R ²	Response Factor (Slope)	P Value	Size Range (µm)	R ²	Response Factor (Slope)	P Value
Naphthalene	355 - 7100	0.455	1.69E-06	0.141	710 - 1400	0.288	1.60E-05	0.272
Fluorene	355 - 7100	0.314	2.14E-06	0.247	710 - 1400	0.614	1.54E-06	0.065
Phenanthrene	355 - 7100	0.671	1.31E-05	0.047	710 - 1400	0.328	9.15E-07	0.234
Anthracene	355 - 7100	0.196	2.29E-06	0.397	710 - 1400	0.634	3.64E-06	0.057
Fluranthene	355 - 7100	0.76	1.77E-06	0.023	710 - 1400	0.751	2.06E-06	0.025
Pyrene	355 - 7100	0.274	1.14E-06	0.285	710 - 1400	0.628	1.50E-06	0.060
Benzo(a)anthracene	355 - 7100	0.188	1.65E-06	0.389	710 - 1400	0.550	1.37E-06	0.091
Chrysene	355 - 7100	0.268	1.68E-06	0.292	710 - 1400	0.698	1.97E-06	0.038
Benzo(b)flouranthrene	355 - 7100	0.398	2.26E-06	0.178	710 - 1400	0.845	4.36E-06	0.009
Benzo(a)pyrene	355 - 7100	0.802	5.43E-06	0.015	710 - 1400	0.700	7.46E-06	0.037
Indeno(1,2,3-cd)pyrene	355 - 7100	0.618	5.31E-06	0.063	710 - 1400	0.700	4.76E-06	0.037
Dibenz(a,h)anthracene	355 - 7100	0.452	4.92E-06	0.143	710 - 1400	0.690	3.65E-06	0.047
Benzo(ghi)perylene	355 - 7100	0.612	5.78E-06	0.062	710 - 1400	0.219	3.67E-06	0.356

Continuation of above table

Analyte	Size Range (µm)	R ²	Response Factor (Slope)	P Value	Size Range (µm)	R ²	Response Factor (Slope)	P Value
Naphthalene	1400 - 2800	0.352	1.62E-05	0.212	> 2800 (w/o LOM)	0.716	8.84E-07	0.033
Fluorene	1400 - 2800	0.625	1.87E-06	0.061	> 2800 (w/o LOM)	0.636	9.80E-07	0.057
Phenanthrene	1400 - 2800	0.629	3.65E-06	0.059	> 2800 (w/o LOM)	0.414	1.28E-06	0.167
Anthracene	1400 - 2800	0.671	1.01E-05	0.046	> 2800 (w/o LOM)	0.713	1.67E-06	0.034
Fluranthene	1400 - 2800	0.908	2.69E-06	0.003	> 2800 (w/o LOM)	0.741	1.10E-06	0.027
Pyrene	1400 - 2800	0.817	1.71E-06	0.013	> 2800 (w/o LOM)	0.766	2.26E-06	0.022
Benzo(a)anthracene	1400 - 2800	0.574	2.63E-06	0.080	> 2800 (w/o LOM)	0.694	1.41E-06	0.039
Chrysene	1400 - 2800	0.664	2.59E-06	0.048	> 2800 (w/o LOM)	0.728	1.26E-06	0.030
Benzo(b)flouranthrene	1400 - 2800	0.745	4.90E-06	0.026	> 2800 (w/o LOM)	0.747	2.39E-06	0.026
Benzo(a)pyrene	1400 - 2800	0.354	1.63E-05	0.212	> 2800 (w/o LOM)	0.959	4.98E-06	0.000
Indeno(1,2,3-cd)pyrene	1400 - 2800	0.422	7.88E-06	0.162	> 2800 (w/o LOM)	0.747	2.14E-06	0.026
Dibenz(a,h)anthracene	1400 - 2800	0.431	1.10E-05	0.156	> 2800 (w/o LOM)	0.699	2.95E-06	0.037
Benzo(ghi)perylene	1400 - 2800	0.72	3.72E-06	0.032	> 2800 (w/o LOM)	0.916	3.19E-06	0.002

Continuation of above Table

Analyte	Size Range (μm)	R²	Response Factor (Slope)	P Value
Naphthalene	LOM	0.846	1.41E-06	0.009
Fluorene	LOM	0.877	1.25E-06	0.005
Phenanthrene	LOM	0.738	1.68E-06	0.028
Anthracene	LOM	0.76	1.34E-06	0.023
Fluranthene	LOM	0.768	1.10E-06	0.022
Pyrene	LOM	0.849	1.27E-06	0.009
Benzo(a)anthracene	LOM	0.736	1.60E-06	0.028
Chrysene	LOM	0.884	1.42E-06	0.005
Benzo(b)flouranthrene	LOM	0.688	1.39E-06	0.040
Benzo(a)pyrene	LOM	0.696	1.43E-06	0.038
Indeno(1,2,3-cd)pyrene	LOM	0.789	1.24E-06	0.018
Dibenz(a,h)anthracene	LOM	0.91	1.21E-06	0.003
Benzo(ghi)perylene	LOM	0.684	1.06E-06	0.042

Table C.44 Analyte Concentration and COD Regression Analysis Results for Hunter Creek Sediment

Analyte	Size Range (µm)	R ²	Response Factor (Slope)	P Value	Size	R ²	Response Factor (Slope)	P Value
Naphthalene	< 45	0.539	1.94E-06	0.096	45 - 90	0.703	1.81E-06	0.059
Fluorene	< 45	0.427	6.40E-06	0.159	45 - 90	0.516	5.15E-06	0.107
Phenanthrene	< 45	0.815	9.86E-06	0.0137	45 - 90	0.482	6.99E-06	0.125
Anthracene	< 45	0.392	8.80E-06	0.183	45 - 90	0.490	9.13E-06	0.120
Fluoranthene	< 45	0.784	2.85E-05	0.018	45 - 90	0.940	3.34E-05	0.001
Pyrene	< 45	0.875	2.69E-05	0.006	45 - 90	0.854	2.44E-05	0.008
Benzo(a)anthracene	< 45	0.512	1.20E-05	0.109	45 - 90	0.338	1.16E-05	0.226
Chrysene	< 45	0.706	1.29E-05	0.036	45 - 90	0.638	1.52E-05	0.056
Benzo(b)fluoranthrene	< 45	0.719	1.13E-05	0.0429	45 - 90	0.768	1.98E-05	0.021
Benzo(a)pyrene	< 45	0.591	6.02E-05	0.073	45 - 90	0.778	1.07E-04	0.019
Indeno(1,2,3-cd)pyrene	< 45	0.736	1.65E-05	0.047	45 - 90	0.685	2.00E-05	0.047
Dibenz(a,h)anthracene	< 45	0.515	4.72E-05	0.107	45 - 90	0.807	3.94E-05	0.014
Benzo(ghi)perylene	< 45	0.617	2.13E-05	0.063	45 - 90	0.430	1.35E-05	0.156

Continuation of above Table

Analyte	Size Range (µm)	R ²	Response Factor (Slope)	P Value	Size	R ²	Response Factor (Slope)	P Value
Naphthalene	90 - 180	0.376	5.13E-06	0.194	180- 355	0.318	1.97E-05	0.242
Fluorene	90 - 180	0.414	1.92E-05	0.167	180 - 355	0.644	2.18E-05	0.054
Phenanthrene	90 - 180	0.296	1.52E-05	0.267	180- 355	0.653	4.00E-05	0.098
Anthracene	90 - 180	0.74	4.14E-05	0.027	180 - 355	0.784	8.0-05	0.046
Fluranthene	90 - 180	0.62	5.99E-05	0.062	180- 355	0.456	9.41E-05	0.140
Pyrene	90 - 180	0.576	8.04E-05	0.080	180 - 355	0.527	7.38E-05	0.102
Benzo(a)anthracene	90 - 180	0.338	1.07E-04	0.304	180- 355	0.485	4.66E-05	0.124
Chrysene	90 - 180	0.665	2.73E-05	0.047	180 - 355	0.504	4.36E-05	0.113
Benzo(b)flouranthrene	90 - 180	0.366	4.25E-05	0.202	180- 355	0.537	5.33E-05	0.097
Benzo(a)pyrene	90 - 180	0.777	4.63E-05	0.202	180- 355	0.467	8.83E-05	0.134
Indeno(1,2,3-cd)pyrene	90 - 180	0.4107	2.73E-05	0.170	180 - 355	0.563	7.89E-05	0.085
Dibenz(a,h)anthracene	90 - 180	0.452	3.88E-05	0.143	180- 355	0.498	3.06E-06	0.097
Benzo(ghi)perylene	90 - 180	0.678	1.42E-05	0.045	180- 355	7.89E-01	2.29E-05	0.020

Continuation of above Table

Analyte	Size Range (µm)	R ²	Response Factor (Slope)	P Value	Size	R ²	Response Factor (Slope)	P Value
Naphthalene	355 - 7100	0.47	1.16E-05	0.132	710 - 1400	0.879	3.22E-06	0.020
Fluorene	355 - 7100	0.693	3.66E-05	0.047	710 - 1400	0.933	3.06E-06	0.001
Phenanthrene	355 - 7100	0.722	2.03E-05	0.032	710 - 1400	0.939	3.29E-06	0.001
Anthracene	355 - 7100	0.69	2.40E-05	0.040	710 - 1400	0.892	4.38E-06	0.021
Fluranthene	355 - 7100	0.441	6.12E-05	0.150	710 - 1400	0.492	5.01E-06	0.120
Pyrene	355 - 7100	0.277	5.43E-05	0.282	710 - 1400	0.923	4.48E-06	0.002
Benzo(a)anthracene	355 - 7100	0.323	2.42E-05	0.239	710 - 1400	0.775	2.65E-06	0.020
Chrysene	355 - 7100	0.724	2.23E-05	0.031	710 - 1400	0.370	1.44E-06	0.199
Benzo(b)flouranthrene	355 - 7100	0.545	2.80E-05	0.093	710 - 1400	0.706	3.38E-06	0.036
Benzo(a)pyrene	355 - 7100	0.793	7.38E-05	0.032	710 - 1400	0.786	5.65E-06	0.018
Indeno(1,2,3-cd)pyrene	355 - 7100	0.896	5.00E-05	0.004	710 - 1400	0.908	1.72E-05	0.012
Dibenz(a,h)anthracene	355 - 7100	0.857	5.35E-05	0.008	710 - 1400	0.909	7.30E-06	0.003
Benzo(ghi)perylene	355 - 7100	0.877	3.18E-05	0.005	710 - 1400	0.976	9.35E-06	0.000

Continuation of above Table

Analyte	Size Range (µm)	R ²	Response Factor (Slope)	P Value	Size	R ²	Response Factor (Slope)	P Value
Naphthalene	1400 - 2800	0.291	1.53E-06	0.268	> 2800 (w/o LOM)	0.678	2.16E-06	0.043
Fluorene	1400 - 2800	0.391	2.47E-06	0.183	> 2800 (w/o LOM)	0.597	2.86E-06	0.071
Phenanthrene	1400 - 2800	0.412	1.28E-06	0.169	> 2800 (w/o LOM)	0.692	3.54E-06	0.039
Anthracene	1400 - 2800	0.823	2.68E-06	0.012	> 2800 (w/o LOM)	0.632	6.24E-06	0.058
Fluranthene	1400 - 2800	0.489	2.43E-06	0.121	> 2800 (w/o LOM)	0.677	7.39E-06	0.044
Pyrene	1400 - 2800	0.886	2.28E-06	0.005	> 2800 (w/o LOM)	0.500	2.61E-06	0.116
Benzo(a)anthracene	1400 - 2800	0.575	2.65E-06	0.080	> 2800 (w/o LOM)	0.696	3.02E-06	0.038
Chrysene	1400 - 2800	0.641	1.37E-06	0.055	> 2800 (w/o LOM)	0.843	2.13E-06	0.009
Benzo(b)flouranthrene	1400 - 2800	0.912	2.83E-06	0.002	> 2800 (w/o LOM)	0.770	5.74E-06	0.022
Benzo(a)pyrene	1400 - 2800	0.887	6.03E-06	0.004	> 2800 (w/o LOM)	0.792	7.20E-06	0.017
Indeno(1,2,3-cd)pyrene	1400 - 2800	0.896	7.73E-06	0.004	> 2800 (w/o LOM)	0.482	1.36E-05	0.125
Dibenz(a,h)anthracene	1400 - 2800	0.838	1.48E-06	0.010	> 2800 (w/o LOM)	0.698	6.82E-06	0.038
Benzo(ghi)perylene	1400 - 2800	0.813	4.34E-06	0.014	> 2800 (w/o LOM)	0.283	6.06E-06	0.277

Continuation of above Table

Analyte	Size	R²	Response Factor (Slope)	P Value
Naphthalene	LOM	0.732	2.83E-06	0.029
Fluorene	LOM	0.609	8.48E-07	0.066
Phenanthrene	LOM	0.625	8.13E-07	0.061
Anthracene	LOM	0.858	1.65E-06	0.007
Fluranthene	LOM	0.709	6.88E-07	0.035
Pyrene	LOM	0.75	1.10E-06	0.025
Benzo(a)anthracene	LOM	0.779	1.11E-06	0.019
Chrysene	LOM	0.87	8.21E-07	0.006
Benzo(b)flouranthrene	LOM	0.657	1.26E-06	0.050
Benzo(a)pyrene	LOM	0.523	1.73E-06	0.104
Indeno(1,2,3-cd)pyrene	LOM	0.818	8.78E-07	0.013
Dibenz(a,h)anthracene	LOM	0.808	7.12E-07	0.014
Benzo(ghi)perylene	LOM	0.739	2.28E-06	0.028

Table C.45 Analyte Concentration and COD Regression Analysis Results for Carroll's Creek Sediments

Analyte	Size Range (µm)	R ²	Response Factor (Slope)	P Value	Size Range (µm)	R ²	Response Factor (Slope)	P Value
Naphthalene	< 45	0.288	2.96E-06	0.272	45 - 90	0.419	5.60E-06	0.164
Fluorene	< 45	0.694	2.64E-06	0.039	45 - 90	0.815	6.17E-06	0.013
Phenanthrene	< 45	0.635	2.10E-06	0.057	45 - 90	0.441	3.11E-06	0.149
Anthracene	< 45	0.798	4.87E-06	0.016	45 - 90	0.962	3.15E-06	0.000
Fluranthene	< 45	0.945	1.83E-06	0.001	45 - 90	0.708	3.26E-06	0.035
Pyrene	< 45	0.747	1.85E-06	0.026	45 - 90	0.448	3.69E-06	0.145
Benzo(a)anthracene	< 45	0.612	1.73E-06	0.065	45 - 90	0.404	2.79E-06	0.174
Chrysene	< 45	0.709	5.55E-06	0.035	45 - 90	0.548	6.71E-06	0.092
Benzo(b)fluoranthrene	< 45	0.702	3.21E-06	0.037	45 - 90	0.371	6.67E-06	0.199
Benzo(a)pyrene	< 45	0.805	5.07E-06	0.015	45 - 90	0.765	1.18E-05	0.022
Indeno(1,2,3-cd)pyrene	< 45	0.732	1.60E-05	0.029	45 - 90	0.681	6.41E-06	0.039
Dibenz(a,h)anthracene	< 45	0.883	7.77E-06	0.005	45 - 90	0.892	5.61E-06	0.004
Benzo(ghi)perylene	< 45	0.734	5.47E-06	0.029	45 - 90	0.723	6.41E-06	0.030

Continuation of the above Table

Analyte	Size Range (μm)	R ²	Response Factor (Slope)	P Value	Size Range (μm)	R ²	Response Factor (Slope)	P Value
Naphthalene	90 - 180	0.565	5.00E-06	0.084	180 - 355	0.683	6.27E-06	0.042
Fluorene	90 - 180	0.0652	6.41E-06	0.0502	180 - 355	0.682	1.13E-05	0.042
Phenanthrene	90 - 180	0.582	2.24E-06	0.0721	180 - 355	0.432	6.41E-06	0.135
Anthracene	90 - 180	0.682	3.21E-06	0.0402	180 - 355	0.683	1.12E-05	0.042
Fluranthene	90 - 180	0.817	7.72E-06	0.013	180 - 355	0.771	5.96E-06	0.021
Pyrene	90 - 180	0.587	7.62E-06	0.075	180 - 355	0.728	9.72E-06	0.030
Benzo(a)anthracene	90 - 180	0.646	6.45E-06	0.053	180 - 355	0.821	5.96E-06	0.012
Chrysene	90 - 180	0.404	1.32E-05	0.174	180 - 355	0.762	6.41E-06	0.023
Benzo(b)flouranthrene	90 - 180	0.661	1.12E-05	0.049	180 - 355	0.873	4.08E-06	0.006
Benzo(a)pyrene	90 - 180	0.513	5.68E-05	0.109	180 - 355	0.257	6.89E-06	0.304
Indeno(1,2,3-cd)pyrene	90 - 180	0.618	1.18E-05	0.068	180 - 355	0.431	1.64E-05	0.156
Dibenz(a,h)anthracene	90 - 180	0.562	5.67E-05	0.085	180 - 355	0.874	1.31E-05	0.006
Benzo(ghi)perylene	90 - 180	0.39	5.82E-05	0.184	180 - 355	0.792	1.20E-05	0.017

Continuation of above Table

Analyte	Size Range (µm)	R ²	Response Factor (Slope)	P Value	Size Range (µm)	R ²	Response Factor (Slope)	P Value
Naphthalene	355 - 710	0.355	2.75E-06	0.211	710 - 1400	0.368	1.90E-06	0.201
Fluorene	355 - 710	0.75	2.44E-06	0.025	710 - 1400	0.62	1.12E-05	0.061
Phenanthrene	355 - 710	0.624	2.24E-06	0.061	710 - 1400	0.767	4.26E-07	0.022
Anthracene	355 - 710	0.532	1.83E-06	0.099	710 - 1400	0.681	5.96E-06	0.041
Fluranthene	355 - 710	0.826	1.23E-06	0.012	710 - 1400	0.543	4.87E-07	0.094
Pyrene	355 - 710	0.61	2.12E-06	0.066	710 - 1400	0.508	9.39E-07	0.111
Benzo(a)anthracene	355 - 710	0.694	2.04E-06	0.039	710 - 1400	0.486	1.05E-06	0.123
Chrysene	355 - 710	0.691	2.97E-06	0.04	710 - 1400	0.812	3.69E-06	0.014
Benzo(b)flouranthrene	355 - 710	0.717	3.31E-06	0.033	710 - 1400	0.501	3.73E-07	0.115
Benzo(a)pyrene	355 - 710	0.724	1.12E-05	0.03	710 - 1400	0.843	3.89E-06	0.010
Indeno(1,2,3-cd)pyrene	355 - 710	0.678	3.88E-06	0.043	710 - 1400	0.745	1.60E-05	0.026
Dibenz(a,h)anthracene	355 - 710	0.825	5.12E-06	0.012	710 - 1400	0.846	2.44E-06	0.010
Benzo(ghi)perylene	355 - 710	0.626	5.96E-06	0.061	710 - 1400	0.692	1.60E-05	0.037

Continuation of above Table

Analyte	Size Range (µm)	R ²	Response Factor (Slope)	P Value	Size Range (µm)	R ²	Response Factor (Slope)	P Value
Naphthalene	1400 - 2800	0.35	2.00E-06	0.215	>2800	0.728	1.34E-06	0.030
Fluorene	1400 - 2800	0.821	1.67E-06	0.011	>2800	0.736	3.44E-06	0.028
Phenanthrene	1400 - 2800	0.508	6.21E-07	0.111	>2800	0.547	1.82E-06	0.092
Anthracene	1400 - 2800	0.621	2.12E-06	0.062	>2800	0.689	1.40E-06	0.040
Fluranthene	1400 - 2800	0.77	5.67E-07	0.021	>2800	0.618	1.23E-06	0.063
Pyrene	1400 - 2800	0.605	1.11E-06	0.068	>2800	0.757	1.25E-06	0.024
Benzo(a)anthracene	1400 - 2800	0.543	1.35E-06	0.094	>2800	0.799	2.63E-06	0.016
Chrysene	1400 - 2800	0.473	1.79E-06	0.13	>2800	0.669	2.29E-06	0.046
Benzo(b)flouranthrene	1400 - 2800	0.555	1.52E-06	0.088	>2800	0.823	1.95E-06	0.012
Benzo(a)pyrene	1400 - 2800	0.381	1.78E-06	0.191	>2800	0.902	2.32E-06	0.003
Indeno(1,2,3-cd)pyrene	1400 - 2800	0.549	2.02E-06	0.091	>2800	0.821	1.91E-06	0.012
Dibenz(a,h)anthracene	1400 - 2800	0.526	2.11E-06	0.102	>2800	0.924	1.81E-06	0.002
Benzo(ghi)perylene	1400 - 2800	0.689	2.40E-06	0.04	>2800	0.961	2.52E-06	0.000

Continuation of above Table

Analyte	Size Range (μm)	R ²	Response Factor (Slope)	P Value
Naphthalene	LOM	0.746	1.23E-06	0.026
Fluorene	LOM	0.784	1.46E-06	0.018
Phenanthrene	LOM	0.776	1.52E-06	0.02
Anthracene	LOM	0.761	1.57E-06	0.023
Fluranthene	LOM	0.623	1.14E-06	0.061
Pyrene	LOM	0.755	1.74E-06	0.024
Benzo(a)anthracene	LOM	0.869	1.48E-06	0.006
Chrysene	LOM	0.876	1.43E-06	0.005
Benzo(b)flouranthrene	LOM	0.751	1.79E-06	0.025
Benzo(a)pyrene	LOM	0.711	1.56E-06	0.034
Indeno(1,2,3-cd)pyrene	LOM	0.793	1.47E-06	0.017
Dibenz(a,h)anthracene	LOM	0.832	1.14E-06	0.011
Benzo(ghi)perylene	LOM	0.709	1.27E-06	0.035